

University of Strathclyde

**Strathclyde Institute of Pharmacy and Biomedical
Sciences**

**Characterization of *Acanthamoeba*
macrophage activation**

By

Antonella Cano

**A thesis submitted in the fulfillment of the requirements for
the degree of Doctor of Philosophy**

2015

This thesis is the result of the author's original research.

It has been composed by the author and has not been previously submitted for examination, which has led to the award of a degree.

The copyright of this thesis belongs to the author under the terms of the United Kingdom Copyrights Acts as qualified by the University of Strathclyde Regulation 3.50.

Due acknowledgement must always be made of the use of any material contained in, or derived from, this thesis.

Signed:



Date:

Acknowledgements

I would like to thank my supervisors Prof. Craig Roberts and Prof. James Alexander for giving me the opportunity to undertake this experience which helped me to mature from a personal and working point of view. I would like to thank them for their supervision and guidance throughout the course of the PhD. I would like to thank Dr. Fiona Henriquez for her constant support inside and outside the laboratory and for being my family here in Scotland. I would like to thank my mentor Dr. Antonella Mattana, for introducing me into research, for supporting me and for her advices and encouragement to always do my best.

I would like to thank Prof. Andrew MacDonald, Prof. Robin Plevin and Prof. Claire Bryant for providing me with, respectively MyD88^{-/-} and TRIF^{-/-} mice, PAR₂^{-/-} and MKP-2 mice, TLR2^{-/-}, TLR4^{-/-} and TLR2/4^{-/-} mice. I would like to thank Dr. Stuart Woods for helping me with the microscopy and metabolomics experiments.

I would like to thanks the friends I have met throughout this experience, with whom I shared the everyday ups and downs of the PhD, for the good laughs and for the break-downs! Bharath, Chris, Jeehan, Stuart, Selina, Caroline, Farzana and all the friends in level 6..I would have like to name you all..but this thesis is already way too long ;-)

Un ringraziamento speciale ai miei genitori e a mia sorella Deny per il loro esempio, per aver sempre creduto in me e nelle mie scelte, per avermi spronato a fare del mio meglio. Claudia, Valentina e Valeria, grazie di cuore sempre presenti amiche mie! Ale, lo sai, non esistono abbastanza parole per ringraziarti...ti dico solo: ce l'abbiamo fatta, e che la nostra vita insieme inizi!!!

Abstract

Acanthamoeba castellanii is a free-living amoeba ubiquitous in nature, with worldwide distribution. Although it is capable of living and proliferating without invading hosts, it can occasionally cause opportunistic as well as non opportunistic diseases in humans. Dissecting the immunology of *Acanthamoeba* infections has been always considered problematic due to the very low incidence despite the high exposure rates. The aim of this study was to investigate the effects of *Acanthamoeba* on the activation of resting macrophages. Towards this purpose bone marrow derived macrophages were co-cultured with either a laboratory strain, named Neff, or a clinical isolate of *A. castellanii*. *Acanthamoeba* was found to induce a pro-inflammatory macrophage phenotype following exposure to Neff strain, characterized by significant production of TNF- α , IL-12 and IL-6 from macrophages. In comparison the clinical isolate induced IL-12 and IL-6 to a significantly lesser degree than the Neff strain ($p < 0.0005$) and did not induce TNF- α . The utilization of macrophages derived from MyD88, TRIF, TLR2, TLR4, TLR2/4, and PAR₂ deficient mice along with a PAR₁ specific antagonist indicated that *Acanthamoeba*-induced pro-inflammatory cytokine production was through MyD88-dependent ($p < 0.0005$), TLR4-induced events ($p < 0.0005$), with a further contribution from PAR₁ ($p < 0.05$). *Acanthamoeba* trophozoites were also found to induce arginase activity in macrophages ($p < 0.0005$). Conversely, nitric oxide (NO) was not significantly detected in macrophages co-incubated with *Acanthamoeba*. By inducing arginase activity in macrophages, *Acanthamoeba* trophozoites were also found to be capable of inducing a tissue-repair, wound healing phenotype. Macrophage/*Acanthamoeba* co-incubation, analysed using a metabolomics approach, showed a peculiar metabolic snap-shot where both amoeba and macrophage metabolites might play a role in modulating the development and outcome of infection. The information

obtained from this experimental study has provided new and interesting insights about the immunological aspects of *Acanthamoeba* infections, which may be helpful for future practical applications in pharmaceutical, immunological and diagnostic fields.

Table of Content

<i>Copy Right</i>	II
<i>Acknowledgements</i>	III
<i>Abstract</i>	IV
<i>Table of Content</i>	VI
<i>List of figures</i>	XI
<i>List of tables</i>	XIV
<i>Abbreviation</i>	XV

CHAPTER 1 Introduction	1
1.1 Free Living Amoebae	2
1.2 <i>Acanthamoeba</i> , a free living amoeba	3
1.2.1 History	3
1.2.2 Life cycle	3
1.2.3 Distribution	6
1.2.4 Classification	6
1.3 <i>Acanthamoeba</i> , a potential pathogen for humans.....	10
1.3.1 History	10
1.3.2 <i>Acanthamoeba</i> diseases.....	11
1.3.2.1 Granulomatous amoebic encephalitis.....	11
1.3.2.2 Cutaneous acanthamoebiasis.....	14
1.3.2.3 <i>Acanthamoeba</i> Keratitis	15
1.3.3 <i>Acanthamoeba</i> virulence factors	21
1.3.4 GAE pathogenic cascade	25
1.3.5 AK pathogenic cascade	26
1.3.6 <i>Acanthamoeba</i> Immunoepidemiology	31
1.3.7 Host immune response in <i>Acanthamoeba</i> Infection.....	32
1.3.7.1 Blood components: the complement system and circulating monocytes	33
1.3.7.2 The corneal surface: physical, molecular, cellular barriers and innate immune receptors	34
1.3.7.3 Innate immune cells: neutrophils and macrophages	39
1.3.7.4 Humoral and cellular adaptive immune responses	45
1.3.7.5 <i>Acanthamoeba</i> immune evasion mechanisms.....	47
1.3.8 Aims.....	51

CHAPTER 2 General Materials and Methods.....	54
2.1 <i>Acanthamoeba castellanii</i> cultures	55
2.2 Culture of murine bone marrow derived macrophages	55
2.3 Infection of BMD macrophages with <i>Acanthamoeba castellanii</i> trophozoites.	56
2.4 Production of amoeba-derived cell free conditioned medium	57
2.5 Stimulation of murine BMD macrophages with amoeba-derived cell free conditioned medium	58
2.6 Stimulation of BMD macrophages with specific agonists	58
2.7 Quantitative analysis of murine cytokines production	59
2.8 Determination of arginase activity in BMD murine macrophages	61
2.9 Determination of nitric oxide production by BMD murine macrophages	63
2.10 Statistical analyses	64
CHAPTER 3 <i>Acanthamoeba castellanii</i> stimulates the production of pro-inflammatory cytokines in murine bone marrow derived macrophages.....	68
3.1 Abstract.....	69
3.2 Introduction.....	70
3.3 Materials and Methods	72
3.3.1 Real time microscopy of a co-culture of murine BMD macrophages and trophozoites of <i>A. castellanii</i> at 37°C	72
3.3.2 Evaluation of morphological changes of <i>A. castellanii</i> trophozoites when cultured at 37°C 5%CO ₂	73
3.3.3 Inhibition of secreted amoebic proteases	73
3.3.4 Statistical analyses.....	74
3.4 Results.....	75
3.4.1 <i>In vitro</i> real time imaging of <i>A. castellanii</i> infection shows cell-cell interactions between murine BMD macrophages and trophozoites of either the Neff strain or clinical isolate	75
3.4.2 Incubation of <i>A. castellanii</i> at 37°C, 5%CO ₂ for 24 hours induces differential changes in trophozoite morphology	76
3.4.3 <i>A. castellanii</i> Neff induces TNF- α , IL-12 and IL-6 production in murine BMD macrophages in a time and trophozoite density dependent manner	84
3.4.4 Clinical isolate of <i>A. castellanii</i> , belonging to genotype T4, stimulates lower cytokine production than Neff, classical laboratory strain	86

3.4.5	Amoeba-derived cell free conditioned medium fails to induce pro-inflammatory cytokines by murine BMD macrophage	89
3.4.6	<i>A.castellanii</i> -secreted proteases stimulate the production of pro-inflammatory cytokines by murine BMD macrophages.....	92
3.5	Discussion	98

CHAPTER 4 Innate immune receptors expressed on murine macrophages recognize and respond to *Acanthamoeba castellanii* trophozoites.....104

4.1	Abstract.....	105
4.2	Introduction.....	106
4.3	Materials and Methods	108
4.3.1	Inhibition of TLR2 and TLR4 expression on BMD murine macrophages with specific IgG antibody.....	108
4.3.2	Stimulation of PAR ₂ deficient BMD macrophages with specific PAR ₂ agonist	108
4.3.3	Inhibition of PAR ₁ using RWJ 56110 synthetic antagonist and stimulation with PAR ₁ agonist.....	109
4.3.4	Statistical analyses.....	110
4.4	Results.....	111
4.4.1	<i>Acanthamoeba</i> -induced IL-12 and IL-6 production is MyD88-dependent and partially TRIF-dependent.....	111
4.4.2	Anti-CD282 (TLR2) monoclonal antibody inhibits IL-12 and IL-6 cytokine production by murine macrophages in response to PAM3CSK4.....	114
4.4.3	<i>Acanthamoeba</i> -induced macrophage IL-12 and IL-6 production is TLR4-dependent but TLR2-independent	120
4.4.4	<i>Acanthamoeba</i> -induced IL-12 and IL-6 production by murine macrophages is PAR ₂ -independent	123
4.4.5	<i>Acanthamoeba castellanii</i> clinical strain induces IL-12 production by murine macrophages in a PAR ₁ -dependent manner.....	125
4.5	Discussion	128

CHAPTER 5 *Acanthamoeba* trophozoites induce arginase activity in murine macrophages.....134

5.1	Abstract.....	135
5.2	Introduction.....	136

5.3	Materials and methods	139
5.3.1	Effect of <i>Acanthamoeba</i> on LPS-induced NO production by murine macrophages	139
5.3.2	Bioinformatical analysis	139
5.4	Results	129
5.4.1	<i>Acanthamoeba</i> trophozoites induce murine macrophage arginase activity; whereas <i>Acanthamoeba</i> -induced macrophage NO production was not significantly induced.....	141
5.4.2	PAM3CSK4-induced arginase activity by macrophages is TLR2-dependent.....	144
5.4.3	Trophozoite-induced arginase activity by macrophages is TLR2-independent.....	146
5.4.4	LPS-induced NO production by macrophages is reduced by <i>Acanthamoeba</i> trophozoites.....	148
5.4.5	<i>Acanthamoeba</i> FlaHb putative protein presents a similar amino acid sequence to other FlaHb protein sequences.	150
5.5	Discussion	152

CHAPTER 6 Qualitative characterization of macrophage metabolism after stimulation with amoeba-derived cell free conditioned medium: preliminary data.....157

6.1	Abstract.....	158
6.2	Introduction	159
6.3	Materials and Methods	162
6.3.1	Extraction of metabolites from whole macrophages, from macrophage spent medium and amoeba-derived conditioned medium.....	162
6.3.2	Liquid chromatography and mass spectrometry	163
6.3.3	Data processing	164
6.3.4	Data analysis.....	164
6.4	Results	165
6.4.1	<i>Acanthamoeba</i> modifies the complete RPMI composition by the release and the uptake of metabolites	165
6.4.2	Amoeba-derived conditioned medium and LPS differently modulate macrophage metabolism.	169
6.4.2.1	Amino acid metabolism	170

6.4.2.2 Carbohydrate metabolism	171
6.5 Discussion	178
CHAPTER 7 Conclusion.....	184
CHAPTER 8 References.....	194

List of figures

Fig 1.1 <i>Acanthamoeba</i> life-cycle.....	5
Fig 1.2 <i>Acanthamoeba</i> classification.....	9
Fig 1.3 AK epidemiological studies reported world-wide.....	20
Fig 1.4 Toll like receptor ligands, structure and signalling pathways.....	49
Fig 1.6 Protease activated receptors (PARs) structure, activation and functions.....	50
Fig 3.1. Real time images of cell-cell interactions in co-cultures of either <i>A. castellanii</i> Neff strain, or clinical isolate strain trophozoites (Tr) with murine BMD macrophages (M ϕ).....	77-82
Fig 3.2 Morphological changes in Neff trophozoites as shown at time 0 (A) and after 24h incubation at 37°C, 5%CO ₂ (B).....	84
Fig 3.3 Morphological changes in clinical trophozoites at time 0 (A) and after incubation at 37°C, 5%CO ₂ (B).....	85
Fig 3.4 Release of TNF- α (A), IL-12 (B) and IL-6 (C) at 4, 6, 8, 10, 24 h after co-incubation with <i>A. castellanii</i> Neff trophozoites.....	88
Fig 3.5 Release of TNF- α (A), IL-12 (B) and IL-6 (C) at 8 and 24 h after co-incubation with <i>A. castellanii</i> trophozoites.....	91
Fig 3.6 Release of TNF- α (A), IL-12 (B) and IL-6 (C) at 24 h after co-incubation with <i>A. castellanii</i> trophozoites or amoeba-derived conditioned medium.....	94
Fig 3.7 Release of IL-12 (A) and IL-6 (B) at 24 h after treatment with protease inhibitors prior co-incubation with <i>A. castellanii</i> trophozoites.....	97
Fig 4.1 Release of IL-12 (A) and IL-6 (B): comparison between C57BL/6 WT and C57BL/6 MyD88 ^{-/-} macrophages at 24 h after co-incubation with <i>Acanthamoeba</i> trophozoites.....	113
Fig 4.2 Release of IL-12 (A) and IL-6 (B): comparison between C57BL/6 WT and C57BL/6 TRIF ^{-/-} macrophages at 24 h after co-incubation with <i>Acanthamoeba</i> trophozoites.....	114

Fig 4.3 IL-12 (A), and IL-6 (B) production by murine macrophages after 24h pre-treatment with anti IgG TLR2 antibody.....	117
Fig 4.4 IL-12 (A), and IL-6 (B) production by murine macrophages after 24h pre-treatment with anti IgG TLR4 antibody.....	118
Fig 4.5 Release of IL-12 (A) and IL-6 (B): comparison between C57BL/6 WT and C57BL/6 TLR2 ^{-/-} , TLR4 ^{-/-} , TLR2/4 ^{-/-} macrophages 24 h after co-incubation with <i>Acanthamoeba</i> trophozoites.....	121
Fig 4.6 Release of IL-12 (A) and IL-6 (B): comparison between C57BL/6 WT and C57BL/6 PAR ₂ ^{-/-} macrophages at 24 h after co-incubation with <i>Acanthamoeba</i> trophozoites.....	124
Fig 4.7 IL-12 (A), and IL-6 (B) production by murine macrophages after 24 h pre-treatment with the PAR ₁ antagonist RWJ 56110.....	127
Fig 5.1 Macrophage Activation.....	138
Fig 5.2 Arginase activity (A) and NO ₂ ⁻ concentration (B) at 24 h after infection.....	143
Fig 5.3 Arginase activity by murine macrophages at 24 h, either pre-treated or not pre-treated with either anti IgG TLR2 antibody (A), or anti IgG TLR4 antibody (B).....	145
Fig 5.4 <i>Acanthamoeba</i> -induced murine macrophage arginase activity at 24 h pre-treated or not pre-treated with anti IgG TLR2 antibody.....	147
Fig 5.5 LPS-induced NO ₂ ⁻ production by macrophages following pre-incubation with, or without, <i>Acanthamoeba</i> trophozoites (A), or amoeba-derived conditioned medium (B).....	149
Fig 5.6 Flavohemoglobin protein sequence multi-alignment across several organisms and comparison with <i>A. castellanii</i> FlaHb predicted protein sequence.....	151
Fig 6.1 Characterization of amoeba-derived conditioned medium.....	167
Fig 6.2 Fold change differences of metabolites in amoeba-derived conditioned medium.....	168

Fig 6.3 Characterization of whole stimulated-macrophages metabolome.....	174
Fig 6.4 Characterization of the metabolome of the spent medium from stimulated macrophage cultures.....	175
Fig 6.5 Schematic representation of the amino acid metabolism detected by LC/MS.....	176
Fig 6.6 Schematic representation of the carbohydrate metabolism detected by LC/MS.....	177
Fig 7.1 Schematic summary of the results.....	193

List of tables

Table 2.1 ELISA antibody and second reagents applied concentrations.....65

Table 2.2 Urea standard curve dilution patterns.....66

Abbreviation

ACAID, anterior chamber associated immune deviation

ADP, adenosine diphosphate

AIDS, acquired immune deficiency syndrome

AK, *Acanthamoeba* keratitis

AMP, adenosine monophosphate

AMPs, antimicrobial peptides

AP, activator protein

APC, antigen-presenting cell

Arg 1, arginase 1

ATP, adenosine triphosphate

BBB, blood-brain barrier

BMD, bone marrow derived

BSC, biological safety cabinet

BV-2, mouse microglia cell line

C12MDP, dicloromethylene diphosphonate

CD4, cluster of differentiation

CLs, contact lens

CMP, cytidine monophosphate

CNS, central nervous system

cPLA_{2 α} , cytosolic phospholipase A₂ alpha

CTP, cytidine triphosphate

CXCL, chemokine ligand

DALK, deep anterior lamellar keratoplasty

DC, dendritic cell

dCTP, deoxycytidine triphosphate

DF3, diagnostic fragment 3

DMEM, Dulbecco's modified eagle medium

DNA, deoxyribonucleic acid

ELISA, linked immuno sorbent-assay

EMC, extracellular matrix components

ESI, electrospray ionization

FCS, foetal calf serum

Fhs-24, small intestinal epithelial

FLA, free living amoeba

FlaHb, flavohemoglobins

FPLC, fast protein liquid chromatography

GAE, granulomatous amoebic encephalitis

GC, glucocorticoids

GIPLs, glycoinositolphospholipids

GPI, glycosylphosphatidylinositol

GPs, glyco-proteines

hBD, β -defensine

HBMEC, human brain microvascular endothelial cells

HCE, human corneal epithelial

HCORN, Chinese hamster corneal epithelial cells

HIV, *human immunodeficiency virus*

HLA-DR, human leucocyte antigen-determinant receptor

HPLC, high-performance liquid chromatography

HSV, *Herpes simplex virus*

HUCLs, human telomerase-immortalized corneal epithelial cells

ID-3, inhibitor of differentiation-3

IDO, indole amine 2,3-dioxygenase

IFN, interferon

Ig, immunoglobuline

IL, interleukin

iNOS, inducible nitric oxide synthase

IRF, interferon regulator factor

KYNU, kynureninase

LASIK, laser-assisted *in situ keratomileusis*

LC/MS, liquid chromatography/mass spectrometry

LEAP, liver-expressed antimicrobial peptide

LPA, lipoprotein A

LPG, lipophosphoglycans

LPS, Lipopolysaccharide

Ly6C, lymphocyte antigen 6C

MAPK, mitogen-activated protein kinases

MBP, mannose binding protein

MCP, monocyte chemoattractant protein

MHC, major histocompatibility complex

MIP, macrophage inflammatory protein

MIP-133, mannose-induced, cytotoxic serine protease of 133 kDa

MMP, metallo-proteases

mRNA, messenger ribonucleic acid

MyD88, myeloid differentiation primary response gene 88

NAD, nicotinamide adenine di nucleotide

Nfkbiz, NF- κ B inhibitor Z

NF- κ B, nuclear factor kappa-light chain-enhancer of activated B cells

NHS, normal human serum

NMS, normal mouse serum

NO, nitric oxide

NO₂⁻, nitrite

P₂Y, purinergic receptor

PAM, primary amoebic meningoencephalitis

PAM3CSK4, tripalmitoylated lipopeptide

PAMPs, pathogens associated molecular patterns

PAR, Proteases Activated Receptor

PCR, polymerase chain reaction

PHMB, polyhexamethylene biguanide

PK, penetrating keratoplasty

PMSF, phenylmethanesulfonyl fluoride

POLY I:C, polyinosinic:polycytidylic acid

PPP, pentose phosphate pathway

PYG, peptone-yeast-glucose

rDNA, ribosomal

RFLP, restriction fragment length polymorphisms

RGS, regulator of G-protein signalling

Sbno2, strawberry notch homologue 2

SDS-PAGE, sodium dodecyl sulphate-polyacrylamide gel electrophoresis

s.e.m. standard error of the means

SEM, scanning electronic microscopy

SOCS, suppressor of cytokine signalling proteins

STAT, signal transducer and activator of transcription

TCA, tricarboxylic acid

TCR, T cell receptor

TEM, transmission electron microscopy

TGF, transforming growth factor

T_H, T helper

TIR, Toll-IL-1 receptor

TIRAP/MAL, MyD88 adapter-like

TLR, Toll Like Receptor

TNF, tumor necrosis factor

TRAM, TRIF-related adaptor molecule

TRIF, TIR-domain-containing adapter-inducing interferon β

CHAPTER 1

Introduction

1.1 Free Living Amoebae

Free Living Amoebae (FLA) are ubiquitous unicellular aerobic microorganisms, that normally have a free living mode of life and thus do not rely on finding or invading a host to survive or perpetuate their life cycle. Despite this, some FLA can also act as facultative pathogens, causing serious and deadly diseases in humans and animals. *Acanthamoeba*, *Balamuthia*, *Naegleria* and *Sappinia* are the major genera of FLA responsible for clinical diseases. However, other genera, such as *Hartmannella*, *Paravahlkampfia* and *Vahlkampfia* have also been found to cause disease in humans (Lorenzo-Morales *et al.*, 2007; Visvesvara *et al.*, 2009; Arnalich-Montiel *et al.*, 2013). Some of these amoebae are considered opportunistic due to causing disease in immune compromised individuals, whereas others can cause disease in apparently healthy individuals (Visvesvara *et al.*, 2007). According to taxonomy, both *Acanthamoeba* and *Balamuthia* belong to the Amoebozoa: Acanthamoebidae super-group; *Naegleria* is included in the super-group Excavata: Heterolobosia: Vahlkampfiidae, whereas *Sappinia* is included within the Amoebozoa: Flabellinea: Thecamoebidae. Within the *Naegleria* genus, *Naegleria fowleri* is the only pathogenic species and it is the most insidious among FLA, being the causative agent of an acute, non-opportunistic, primary amoebic meningoencephalitis (PAM). This disease is generally deadly especially for young individuals (Visvesvara *et al.*, 2007). *Acanthamoeba* spp and *Balamuthia mandrillaris* have been associated with skin, and lung infections as well as with fatal granulomatous encephalitis mainly in immune-compromised conditions (Visvesvara *et al.*, 2007).

In contrast with other genera, several species of *Acanthamoeba* have been reported as pathogens of humans and unlike other amoebae are facultative parasites capable of causing a non-opportunistic, potentially blinding eye infection (Visvesvara, *et al.*, 2007). Notwithstanding this, they are also opportunistic

pathogens capable of causing granulomatous amoebic encephalitis (Visvesvara, *et al.*, 2007). These adaptable amoebae and their occasional interactions with the mammalian host comprise the subject of this thesis.

1.2 *Acanthamoeba*, a free living amoeba

1.2.1 History

Acanthamoeba was first described by Castellani in 1930 in Oxford as a contaminant of a *Cryptococcus pararoseus* culture (Castellani, 1930). He named it *Hartmanella castellanii*, believing it to be a member of the *Hartmanella* genus. However, it was later reclassified as *Acanthamoeba castellanii* (Martinez & Visvesvara, 1997).

1.2.2 Life cycle

Acanthamoeba has two life-cycle stages: the active feeding and dividing trophozoite, and the dormant and resistant cyst. Trophozoite size varies from 25 µm to 40 µm among the different species. Their plasma membrane is composed of proteins, phospholipids, fatty acids, sterols, glycolipids and lipophosphoglycans. Their cytoplasm presents the characteristic eukaryotic structures: the nucleus with a prominent central nucleolus and organelles such as several mitochondria, small digestive vacuoles, Golgi complex, smooth and rough endoplasmic reticula (Siddiqui & Khan, 2012). In addition to the common eukaryotic characteristics mentioned, *Acanthamoeba* also possess a contractile vacuole that regulates cell osmolarity. The cytoskeleton is an essential structure for *Acanthamoeba* motility, division and feeding. Trophozoites can move at 0.8 µm/sec and their movements are characterized by the formation of long spine-like plasma membrane extensions, called acanthopodia (Siddiqui & Khan, 2012). *Acanthamoeba* trophozoites feed on

bacteria, algae and yeast facilitated by capture through acanthopodia, formation of a food cup, phagocytosis or pinocytosis. Trophozoite division occurs by binary fission (Marciano-Cabral & Cabral, 2003).

Acanthamoeba cysts have a characteristic double wall structure, and their size varies from 5 μm to 20 μm . Specifically, the double wall consists of an outer layer (ectocyst) and an inner layer (endocyst). The ectocyst shows an irregular wrinkled surface mainly composed of proteins and lipids, whereas the endocyst, is mainly composed of cellulose and can have different forms (rounded, squared, polygonal, stellate) depending on the species. The two walls are usually separated by an intermediate space with occasional points of contact. Pores, known as ostioles, are localized at these junction points between the two walls and they are covered by an operculum. These structures are used by trophozoites as points of egress from the cyst during the excystment process (Siddiqui & Khan, 2012; Martinez & Visvesvara, 1997).

Acanthamoeba exist either as the cyst or the trophozoite form dependent upon the environmental conditions. Under harsh conditions, such as lack of food, hyper- or hypo- osmolarity, extreme temperature and pH, trophozoites transform into cysts. When the external conditions become favorable, the trophozoite emerges from the cyst, leaving behind the empty shell. The ability to encyst and survive hostile environments has undoubtedly contributed to the success of *Acanthamoeba* in diverse environments (Fig 1.1).

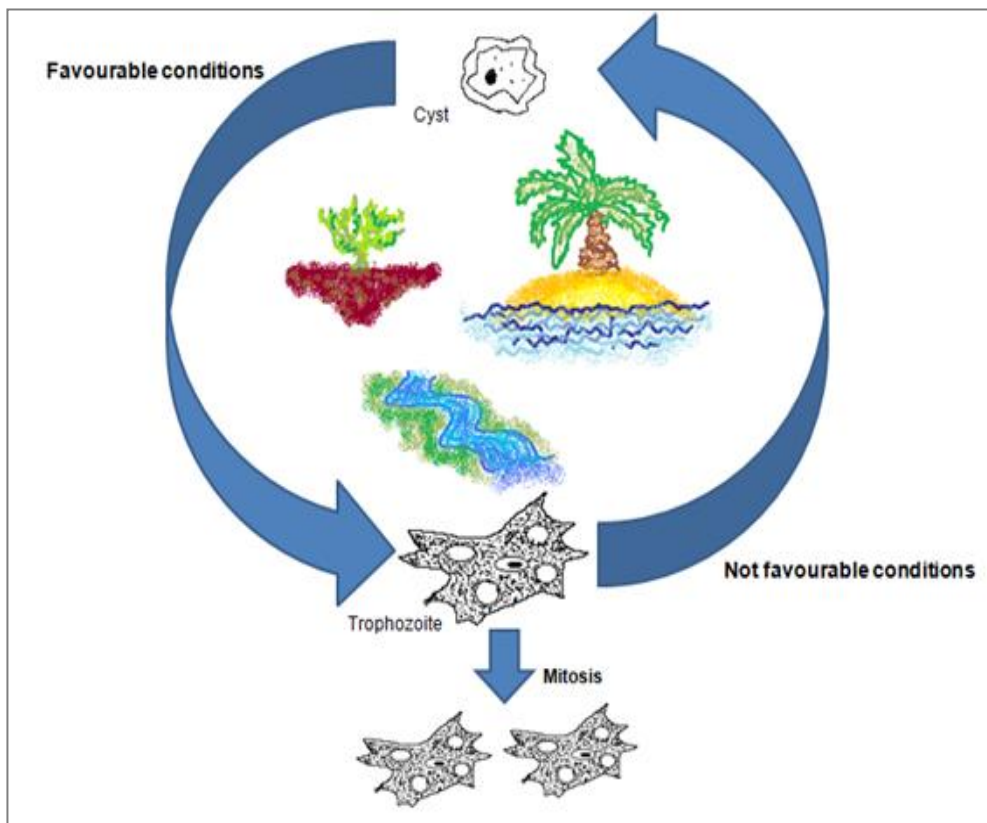


Fig 1.1 *Acanthamoeba* life-cycle. *Acanthamoeba* is ubiquitous in nature. It has been isolated from soil, sea-water, hot springs, rivers and lakes. It can exist in the environment as a dormant and resistant cyst or as the active feeding active dividing form, the trophozoite. Harsh conditions induce the trophozoite to turn into a cyst; however when the external conditions are again favourable, the trophozoite exits from the cyst.

1.2.3 Distribution

Acanthamoeba is ubiquitous in nature and found worldwide. It has been isolated from soil, seawater, lake and river water, hot springs (Reyes-Batlle *et al.*, 2014; Kao *et al.*, 2013); as well as from domestic tap water, swimming pools, bottle water, air conditioning units, contact lenses and their cases (Tanveer *et al.*, 2013; Astorga *et al.*, 2011; Gianinazzi *et al.*, 2009). It has also been recovered from hospitals, dialysis units, surgical instruments and from clinical samples as nasal and pharyngeal swabs; lungs, skin and corneal biopsies, cerebrospinal fluid and brain necropsies (Lasjerdi *et al.*, 2011; Gatti *et al.*, 2010; Yagi *et al.*, 2007; Petry *et al.*, 2006) (Khan, 2006). *Acanthamoeba* spp. have been isolated from all continents.

1.2.4 Classification

Classification of the genus *Acanthamoeba* was historically based on the morphology of the cysts (Pussard & Pons, 1977). According to the size of the cysts and the shape of the ecto and endocysts, *Acanthamoeba* species were divided into 3 morphological groups. Group I includes species characterized by larger trophozoites and cysts (diameter from 16 to 30 μm): *Acanthamoeba astronyxis*, *Acanthamoeba comandoni*, *Acanthamoeba echinulata*, *Acanthamoeba tubiashi*. Species belonging to Group II have cysts with a diameter of $\leq 18 \mu\text{m}$. This group includes 10 different species of *Acanthamoeba*, the most commonly found and wide spread: *A. castellanii*, *Acanthamoeba polyphaga*, *Acanthamoeba rhyodes*, *Acanthamoeba griffini*, *Acanthamoeba hatchetti*, *Acanthamoeba triangularis*, *Acanthamoeba divionensis*, *Acanthamoeba paradivionensis*, *Acanthamoeba mauritaniensis*, *Acanthamoeba lugdunensis*, and *Acanthamoeba quina*. Group III includes species characterized by cysts of $\leq 18 \mu\text{m}$ in diameter. *Acanthamoeba culbertsoni*, *Acanthamoeba palestinensis*, *Acanthamoeba pustulosa*, *Acanthamoeba royreba*,

and *Acanthamoeba lenticulata* belong to Group III (Visvesvara, 1991; Visvesvara *et al.*, 2007) (Fig 1.2-A). Preliminary identification of the genus *Acanthamoeba* based on morphology is still accepted, given the characteristic and unique trophozoite and cyst structures. However, the classification, among *Acanthamoeba* species, based on these criteria, shows several obstacles as cyst morphology can change depending on the culture conditions (Stratford & Griffiths, 1978; Marciano-Cabral & Cabral, 2003).

Further classifications of these organisms have been based on their immunogenic or isoenzyme profile (Costas & Griffiths, 1985; Moura *et al.*, 1992) or on the analysis of the DNA mitochondrial restriction fragment length polymorphisms (RFLP) (Bogler *et al.*, 1983; Gautom *et al.*, 1994; Kong *et al.*, 2002). However, none of these criteria could be considered as ideal tools to discriminate *Acanthamoeba* species. Indeed, different species of *Acanthamoeba* present the same antigen profile; furthermore the analysis of the *Acanthamoeba* isoenzyme patterns shows similarities within strains of different species or differences among the strains of the same species (Marciano-Cabral & Cabral, 2003). Enzymatic activity also can change depending on the external conditions (Weekers & De Jonckheere, 1997). Although RFLP analysis was considered a consistent tool for *Acanthamoeba* isolate classification, it required a consistently high number of trophozoites for the extraction of the DNA, a potential limitation for fresh environmental or clinical samples (Marciano-Cabral & Cabral, 2003).

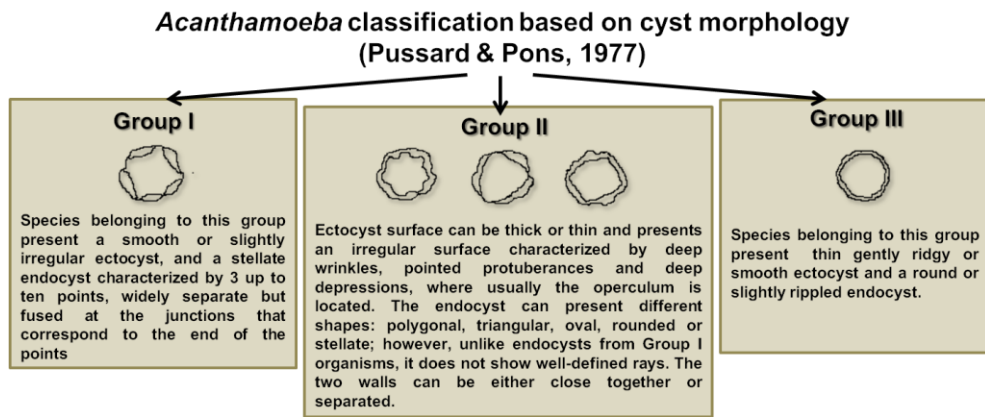
Current methods rely on the sequencing the ASA-S1 region of the small subunit ribosomal RNA gene (18S rDNA) which is highly specific for *Acanthamoeba* genus. A small portion of this region, called diagnostic fragment 3 (DF3) shows high variance (5%) (Schroeder *et al.*, 2001; Gast *et al.*, 1996; Stothard *et al.*, 1998), and has allowed the identification and classification of 19 different genotypes (T1-T19)

within the *Acanthamoeba* genus (Magnet *et al.*, 2014). As this method is based on PCR, *Acanthamoeba* can now be identified and classified with confidence, even starting from a small cell quantity (Fig 1.2-B).

Genotyping *Acanthamoeba* allowed researchers to determine the pathogenicity, environmental and world distribution and host preferences of each genotype. *Acanthamoeba* T4 was found to be the most widely distributed in the environment and the major genotype associated with Acanthamoebic diseases. T2, T3, T5, T6, T10, T11, T12, T15 and T18, also have been associated with human diseases and therefore, recognized as pathogenic. T4 is the most common genotype isolated from indoor environments and this might explain the majority of clinical cases are caused by T4, followed by the phylogenetically close T3 and T11 genotypes (Magnet *et al.*, 2014, Maciver *et al.*, 2013) (Fig 1.2-C).

Fig 1.2 *Acanthamoeba* classification. The first classification in 1977, was based on the cyst morphology: in particular based on cyst size and on the different endocyst shape, *Acanthamoeba* species were divided into three distinct groups (A). In 2001, the new classification method based on 18S Ribosomal DNA, allowed the identification of 19 different genotypes. JDP1, JDP2 are the primers used to amplify the diagnostic fragment DF3 (B). Classification in genotypes can also be supplemented by the first classification suggested by Pussard and Pons in 1977, finding relationship between more closely related genotypes, T4-T3-T11 for example, and associating them to the morphological group (Fuerst, 2014). Furthermore, sequencing *Acanthamoeba* isolates allowed to obtain more information regarding the preferential environmental distribution and different rates of pathogenicity (C).

A



B

**Acanthamoeba genotypic classification based on 18S Ribosomal DNA
(Schroeder et al. 2001)**



C

Specie Name	Genotype	Morphology Group	Isolation
<i>A. hatchetti</i>	T11	II	AK
<i>A. griffinii</i>	T3	II	AK
<i>A. castellanii</i> <i>A. polyphaga</i> <i>A. culbertsoni</i>	T4	II	GAE/AK/Cutaneous Acanthamoebiasis
<i>A. culbertsoni</i>	T10	III	GAE/AK
<i>A. lenticulata</i>	T5	III	AK
<i>A. palestiniensis</i>	T6	III	AK
<i>A. palestiniensis</i>	T2	III	GAE
<i>A. healyi</i>	T12	III	GAE
<i>Acanthamoeba spp.</i>	T14	III	?
<i>A. byersi</i>	T18	I	GAE
<i>A. astronixis</i>	T7	I	Environment
<i>A. tubiashi</i>	T8	I	Environment
<i>A. comandoni</i>	T9	I	Environment
<i>Acanthamoeba spp.</i>	T17	I	Environment
<i>Acanthamoeba spp.</i>	T16	?	Rare isolation (Environm)
<i>Acanthamoeba spp.</i>	T13	?	Rare isolation (Environm)
<i>A. jacobsi</i>	T15	?	AK

1.3 *Acanthamoeba*, a potential pathogen for humans

1.3.1 History

The pathogenic potential of *Acanthamoeba* was first suggested by Culbertson (Culbertson *et al.*, 1958; Culbertson *et al.*, 1959). At that time, the company Eli Lilly Laboratories from Indianapolis was producing a polio vaccine and its efficacy and safety was tested *in vitro* using monkey kidney cell cultures. While performing these trials an unknown contamination was observed in the cell culture treated with the vaccine. Initially it was thought to be due to a virus, however further investigations were thankfully carried out by Culbertson and his collaborators. They inoculated cortisone treated mice and monkeys with unprocessed contaminated culture fluids. These animals developed illness and subsequently died. *Post-mortem*, investigation of the brain tissues showed the presence of atypical cells that were causing the infection. *In vitro*, microscopic analysis of the culture fluids demonstrated the presence of amoebae, identified as *Acanthamoeba* spp. Lilly A-1 strain. Culbertson included these amoebae into the *Hartmanella-Acanthamoeba* group (H-A amoebae). For demonstrating the pathogenic potential of this *Acanthamoeba* spp. Lilly A-1 strain was then named after Dr. Clyde G. Culbertson, as *Acanthamoeba culbertsoni*.

Over the years, cases of encephalitis in humans due to FLA were reported; many of them erroneously attributed to *Acanthamoeba*, and actually caused by other FLA such as *Naegleria* and *Balamuthia*. The first confirmed amoebic encephalitis cases caused by *Acanthamoeba* were reported in a patient with Hodgkin's disease (Jager & Stamm, 1927) and in a 58-year old man, who had been in contact with contaminated water 2 weeks prior to the manifestation of the symptoms. The differences between encephalitis caused by either *Naegleria* or *Acanthamoeba* were

first described in a clinical report (Robert & Rorke, 1973). Martinez, in 1980, first used the term granulomatous amoebic encephalitis (GAE) to describe infection of the central nervous system (CNS) caused by *Acanthamoeba* and to discriminate it from PAM caused by *Naegleria* (Martinez, 1980) (Martinez & Visvesvara, 1997).

In the early 1970s, several cases of *Acanthamoeba* infections, within the brain, eye (Jones *et al.*, 1975; Nagington *et al.*, 1974) and skin (Gullett *et al.*, 1979), were reported in humans. *Acanthamoeba* was thus established as a causative agent of disease in humans (Marciano-Cabral & Cabral, 2003).

1.3.2 *Acanthamoeba* diseases

It is now known that *Acanthamoeba* can act as an opportunistic as well as a non-opportunistic pathogen. In immune-compromised patients, who are particularly susceptible, it causes a fatal infection of the central nervous system, GAE, but also lesions within the skin, lungs and bones. In immune competent individuals *Acanthamoeba* is the agent of a painful, progressive sight-threatening corneal infection, termed *Acanthamoeba* keratitis (AK).

1.3.2.1 Granulomatous amoebic encephalitis

GAE is a fatal disease, characterized by an intense and progressive chronic inflammation of the CNS. Individuals with pre-existing clinical conditions such as tumors, systemic lupus erythematosus, diabetes, renal failure, cirrhosis, tuberculosis, skin ulcers, human immunodeficiency virus (HIV) infection or Hodgkin's disease are more susceptible to GAE than others (Castillo *et al.*, 2012; Maritschnegg *et al.* 2011; Pietrucha-Dilanchian *et al.*, 2012; Seijo Martinez *et al.* 2000). Other risk factors, associated with this disease, are alcohol and drug abuse, steroid treatment, cancer chemotherapy, radiotherapy and organ transplantation (Cabral & Marciano-Cabral, 2004; Satlin *et al.*, 2013; Akpek *et al.* 2011; Fung *et al.*,

2008). Recently, GAE has been also reported in apparently healthy individuals (Webster *et al.* 2012; Binesh *et al.* 2011, Reddy *et al.* 2011; Lackner *et al.* 2010; Marciano-Cabral & Cabral, 2003).

GAE is a rare disease with only approximately 150 cases confirmed world-wide. It is easily misdiagnosed by clinicians and, therefore, most frequently diagnosed post-mortem, when autopsy is permitted. For all these reasons, the epidemiological data may represent just a small portion of the actual number of GAE cases (Trabelsi *et al.*, 2012; Webster *et al.*, 2012).

Individuals may develop GAE, after contact with contaminated water or soil, or through exposed skin lesions. In some cases, GAE patients have a history of chronic sinusitis, rhinitis or pneumonia (Akpek *et al.*, 2011), suggesting that *Acanthamoeba* can reach the CNS through three main “portals of entry”: skin lesions, the respiratory tract and the olfactory neuroepithelium. From skin lesions or the respiratory tract, *Acanthamoeba* dissemination occurs through the bloodstream, whereas from the olfactory neuroepithelium, *Acanthamoeba* reaches the CNS, migrating along the nerves and invading the olfactory bulb (Khan, 2008).

Within the 19 *Acanthamoeba* genotypes, T4 is the most commonly isolated from cases of GAE, followed by T1, T10 and T12 (Booton *et al.*, 2005). The first cases of GAE caused by T2 (Walochnik *et al.*, 2008) and T5 (Lackner *et al.*, 2010), previously known as AK causative agents, were described in Austria. Recently a new pathogenic *Acanthamoeba*, belonging to genotype T18 has been isolated from the skin and the brain of a fatal case of GAE (Qvarnstrom *et al.*, 2013).

Clinical symptoms of GAE are headache, dizziness, confusion, lethargy, nausea, seizures, neurological deficit and increased cranial pressure. Patients might present cutaneous infections or pneumonia for months; GAE is the final step of this

escalation of disease manifestations at which time treatment is unlikely to be successful. Diagnosis antemortem is rare and difficult due to similarities in the symptoms with other viral, bacterial, fungal and protozoan infections. Radiological studies, examination of the cerebrospinal fluid, tissue samples and blood samples are useful tools for the diagnosis of GAE. Post-mortem analysis of brain tissue, presents hemorrhagic necrosis and edema. The presence of granulomas composed of immune cells, such as CD4, CD8, T-lymphocytes, B-lymphocytes and macrophages, is an important patho-histological feature in GAE, although these might be absent in severely immune-compromised individuals (Akpek *et al.*, 2011).

There is no established effective drug treatment for GAE and consequently therapy usually consists of a wide range of aggressive antifungal, antibacterial, and anti-protozoan drugs in combinations given intravenously for long periods. Miltefosine, an alkyphosphocholine normally used for treating visceral leishmaniasis has been successfully used in combination with other drugs for the treatment of GAE and is now considered a fundamental drug to include in the treatment regime of *Acanthamoeba* CNS infections (Schuster *et al.*, 2006; Aichelburg *et al.*, 2008). The case of GAE in a 2 years old boy with acute lymphoblastic leukemia, reported in Austria, had a positive outcome, after treatment with a combination of trimethoprim-sulfamethoxazole, fluconazole, pentamidine and miltefosine in combination with hyperbaric oxygen therapy (Maritschnegg *et al.*, 2011). Over the years, other successful treatments of GAE with multi-drug therapy have been reported (Walochnik *et al.*, 2008). However, the consequences of the harsh treatments, or of the surgical approaches sometimes also employed have resulted in neurological damage and loss of vision (Fung *et al.*, 2008; Lackner *et al.*, 2010; Seijo Martinez *et al.*, 2010; Aichelburg *et al.*, 2008). In some cases, patients treated successfully for GAE have died from the pre-existing diseases (Gupta *et al.*, 2008).

1.3.2.2 Cutaneous acanthamoebiasis

Acanthamoeba diseases involving skin, lungs, bones and sinuses are extremely rare. In 1976 and 1979 the first disseminated granulomatous acanthamoebic infections were described (Ringsted *et al.*, 1976; Gullett *et al.*, 1979). For a long time these diseases were mainly associated with acquired immunodeficiency syndrome (AIDS) (Gonzalez *et al.*, 1986; Nachega *et al.*, 2005; Torno *et al.*, 2000; Kim *et al.*, 2000; Selby *et al.*, 1998). In the early 1990s, infections were noted in renal and lung transplant individuals and the first successful treatments of disseminated disease achieved (Slater *et al.*, 1994; Oliva *et al.*, 1999). So far, cases of disseminated *Acanthamoeba* infections have been described in individuals following lung (Afshar *et al.*, 2013; Walia *et al.*, 2007; Duarte *et al.*, 2006), renal (Mutreja *et al.*, 2007; Steinberg *et al.*, 2002), liver (Young *et al.*, 2010), hematopoietic stem cell (Kaul *et al.*, 2008) and heart transplant (Barete *et al.*, 2007) patients. In these cases infection was noted in the skin, lungs, bones and pancreas.

Cutaneous acanthamoebiasis, lung infections and sinusitis, should be considered as risk factors for the potential development of fatal GAE. These acanthamoebic infections, if diagnosed in time before escalation into the CNS, can be treated and the mortality rate is 75% compared with the almost 100% mortality in those with CNS involvement (Torno *et al.*, 2000). Osteomyelitis caused by *Acanthamoeba* can occur through the hematopoietic stream or more likely from the extension of the local cutaneous infection (Steinberg *et al.*, 2002).

A definitive therapeutic regime for disseminated *Acanthamoeba* infection, as a consequence of cutaneous infection has not been developed. However, successful treatment of a lung transplant patient that developed cutaneous acanthamoebiasis was achieved with a combination of amphotericin B and voriconazole (Walia *et al.*, 2007). However, the combination of oral miltefosine and voriconazole did not have

a positive outcome in a hematopoietic stem cell transplanted patient with disseminated acanthamoebic infection (Kaul *et al.*, 2008). Pentamidine in combination with 5-fluorocytosine, itraconazole, as well as topical application of chlorhexidine gluconate and fluconazole achieved cure in a lung transplant patient (Oliva *et al.*, 1999). The combination of surgical approaches and high doses of amphotericin-B and 5-fluorocytosine was shown to be effective in a case of rhinosinusitis in an AIDS patient (Nachegea *et al.*, 2005).

1.3.2.3 *Acanthamoeba* Keratitis

AK is a rare, severe, potentially blinding, non opportunistic infection of the eye caused by *Acanthamoeba* spp. The disease primarily affects the corneal epithelium, but the infection can progress into the deeper layers of the eye and, if not promptly diagnosed, can lead to partial or complete loss of vision. AK occurs in immune-competent individuals and it is mainly associated with use of contact lens (CLs). CLs can cause micro corneal trauma predisposing the eye to infection. Inappropriate use, maintenance and cleaning of CLs can result in their contamination with *Acanthamoeba* and facilitate transmission to the eye. It has been demonstrated that trophozoites and cysts can bind to both soft and rigid CLs (John *et al.*, 1989; Kilvington, 1993; Sharma *et al.*, 1995). Furthermore a lower concentration of chemokines, cytokines and other pro-inflammatory mediators has been shown in individuals with history of prolonged CL use (Thakur & Willcox, 2000). Consequently these individuals have reduced recruitment and activation of macrophages and neutrophils and as a result impaired innate immune responses in the eye (Thakur & Willcox, 2000). For this reason, it has been suggested that there is a link between innate immune impairment at the ocular surface caused by a prolonged use of CLs, and the possibility of contracting AK (Li & Sun, 2008).

Although the majority of AK cases occur in CLs wearers, 10-15% are reported in non-contact lens wearers. In these cases, infection was subsequent to corneal trauma, either accidental or after laser vision correction surgery (LASIK), or invasive or radial keratoplastia (Lorenzo-Morales *et al.*, 2013).

Since the first AK cases were reported in the US (Jones *et al.*, 1975) and UK (Naginton *et al.*, 1974), a significant increased number of cases have been reported world-wide. Over these years, epidemiological studies have been performed in North America (Yoder *et al.*, 2012; Verani *et al.*, 2009), South America (Cariello *et al.*, 2011), Europe (Radford *et al.*, 2002, Seal 2003, Iovieno *et al.*, 2014; Chawla *et al.*, 2014; Di Cave *et al.*, 2014; Walochnik *et al.*, 2014), Asia (Lalitha *et al.*, 2012; Por *et al.*, 2009), and Australia (Ku *et al.*, 2009) (Fig 1.3). AK cases are concentrated in industrialized, developed countries, probably due to a higher use of soft CLs and of the corrective LASIK surgery; however this disease has also now been reported in developing countries, probably correlated to water sanitation and quality, as well as the occurrence of environmental disasters such as flooding (Ibrahim *et al.*, 2007).

T4 is the predominant genotype found as a causative agent of *Acanthamoeba* ocular infections world-wide. Other genotypes found in AK patients are T3 and T11, which together with T4 are members of 'group II' organisms as originally classified by morphology (Boaton, *et al.*, 2009, Walochnik *et al.*, 2014). Genotype T5 (Iovieno *et al.*, 2010; Ledee *et al.*, 2009; Spanakos *et al.*, 2006) and T6 (Walochnik *et al.*, 2000) have also rarely been isolated from AK patients. T10 genotype and T2, more normally associated with GAE, were also isolated from the eyes of patients in Thailand (Nuprasert *et al.*, 2010), and from the CLs of a French AK patient (Risler *et al.*, 2013). AK caused by genotype T15 was reported in Italy (Di Cave *et al.*, 2009) and in Slovakia (Nagyová *et al.*, 2010). Recently T13 has also been isolated from a

persisting keratitis in a young female, expanding the number of genotypes responsible for causing AK in humans to 9 (Grün *et al.*, 2014).

AK mainly manifests in just one eye; however, cases with the involvement of both eyes (bilateral keratitis) have also been reported (Kim & Kim, 2010). The initial, and less distinctive symptoms are redness, substantial production of tears, photophobia, pain and foreign body sensation in the eye. With the progression of the infection, the severity and the specificity of the symptoms increase: firstly epithelial opacity develops and subsequently keratoneuritis is more evident along with epithelial keratitis. Stromal opacity, focal stromal infiltration and eventually formation of a ring-like infiltrate are the latest symptoms to develop and the one that allows the differential diagnosis of AK (Por *et al.*, 2009).

AK is a challenging disease to diagnose on the basis of the clinical symptoms. Early AK-like symptoms are commonly observed in keratitis caused by viruses, fungi and bacteria. The epithelial opacity, characterized by a pseudodendritic pattern is also seen in the dendritic keratitis caused by *Herpes simplex virus* (HSV). For all these reason AK is frequently misdiagnosed and treated with antiviral or antibacterial drugs that are not effective. This eventually leads to an exacerbation of the disease and the manifestation of the characteristic clinical features (Visvesvara, 2013). The isolation of *Acanthamoeba* from CLs, their cases or solutions is a useful indicator of potential AK, but since this has also been achieved from asymptomatic individuals, it is necessary to confirm infection microscopically from corneal scrapings or biopsies. Molecular techniques help to reinforce the diagnosis based on the microscopic investigation and confocal microscopy has been applied, as a less invasive method of diagnosis (Trabelsi *et al.*, 2012).

The ability of *Acanthamoeba* to encyst as a consequence of the immune response or as a reaction to therapies, constitutes the main obstacle in the treatment of AK. The two binary aims of the treatment in AK are to eradicate trophozoites and cysts from the site of infection and to attenuate the associated inflammatory response. Biguanides, specifically polyhexamethylene biguanide (PHMB) and chlorhexidine, are the most effective drugs against both trophozoites and cysts. These disinfectants have been used successfully alone or in combination with diamines, such as propamidine isethionate or hexamidine. Diamines show both trophozoicidal and cysticidal activity, however effective concentrations are high and preclude their use as monotherapy. Therefore the most applied therapeutic protocol for AK consists in the topical application of a biguanide PHMB 0.02%, or chlorhexidine 0.02%, in combination with either propamidine isethionate 0.1%, or hexamidine 0.1% (Clark *et al.*, 2012). Early intensive administration is applied, in order to avoid the formation of mature cysts. It consists of a high frequency drop administration, every hour, day and night, for 48 hrs and then every hour, during the day, for the following 72 hr. In order to avoid complications, the frequency of administration is then lowered for the following weeks and then modified as appropriate for the specific case. Topical or systemic administration of azoles, such as itraconazole, cotrimaxole, miconazole, voriconazole, in association with the biguanide/diamine therapy have been shown effective especially in the most difficult cases (Clark *et al.*, 2012). Steroid use is considered controversial in AK although they have been used to attenuate the pain and inflammation especially after surgery. When the corneal epithelium is highly scarred, or if infections are recurrent drug therapy is combined with surgery. Penetrating keratoplasty (PK) has been successfully applied, after drug therapy, when there was not an ongoing or latent infection. In refractive AK, deep anterior lamellar keratoplasty (DALK) has also been used. Lately, laser phototherapeutic keratectomy has been performed to remove thickness in the

stroma (Clark *et al.*, 2012). The positive prognosis of AK closely depends on a prompt diagnosis and effective treatment (Dart *et al.*, 2009).

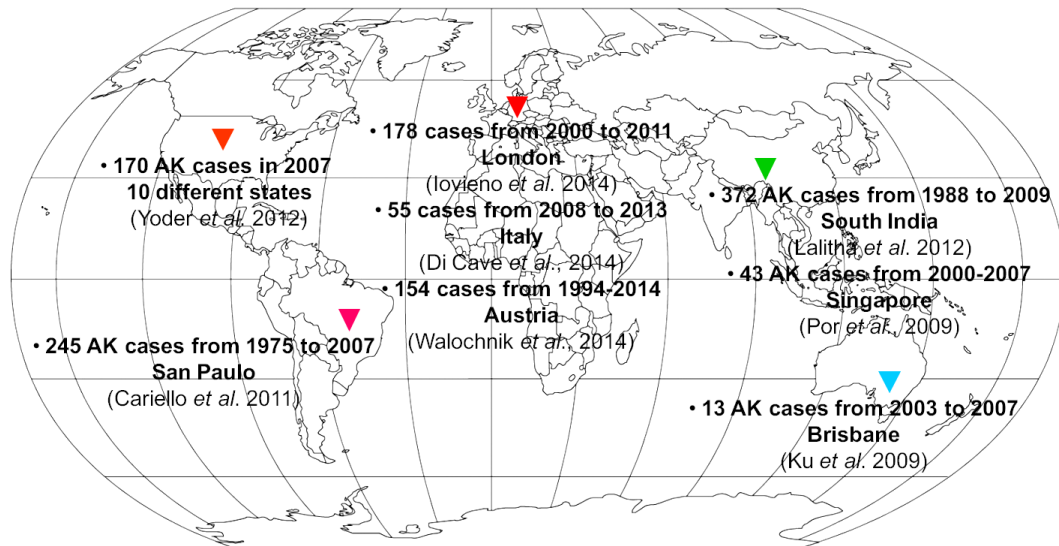


Fig 1.3 AK epidemiological studies reported world-wide. Through the analysing of AK cases, registered by ophthalmologist over a period of years, a series of epidemiological studies could be reported, and the incident of AK could be evaluated in specific countries. The majority of these studies presented AK outbreaks during specific years, months or seasons. The incidence of AK in CLs wearers or non-CLs wearers was also indicated as well as the outcome of the infection. AK incidence generally appears to be very low, however these studies are not providing the full picture and the real incidence of the disease across the globe.

1.3.3 *Acanthamoeba* virulence factors

The potential pathogenicity of *Acanthamoeba* in humans depends on several factors. Genotype T4, as has been already mentioned, is the most frequent genotype isolated from outdoor and indoor environments, along with T3, T11, and T5 as well as T7, T8, and T9 that are specifically found in soil and water. Nevertheless, T4 has been recognized as the most virulent genotype and the main causative agent of AK and non-AK diseases. Environmental distribution is, therefore, an important factor, but not the only one responsible for over-representation of certain genotypes associated with disease. For this reason, many studies have been performed in order to characterize the differences between pathogenic and non-pathogenic *Acanthamoeba*.

Acanthamoeba resistance and growth rate under extreme physical (temperature, pH, osmolarity) and chemical (drugs, disinfectants) conditions, as well as the expression of extracellular molecules and induced-cell cytotoxicity are the main parameters used to discriminate between pathogenic and non pathogenic *Acanthamoeba* isolates (Griffin, 1972; Cursons & Brown, 1978; De Jonckheere, 1980; Khan *et al.*, 2002).

Acanthamoeba grows at the optimal temperature of 25°C, but thermo tolerance has been observed in some clinical isolates, obtained from infected cornea and brain samples and these have been found to proliferate optimally at higher temperatures (Walochnik *et al.*, 2000). The high growth rate at temperatures between 30 and 42 degrees is considered an important virulence factor, associated with resistance, viability and ability to proliferate in the sites of infection. However, some non-pathogenic strains have been observed to tolerate increased temperature (Nagyová *et al.*, 2010). The ability of trophozoites to survive in hyper-osmolar conditions has

been used to discriminate between virulent and non-virulent isolates of *Acanthamoeba*. Resistance to hypertonic conditions can be important in AK development. Indeed it is known that contact lenses can increase some of the tear film components or induce evaporation, thus changing the tear film osmolarity (Mann & Tighe, 2013).

Both pathogenic and non-pathogenic strains release extracellular proteases. Using colorimetric and zymography techniques, a higher protease production in clinical, than in environmental isolates of *Acanthamoeba* has been observed (Khan *et al.*, 2000). Enzymes involved in cell growth, differentiation mechanisms and host-pathogen interactions, such as peroxidases, superoxide dismutase, and ecto-ATPases, have been found in *Acanthamoeba* and correlated to its virulence. An *In vivo* study has reported higher peroxidase and lower superoxidase activities in a virulent isolate of *Acanthamoeba* (Hadas & Mazur, 1993). Adenosine triphosphate (ATP) and its hydrolysis products are involved in several cellular biological processes. Ecto-ATPases are enzymes, expressed on the cell surface, that catalyse ATP hydrolysis. An *in vitro* study has demonstrated differences in their expression between clinical and non-clinical isolates of *Acanthamoeba*. Trophozoite lysate analysed by electrophoretic techniques showed that both types of isolates express ATP-ases; however, the clinical isolates showed a different pattern of expression and this discrepancy was also observed between GAE and AK isolates (Sissons *et al.*, 2004).

Acanthamoeba pathogenic potential is also related to the ability to induce cytotoxicity in mammalian cells. Indeed, it has been demonstrated, in several *in vivo* and *in vitro* studies, that *Acanthamoeba* induces cytopathic effects both through the release of toxic molecules or through phagocytosis (Kinnear, 2003). Images of an experimental acanthamoebic infection *in vitro*, obtained using transmission electron

microscopy (TEM), showed trophozoites to be able to phagocytose whole corneal epithelial cells as well as cell debris (Omaña-Molina *et al.*, 2013). Phagocytosis, in the site of infection has a dual function: first the progression and dissemination within the host's tissues and second the uptake of food (Garner, 1993).

Acanthamoeba spp. produce, and secrete extracellular serine, and cysteine proteases (amoebic secretome), and their role in the pathogenicity process has been widely investigated (Mitro *et al.*, 1994; Alfieri *et al.*, 2000; Sant'ana *et al.* 2014). Serine proteases have been shown to be the major component of the amoebic secretome and several studies achieved the purification and characterization of different amoebic serine proteases, highlighting their importance in the invasion and cytotoxicity processes. A serine protease of 40 kDa from an ocular isolate of *A. castellanii* has been purified and characterized; this protease elicits plasminogen activation factor, potentially starting the biochemical cascade that leads to fibrinogen degradation, and therefore enhancing the invasion of trophozoites within the tissues (Mitra *et al.* 1995). Later, a serine protease of 42 kDa was purified from the conditioned medium of *A. castellanii*, maintained 3 days in peptone-yeast-glucose (PYG) medium culture (Cho *et al.*, 2000). Its maximum activity was detected at pH 8, but decreased below pH 7 and above pH 10. Optimal activity was shown at temperatures between 30° C and 50° C; whereas at 80° C the protease was rapidly inactivated. Moreover this 42 kDa serine protease induced collagen degradation, and after incubation with either corneal epithelial cells and corneal fibroblasts an 86% of cell loss could be observed, microscopically, and through spectrophotometry, within 6 hrs. In the presence of phenylmethanesulfonyl fluoride (PMSF), a serine protease inhibitor, the cytopathic effect was ablated (Cho *et al.*, 2000). *In vitro* and *in vivo* experiments studied the cytopathic effect of a purified serine protease of 12 kDa obtained from the conditioned medium of *A. castellanii*

isolated from a case of keratitis (Na *et al.*, 2001). A secreted serine protease of 33 kDa, was purified and characterized from the conditioned medium of *A. healyi* isolated from a case of GAE. It was shown to be active at an optimal pH of 8 and at 40°C and although there is no reported data about the cytopathic effect, this serine protease degraded a wide range of substrates including collagen, fibronectin, fibrinogen and immunoglobulins (Kong *et al.*, 2000). A 33 kDa serine protease has also been found in ocular and environmental isolates; the enzyme purified from either clinical or environmental isolates elicited different rates of cytotoxicity according to the type and severity of infection caused (Kim *et al.*, 2006). This observation was confirmed by a screening clinical study of AK patients, where the severity of the symptoms observed in these patients was associated with the characteristics of the amoebic secretome. It has been demonstrated that a high diversity and the activity of enzymes of small molecular mass is associated with most severe clinical manifestations (de Souza Carvalho *et al.*, 2011).

Acanthamoeba can elicit cytotoxic effects inducing an increase of the intracellular calcium concentration, as well as morphological and cytoskeleton modifications. These events, characteristic of apoptosis (programmed cell death), along with membrane blebbing, chromatin condensation and chromosomal DNA fragmentation, have been observed in several mammalian cell types after contact with either trophozoites or their soluble molecules or trophozoite lysate (Alizadeh *et al.*, 1994; Shin *et al.*, 2000; Zheng *et al.*, 2004). A low molecular weight, heat resistant molecule secreted by *A. castellanii* has been shown to induce increased intracellular calcium concentration in human epithelial cells. An increase in secretion preceded a trans-membrane influx of extracellular calcium. Subsequent to this event, cell modification, cytoskeleton damage, DNA fragmentation and a decrease in cell viability were observed, suggesting apoptotic processes (Mattana *et al.*,

1997). Later, adenosine diphosphate (ADP) released into the medium by *Acanthamoeba* was shown to be the molecule responsible for the increased cytoplasmic calcium and for the induction of apoptosis both in human epithelial cells and in human monocytes. These events were inhibited by suramine, an inhibitor of the purinergic receptor P₂Y₂, suggesting that the ADP cytotoxic effect is elicited through binding to purinergic receptors expressed on the surface of mammalian cells (Mattana *et al.*, 2001; Mattana *et al.*, 2002). *Acanthamoeba* infections within either the brain or the eye are the result of a serial sequence of pathogenic events where both host and amoebic factors are involved.

1.3.4 GAE pathogenic cascade

The CNS is an inaccessible organ, protected by the blood-brain barrier (BBB) that is constituted of endothelial cells joined by tight junctions. Water, gasses and lipids passively diffuse, whereas glucose and amino acids are actively transported from the blood to the CNS through the BBB. Another important action of the BBB is to prevent the entry of microbes and the diffusion of toxins into the CNS. It has been suggested that *Acanthamoeba* can reach the CNS through the olfactory neuroepithelium, the respiratory track and skin lesions; the last two “portals of entry” are more likely to happen and they allow a faster dissemination of *Acanthamoeba* through haematogenous spread. Once *Acanthamoeba* trophozoites are in the blood-stream, the first and critical step in the pathogenic cascade of GAE is the adhesion of the trophozoites to the BBB endothelial cells. Experiments, performed *in vitro*, investigated the binding of *Acanthamoeba* trophozoites to human brain microvascular endothelial cells (HBMEC). It was shown that trophozoites bind HBMEC, and this binding was prevented by the incubation of trophozoites in α -mannose solution prior to the adhesion assay. These results suggested that *Acanthamoeba* trophozoites bind to BBB endothelial cells through a mannose

binding protein expressed on their surface. Furthermore this binding was observed in a higher percentage in pathogenic rather than in non-pathogenic isolates, highlighting the importance of the adhesion step in the pathogenicity cascade (Alsam *et al.*, 2003).

After binding to the endothelial cells, *Acanthamoeba* can induce BBB structural and functional loss by disruption of the tight junctions (Khan & Siddiqui, 2009), phagocytosis and cytotoxic activity (Alsam *et al.*, 2003; Sissons *et al.*, 2005; Sissons *et al.*, 2004). The basement membrane that lies between the BBB and the brain tissue consists of extracellular matrix components (EMC) such as laminin and collagen IV. Studies have demonstrated the ability of *Acanthamoeba* trophozoites to recognize and bind EMC. The recognition and binding was shown to be mannose, as well as protein-binding dependent (Gordon *et al.*, 1993; Rocha-Azevedo *et al.*, 2009). Through the released of serine proteases and the activation of metallo-proteases, trophozoites can degrade collagen, laminin and fibronectin, progressing their invasion within the deeper matrix layer and eventually the brain (Rocha-Azevedo *et al.*, 2010). Both amoebic cytotoxicity activity and the consequent host immune response within the cerebral tissue play a role in the final steps of the pathogenic cascade that result in GAE development.

1.3.5 AK pathogenic cascade

The pathogenic events involved in the development of AK have been broadly examined both *in vivo* and *in vitro*, as well as analyzing the patho-physiology in patients affected by AK, through histopathological examination. Human cornea consists of 5 different layers: the outer is the corneal epithelium, a thin layer of specialized epithelial cells. The AK pathogenic cascade starts with the adhesion of the trophozoites to the corneal epithelium. *In vitro* experiments, using radiolabeled

trophozoites, evaluated *Acanthamoeba* adhesion to rabbit corneal epithelial cells, in relation to temperature, presence of carbohydrates and different isolates. Pathogenic strains showed higher adherence than non-pathogenic strains at all experimental temperatures: 4° C, 25° C and 37° C. However, the optimal temperature was shown to be 25° C, since at 37° C trophozoites started to detach and encyst. Furthermore, adherence was prevented after pre-incubation of trophozoites with either mannose or methyl- α -D-mannopyranoside (Morton *et al.*, 1991). Therefore, more studies have been subsequently performed in order to study the nature of the structures involved in the amoebic binding to the corneal epithelium. Using an electrophoresis-blot overlay assay, it was demonstrated that an AK isolate of *Acanthamoeba* binds to membrane associated mannose-glycoproteins (GPs) expressed on primary rabbit corneal cells. *Acanthamoeba* trophozoites did not show any preference for the nature of the GPs or the number of the linked mannose residues involved. A putative mannose binding protein of 135 kDa (135 kDa-MBP) was then isolated, through affinity chromatography, from the membrane of trophozoites, and characterized. This protein has been shown to be the main amoebic structure involved in the binding to the mannose-GPs expressed on corneal epithelial cell surface (Yang *et al.*, 1997). More recent investigations on MBP structure and function, reported the isolation and purification of a 400 kDa MBP, consisting of 3 subunits of 130 kDa each. MBP showed an intracellular, a transmembrane and an extracellular domain, presenting similarity to the structure of a transmembrane receptor; furthermore mannose molecules bind to each 130 kDa subunit (Garate *et al.*, 2004; Garate *et al.*, 2005). Expression of MBP in trophozoites of different isolates of *Acanthamoeba* and in cysts has been investigated using polyclonal antibody anti-MBP immunoglobulin (Ig)G; these antibodies were obtained from chickens, using the purified protein. Immunostaining experiments showed a lower expression of MBP in cysts and in non-pathogenic isolates in comparison with

highly pathogenic isolates. Therefore the expression of the 130 kDa-MBP is directly correlated with the virulent potential of *Acanthamoeba* (Garate *et al.*, 2006). It has been demonstrated that the surface of CLs, that have been worn for a long period, are coated with mannose or other saccharide residues attached to protein or lipids (Klotz *et al.* 1987). Furthermore CLs wearing as well as micro-traumas at the ocular surface can induce an increase of mannose-GPs expression on corneal epithelial cells (van Klink *et al.*, 1993; Jaison *et al.*, 1998). These reports reinforce the role of CLs as optimal carriers for *Acanthamoeba* trophozoites and as a risk factor for the development of *Acanthamoeba* keratitis. The ability of *Acanthamoeba* to bind GPs through 130 kDa-MBP is an essential step for the pathogenic cascade, however it does not imply the development of the infection. Further steps, such as the disruption of the corneal epithelium and the invasion of the deeper layers of the cornea are responsible for the clinical manifestations of AK (Clarke & Niederkorn, 2006).

In vitro studies, using Chinese hamster corneal epithelial cells (HCORN), have demonstrated that in the presence of mannose, trophozoites release into the medium serine proteases of approximately 100 kDa that cause cytopathic effects on corneal epithelial cells (Leher *et al.*, 1998). Therefore, it has been suggested that amoebic MBP can act as a mannose-receptor: the binding to mannose structures, induces activation of intracellular signaling pathways that eventually lead to the release of cytotoxic molecules by the trophozoites (Leher *et al.*, 1998). Later studies characterized the effect of mannose on the growth and excystment of *Acanthamoeba*, as well as the cytopathic effect of the whole or fractioned supernatant obtained from trophozoites treated or not with mannose on HCORN, human corneal epithelial (HCE) cells and small intestinal epithelial (Fhs-24) cells (Hurt *et al.*, 2003). It was found that mannose inhibits the growth of trophozoites and

increases cyst formation *in vitro*. Furthermore, cysts incubated in the presence of mannose slowly excyst reaching 50% of excystation on day 10, whereas in the absence of mannose 100% excystation was observed after 7 days. Whole amoebic supernatant obtained in the presence of mannose, showed cytopathic effects on HCORN, HCE cells but not on Fhs-24 cells. Similarly, the fraction above 100 kDa, showed higher cytopathic effects on HCORN and HCE cells, but not Fhs-24 cells (Hurt *et al.*, 2003). Sodium Dodecyl Sulphate-PolyAcrylamide Gel Electrophoresis (SDS-PAGE) analysis of whole supernatant showed two bands at 70 kDa and 133 kDa; these bands were not observed without pre-treatment with mannose. Subsequently, using fast protein liquid chromatography (FPLC), an amoebic, mannose-induced, cytotoxic serine protease of 133 kDa (MIP-133) was purified and characterized (Hurt *et al.*, 2003). Recently, it was shown that MIP-133 cytopathic effect towards HCE cells is elicited by induction of apoptosis through the activation of the cytosolic phospholipase $A_{2\alpha}$ pathway (Tripathi *et al.*, 2012). Although, corneal trauma is considered an important pre-condition for the *Acanthamoeba* adhesion and invasion processes, recent studies performed with scanning electronic microscopy (SEM) showed that trophozoites can bind and invade intact human cornea *in vitro* by disruption of the tight junctions and invasion through the separated cells. Once trophozoites reached the deeper layers, division and ingestion of basal cells was observed by light microscopy of thin sections (Omaña-Molina M *et al.*, 2010). The effect of amoebic conditioned medium on intact human cornea was also investigated; in this case the loss of epithelium integrity increased throughout the period of co-incubation, however it was mainly a superficial effect. After 3 hrs incubation separation of the tight junctions and a lytic effect was observed. Taken together, the disruption of the corneal epithelium and the subsequent invasion of *Acanthamoeba* are caused by soluble cytotoxic molecules, which may, or may not, be

released after binding to the corneal epithelial cells, and by the mechanical action and phagocytosis of trophozoites (Omaña-Molina M *et al.*, 2010).

Invasion and degradation of corneal stroma is the following step in the AK pathogenic cascade. Collagen, laminin and fibronectin are important structural proteins in the anterior and posterior portion of the cornea. *Acanthamoeba* can degrade these structural proteins through the release of serine and cysteine proteases; this leads to corneal structural and functional loss, and the development of the characteristic AK patho-physiological features (Ferrante & Bates, 1988; He *et al.*, 1990; Sant'ana *et al.*, 2014). In the degradation of EMC, proteases can also act indirectly, inducing the release and activation of metallo-proteases (MMP) from epithelial and stromal corneal cells. MMPs by digesting ECM play an important role in the remodelling of corneal layers and the wound healing processes in the eye; proteases can therefore play a role in both physiological and pathological conditions. MMP-1, MMP-2, MMP-3 and MMP-9 are physiologically expressed in corneal epithelial and stromal cells. Incubation with MIP-133 induces an increase of MMP-2 and MMP-3 gene expression in corneal epithelial cells, whereas in stromal corneal cells, this increase was seen for MMP-2 and 3 both for gene expression and protein (Alizadeh *et al.*, 2008). Expression of mRNA of MMPs was verified in *Acanthamoeba* trophozoites, but they have not been shown to produce these molecules (Alizadeh *et al.*, 2008). In the corneal stroma, trophozoites can induce apoptosis in keratocytes (Takaoka-Sugihara *et al.*, 2012) and nerve cell death, both by cytolysis and phagocytosis (Pettit *et al.*, 1996); this last event is responsible for the pain experienced by AK patients.

Acanthamoeba trophozoites that have penetrated into the corneal stroma, seem to then be arrested and unable to progress through the Descemet's membrane, the corneal endothelium and to reach the anterior chamber, and are therefore unable to

induce anterior eye infection (Clarke & Niederkorn, 2006). While it has been demonstrated that *Acanthamoeba* trophozoites can actually cross the Descemet's membrane and the endothelium, through the cytopathic effect of MIP-133 (Clarke *et al.*, 2005), *in vivo* experiments have demonstrated that the inability of *Acanthamoeba* to induce intraocular infections is due to an aggressive and effective clearance of trophozoites in the aqueous humor by recruited neutrophils (Clarke *et al.*, 2005).

Acanthamoeba virulence factors are important in the pathogenic cascade of GAE and AK diseases. The immune response, induced by *Acanthamoeba* within host tissues, if too intense, might contribute to the severity of the clinical symptoms and therefore impair the resolution of the disease.

1.3.6 *Acanthamoeba* Immunoepidemiology

Although the distribution of *Acanthamoeba* is pretty much ubiquitous and there is high exposure to this organism, very few cases of *Acanthamoeba* infections in humans have been reported. Interestingly, serological analysis of healthy individuals has shown the presence of high levels of antibody against *Acanthamoeba*, especially IgG and IgM in 50-100% of individuals (Cursons *et al.*, 1980). In a later study 20 human sera, including two samples belonging to AK patients and one from a newborn, were tested for anti-*Acanthamoeba* IgG, IgM and IgA antibody using immunoblotting techniques. It was found that all the sera, including the newborn serum, presented anti-*Acanthamoeba* antibodies, suggesting that antibodies can be transferred transplacentally. In the same study it was also demonstrated that AK patients present less IgA immunoreactivity to pathogenic strains, suggesting that lower titer of IgA in individuals might enhance the possibility of developing AK (Walochnik *et al.*, 2001). Alizadeh *et al.*, also in 2001, reported that AK patients

showed the same titer of serum IgG against *Acanthamoeba* as healthy individuals; whereas, lower tear IgA titers were detected in AK patients in comparison with healthy individuals. This finding confirms the importance of IgA in *Acanthamoeba* ocular infections. In order to evaluate whether different genotypes induce different immunoreactivity profiles, IgG IgM and IgA antibodies against seven different *Acanthamoeba* genotypes, representing the three different morphological groups, were measured in the serum of healthy individuals. It was shown that human sera had high IgG, IgM and IgA immunoreactivity against Group II and Group III strains, but lower immunoreactivity against Group I strains. In addition, although human serum displayed antibody against all the genotypes tested, IgG, IgA and IgM immunoreactivity was extremely high against T4, T5 and T6 strains, whereas IgG and IgA immunoreactivity, against T7 and T9, was relatively weak or non-detectable (Pumidonming *et al.*, 2014).

1.3.7 Host immune response in *Acanthamoeba* Infection

Acanthamoeba infects preferentially immune privileged sites, such as the brain and the eye. Cerebral and ocular tissues are characterized by a limited regenerative capacity, and the maintenance of their structural and functional features is essential for the survival of the hosts (Niederhorn, 2006; Forrester *et al.*, 2008). Therefore, *Acanthamoeba* interactions with the host's immune response has been studied through *in vivo* and *in vitro* experiments, as well as by cyto-pathological analyses of infected eye and brain tissues. These studies suggest that both humoral and cell mediated adaptive immunity is induced by *Acanthamoeba*. However, this is not efficient in avoiding the recrudescence of AK and in resolving the infection. Consequently, it is the general consensus that the innate immune apparatus plays the main role in avoiding the development of *Acanthamoeba* infections and the clearance of the amoeba from the host tissues.

1.3.7.1 Blood components: the complement system and circulating monocytes

Acanthamoeba trophozoites reach cerebral tissues mainly through the blood stream. There, components of innate immune system, such as the complement system and circulating monocytes, represent the first defence against *Acanthamoeba*. From as long ago as the early nineteen eighties it was demonstrated that *A. culbertsoni* trophozoites were susceptible to exposure to normal human serum (NHS). Indeed, 80% of trophozoites were killed after incubation with NHS; heat-inactivation at 37°C for 30 min ablated the amoebae death. This event was further investigated and it was found that trophozoites were able to activate the alternative complement pathway. This activation was observed using both pathogenic and non pathogenic *Acanthamoeba* isolates. Therefore, *in vivo* trophozoite death can be the result of either plasma membrane disruption via induction of the membrane attack complex or phagocytosis after C3b opsonisation (Ferrante & Rowan-Kelly, 1983). A recent study confirmed that NHS-induced trophozoite lysis, via alternative complement pathway activation by *Acanthamoeba* and the binding of C3 and C9 to the amoebic surface. In contrast to studies using NHS it was demonstrated that normal mouse serum (NMS), did not kill *Acanthamoeba*; although activation of the complement system was still observed (Pumidonming *et al.*, 2011). Using mannose binding lectin, complement factor B and complement factor C1_q deficient mice it was confirmed that the activation of complement induced by *Acanthamoeba* is alternative pathway dependent, but classical and lectin pathway independent (Pumidonming *et al.*, 2011). Circulating monocytes can act in order to prevent the dissemination of *Acanthamoeba* trophozoites in the host. It has been demonstrated that soluble molecules, released by *A. castellanii*, induce release of pro-inflammatory cytokines, such as tumor necrosis factor-alpha (TNF- α), interleukin-1 beta (IL-1 β), and

interleukin-6 (IL-6) from the human monocytic cell line THP-1 (Mattana *et al.*, 2002). TNF- α production was ablated by suramin treatment, suggesting purinergic receptor activation by amoebic ADP to be responsible for this event. On the other hand, neither IL-6 nor IL-1 β production were induced by amoebic ADP; in particular, IL-1 β production was stimulated by an unknown molecule of <10 kDa, that was susceptible to heat inactivation (Mattana *et al.*, 2002). In immune competent individuals, the initial innate immune response at the blood stream level and the formation of granulomas in the brain are essential events for avoiding invasion, dissemination and clearance of *Acanthamoeba* trophozoites and therefore the manifestation of GAE.

1.3.7.2 The corneal surface: physical, molecular, cellular barriers and innate immune receptors

Ocular defence against pathogens, at the interface with the external environment, relies on physical, molecular and cellular innate features that constitute the ocular surface. The ocular surface is the outer component of the eye and it consists of the eyelid, tear film, cornea and conjunctiva (Lambiase *et al.*, 2011). Eyelid movements and tear film provide the first innate defence against *Acanthamoeba* both through mechanical and biological mechanism. Frequent blinking and the tears can mechanically wash trophozoites from the ocular surface and prevent their adherence to the epithelium. Tear film that constantly coat cornea and conjunctiva elicits anti-microbial activity through enzymes, glycoproteins, amino acids, and immunoglobulins. It is know that epithelial cells release antimicrobial peptides (AMPs) in response to immune stimuli and/or to pathogens. The expression of AMPs was then investigated in response to *Acanthamoeba*, *in vitro*. Human corneal limbal epithelial cells, stimulated with live trophozoites, showed up-regulation of β -

defensin 3 (hBD3), liver-expressed antimicrobial peptide 1 (LEAP-1), hBD2 and RNase-7 in a time-dependent manner (Otri *et al.*, 2010). It was therefore suggested that these molecules might play a role in the early stages of the innate immune response to *Acanthamoeba* (Otri *et al.*, 2010). Tear IgA has a fundamental role in preventing the adhesion of trophozoites to the cornea and therefore limiting the chance of infection (Leher *et al.*, 1999; Said *et al.*, 2004).

Cornea consists of a multilayer epithelium; the Bowman's layer which separates the corneal epithelium from the underlying thick stroma, consisting of fibroblasts and keratocytes, which is underlain by the Descemet's membrane and by the endothelium (Shaharuddin *et al.*, 2013). Corneal histological structure consists of epithelial cells glued together by tight junctions, that represents a solid barrier that protects the inner layers of the cornea from invading pathogens. An *in vitro* study has demonstrated the higher resistance of human corneal epithelium, in comparison to human keratocytes, to amoebic cytopathic effects (Kinnear, 2004). Corneal epithelium damage was found to occur at the latest time points after infection at the higher trophozoite density. This same temporal and infection rate pattern was observed in keratocytes/trophozoite co-infections, but with more severe damage. Kinnear (2004) suggests that this difference is a result of the anatomical structure of the corneal epithelium that physically impedes trophozoite invasion.

Corneal epithelial and stromal cells are also immunologically active components of the cornea and produce cytokines and chemokines such as IL-1 α , IL-6, TNF- α , IL-8 and α -defensin, and participate in the recruitment of leucocytes into the cornea in response to microbial invasion or physical trauma (Lambiase *et al.*, 2011). Indeed, corneal epithelial cells express several receptors on their surface, that are able to recognize and respond to microbes, such as Toll Like Receptors (TLRs) and Proteases Activated Receptors (PARs). Since their first identifications, several TLRs

have been included in the TLR family, 10 have been identified in humans (TLR1-TLR10) and 12 have been identified in mice (TLR1-TLR13) where TLR10 is missing (Kawasaki & Kawai, 2014). Due to their important role in the first recognition of pathogens and in the rapid activation of immune responses, TLRs are strategically expressed in innate immune cells such as macrophages, neutrophils, dendritic cells (DCs), epithelial cells and in fibroblasts (Kawasaki & Kawai, 2014; McClure & Massari, 2014). TLRs are transmembrane proteins, that can recognize highly conserved and specific pathogens associated molecular patterns (PAMPs) (Kawai & Akira, 2009). TLRs are classified based on their cellular localization and on the nature of the PAMPs they recognize. TLR1, 2, 4, 5 and 6 are localized on the cell surface, sensing the extracellular microenvironment for PAMPs expressed by bacteria, fungi and protozoa. TLR3, 7, 8 and 9 are localized within cytoplasmic vesicles, called endosomes, and they mainly recognize viral and bacterial nucleic acids (Kumar *et al.*, 2011). Upon the binding of specific ligands to TLRs, intracellular signalling pathways are activated and culminate with the induction of appropriate immunological responses. Upstream molecules, involved in initiation of the intracellular signal are TIR-domain containing adaptors, such as MyD88, TRIF, and their sorting adaptors TIRAP/MAL and TRAM (Kawasaki & Kawai, 2014). The signalling pathway depending on MyD88 is associated with all TLRs, with the exception of TLR3, and it induces NF- κ B and MAPKs activation. MyD88 requires the sorting adaptor TIRAP/MAL for the engagement with the activated receptors, in particular TLR2 and TLR4 (Takeda & Akira, 2004). The signalling pathway dependent on TRIF is associated with TLR3 and TLR4 and it leads to activation of IRF3, NF- κ B and MAPKinases. TRAM is the sorting adaptor required for the engagement of TRIF to TLR4 (Kawasaki & Kawai, 2014). Therefore TLR activation can induce either a MyD88-dependent pathway or a TRIF-dependent pathway

leading to, respectively, either pro-inflammatory cytokine and chemokine production or type I interferon induction as well as cytokine production (Kawai & Akira, 2010) (Fig. 1.4).

PARs belong to the family of G-protein-coupled receptors, characterized by seven transmembrane domains connected by extracellular and intracellular loops, and presenting the N-terminus in the extracellular portion. These receptors are not activated through ligand binding, but by the proteolytic activity of endogenous and exogenous proteases (Macfarlane *et al.*, 2001). So far, 4 PARs have been identified: PAR₁, PAR₂, PAR₃, PAR₄. While PAR₁, PAR₃, PAR₄ are naturally activated by thrombin, PAR₂ is activated by trypsin. Nevertheless, each PAR presents a different cleavage site and a different tethered peptidic sequence (Macfarlane *et al.*, 2001). PARs are expressed in various types of immune cells such as monocytes, macrophages, neutrophils, eosinophils, mast cells, DCs and Tcells, as well as non immune cells such as fibroblasts, epithelial cells, smooth muscle cells, glial cells, neurons and nerves. This ubiquitous expression explains their wide range of physiological functions associated with maintenance of the tissue integrity as well as with inflammatory and immunological responses (Vergnolle, 2003). PARs are involved in initiating the release of inflammatory mediators, recruitment of leucocytes and the recovery and regeneration of tissue integrity. PARs, especially PAR₁ and PAR₂, are expressed on human corneal epithelial cells, predominantly in the outer cell layers of the corneal epithelium. Their activation leads to production of pro-inflammatory cytokines, as well as wound healing processes (Lang, *et al.*, 2003) (Fig 1.5). Therefore, the role of innate immune receptors in *Acanthamoeba* recognition and response at the ocular surface has been an area of recent interest.

It has been demonstrated that TLR2 and TLR4 expression in human telomerase-immortalized corneal epithelial cells (HUCLs) is significantly increased, both at

mRNA and protein level, after challenge with *Acanthamoeba* trophozoites (Ren *et al.*, 2010). Furthermore, an augmented expression of TLR2 and TLR4 on cell surface was observed. *Acanthamoeba* trophozoites, through early activation of TLR4-MyD88-NF- κ B pathway, induced production of TNF- α , and IL-8 in HUCLs (Ren *et al.*, 2010). In addition, later stimulation of the TLR4-ERK1/2 pathway resulted in interferon- β (IFN- β) release by HUCLs. Although TLR2 expression in HUCL was up-regulated after *Acanthamoeba* challenge, it was not involved in cytokine production (Ren *et al.*, 2010). These results were also confirmed *in vivo*, using a rat model of AK (Ren & Wu, 2011). More recent findings, further underlined the role of TLR4 in AK (Alizadeh *et al.*, 2014). Indeed, TLR4 activation by *Acanthamoeba* trophozoites, induces up-regulation of IL-8 mRNA expression and secretion in human corneal epithelial cells and of chemokine CXCL2 in HCORN (Alizadeh *et al.*, 2014). Furthermore, it was demonstrated that clinical isolates of *Acanthamoeba* induce higher expression of TLR4 and CXCL2 mRNA and secretion of CXCL2 in HCORN cells in comparison with soil isolates (Alizadeh *et al.*, 2014). This difference resulted in a more intense inflammatory response and neutrophil recruitment caused by clinical rather than soil isolate, in an *in vivo* AK model (Alizadeh *et al.*, 2014). Although keratocytes in the stroma do not provide a resistant physical barrier for *Acanthamoeba*, they are able to produce pro-inflammatory cytokines such as IL-8, TNF- α and IFN- β , in response to trophozoites. The production of these cytokines by human telomerase-immortalized corneal stromal fibroblasts after challenge with *Acanthamoeba* trophozoites is TLR4-dependent (Ren *et al.*, 2010). Amoebic serine protease MIP-133 was found to induce the production of IL-8, IL-6, IL-1 β and IFN- γ by HCE cells, and CXCL2/MIP-2 in HCORN cells via a cPLA₂ α dependent pathway (Tripathi *et al.*, 2012). A very recent study demonstrated that *Acanthamoeba* plasminogen activator stimulates, in HCE

cells, the production of IL-8 in a PAR2 dependent, but PAR1 independent manner (Tripathi *et al.*, 2014).

Corneal epithelial cells and stromal fibroblasts are able to recognize and respond to *Acanthamoeba* through the production of AMPs, cytokines and chemokines. These inflammatory mediators might be responsible for the recruitment of neutrophils and macrophages in the corneal stroma, the major immune cell types found in *Acanthamoeba* site of infections.

1.3.7.3 Innate immune cells: neutrophils and macrophages

The cellular components of the innate immune system derive from myeloid stem cells in the bone marrow and they include monocytes, macrophages, dendritic cells, granulocytes and mast cells. These cells are the main effectors of the initial recognition and response against invading microbes, as well as of their clearance from host tissues. They play important functions in the initiation, progression and intensification of the inflammatory response and represent the essential bridge between the innate and the adaptive immune response (Murphy, 2011).

Neutrophils are the main cell population within the granulocytes and the first innate immune cells to appear at the site of infection. They elicit their immune functions through phagocytic and non-phagocytic mechanisms such as degranulation and release of antimicrobial molecules and reactive oxygen species and are involved in cell-cell cross talk via the release of wide range of cytokines and chemokines (Jaillon *et al.*, 2013). Macrophages are heterogeneous white blood cells present in all tissues where they elicit important functions in both homeostatic and stress conditions.

Macrophages can be long-lived cells localized in specific tissues, called “resident tissue macrophages” or can they can originate in sites of infection/inflammation from

incoming Ly6C⁺ monocytes, and these are generally referred to as “elicited macrophages” (Gordon *et al.* 2014; Owen *et al.*, 2012). Tissue resident macrophages present different morphology, phenotype and activity, depending on their localization. They are strategically distributed throughout the body and also express several recognition receptors, such as TLRs and proteins on their surface. These two aspects confer upon them a special role in the immune surveillance of host tissues, initially recognizing invading pathogens and subsequently initiating the immune response. Indeed, upon pathogen recognition they recruit neutrophils and monocytes; the latter differentiating into macrophages, in the site of infection. Therefore, both resident and monocyte-derived macrophages, that are usually present in higher numbers, are present in the site of infection. Resident macrophages are, not only important in the initiation of the immune response, but also persist at the site of infection along with monocyte-derived macrophages, to modulate the evolution of the immune response leading eventually to recovery of homeostasis (Davies *et al.*, 2013). While tissue resident macrophages are specialized in the initiation of immune response and in the recovery of the homeostatic tissue conditions, monocyte-derived macrophages are important in the inflammatory phase where they can kill invading pathogens, through phagocytosis and the release of reactive oxygen and nitrogen species, and orchestrate innate and adaptive immune responses, through the release of cytokines and chemokines.

Granulomas, within the brain, consist of different immune cell populations such as microglia, neutrophils, T and B lymphocytes, all working in concert to clear trophozoites and cysts from the site of infection and to prevent *Acanthamoeba* spread through both contact-dependent and independent mechanisms (Harrison *et al.*, 2010). It has been demonstrated that microglia cells are chemoattracted by trophozoite conditioned medium. In particular cannabinoid receptors are involved in

these events: amoebic proteases and phospholipases cleave lipid molecules expressed on the plasma membrane that induce chemotaxis of microglia in a paracrine and/or autocrine mechanism (Cabral *et al.*, 2008). Microglia cells can then induce trophozoite death by both phagocytosis and chemokines/cytokines production.

Through TEM and SEM techniques, it was observed that rat cortical microglia cells can phagocytose *A.castellanii* trophozoites *in vitro* (Marciano-Cabral *et al.*, 2000; Marciano-Cabral *et al.*, 2004). After co-incubation of BV-2, mouse microglia cell line, with trophozoites of *A. culbertsoni*, increased chemokines, such as monocyte chemoattractant protein-1 (MCP-1), macrophage inflammatory protein (MIP-2), MIP-1 α and MIP-1 β , and cytokines, such as IL-1 α , IL-1 β and IL-6, mRNA expression were observed. The same cytokine pattern was detected at the protein level (Harrison *et al.*, 2010). Also in neonatal rat cortical microglia cells, *A. castellanii* trophozoites induced an increase of IL-1 β , IL-1 α and TNF- α mRNA expression (Marciano-Cabral *et al.*, 2000).

In immune compromised individuals, the formation of a distinctive granuloma is not observed. The decreased recruitment of microglia cells, and consequently a limitation of their immune functions, leads to dissemination of trophozoites within the cerebral tissue with an exacerbation of the infection and a poor outcome for the patient. As previously reported, an increased number of GAE cases have been observed in immune competent individuals (Webster *et al.* 2012). Potentially, the manifestation of GAE in these patients is more likely due to an excessive and detrimental immune response in the brain, whereas in immune compromised individuals GAE pathogenesis is more linked to the virulence of *Acanthamoeba* and its direct cytopathic activity.

Originally it had been thought that innate immune cells were not present in the cornea, as part of it being an immune privileged site. Subsequently, a series of studies reported the presence of macrophages in the healthy murine cornea (Brissette-Storkus *et al.*, 2002; Yamagami *et al.*, 2005; Pearlman *et al.*, 2013). Innate immune cells, such as macrophages and neutrophils, are also recruited following corneal trauma, that may or may not be associated with microbial infections. These cells act in order to clear the tissue of invading pathogens and/or cell debris, they inhibit the replication and invasion of pathogens (Sun *et al.*, 2010; McClellan *et al.*, 2003) and participate in the eventual recovery of corneal structural and functional features (Li *et al.*, 2013).

Many studies have been performed to investigate the importance of neutrophils and macrophages in AK. *In vivo* models of AK have been widely and successfully used for this purpose (van Klink *et al.*, 1996; Hurt *et al.*, 2001). Furthermore, histopathological analysis of AK patients' corneas have allowed, over the years, an understanding of the kinetics of the involvement of neutrophils and macrophages in human infections. In an early study, examination of AK patients' corneas, using both light and electronic microscopy techniques, indicated the presence in the stroma of polymorphonuclear leucocytes and human leucocyte antigen-determinant receptor (HLA-DR) macrophages (Mather *et al.*, 1987). Experimental AK infection in the rat, and use of immunohistochemical techniques, have allowed reconstruction of the sequential immunological events and the recruitment of the different immune cells during the development of the infection (Larkin & Easty, 1991). On day 1, an important influx of neutrophils was observed in the stroma. At day 3, macrophages were detected and by day 7, these cells constituted the predominant cell type, whereas neutrophil numbers at this time had declined. At day 7, T-cells were found within the tissue. By day 14, macrophages were still predominantly present in the

site of infection, and both activated and non activated T-cells were also found. With further disease progression, neutrophil numbers progressively decreased, whereas macrophages and T-cells persisted in the area, and were detected constantly up to day 84 after infection. B-cells were not found at any stage within the infected stroma, probably due to lack of vascularisation of the cornea and its immune privileged status (Larkin & Easty, 1991). A more recent study analysed the cornea of an AK patient that underwent a therapeutic PK (Knickelbein *et al.*, 2013). Using immunohistochemical analysis, neutrophils and macrophages were found to be the major cell types present in agreement with the previous findings in animal AK models (Larkin & Easty, 1991). Macrophages and neutrophils were observed moving towards *Acanthamoeba*. Although T-cells and B-cells were detected within the corneal stroma, they were not seen in proximity to *Acanthamoeba* cysts (Knickelbein *et al.*, 2013). Neutrophils and macrophages are the effector cells in the clearance of *Acanthamoeba* and therefore the resolution of infection. Indeed, depletion of macrophages, by subconjunctival injection of dichloromethylene diphosphonate (C12MDP) in a hamster AK model, resulted in an increase of the incidence and severity of the infection (van Klink *et al.*, 1996). In C12MDP treated animals, clinical manifestations appeared earlier and AK became chronic (van Klink *et al.*, 1996). Depletion of neutrophils was also investigated *in vivo* (Hurt *et al.*, 2001). After administration of anti-macrophage inflammatory protein 2 or anti-neutrophil antibody, an exacerbation of AK in chinese hamsters was observed, characterised by an early manifestation of the clinical symptoms and eventual development into chronic infection. Inhibition of neutrophil recruitment was responsible for this negative outcome (Hurt *et al.*, 2001). Instillation of sterile latex beads in the cornea of hamsters conferred resistance to AK. Using either C12MPD or anti-neutrophil antibody, it was suggested that the observed resistance was principally due to macrophage activity (Clarke *et al.*, 2006). Furthermore the role of

neutrophils in the early stages of infection was confirmed, whereas macrophage significant activity commenced after the 4th day and proceeded until the resolution of AK (Clarke *et al.*, 2006). Neutrophils and macrophages may be recruited in the site of infection by host mediators such chemokines and pro-inflammatory cytokines, released by corneal epithelial cells and stromal fibroblasts (Lambiase *et al.*, 2011). Although neutrophils are present in large numbers in the site of corneal infection they are not as effective as macrophages in killing *Acanthamoeba* trophozoites (Marciano-Cabral & Cabral, 2003). Studies have demonstrated that neutrophil amoebicidal activity can be enhanced by the influence of mononuclear leukocyte mediators in the presence of both antibody and complement (Ferrante & Abell, 1986). On the other hand, it has been demonstrated that neutrophils are extremely effective in killing trophozoites in the anterior chamber, and therefore, in this role they prevent the development of intraocular *Acanthamoeba* infections (Clarke *et al.*, 2005). Rat macrophages are chemotactically attracted by *Acanthamoeba* trophozoites *in vitro* (Stewart *et al.*, 1992). Macrophages are able to kill *Acanthamoeba* through phagocytosis and contact-dependent trophozoite lysis (Marciano-Cabral & Toney, 1998). Activation of murine macrophages, with bacterial components, increases their amoebicidal activity relative to non-activated macrophages. However, supernatants of macrophages primed with LPS or IFN- γ did not induce cytotoxic or cytostatic effects on trophozoites (Marciano-Cabral & Toney, 1998). *In vitro* experiments showed that macrophages stimulated with IFN- γ containing supernatant killed a high number of trophozoites. This cytotoxic activity was inducible NO synthase independent (Alizadeh *et al.*, 2007). Furthermore, in the presence of *Acanthamoeba* specific antibody macrophages demonstrated an increased amoebicidal activity (Stewart *et al.*, 1992). Although neutrophils and macrophages are not chemotactically attracted to intact cysts, they can kill them:

macrophages through phagocytosis, neutrophils through the secretion of myeloperoxidase (Hurt *et al.*, 2003). Although many studies have been performed to investigate the role of macrophages in killing *Acanthamoeba*, the nature of the host/parasite interaction awaits clarification: in particular the immune receptors involved in pathogen recognition await characterisation, as well as the amoebic molecules that influence macrophage function.

1.3.7.4 Humoral and cellular adaptive immune responses

Immune privilege in the eye is maintained through three distinctive features: firstly, anatomical, cellular and molecular barriers identified in the blood ocular barriers, the absence of lymphoid draining routes, reduced MHC I and II expression on parenchymal cells and expression of FasL throughout the eye; secondly, the creation of an immune-suppressive microenvironment through the presence of immune suppressive molecules such as cytokines, hormones, neuropeptides and complement inhibitors; thirdly, the ability to deviate the systemic immune response subsequent to the recognition of antigens in the anterior chamber of the eye, a mechanism named anterior chamber associated immune deviation (ACAID) (Streilein, 1997; Shaharuddin *et al.*, 2013). The detection of IgG and IgM against *Acanthamoeba* in healthy individuals suggests a natural sensitization of individuals, as a result of the frequent contact with the organism, and the involvement of the adaptive immune response in *Acanthamoeba* infections. One study has reported human T cell clones responsive to *Acanthamoeba* that are CD4 positive, CD8 negative and TCR- $\alpha\beta$ positive (Tanaka *et al.*, 1994). These T-cell clones were shown to be active towards both a GAE and an AK isolate of *Acanthamoeba* and predominantly showed a T_H1 activity, with release of IFN- γ (Tanaka *et al.*, 1994).

Some studies have examined the development of immunity following an immunization protocol against *Acanthamoeba*, especially in AK. Using a pig model,

subconjunctival injection of *Acanthamoeba* antigen prevented the development of AK, and this protection was not correlated with either IgG or the activation of lymphocytes. Furthermore, animals that were affected by AK and recovered, were not protected from a subsequent infection (Alizadeh *et al.*, 1995). In a later study pigs were immunized through oral administration of *Acanthamoeba* antigen and cholera toxin as adjuvant, before and after inducing experimental AK. Immunization prior to AK was effective in protecting the animals from the development of infection, whereas animals that were immunized after the experimental induction of AK developed the same disease severity as the controls. The protective immunization was correlated with high titers of *Acanthamoeba* specific IgA in the animal tears (Leher *et al.*, 1998). The same protocol of oral immunization was used in chinese hamsters, and in a similar manner a lower infection rate was observed relative to unvaccinated control hamsters. By enzyme linked immuno sorbent-assay (ELISA) high titers of anti-*Acanthamoeba* IgA were found in the animal tears. IgA was found not to induce trophozoite death, but it inhibited their binding to the corneal epithelium preventing the infection (Leher *et al.*, 1998a). Further studies were performed to address the role of mucosal IgA in protection from the development of AK. Therefore anti-*Acanthamoeba* IgA monoclonal antibody were obtain from chinese hamsters after oral immunization with acanthamoebic antigen and cholera toxin as adjuvant. Using immune staining techniques it was demonstrated that anti-*Acanthamoeba* IgA recognized antigen expressed on the amoeba surface. These specific antibodies protected the animal from AK. The protection was a result of the inhibition of trophozoite adhesion to the corneal cells but not to an amoebicidal activity (Leher *et al.*, 1999).

Rabbits immunized with *Acanthamoeba*-antigens, prior the induction of AK, showed milder symptoms than non-immunised control rabbits. Furthermore it was shown

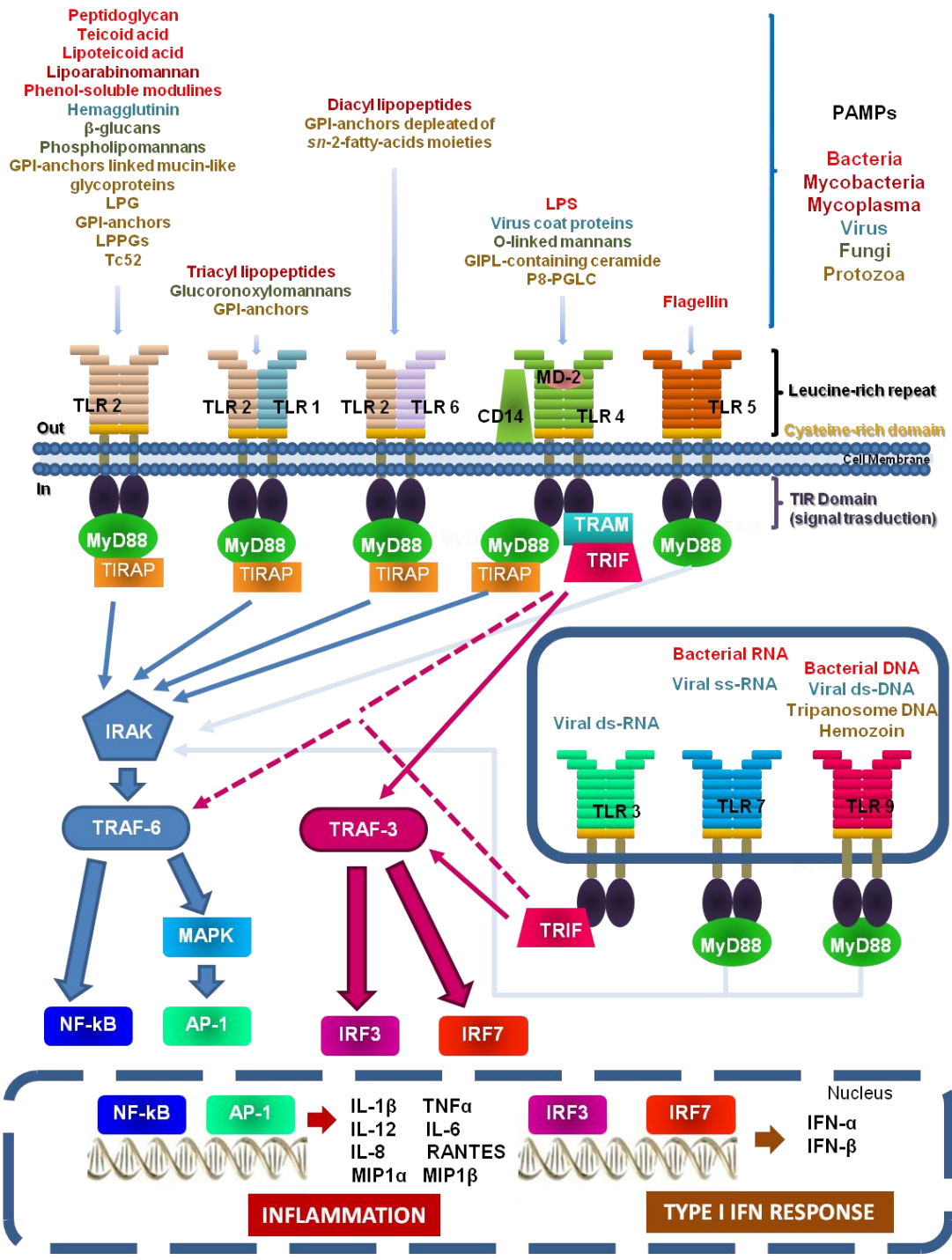
that IgA could operate through both an “innate” role via the mannosylated residues of the heavy chains inhibiting the adherence of trophozoites to corneal epithelium; and an adaptive immunological role, by increasing the neutrophil-mediated killing of trophozoites and antigen recognition (Said *et al.*, 2004).

1.3.7.5 *Acanthamoeba* immune evasion mechanisms

The ability of *Acanthamoeba* to differentiate into cysts has been considered an effective mechanism of immune evasion. As previously reported, neither macrophages nor neutrophils are chemotactically attracted to *Acanthamoeba* cysts and this enables them to persist within the tissues with the potential to initiate the recrudescence of the infection. *In vivo* experiments have been reported that cysts are immunogenic. Intraperitoneal immunization with either *Acanthamoeba* trophozoites or cysts elicits T cell proliferation in mice, although this event was stronger after immunization with cysts. Furthermore, pre-exposure to cysts leads to T cell mediated responses against both cysts and trophozoites, whereas pre-exposure to trophozoites fails to induce a T cell response towards cysts (McClellan *et al.* 2002). Therefore, a first contact with the infectious trophozoite form will not provide protection against cysts, allowing them to persist within the tissues. Under these conditions the failure of the systemic immune system to protect the host from the reactivation of AK is perhaps not surprising (McClellan *et al.* 2002). It has been reported that *Acanthamoeba culbertsoni* is able to destroy microglia cells, *in vitro*, through the induction of necrosis, plasma membrane lysis and apoptosis. By inducing macrophage death, pathogenic *Acanthamoeba* can survive within the host's tissue (Shin *et al.* 2001, Marciano-Cabral *et al.*, 2004; Harrison *et al.*, 2010). Pathogenic isolates of *Acanthamoeba* induce higher cytokine and chemokine production by microglia cells and corneal epithelial cells (Marciano-Cabral *et al.*, 2004; Alizadeh *et al.*, 2014). Cytokines and chemokines alone have not a cytostatic

or cytotoxic effect, however they can induce stronger and detrimental inflammation within the brain and eye. On the other hand, it has also been demonstrated that *A. culbertsoni*, through serine proteases activity, is able to degrade cytokines and chemokines produced by microglia cells *in vitro* (Harrison *et al.*, 2010). Immunoglobulins, especially IgA, are important defence factors in AK. It has been demonstrated that *A. castellanii* proteases can degrade IgA, IgG and IgM *in vitro*. Abrogation of IgA effects allow adherence of trophozoites to corneal epithelium and therefore the initiation of the pathogenic cascade (Na *et al.*, 2002). Recently it has been found that the iron superoxide dismutase gene in *A. castellanii* can protect *Acanthamoeba* from the oxidative killing mechanisms of immune cells by detoxifying oxygen reactive species (Kim *et al.*, 2012).

Fig 1.4 Toll like receptor ligands, structure and signalling pathways. TLRs are characterized by three different domains: the ectodomain, responsible for the recognition of PAMPs and consisting of leucine rich repeats (LRRs), the transmembrane domain and the endodomain, named Toll/IL-1R (TIR) domain for its homology with IL-1R and involved in the initiation of the signalling pathway. TLRs recognize molecular moieties (PAMPs) expressed by bacteria, viruses, fungi, and protozoa. Stimulation of TLR2, TLR4 and TLR5 leads to activation of the MyD88 dependent signalling pathway, characterized by the initial recruitment of IRAK kinase family proteins by MyD88 and subsequently of TRAF6. The IRAK1/TRAF6 complex dissociates from the receptor and TRAF6 itself binds to TGF- β activated kinase 1 (TAK1) in association with TAK1 binding proteins, TAB1 and TAB2; this complex, induces TAK1 activation which leads to the activation of the IKK complex-NF- κ B pathway or the MAPKs-AP1 pathway (Kawai & Akira, 2010). Stimulation of TLR3 and TLR4 induce the activation of the TRIF-dependent signalling pathway. The TRIF-dependent pathway can either lead to activation of NF- κ B and MAPKs, inducing pro-inflammatory cytokine production or to activation of IRF3 and production of type I IFN (Kumar *et al.*, 2011). TLR4 stimulation can lead to induction of both MyD88-dependent and TRIF-dependent pathways. In the first case, TIRAP is required to direct MyD88 engagement with the receptor. Subsequently MyD88/TIRAP forms the complex with IRAKs and TRAF6, which induces activation of TAK1 and consequent activation of the IKK complex-NF- κ B pathway or the MAPKs-AP1 pathway, leading to an early production of proinflammatory cytokines. Subsequently, TLR4 is enclosed into endosomes, where it is associated with the sortin adaptor TRAM. TLR4/TRAM complex associates with TRIF, which leads to activation of TRAF3, TBK1 and IKKi and consequent activation of IRF3 and late activation of NF- κ B and MAPKs (Kawai & Akira, 2010).



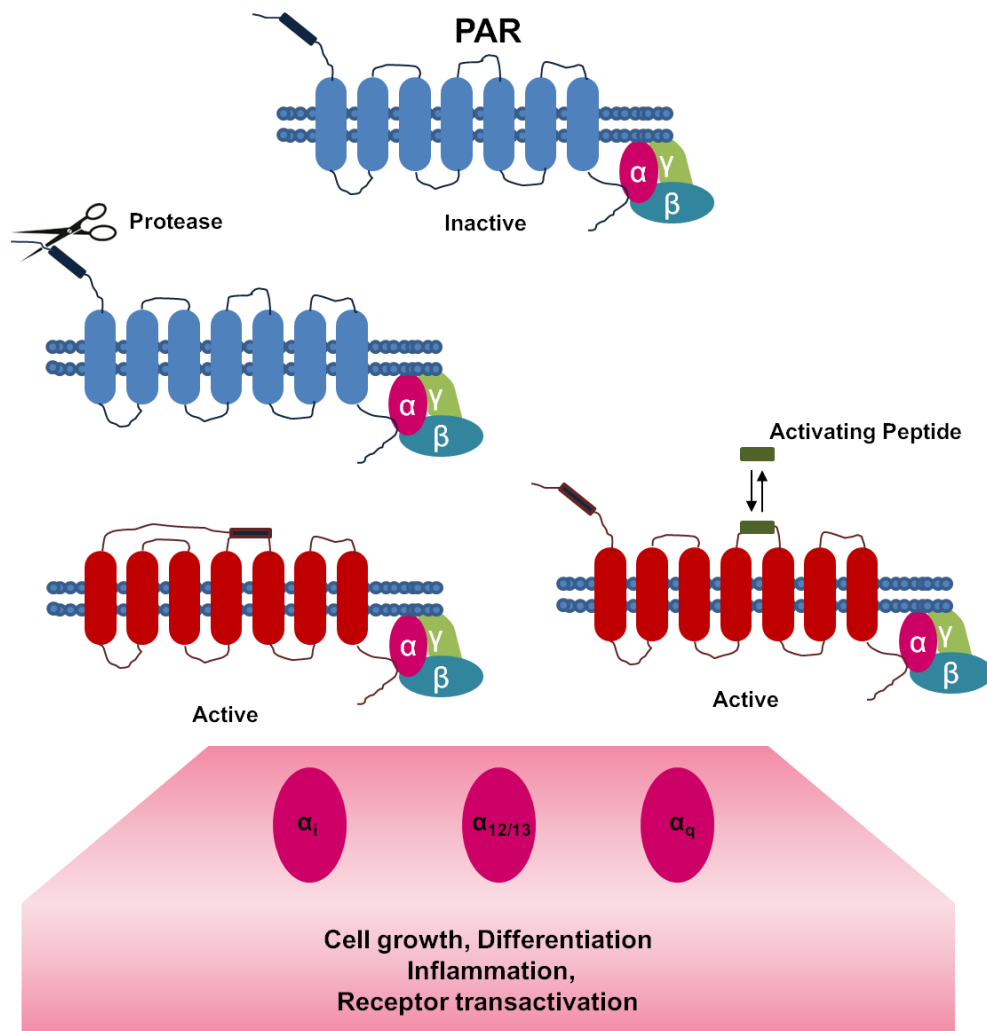


Fig 1.6 Protease activated receptors (PARs) structure, activation and functions. PARs are characterized by seven transmembrane domains connected by extracellular and intracellular loops, presenting the N-terminus in the extracellular portion. Proteases are involved in the activation of these receptors: by cleaving the N-terminus, serine proteases create a new “tethered ligand” which folds and binds to the 2 extracellular loops of the receptor, leading to conformational modification, initiation of the intracellular signalling and cellular responses. Activating peptides do not cleave the receptor, but directly bind the second extracellular loop mimicking the tethered ligands (Adams *et al.*, 2011). Activation of PARs involves the heterotrimeric guanyl nucleotide binding proteins (G proteins): G_q, G_i and G_{12/13}.

1.3.8 Aims

Although *Acanthamoeba* has an ubiquitous distribution and exposure to this organism is extremely frequent, few cases of *Acanthamoeba* infections in humans have been reported. *Acanthamoeba* predominantly infects immune privileged sites, such as the brain and the eye and some individuals, especially the immune compromised are more susceptible than others. A number of studies, as illustrated above, have indicated that adaptive immune response, with the possible exception of IgA generation to protect mucosal surfaces, plays little role in the prevention of clinical infection, and that the innate immune response plays the pivotal role in determining patent disease progression. Amongst those elements of the innate immune response that have been implicated in protective immunity are the phagocytic cells, primarily neutrophils and macrophages. While *Acanthamoeba* infections are characterised by an early influx of these innate cells into the site of infection, with macrophages persisting throughout the infection period, both have been demonstrated to be able to kill the pathogen while macrophages also have a role in tissue repair and homeostasis associated with healing. To date the majority of studies have examined the interaction between corneal epithelial cells and *Acanthamoeba* with comparatively few examining the interaction of these organisms with phagocytic cells.

Consequently, one of the major aims of the present study was to study the effect, if any, of *Acanthamoeba* on the activation state of resting macrophages. Towards this end macrophages were co-incubated with either a classical laboratory strain of *A. castellanii*, named as Neff, and perhaps of greater significance, a clinical isolate of *A. castellanii*, isolated from a case of bilateral keratitis. Both strains utilised were of the T4 genotype that has been associated with the majority of human infections. The ability of trophozoites from either strain to induce macrophage pro-inflammatory

cytokines production was subsequently measured. In particular, TNF- α , IL-12 and IL-6 production by macrophages was investigated for their essential roles during early and late phases of the immune response, as well as for the lack of knowledge regarding the mechanisms and kinetics of release of these three pro-inflammatory cytokines during *Acanthamoeba* infection.

Once an effect of *Acanthamoeba castellanii* on the macrophage activation state had been established a further aim of the project was to determine which pathogen products were influencing macrophage function and whether these were secretory products. Studies involving inhibitors of proteases that have been reported as *Acanthamoeba* virulence factors were used to this purpose.

A further aim of the project was to determine which macrophage PRRs and which signalling pathways were activated by the *Acanthamoeba* isolates. Towards this end macrophages were utilised from TLR or signal transduction gene deficient mice and their activation states compared with gene intact macrophages following co-cultivation with trophozoites of either strain were investigated. In order to determine whether PARs were activated by *Acanthamoeba* trophozoites, PAR gene deficient mice or specific antagonist were used.

As an important role for macrophages is also tissue repair via alternative macrophage activation a further aim of the project was to determine the role of the isolates in L-arginine metabolism and whether the isolates could influence tissue repair.

Finally, in order to better determine, in a global manner, how trophozoites may influence macrophage function, and how clinical and laboratory *A. castellanii* isolates may differ and influence pathogenicity, a metabolomic analysis has been undertaken. In the 1st instance a comparison of the secreted products of 2 *A.*

castellanii isolates was undertaken and secondly a study has been initiated to determine the effect of these trophozoite supernatants on the macrophage metabolome.

CHAPTER 2

General Materials And Methods

2.1 *Acanthamoeba castellanii* cultures

Trophozoites of two different strains of *Acanthamoeba castellanii* were used throughout this study. *Acanthamoeba* Neff strain, a classical laboratory strain, isolated from soil over 50 years ago and kindly donated by Prof. Keith Vickerman (Glasgow, United Kingdom) (Henriquez *et al.*, 2014) and *Acanthamoeba castellanii* genotype T4, isolated from a patient affected by bilateral keratitis in Ancora, Italy (clinical isolate) and provided by Dr. Antonella Mattana (Sassari, Italy) (Henriquez *et al.*, 2014).

Acanthamoeba trophozoites from both strains were grown in a medium consisting of 0.9% w/v D-(+)-maltose monohydrate 95% (AlfaAesar, Heysham UK) and 2% w/v mycological peptone (Oxoid, Basingstoke, UK) and supplemented with 125µg/ml of Penicillin/Streptomycin (Sigma Chemical Co, Poole, UK) and the Neff strain was also treated with 125µg/ml Amphotericin B (Sigma Chemical Co, Poole, UK). Since this medium is characterized by a consistent concentration of nutrients, such as carbohydrates and peptides, it has been named, by our laboratory, rich medium. Trophozoites were cultured in 75 cm² tissue culture flasks (Corning, NY, USA) and incubated at room temperature. They were used when confluent and harvested by mechanical detachment. All procedures were carried out in a biological safety cabinet (BSC) of class II.

2.2 Culture of murine bone marrow derived macrophages

Bone marrow derived (BMD) macrophages, obtained from the femurs of either 7-weeks-old male BALB/c or C57BL/6 mice were used to perform the experiments. Schedule 1 procedure was ordinarily applied to sacrifice the animals. On the bench, intact and clean bones were obtain using sterile scissors and forceps; and then immersed in 70% v/v ethanol for few minutes for sterilisation.

Growth medium (gDMEM), consisting of Dulbecco's medium (DMEM) (Life technologies, Paisley, UK) supplemented with 20% v/v of heat inactivated foetal calf serum (HI-FCS) (Biosera, Sussex, UK), 30% v/v of L-cell conditioned medium, 5 mM L-glutamine, 100 U/ml Penicillin and 100 µg/ml Streptomycin (Sigma Chemical Co, Poole, UK), was freshly prepared in the BSC. Bones pre-treated with ethanol were then transferred into a sterile Petri dish (Thermo Fisher Scientific, USA) and washed with sterile gDMEM. At this point, bones were cut at each end with sterile scissors and bone marrow stem cells were flushed from the femur with 5 ml of gDMEM, using a BD Microlance 25G 5/8 needle (Becton, Dickinson and company, Louth, Ireland). Stem cells were then gently re-suspended with a 10 ml serological pipette and passed through a sterile BD falcon 40 µm cell strainer (Becton, Dickinson and company, Louth, Ireland) in order to obtain a single cell suspension. 10 ml of bone marrow stem cell were distributed into each Petri dish and incubated at 37°C, 5% CO₂ atmosphere. The cell feeding protocol consisted in adding 10 ml of gDMEM at day 4 and changing the media with fresh 20 ml of gDMEM at day 7. At day 10 mature macrophages were harvested and used for the experiments.

L-cell conditioned medium was obtained harvesting the metabolized medium from cultured murine fibroblastic cell line L-929. This conditioned medium provides a source of macrophage colony stimulating factor (M-CSF) necessary for the growth and differentiation of bone marrow cells into mature macrophages.

2.3 Infection of BMD macrophages with *Acanthamoeba castellanii* trophozoites

At day 10 macrophages were harvested with RPMI-1640 medium (Lonza Biowhittaker, Virviers, Belgium), and centrifuged at x 300g 5 minutes (min). Pellets was re-suspended in RPMI supplemented with 10% v/v HI-FCS, 5 mM L-glutamine,

125µg/ml 100 U/ml Penicillin and 100 µg/ml Streptomycin (Sigma Chemical Co, Poole, UK) (complete RPMI, cRPMI) and centrifuged for 5 min at x 300g. Supernatants were discarded and macrophages were then re-suspended in cRPMI and counted using the Neubauer Chamber (Superior Marienfeld, Germany). 1×10^6 macrophages/well were plated in 24-well plates (TPP, Switzerland) and incubated over night at 37°C, 5% CO₂ to allow them to adhere.

The day after, trophozoites were observed using an inverted microscope (to evaluate the presence of any contamination or cysts) and then harvested by mechanical detachment. Trophozoite suspensions were transferred into sterile 50 ml centrifuge tubes (Corning, NY, USA) and centrifuged at x 360g for 10 min. Subsequently, supernatant was discarded and trophozoites were washed once in sterile Phosphate Buffered Saline without Ca₂⁺⁺ or Mg₂⁺⁺ or Phenol Red (PBS) (Lonza, Walkersville, USA) (x 360g 5 min) and once in cRPMI (x 360g 5 min). Trophozoites were then suspended in cRPMI and counted using the Neubauer Chamber. Trophozoite suspensions at specified density, were prepared and subsequently used to infect macrophages at prearranged ratios.

Macrophages were infected with trophozoite suspension in cRPMI of either *Acanthamoeba* Neff strain (Neff) or *Acanthamoeba* clinical isolate (clinical).

2.4 Production of amoeba-derived cell free conditioned medium

Trophozoites of either the Neff or clinical strains were cultured in the rich medium at room temperature. When confluent, they were mechanically detached and washed twice in sterile PBS (x 360g for 10 min). Thereafter, trophozoites were suspended in RPMI supplemented with 20 mM HEPES (Sigma-Aldrich, Saint Louis, Missouri) at a

density of 4×10^6 /ml and incubated for 2 h at room temperature (Mattana *et al.* 1997; Mattana *et al.* 2001, Mattana *et al.* 2002).

To obtain amoeba-derived cell free conditioned medium, trophozoite suspension was centrifuge for 15 min at x 500g. Amoebic cell free conditioned medium was supplemented with 10% HI-FCS, prior to use in the stimulation experiments (Mattana *et al.* 1997; Mattana *et al.* 2001, Mattana *et al.* 2002).

2.5 Stimulation of murine BMD macrophages with amoeba-derived cell free conditioned medium

Macrophages were harvested, as previously described, plated at 1×10^6 macrophage/well in 24-well plates and incubated over night at 37°C 5% CO₂.

The day after, old medium was discarded and replaced with 200 µl of cRPMI supplemented with 20 mM HEPES. Afterwards, 800 µl of amoebic cell free conditioned medium, supplemented with 10% HI-FCS, were added into the wells.

2.6 Stimulation of BMD macrophages with specific agonists

Lipopolysaccharide (LPS) from *Salmonella enterica* serotype abortus equi (Sigma Chemical Co, Poole, UK) and the synthetic tripalmitoylated lipopeptide (PAM3CSK4) (Invivo Gen, San Diego, CA, USA), were used to stimulate macrophages via TLR4 and 2, respectively as positive controls. Prior to stimulation, LPS in cRPMI was prepared from a 1000 µg/ml stock solution, whereas PAM3CSK4 in cRPMI was obtained from a 100 µg/ml stock solution. The final concentration used in wells, was 200 ng/ml for LPS and 320 ng/ml for PAM3CSK4.

After adding the specific stimuli (either trophozoites, amoeba-derived cell free conditioned medium or agonist), plates were incubated at 37°C, 5% CO₂ throughout the duration of the experiment.

2.7 Quantitative analysis of murine cytokines production

Enzyme Linked-Immuno-Sorbent Assay (ELISA) was performed to determine the concentration of TNF- α , IL-12, and IL-6 released by murine macrophages after stimulation. At specific time points after infection/stimulation, plates were observed, using an inverted microscope to examine the morphological changes within either macrophages or trophozoites and possible contamination. Afterwards, plates were centrifuged for 1 min at 480g and supernatants were collected and stored at -20° until performing the ELISA.

The buffers required for the procedure were prepared fresh before the assay: PBS pH either 7.4 or pH 9, consisting of 137 mM NaCl (Sigma Aldrich, Saint Louis, Missouri, USA), 8.10 mM Na₂HPO₄ (May & Baker, Essex, England), 2.7 mM KCl (Fisher Chemicals, Leicestershire, UK) and 1.47 mM KH₂PO₄ (Sigma Aldrich, Saint Louis, Missouri, USA) in distilled water (dH₂O); 0.1 M potassium phosphate buffer pH 6, obtained combining 1 M K₂HPO₄ (Sigma Aldrich, Saint Louis, Missouri, USA) and 1 M KH₂PO₄ solutions and diluted with dH₂O to a 0.1 M solution, and Glycine buffer pH 10.4, consisting of 100 mM Glycine (Sigma Aldrich, Saint Louis, Missouri, USA), 0.998 mM MgCl₂• 6H₂O and 0.997 mM ZnCl₂ (Sigma Aldrich, Saint Louis, Missouri, USA) in dH₂O pH 10.4. Wash buffer, 0.05% Tween20 (Sigma Aldrich, Saint Louis, Missouri, USA) in PBS pH7.4, was also prepared before performing the assay. Antibodies and second step reagents were used diluted, using the appropriate buffer, at the required concentrations (Table 2.1).

96 well ELISA flat bottom and medium binding microplates, (Greiner bio-one, Frickenhausen, Germany) were coated with 50 µl/well of Capture antibody, diluted in the appropriate buffer (PBS pH 9 for IL-12 and IL-6 and Potassium Phosphate Buffer pH 6 for TNF-α). Afterwards plates were covered and incubated over night at 4°C. The day after, Capture antibody was discarded and plates were washed by adding 400 µl of wash buffer in each well. Wash buffer was then removed and plates were blotted against paper towels to eliminate the excess. This procedure was repeated three times after each incubation stage. Non-specific binding sites were then blocked by adding 200 µl of block buffer (10% HI-FCS in PBS pH 7.4) in each well and incubating the plates for 1 hour (h) at 37°C. In the meantime, samples were defrosted at room temperature and the appropriate recombinant mouse cytokine of the cytokine being measured was diluted in block buffer (top standard concentration), for the generation of the standard curve. After the washing step, 30 µl/well of samples were added and an eleven point standard curve was generated in duplicate, by adding 60 µl of standard solution in the first two wells and using a 2-fold serial dilution in block buffer. The final two wells did not received standard solution and they were considered the blank. Plates were then sealed and incubated at 37°C for 2 h. After incubation, samples and standard were removed and plates were washed to eliminate the unbound protein. Biotinylated secondary antibody work solution was prepared and distributed at 50 µl/well. Plates were then incubated for 1 h at 37°C. Afterwards, antibody was discarded and washing step repeated. 50 µl of Streptavidin-AKP solution was added to each well and incubated for 45 min at 37°C. In the meantime substrate solution was prepared by dissolving one tablet of 4-nitrophenyl phosphate disodium salt hexahydrate (20 mg) in 20 ml of Glycine Buffer. After washing, 50 µl of substrate solution was added to each well and plates were incubated at 37°C, and covered with tin foil in order to protect them from direct light. Development of the reaction was checked every 10 minutes. The optical

density (OD) of each well was determined at 405 nm using SpectraMax 190 microplate spectrophotometer (Molecular Devices, Sunnyvale, CA, USA). SOFTMAX PRO software (Molecular Devices, Sunnyvale, CA, USA) was used to obtain the values of OD and to calculate cytokine concentration in relation to the standard curve. When samples showed concentrations above the top standard, they were re-assayed at 1:5 dilution of sample in block buffer. Cytokine concentration was expressed in ng/ml

2.8 Determination of arginase activity in BMD murine macrophages

Arginase activity in BMD macrophages, after infection/stimulation experiments, was determined using the modified Schimke's method as previously described (Corraliza *et al.*, 1994).

After collecting the supernatant for ELISA or NO assay, 500 µl of ice cold PBS was added into each well and macrophages were harvested by scraping with a 1000 µl pipette tip. Suspensions were collected and transferred into 1.5 ml microcentrifuge tubes. A further 500 µl of ice cold PBS was added into each well and the remaining cells were scraped from the surface and transferred into the same microcentrifuge tubes as the supernatants. Each well corresponded to one microcentrifuge tube. Afterwards, samples were centrifuged for 4 min at 12500g using a microcentrifuge. PBS was discarded and pellets were re-suspended. 0.1% Triton X-100 (Sigma Aldrich, Saint Louis, Missouri, USA) solution in dH₂O containing 5 µg of Pepstatin A synthetic, 5 µg of Aprotinin, Bovine Lung, Crystalline and 5 µg of Antipain Hydrochloride (Merck KGaA, Darmstadt, Germany) was prepared (solution 1). Stock solutions of these three protease inhibitors were previously prepared at respectively 5 mg/ml in Methanol, 10 mg/ml in dH₂O and 5 mg/ml in dH₂O and the volumes to be

added to 0.1% triton X-100 solution were based on the number of samples to be treated. 50 μl of solution 1 was added to each pellet and mixed by vortexing. Samples were then incubated for 30 min at 25°C on a shaker (230 rpm) to lyse the cells. Later, 50 μl of 10 mM $\text{MnCl}_2 \cdot 4 \text{H}_2\text{O}$ (USB United States Biochemical, Amersham, Cleveland, Ohio, USA), 50 mM TRIS (Sigma Aldrich, Saint Louis, Missouri, USA) solution in dH_2O pH 7.5 (solution 2) was added to the lysates. After mixing vigorously for a few seconds, samples were incubated at 55°C for 10 min in a water bath. Mn^{2+} is necessary for arginase activity and incubation at 55°C will activate the enzyme. In the meantime, 25 μl of 0.5 M arginine hydrochloride (Sigma Aldrich, Saint Louis, Missouri, USA) solution in dH_2O pH 9.7, was distributed into new microcentrifuge tubes (previously marked). Thereafter, in order to initiate the hydrolysis of arginine, 25 μl of the activated lysate was added to the 25 μl of arginine solution in each microcentrifuge tube. After mixing by vortexing for a few min, samples were incubated at 37°C for 1 h on a shaker (230 rpm). In the meantime, 0.00192 g of urea (Sigma Aldrich, Saint Louis, Missouri, USA) was dissolved in 1 ml dH_2O to obtain a stock solution. From this one solution two dilution patterns were prepared to obtain a wide range of urea concentrations (Table 2.2). Arginine hydrolysis reaction was stopped by adding 400 μl of a mixture containing H_2SO_4 (Sigma Aldrich, Saint Louis, Missouri, USA), H_3PO_4 (Fisher Scientific, Leicestershire, UK) and dH_2O , in a ratio of 1:3:7, to each sample and to the urea standards, previously aliquoted out at 100 μl /microcentrifuge tube. To detect urea in our samples and in the standards, 25 μl of 9% α -isonitrosopropiophenone (α -ISPF) (Sigma Aldrich, Saint Louis, Missouri, USA) in absolute ethanol (Sigma Aldrich, Saint Louis, Missouri, USA) was added to the microcentrifuge tubes. After mixing by vortexing, samples were incubated at 95°C for 45 min. α -ISPF reacts with the urea in the sample developing a purple colour. Samples were then allowed to cool at room temperature for 10 min in the dark. Afterwards, 200 μl of each sample and

standard was plated into a 96-well ELISA plate and OD was read at 540 nm using a SpectraMax 190 microplate spectrophotometer. The concentration of urea in the sample was determined in relation to the standard curve generated. One unit (U) of arginase activity was defined as the enzyme activity that catalysed the production of 1 μmol urea/min.

2.9 Determination of nitric oxide production by BMD murine macrophages

Nitric oxide (NO) production by BMD macrophages after infection or stimulation, was assessed by quantifying the nitrite (NO_2^-) present in the supernatants. Concentration of nitrite was relative to a standard curve constituted of serial concentrations of Sodium Nitrite (NaNO_2) solution. First a 10 mM NaNO_2 stock solution was prepared by dissolving 0.069 g of NaNO_2 (Fisher Chemicals, Leicestershire, UK) in 100 ml of dH_2O . From this stock solution, 1 mM standard solution (top concentration) was prepared by diluting with RPMI. Later, Griess reagent A, 0.5 g of sulphanilamide (Sigma Aldrich, Saint Louis, Missouri, USA) dissolved in 5% H_3PO_4 , and Griess reagent B, 0.05 g of naphthylethylenediamine dihydrochloride (Sigma Aldrich, Saint Louis, Missouri, USA) in dH_2O , were prepared. Once all the reagents were ready, 50 μl of each sample were plated into 96-well ELISA plates. An eleven point standard curve was then generated in duplicate, by adding 100 μl of 1 mM standard solution in the first two wells and using a 2-fold serial dilution in RPMI. The final two wells did not received standard solution and they were considered the blank. Griess reagent A and reagent B were combined in a ratio 1:1 and 50 μl was added to each sample and standard. Plates were then incubated at room temperature for 10 minutes in the dark. After incubation the OD of each well was determined at 540 nm using a SpectraMax 190 microplate spectrophotometer and SOFTMAX PRO software to

obtain the values of OD and to calculate NO_2^- concentration in relation to the standard curve.

2.10 Statistical analyses

Experiments were performed in triplicate and repeated at least twice. Data are shown as the mean \pm s.e.m. of 3 replicates. Statistical analyses were performed using GraphPad Prism 5 program. Data, that were normally distributed, were analysed using the parametric statistical tests one way analysis of variance (ANOVA) and student's *t* test accordingly with the nature of experiments and of the hypothesis to be investigated. One way ANOVA was used to analyse statistical significance within several conditions (more than two) and post-hoc tests, either Tukey's or Dunnett's, were applied respectively to set all pairwise comparisons or to compare each condition mean with the control. Student's *t* test was applied to evaluate significant differences between two conditions. Differences were considered significant with a value of $P < 0.05$.

Table 2.1 ELISA antibody and second reagents applied concentrations

Cytokine	Coating Purified rat anti-mouse antibody (BD biosciences)	Standard Recombinant mouse protein (BD bioscience)	Detection Biotin rat anti- mouse antibody (BD bioscience)
TNF-α	Clone TN3-19.12 Isotype Armenian Hamster IgG1, λ 1 Stock conc 500 μ g/ml Work conc 2 μ g/ml	Stock conc 2 μ g/ml Work conc 10 ng/ml	Clone 516D1A1 Isotype Human Ig, κ Dilution Factor 1:2000
IL-12	Clone C15.6 Isotype Rat IgG1 Stock conc 1000 μ g/ml Work conc 2 μ g/ml	Stock conc 1 μ g/ml Work conc 20 ng/ml	Clone C17.8 Isotype Rat IgG2a Dilution Factor 1:1000
IL-6	Clone MP5-20F3 Isotype Rat IgG1 Stock conc 500 μ g/ml Work conc 2 μ g/ml	Stock conc 0.5 μ g/ml Work conc 20 ng/ml	Clone MP5-32C11 Isotype Rat IgG2a Dilution Factor 1:500

Table 2.2 Urea standard curve dilution patterns

Microcentrifuge Tube	Urea μl	dH₂O μl	Dilution	Conc μg/ml	Conc μg/100 μl
1	500	500	1:2	960	96
2	500	500	1:2	480	48
3	500	500	1:2	240	24
4	500	500	1:2	120	12
5	500	500	1:2	60	6
6	500	500	1:2	30	3
7	500	500	1:2	15	1.5
8	300	100	3:4	1440	/
9	200	200	1:2	720	72
10	200	200	1:2	360	36
11	200	200	1:2	180	18
12	200	200	1:2	90	9

500 μ l of 0.00192 urea in 1 ml distilled H₂O (dH₂O) solution was diluted with 500 μ l dH₂O (microcentrifuge tube 1) and a 2 fold serial dilution in dH₂O was used (from 1 to 7). 300 μ l of 0.00192 urea in 1 ml dH₂O solution was diluted with 100 μ l dH₂O (microcentrifuge tube 8), and from this solution a 2 fold serial dilution in dH₂O was used (from 9 to 12) and then

discarded. Standards were applied in the following order 1, 9, 2, 10, 3, 11, 4, 12, 5, 6, 7 in order to obtain a wide range of urea concentrations.

CHAPTER 3

***Acanthamoeba castellanii* stimulates the production of pro-inflammatory cytokines in murine bone marrow derived macrophages**

3.1 Abstract

Acanthamoeba castellanii is an opportunistic, facultative parasitic protist known to be the agent of a serious, painful and potentially blinding keratitis as well as fatal encephalitis in humans. *A. castellanii* is ubiquitous in nature and approximately 50% to 100% of asymptomatic individuals present specific anti-*Acanthamoeba* antibodies, implying that both the amoeba's pathogenic characteristics and the host immune response might be crucial in either the manifestation of the disease or the asymptomatic recovery. While macrophages are acknowledged as playing a significant role in the outcome of *Acanthamoeba* infections little is known about how the parasite influences macrophage functions. Accordingly, herein, the production of TNF- α , IL-12 and IL-6 by murine bone marrow-derived macrophages (BMDM), following co-culture with trophozoites of the laboratory Neff strain, T4 genotype, of *A. castellanii*, as well as a T4 genotype clinical isolate of *A. castellanii*, was studied. Interestingly, not only did the behaviours of the 2 strains differ following co-cultivation with macrophages at 37°C but the morphology of the Neff but not the clinical strain was significantly altered over the study period. In addition, while the Neff strain induced significant levels of TNF- α IL-12 and IL-6 from macrophages, the clinical strain induced only the latter 2 cytokines, and to a significantly lesser degree than the Neff strain. *Acanthamoeba* culture supernatants were not able to induce macrophage cytokine production indicating this was only a function of viable amoeba. Macrophage cytokine production was, however, inhibited in *Acanthamoeba* co-cultures, though not LPS stimulated cultures, in the presence of either serine or cysteine protease inhibitors, indicating that these *Acanthamoeba* proteases contribute to the induction of cytokine production in murine macrophages.

3.2 Introduction

A. castellanii T4 is the most common genotype in the environment and the most often associated with AK and non-AK infections; indeed it is frequently isolated from the site of infections. This is probably due, not only to its wide distribution in nature as well as in indoor environments, but also due to its virulence factors, and its relative resistance to drugs and disinfectants (Maciver *et al.*, 2013; Walochnik *et al.* 2014).

The release of proteases by *Acanthamoeba* spp. has been associated with virulence (de Souza Carvalho *et al.*, 2011). After binding, *Acanthamoeba* releases proteases that enhance the penetration of the parasite into deeper layers of the host tissue (Sant'ana *et al.*, 2014). As proteases are of major importance in the pathogenicity process, the pattern of their secretion is commonly used to discriminate between pathogenic and non-pathogenic strains of *Acanthamoeba* (Khan *et al.*, 2000). It has also been reported that proteases can be used by *Acanthamoeba* to evade the immune response by degrading immunoglobulins, endogenous proteases inhibitors, and cytokines such as IL-1 (Na *et al.*, 2002, Harrison *et al.*, 2010).

The role of IgA, in preventing the attachment of trophozoites and the high levels of IgG anti-*Acanthamoeba* in asymptomatic individuals suggest that both adaptive and innate immunity are involved in the host defense against *Acanthamoeba* (Cursons *et al.*, 1980; Alizadeh *et al.*, 2001). However, the immune privileged nature of the brain and of the eye requires adaptive immunity to be controlled, and consequently a carefully regulated innate immune system is required to lead the response against *Acanthamoeba* (Said *et al.*, 2004; Clarke & Niederkorn, 2006).

Macrophages are mononuclear phagocytic cells of the innate immune system. They act against pathogens by phagocytosis and by releasing pro-inflammatory cytokines

and reactive oxygen and nitrogen species (Biswas & Mantovani, 2010). They can also act to influence the adaptive immune response and are also potent effectors of this response and depending on the activation state induced they can be anti-microbial or wound healing (Mills *et al.*, 2000). The innate immune system has been shown to be involved in *Acanthamoeba* infections. Indeed, macrophages as well as neutrophils are the predominant cell types present at the site of infection, where they are found alongside trophozoites and cyst forms, and are reported to be the major cells involved in the clearance of the parasites (Larkin & Easty, 1991; van Klink *et al.*, 1996; Knickelbein *et al.*, 2013). However, to date little is known about how *Acanthamoeba* influences macrophage function or whether these facultative parasites can do this directly and/or indirectly via protease release. In this study, therefore, we examined the effects of co-cultivation of trophozoites of both a laboratory and a clinically isolated strain of *Acanthamoeba*, and their respective secreted proteases with murine bone marrow-derived macrophages (MBDM).

3.3 Materials and Methods

3.3.1 Real time microscopy of a co-culture of murine BMD macrophages and trophozoites of *A. castellanii* at 37°C

Murine macrophages were harvested and a suspension of 7×10^5 cells/ml in cRPMI was prepared. 30 μ l of cell suspension was quickly added into 3 channels of the μ -slide VI^{0.4} (ibidi GmbH, Martinsried, Germany), in order to avoid trapped air bubbles. After replacing the lid to cover the reservoirs, the μ -slide was incubated at 37°C 5%CO₂ for 1 h and 30 min to allow macrophages to adhere. Afterwards, each reservoir was fill with 60 μ l of free cell cRPMI, and then the μ -slides were incubated at 37°C 5%CO₂ over night.

The following day, either Neff or clinical trophozoites were harvested and 7×10^5 trophozoites/ml suspensions in cRPMI were prepared. μ -slides were removed from the incubator and macrophages were observed using an inverted microscope to verify if they were healthy. Afterwards, cRPMI was removed from the reservoirs. In the control channel (macrophages alone) 30 μ l of cRPMI were applied; in the co-culture channels, 30 μ l of either Neff or clinical trophozoites suspension were added. Reservoirs were then filled with 60 μ l of cRPMI. Prepared μ -slides were then observed, using an inverted epifluorescence microscope (Nikon, Eclipse TE300), provided with a 37°C chamber that allowed maintenance of the samples at the appropriate temperature while images were acquired. Objectives were used with a magnification of X10, X20 or X40. After manually focusing, images were acquired every 30 sec for a period of 1 h using the software MetaMorph (Molecular devices, Sunnyvale, CA, USA). Thereafter, images were processed using the programme Volocity (Perkin Elmer, Massachusetts, USA). Qualitative observations, regarding

movements of either macrophages alone, or trophozoites alone, or macrophage/trophozoite interactions in co-cultures were drawn.

3.3.2 Evaluation of morphological changes of *A. castellanii* trophozoites when cultured at 37°C 5%CO₂

Trophozoites of either Neff or clinical strains were harvested and prepared as previously described. Once re-suspended in cRPMI trophozoites were plated in 24-well plates at 5×10^5 /well. The morphology of trophozoites was then observed using an inverted microscope [Axiovert25 (Zeiss, Oberkochen, Germany)] at time 0 and after 24 h incubation at 37°C 5%CO₂. Images of trophozoites were obtained using a digital camera through an objective with a magnification of x40. Qualitative observations, regarding changes in trophozoites morphology, at both time points, were drawn.

3.3.3 Inhibition of secreted amoebic proteases

To inhibit the activity of proteases secreted by *A. castellanii* strains, two different proteases inhibitors E64 (Sigma Chemical Co, Poole, UK) and leupeptin hemysulfate salt (Sigma Chemical Co, Poole, UK) were used. Macrophages at day 10 were harvested and plated 1×10^6 /well as described in the general materials and methods. The day after, cRPMI in the wells was discarded and replaced with either E64 or with leupeptin solution in cRPMI, at a final concentration in the wells of 10 µM and 50 µM respectively. cRPMI without protease inhibitors was added into the control wells. Macrophages in these three different experimental conditions were then infected with either Neff trophozoites 1×10^6 /well or clinical trophozoites 1×10^6 /well. LPS was used to stimulate macrophages as positive controls to verify that macrophages were responsive and healthy. In order to assess that cells were not naturally pre-activated either at the beginning, or throughout the experiment,

uninfected macrophages represented the negative control. Plates were incubated at 37°C 5%CO₂ throughout the duration of the experiment. The supernatants were collected after 24 h culture and cytokine production evaluated by ELISA.

3.3.4 Statistical analyses

Experiments were performed in triplicates and repeated at least twice. Data are shown as the mean \pm s.e.m. of 3 replicates. Statistical analysis was performed using GraphPad Prism 5 Software. One way analysis of variance (ANOVA) test and Tukey's and Dunnett's post multicomparison tests were applied to verify the differences within the conditions; they were considered significant with a value of $P < 0.05$.

3.4 Results

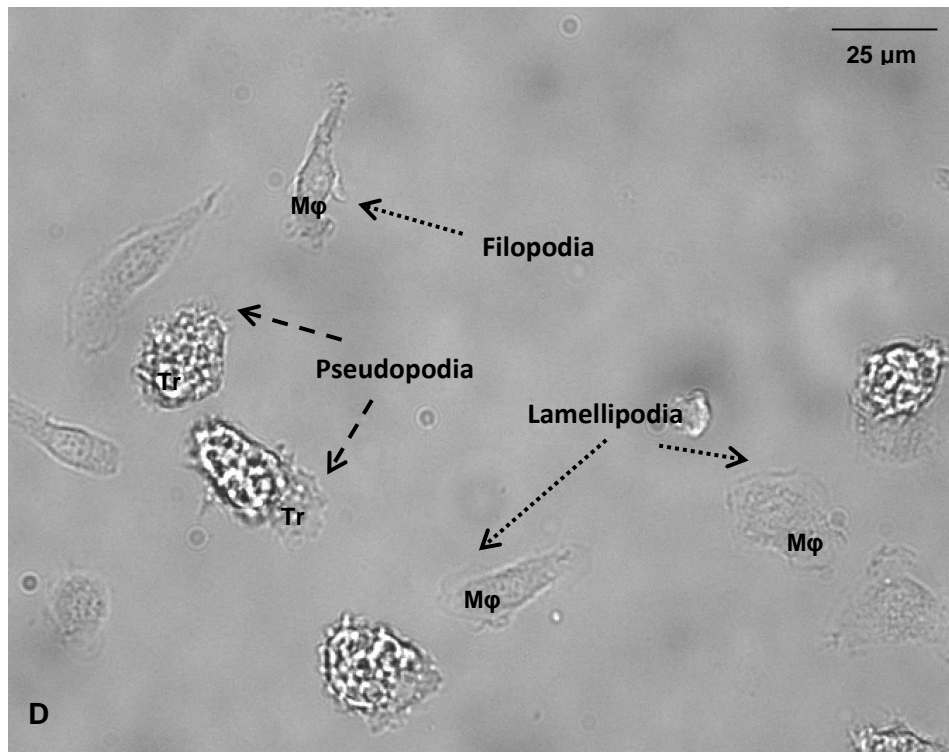
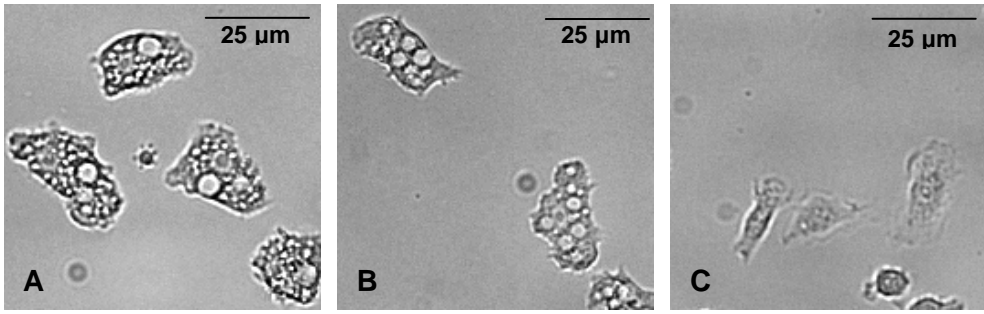
3.4.1 *In vitro* real time imaging of *A. castellanii* infection shows cell-cell interactions between murine BMD macrophages and trophozoites of either the Neff strain or clinical isolate

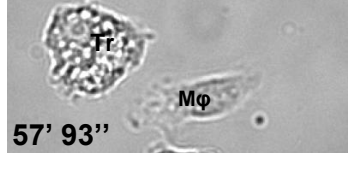
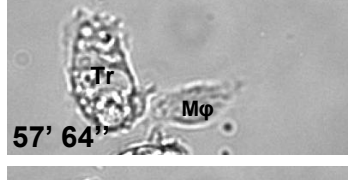
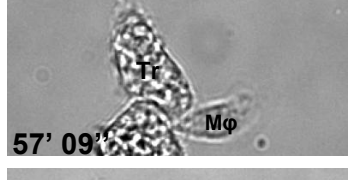
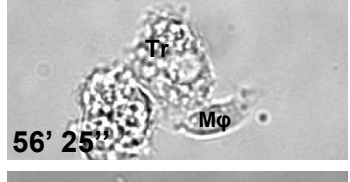
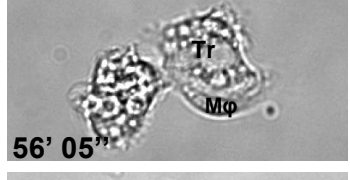
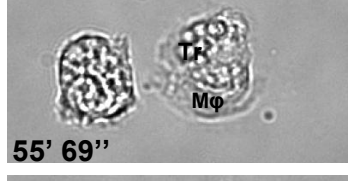
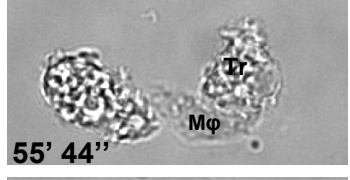
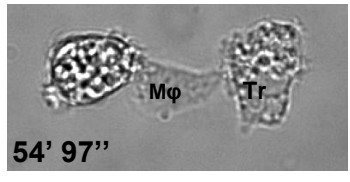
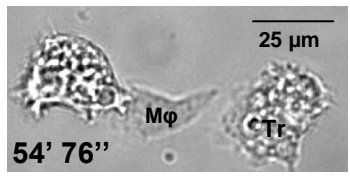
Real time interactions between murine BMD macrophages and trophozoites of either the Neff or clinical strains was investigated *in vitro* by performing time lapse microscopy with an inverted epifluorescence microscope equipped with a 37°C chamber. Macrophages were infected with trophozoites in μ -slides, and images were acquired for 1 h after infection.

Macrophages and Neff trophozoites were found to engage in mutual interactions a few minutes after infection. Trophozoites appeared to increase their activity in the presence of macrophages, showing their characteristic pseudopodia driven amoeboid movement (Fig 3.1 D). Their migration across the field of view was fast and they covered significant distances. Trophozoites were observed to interact with each other. However, this interaction was not prolonged over the time of observation. Macrophages were healthy and actively moving, showing their characteristic features: lamellipodia and filopodia (Fig 3.1-D). However, they were generally less motile than trophozoites. The major features of interactions between macrophages and Neff trophozoites were noted. Trophozoites established contact with macrophages and were observed to roll on the macrophage's surface (Fig 3.1 E); macrophages, after capturing trophozoites with either lamellipodia (Fig 3.1 F) or filopodia (Fig 3.1 G), were unable to maintain this contact and to phagocytose trophozoites. Indeed, no phagocytic invagination was observed at any time during infection.

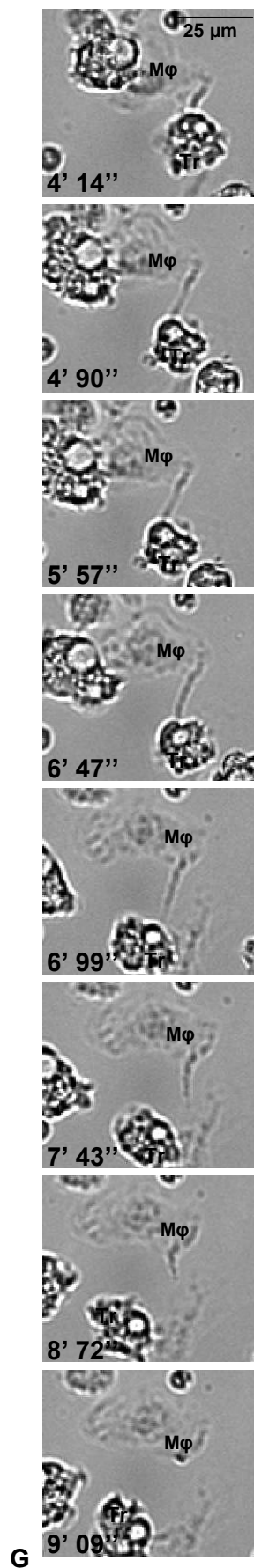
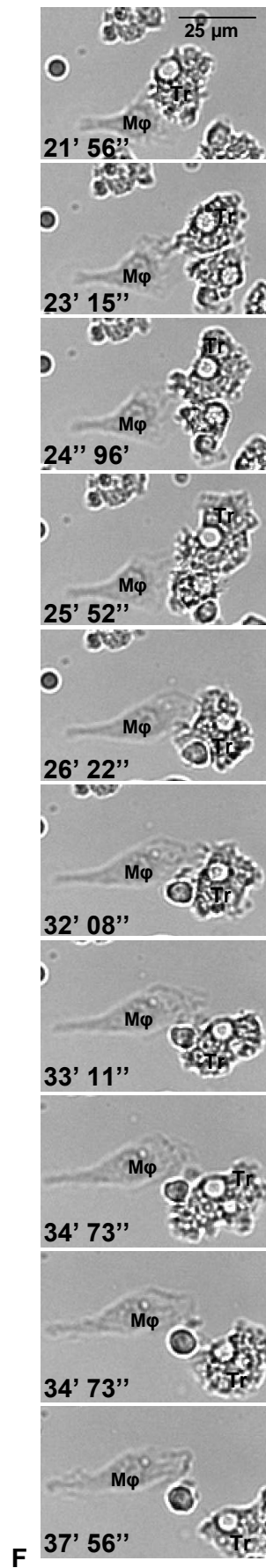
Real time interaction between macrophages and trophozoites of the clinical isolate showed some differences in comparison with macrophage infection with the Neff strain. Both macrophages and trophozoites showed similar motility, distribution and speed, across the field of view. Furthermore, trophozoite division occurred during the observation period (Fig 3.1 H). Trophozoites of the clinical isolate did not engage in any prolonged contact with macrophages nor rolling behavior over their surface. Macrophages were able to actively capture trophozoites through lamellipodia (Fig 3.1 I) and filopodia (Fig 3.1 J). These contacts with macrophages sometimes resulted in trophozoite disruption (Fig 3.1 K) or the induction of their division (Fig 3.1 L). The formation of two wide and long filopodia was often observed in the process of engulfing trophozoites although as far as was observed trophozoites were able to escape phagocytosis (Fig 3.1 M). This event was observed on several occasions during the co-incubation.

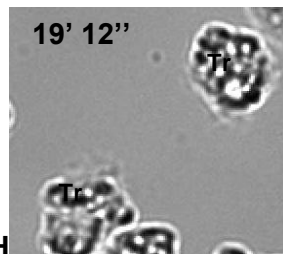
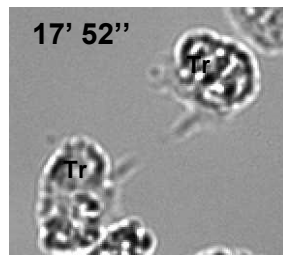
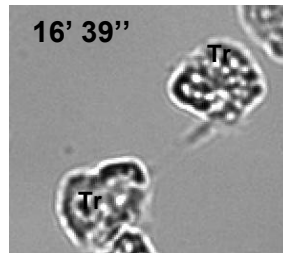
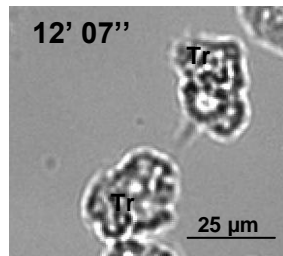
Fig 3.1. Real time images of cell-cell interactions in co-cultures of either *A. castellanii* Neff strain, or clinical isolate strain trophozoites (Tr) with murine BMD macrophages (M ϕ). Murine macrophages were infected with trophozoites in a ratio 1:1 in μ -slides. Images were acquired every 30 sec, for a period of 1 h using an inverted epifluorescence microscope. Sequential observations of cell-cell interactions are presented in a time line constituted of minutes (') and seconds (") from the time 0 (beginning of images acquisition). Selected single images show mono-culture of Neff trophozoites (A), clinical trophozoites (B) and macrophages (C); their characteristic motility features are shown in a micrograph of Neff/macrophage co-culture (D). Micrographs show Neff rolling on macrophage surface (E) or captured by either macrophage lamellipodia (F) or a filopodia (G). Clinical trophozoite division (H); clinical trophozoite captured by either macrophage lamellipodia (I) or fillopodia (J); clinical trophozoites, either disrupted (K) or in division (L) following contact with macrophages; wide and long macrophage filopodia engulfing clinical trophozoite (M)



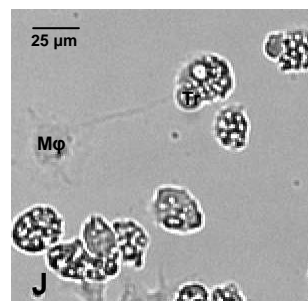
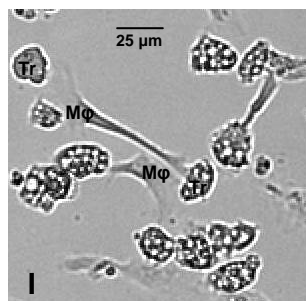


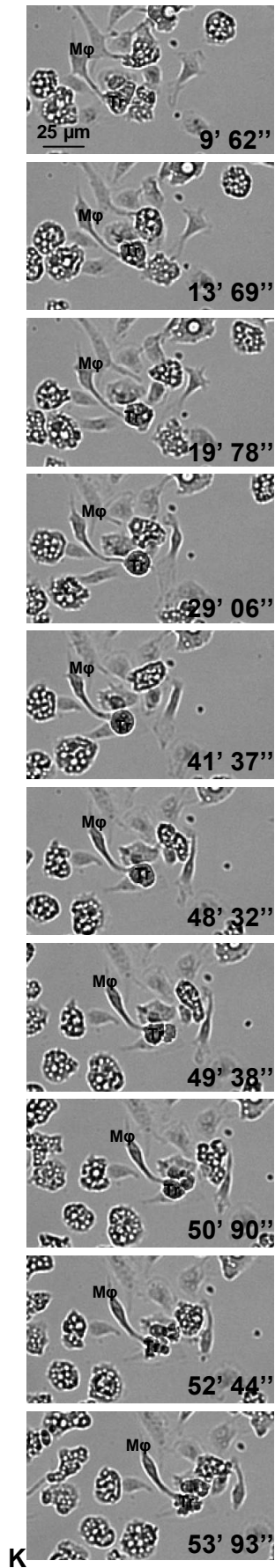
E



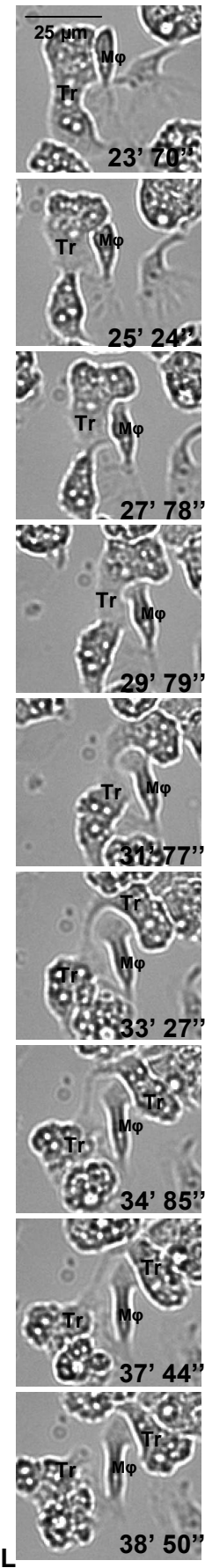


H

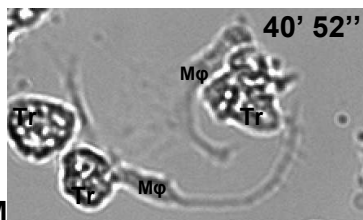
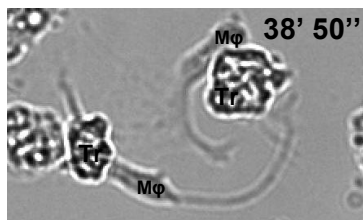
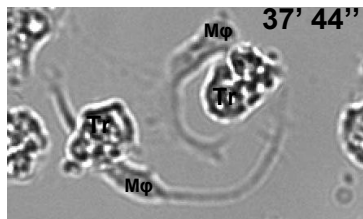
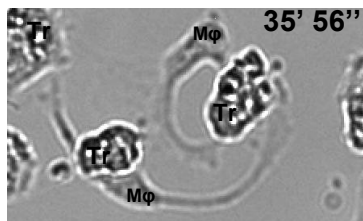
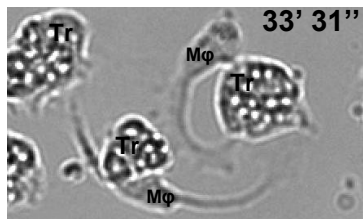
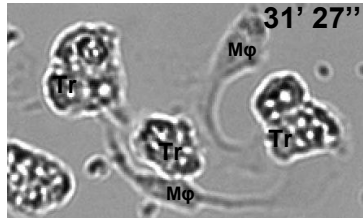
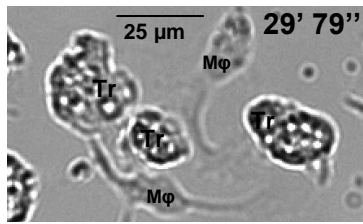




K



L



M

3.4.2 Incubation of *A. castellanii* at 37°C, 5%CO₂ for 24 hours induces differential changes in trophozoite morphology

In order to evaluate if incubation at 37°C, 5%CO₂ was affecting *A.castellanii*, trophozoites of either the Neff stain or the clinical isolate, trophozoites were suspended in cRPMI, plated at a density of 5x10⁵/well in a 24-well plate and placed in the mammalian cell incubator for 24 h. Images were acquired at time 0 and after 24 h.

Incubation of Neff at 37°C, 5% CO₂ induced significant morphological changes in trophozoite morphology. At time 0, Neff strain parasites presented the typical oblong shape, characteristic of attached and moving trophozoites. Furthermore vacuoles (one or two big and several smaller) were visible within amoeba (Fig 3.2 A). After 24 h incubation at 37°C, 5% CO₂, Neff strain trophozoites showed major changes in morphology: trophozoites presented a rounded shape, they had become detached and the cytoplasm generally contained a large single vacuole (Fig 3.2 B).

Conversely, clinical strain trophozoites did not appear to be affected morphologically by incubation at 37°C, 5% CO₂. Prior to incubation, trophozoites appeared healthy and attached to the well. They presented their characteristic internal structures composed of several vacuoles and a visible nucleus (Fig 3.3 A). After 24 h incubation at 37°C 5% CO₂, trophozoites morphology and indeed confluency was similar to that observed at 0 hours (Fig 3.3 B).

Fig 3.2 Morphological changes in Neff trophozoites as shown at time 0 (A) and after 24h incubation at 37°C, 5%CO₂ (B). Trophozoites in cRPMI were plated, in triplicate, at a density of 5×10^5 in 24-well plates. Trophozoite morphology was observed using an inverted microscope with a magnification of x40 and images were acquired using a digital camera. In the images trophozoites were indicated by black (→), and vacuoles by red (→) arrows. Observations were consistent in all three wells.

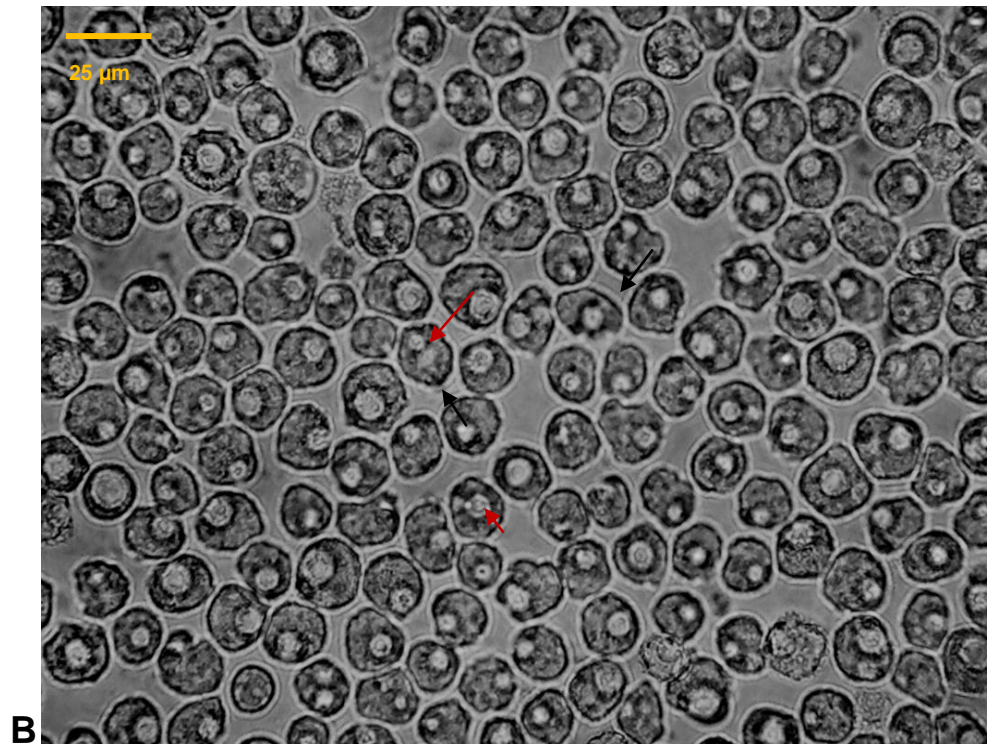
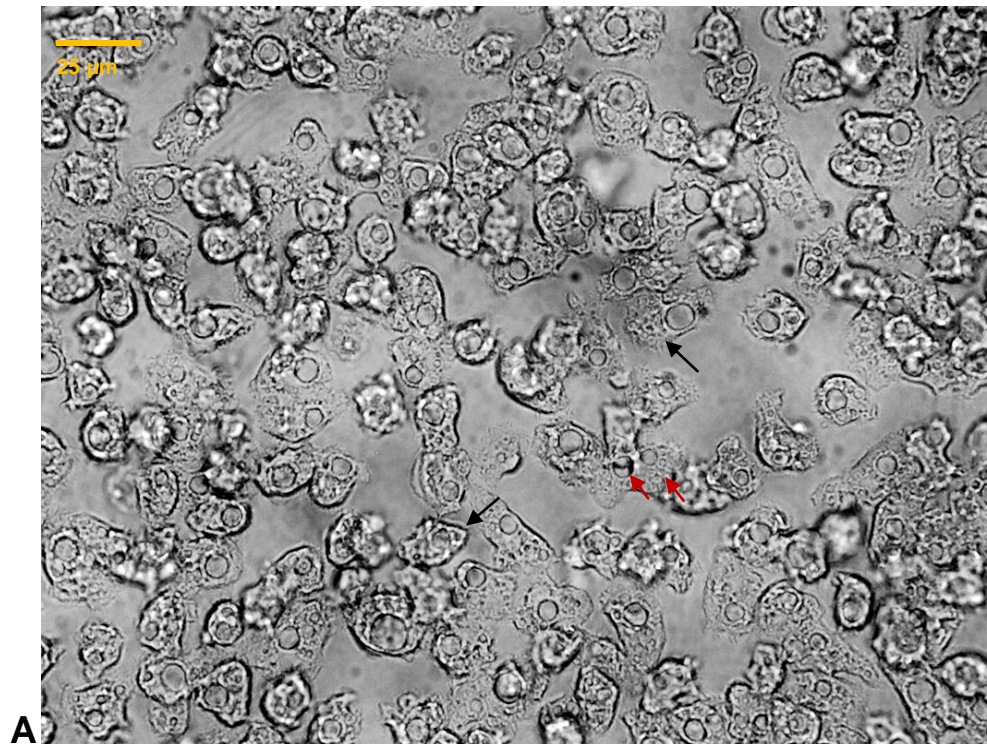
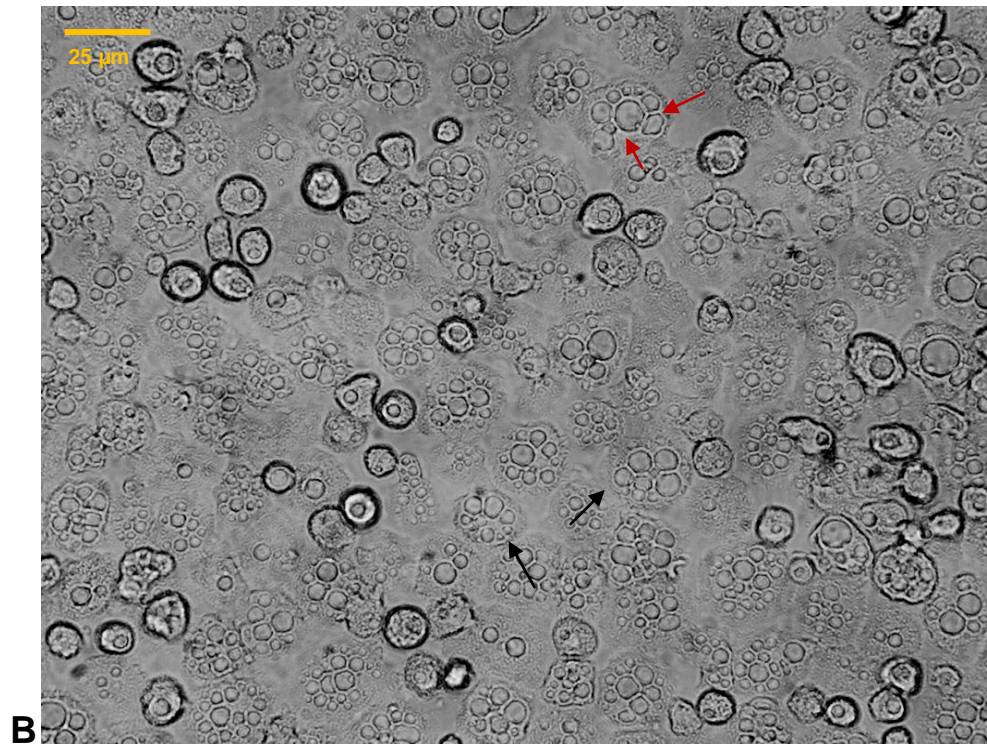
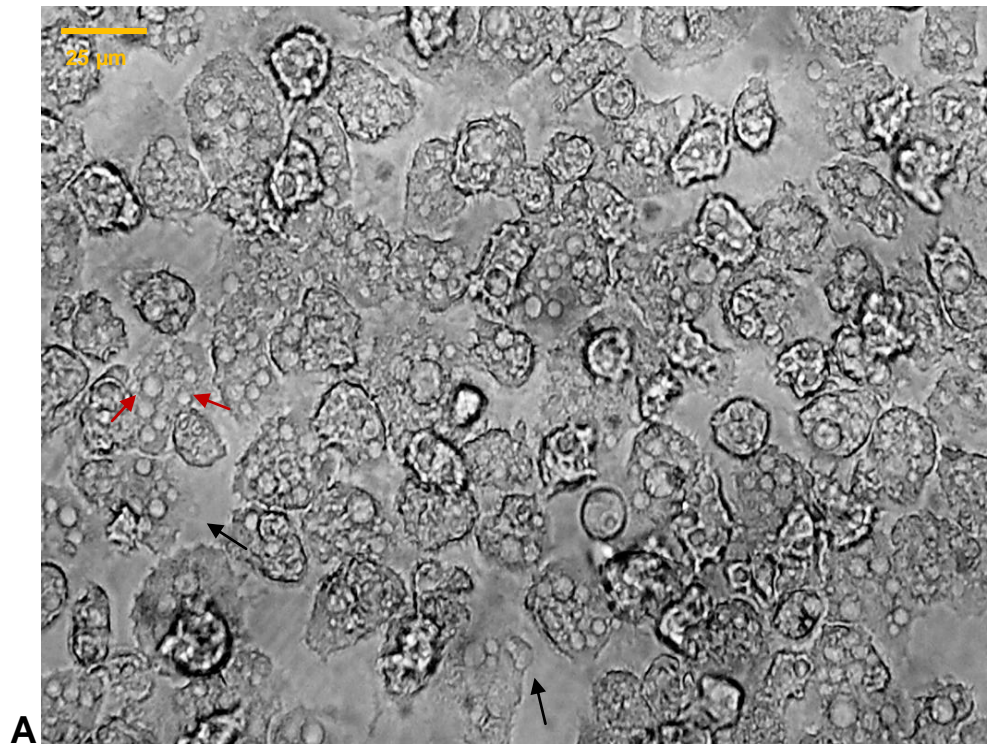


Fig 3.3 Morphological changes in clinical trophozoites at time 0 (A) and after incubation at 37°C, 5%CO₂ (B). Trophozoites in cRPMI were plated, in triplicate, at a density of 5×10^5 in 24-well plates. Trophozoite morphology was observed using an inverted microscope with a magnification of x40 and images were acquired using a digital camera. In the images trophozoites are indicated by black (→), and vacuoles by red (→) arrows. Observations were consistent in all three wells.



3.4.3 *A. castellanii* Neff induces TNF- α , IL-12 and IL-6 production in murine BMD macrophages in a time and trophozoite density dependent manner

In order to evaluate if the production of pro-inflammatory cytokines depends on trophozoite density or on duration of infection, murine macrophages were stimulated with Neff trophozoites at three different ratios trophozoite/macrophage: 1 trophozoite every 1 macrophage (ratio 1:1), 1 trophozoite every 2 macrophages (ratio 1:2) and 1 trophozoite every 10 macrophages (ratio 1:10). Production of TNF- α , IL-12 and IL-6 was then measured at 4, 6, 8, 10, and 24 h after infection.

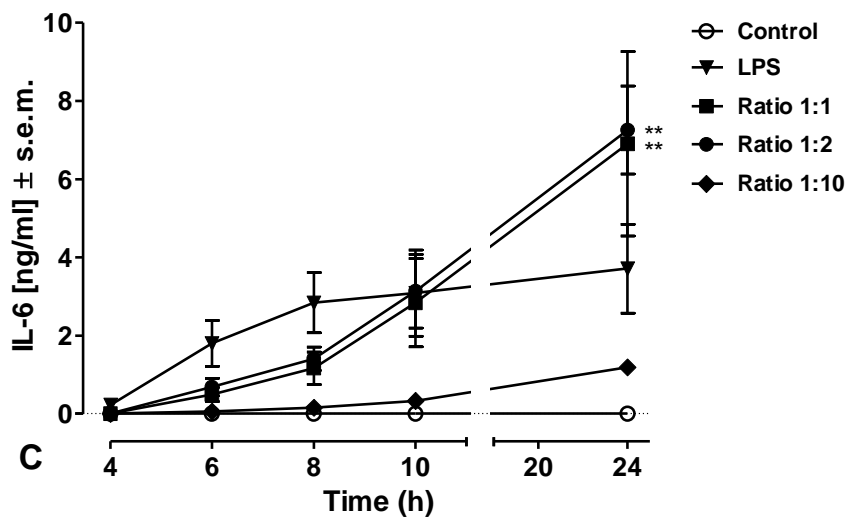
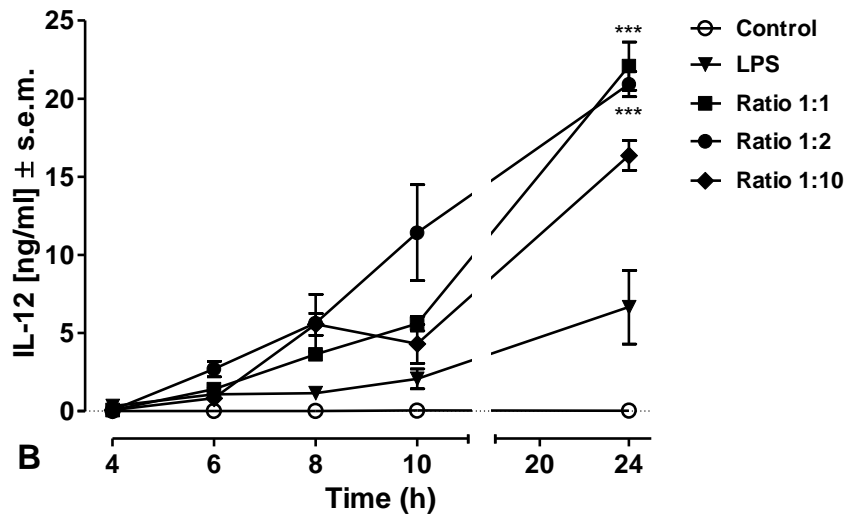
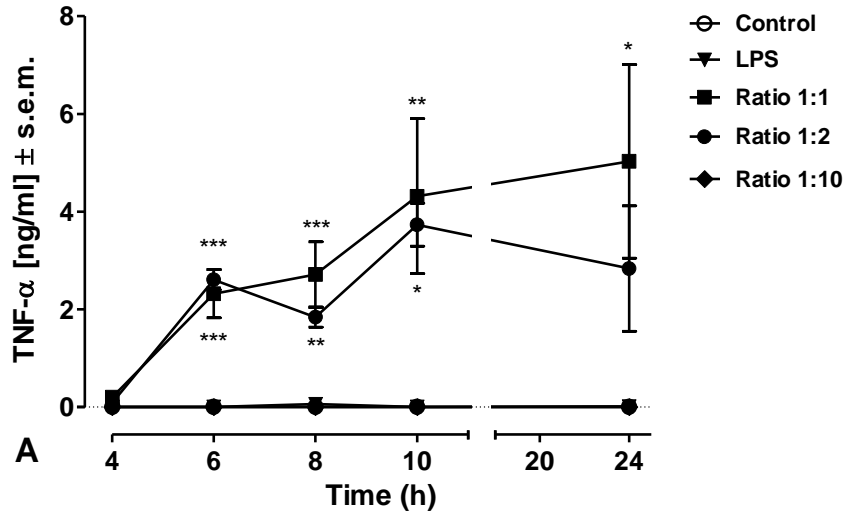
By 6 hrs post-infection significant TNF- α production was detected and at similar levels in cultures with trophozoite/macrophage ratios of 1:2 (2.60 ng/ml, $p < 0.0005$) and 1:1 (2.31 ng/ml, $p < 0.0005$) compared with non-infected controls (Fig 3.4 A). TNF- α production thereafter was maintained at comparably similar levels over 24 hours at these infection ratios. TNF- α production remained significant compared with control non-infected cultures at the higher trophozoite/macrophage 1:1 infection ratio, though not the smaller 1:2 infection ratio at 24h (2.83 ng/ml, $p > 0.05$), throughout the entire time course of the experiment. TNF- α production induced by the trophozoite/macrophage infection ratio 1:10 was below the detectable value at all time points (Fig 3.4 A). No TNF- α was detectable in non-infected macrophage or LPS stimulated macrophage cultures at any time (Fig. 3.4-A).

By comparison with TNF- α production, IL-12 production increased progressively throughout the course of the study in all trophozoite infected groups, reaching the highest concentrations at 24h post-infection compared with control cultures for all three trophozoite/macrophage infection ratios investigated. At 24h the

trophozoite/macrophage infection ratios of 1:1 and 1:2 had induced similar levels of IL-12 to each other but significantly higher IL-12 than the other experimental groups. LPS stimulated macrophages produced IL-12 in a time dependent manner, peaking at 24 h post-stimulation. However, LPS induced less macrophage IL-12 production than trophozoite/macrophage infections. No IL-12 was detectable in non-infected macrophage cultures at any time (Fig 3.4 B).

In a similar manner to IL-12, IL-6 production by murine macrophages infected with trophozoites increased throughout the course of infection and levels recorded were significantly greater from the trophozoite/macrophage infection ratios of 1:1 and 1:2 than non-infected macrophage cultures from 8h post-infection. The trophozoite/macrophage infection ratios of 1:1 and 1:2 were equally effective at inducing IL-6 production and significantly more so than a trophozoite/macrophage infection ratio of 1:10 (Fig 3.4 C). Interestingly the dynamics and profile of LPS induced macrophage IL-6 production are quite dissimilar from that induced by trophozoite infection. LPS induced a significantly more rapid IL-6 production than trophozoite/macrophage infection ratios of 1:1 and 1:2 that peaked at 8 h post-stimulation. No IL-6 was detectable in non-infected macrophage cultures at any time.

Fig 3.4 Release of TNF- α (A), IL-12 (B) and IL-6 (C) at 4, 6, 8, 10, 24 h after co-incubation with *A. castellanii* Neff trophozoites. 1×10^6 murine macrophages, obtained from BALB/c mice, were challenged with either 1×10^6 (Ratio 1:1) or 5×10^5 (Ratio 1:2) or 1×10^5 (Ratio 1:10) trophozoites of *A. castellanii* Neff strain. LPS was used as a positive control at a concentration of 200 ng/ml, whereas uninfected macrophages (Control) were considered the negative control. Experiments were repeated three times. Results represent the mean \pm standard error of n=6. Two way ANOVA could not be applied, since the interaction between the stimuli and time was statistically significant and the statistical analysis for the time and stimuli effects are therefore difficult to interpret. For this reason, one way ANOVA was applied for each time points. Tukey's multiple comparison test was performed to evaluate differences within the conditions means at each time point. In the graphs, significances within the different conditions are indicated as follow: for values of $p < 0.05$ *; $p < 0.005$ **; $p < 0.0005$ ***. In the table A LPS, Ratio 1:10 and control show values equal to 0. Note that trophozoite/macrophage infection higher ratios induce higher cytokine production. Trophozoite-induced TNF- α production is induced early in infection and is maintained thereafter, whereas IL-6 and IL-12 production peaks at 24 hrs.



3.4.4 Clinical isolate of *A. castellanii*, belonging to genotype T4, stimulates lower cytokine production than Neff, classical laboratory strain

Differences in the levels of macrophage cytokines induced by infection with either a clinical isolate (clinical) or a classical laboratory strain (Neff) of *A. castellanii* were investigated. Based on the effectiveness of cytokine induction in the studies above, murine BMD macrophages were infected at the ratios of trophozoites/macrophages 1:1 and 1:2. Samples were collected at an early time point and a late time point, respectively 8 h and 24 h after infection.

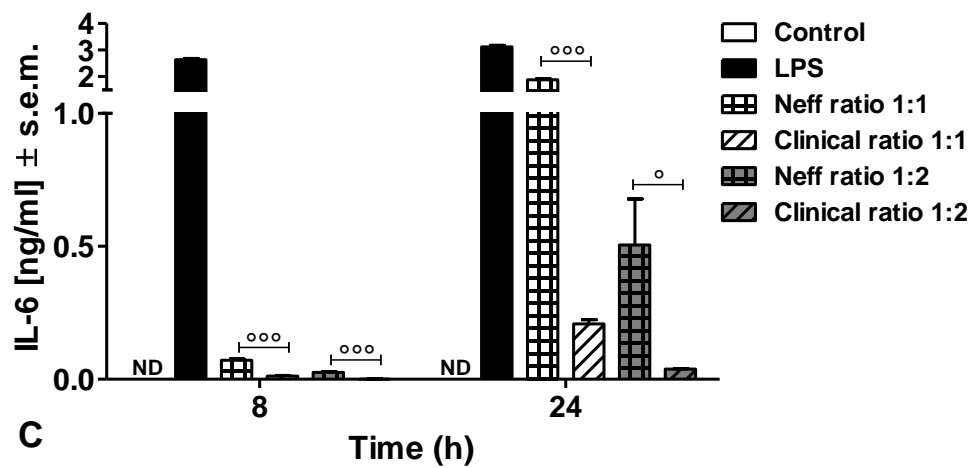
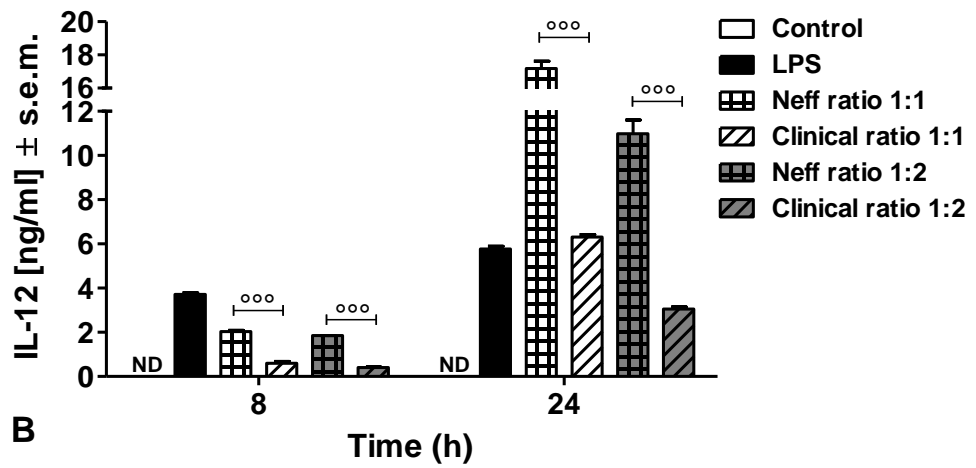
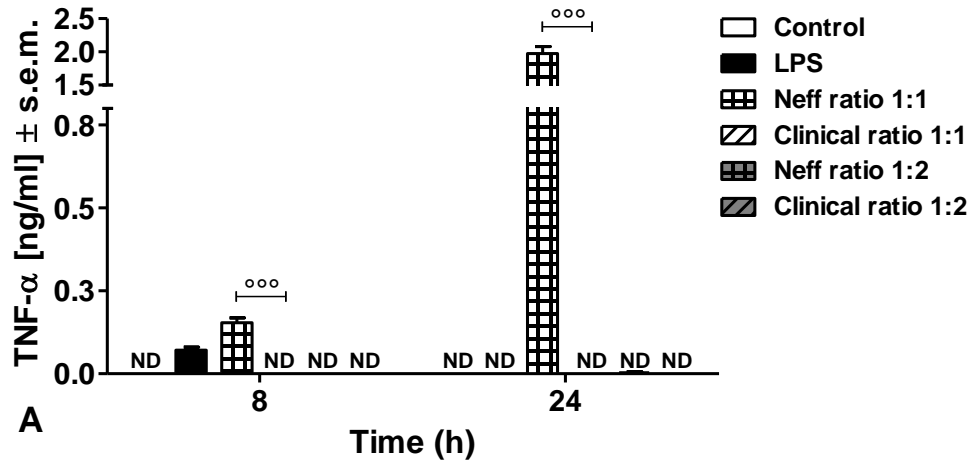
TNF- α production was induced significantly by the Neff strain trophozoites at the 1:1 trophozoite/macrophage infection level both at 8 and 24 h ($p < 0.0005$) post-infection. In comparison, TNF- α levels at these times after challenge with clinical trophozoites, was below detectable values. This discrepancy in macrophage induced TNF- α production, between Neff and clinical isolate trophozoites of *Acanthamoeba* was significant ($p < 0.0005$) (Fig 3.5 A).

In comparison, IL-12 production by macrophages was induced by incubation with Neff, and with clinical trophozoites with highest levels being detected at 24 h post-infection. IL-12 production by macrophages was greater following incubation with Neff strain trophozoites than the clinical isolate at both 8 h and 24 h ($p < 0.0005$) (Fig 3.5 B). These results were consistent at both trophozoite/macrophage infection levels.

IL-6 production by macrophages was significantly induced by Neff strain trophozoites compared with non-infected macrophage cultures at both at 8 and 24 h ($p < 0.0005$) post-infection. In addition macrophages incubated with Neff strain

trophozoites produced significantly more IL-6 than macrophages incubated with clinical strain trophozoites. By comparison trophozoites of the clinical strain failed to induce IL-6 production significantly above that produced by non-infected macrophages at 8 h post-infection. (Fig 3.5 C). The kinetics of LPS and Neff trophozoite induced macrophage IL-6 production were quite distinct with LPS inducing a significantly earlier peak induction of this cytokine.

Fig 3.5 Release of TNF- α (A), IL-12 (B) and IL-6 (C) at 8 and 24 h after co-incubation with *A.castellanii* trophozoites. 1×10^6 murine macrophages, obtained from BALB/c mice, were challenged with either 1×10^6 or 5×10^5 trophozoites of either the Neff strain (respectively Neff ratio 1:1 and Neff ratio 1:2) or clinical isolate (respectively Clinical ratio 1:1 and Clinical ratio 1:2). LPS, at a concentration of 200 ng/ml, (LPS) was used as a positive control, whereas uninfected macrophages (Control) were considered the negative control. The experiment was repeated twice. Results represent the mean \pm standard error of $n=3$. One way ANOVA was applied for each time point and Tukey's multiple comparison test was performed to evaluate differences within the conditions means at each time point. In the graphs, significant differences between Neff and clinical strains are indicated as follow: for values of $p < 0.05$ °; $p < 0.0005$ °°. Values below the detectable levels are indicated in the graphs as ND (not detected). Note that *Acanthamoeba* Neff strain induces higher levels of macrophage pro-inflammatory cytokines than *Acanthamoeba* clinical isolates. This event is observed both at the early time points (8 hrs post co-incubation) and later time points (24 hrs post co-incubation).



3.4.5 Amoeba-derived cell free conditioned medium fails to induce pro-inflammatory cytokines by murine BMD macrophage

In order to evaluate if molecules released in the medium by *A. castellanii* were able to induce cytokine production by murine macrophages, amoeba-derived cell free conditioned medium from either Neff or Clinical strain cultured trophozoites was obtained and used undiluted and non-fractionated to stimulate macrophages. Furthermore, the differences between whole trophozoite and trophozoite-secreted molecules in stimulating pro-inflammatory cytokines were investigated. In these experiments, the synthetic triacetylate lipopeptide PAM3CSK4, specific TLR1/2 agonist, was included as a positive control as well as LPS. Supernatant samples for evaluating cytokine production were taken at 24 h after infection.

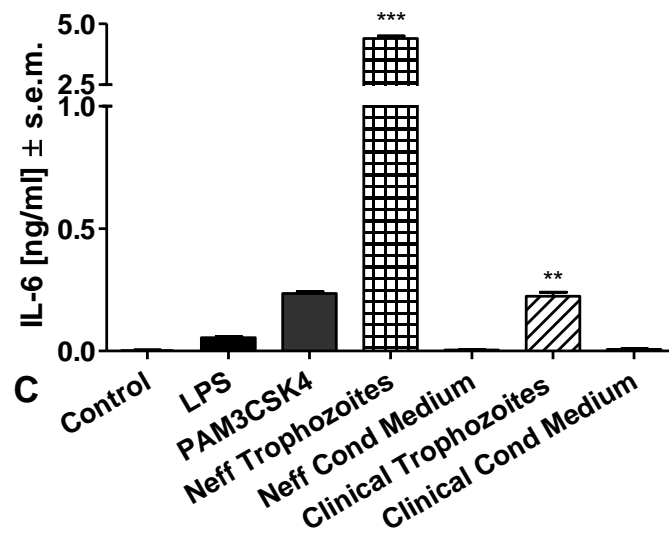
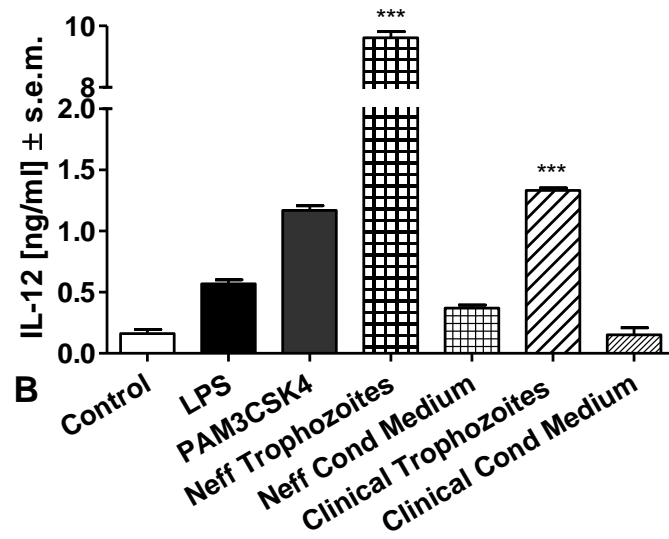
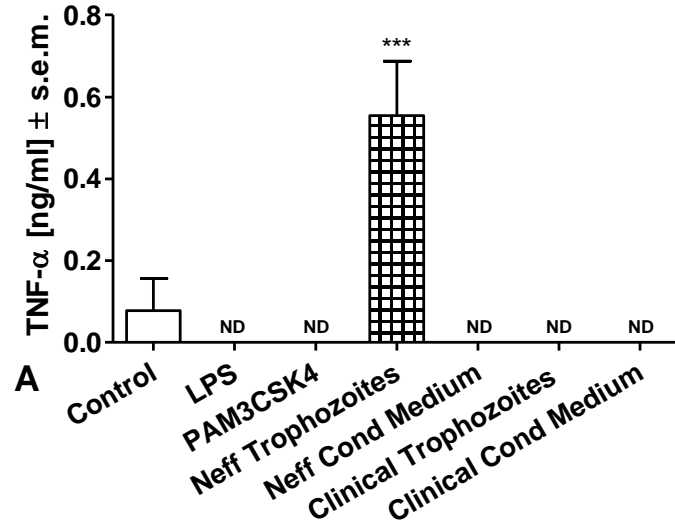
Significant TNF- α production by stimulated or infected macrophages, compared with non-stimulated control macrophages, was only detected after challenge with Neff strain trophozoites, reaching a value of 0.554 ng/ml ($p < 0.0005$) (Fig 3.6 A).

IL-12 production by macrophages was induced significantly by the trophozoites of both the Neff and Clinical strains with concentrations of 9.611 ng/ml ($p < 0.0005$) and 1.331 ng/ml ($p < 0.0005$) respectively. In addition Neff trophozoites stimulated more IL-12 production from macrophages than their clinical strain counterparts. By comparison, trophozoite-derived cell free conditioned medium obtained from either Neff (0.371 ng/ml, $p > 0.05$) or clinical (0.152 ng/ml, $p > 0.05$) trophozoite cultures failed to stimulate any significant production of IL-12 by murine macrophages (Fig 3.6 B).

As with IL-12 production IL-6 production by macrophages was induced significantly by the trophozoites of both the Neff and Clinical strains with concentrations of 4.397 ng/ml ($p < 0.0005$) and 0.225 ng/ml ($p < 0.005$) respectively. In addition Neff

trophozoites stimulated more IL-6 production from macrophages than their clinical strain counterparts. By comparison, trophozoite-derived cell free conditioned medium obtained from either Neff or clinical trophozoite cultures failed to stimulate any significant production of IL-6 by murine macrophages (respectively 0.004 ng/ml and 0.007 ng/ml) (Fig 3.6 C).

Fig 3.6 Release of TNF- α (A), IL-12 (B) and IL-6 (C) at 24 h after co-incubation with *A. castellanii* trophozoites or amoeba-derived conditioned medium. 1×10^6 murine macrophages, obtained from BALB/c mice, were challenged with 1×10^6 trophozoites of either *A. castellanii* Neff strain (Neff trophozoites) or clinical isolate (clinical trophozoites). Furthermore, they were stimulated with undiluted and not fractionated amoeba-derived cell free conditioned medium obtained from either the Neff (Neff cond medium) or clinical (clinical cond medium) strains. LPS and PAM3CSK4 at respectively 200 ng/ml (LPS) and 320 ng/ml (PAM3CSK4) were used to stimulate macrophages as positive controls. Uninfected macrophages (Control) were considered the negative control. The experiment was repeated twice. Results represent the mean \pm standard error of $n=3$. One way ANOVA was applied and Dunnett's multiple comparison test was performed to evaluate differences within the conditions means. In the graphs, significant differences between each stimuli and Control are indicated as follow: for values of $p < 0.005$ **; $p < 0.0005$ ***. Values below the detectable levels are indicated in the graphs as ND (not detected). Cytokines production in trophozoite/macrophage infection conditions has confirmed the results previously found. In addition, amoeba-derived cell free conditioned medium, obtained from either Neff strain or clinical, failed to induce significant production of cytokines in murine macrophages.



3.4.6 *A.castellanii*-secreted proteases stimulate the production of pro-inflammatory cytokines by murine BMD macrophages

The role of *Acanthamoeba* secreted proteases in influencing trophozoite mediated macrophage cytokine production was investigated. For this purpose murine macrophages were treated prior to infection with either leupeptin, a serine and cysteine proteases inhibitor, or E64 that selectively inhibits cysteine proteases. The choice of these two protease inhibitors relied on the specific composition of the *Acanthamoeba* secretome that mainly comprises serine and cysteine proteases. Macrophages in cRPMI were considered the negative inhibitor control. Immediately after addition of inhibitors macrophage cultures were infected with either Neff or clinical strain trophozoites. Pro-inflammatory cytokine production was evaluated after 24 h.

TNF- α production by macrophages induced by *Acanthamoeba* in these studies was below the detectable levels.

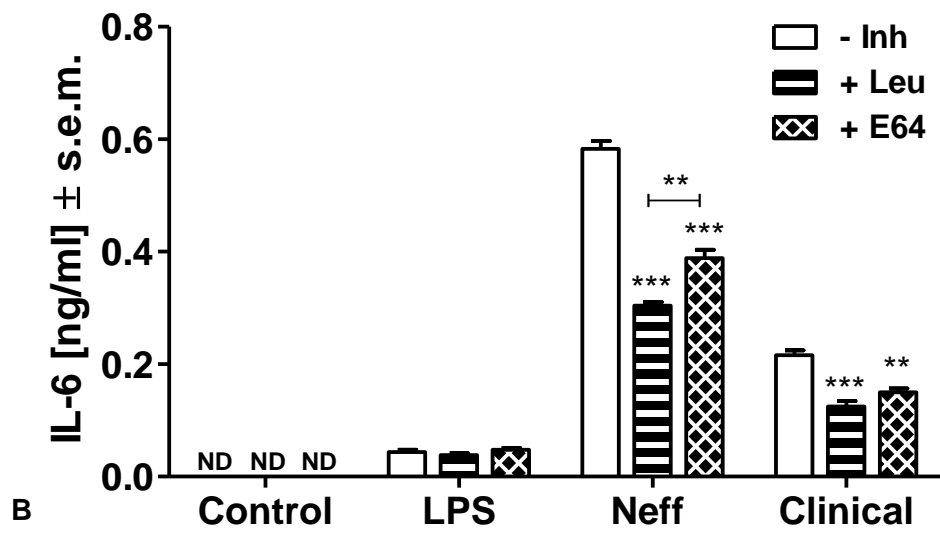
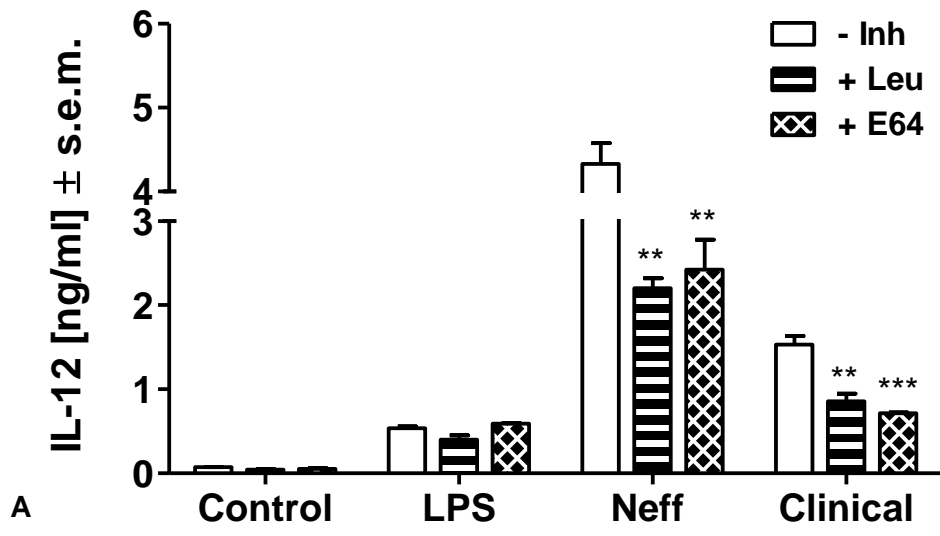
IL-12 production by macrophages was induced by co-culture with either the Neff or clinical strains of trophozoites in the absence of protease inhibitors, with a concentration of 4.329 ng/ml and 1.530 ng/ml respectively. Macrophage production of this cytokine was significantly reduced when leupeptin was present, after infection with either Neff (2.203 ng/ml, $p < 0.005$) or clinical (0.857 ng/ml, $p < 0.005$) strain trophozoites. Similarly, macrophage IL-12 production was significantly lower after challenge with either Neff (2.422 ng/ml, $p < 0.005$) or Clinical strain (0.717 ng/ml, $p < 0.0005$) trophozoites when macrophages were treated with E64 in comparison with the control cultures lacking inhibitor (Fig 3.7 A).

Both Neff (0.583 ng/ml) and clinical (0.216 ng/ml) trophozoites induced IL-6 production by murine macrophages in the absence of proteases inhibitors. As with

macrophage IL-12 production, IL-6 levels were significantly reduced when macrophages were challenged with Neff or clinical strains trophozoites ($p < 0.0005$) and treated with leupeptin. Treatment of cultures with E64 also induced a significant reduction in the levels of IL-6 produced by macrophages after challenge with either Neff (0.388 ng/ml, $p < 0.0005$) or clinical (0.149 ng/ml $p < 0.005$) strains of *Acanthamoeba* trophozoites. Furthermore, a difference in IL-6 production was found between the protease inhibitors in macrophage cultures incubated with Neff trophozoites; leupeptin (0.303 ng/ml) was more efficient at inhibiting IL-6 than E64 ($p < 0.005$). This difference in macrophage IL-6 production was not demonstrated following incubation with clinical strain trophozoites (Fig 3.7 B).

Neither of the inhibitors significantly influenced LPS induced macrophage IL-12 or IL-6 production indicating that their activities were targeting trophozoite protease activity specifically (Fig 3.7 A and B).

Fig 3.7 Release of IL-12 (A) and IL-6 (B) at 24 h after treatment with protease inhibitors prior co-incubation with *A. castellanii* trophozoites. 1×10^6 murine macrophages, obtained from BALB/c mice, were infected with 1×10^6 trophozoites of either *A.castellanii* Neff (Neff) strain or *A.castellanii* clinical isolate (Clinical) in three different experimental conditions: in cRPMI (- Inh), in cRPMI supplemented with leupeptin 50 μ M (+ Leu) and in cRPMI supplemented with E64 10 μ M (+ E64). LPS, at a concentration of 200 ng/ml (LPS) was included as positive control, whereas uninfected macrophages (Control) consisted of the negative control. The experiment was repeated twice. Results represent the mean \pm standard error of n=3. One way ANOVA was applied and Tukey's multiple comparison test was performed to evaluate differences within the three different conditions means. In the graphs, significant differences within each condition are indicated as follow: for values of $p < 0.005$ **; $p < 0.0005$ ***. Values below the detectable levels are indicated in the graphs as ND (not detected). Note that *Acanthamoeba*-induced macrophage production of IL-6 and IL-12 is significantly inhibited in the presence of serine and cysteine proteases. This inhibition is observed in both the infection with either Neff or clinical trophozoites. In this experiment, TNF- α was below the detectable levels for all the condition.



3.5 Discussion

A. castellani is a free-living organism and individuals are constantly exposed to these amoebae in their everyday life. Although the opportunities of becoming infected with this protozoan are high, few cases have been reported. Patients with an immune deficiency are particularly susceptible to infection with these organisms and they usually present with the most severe and deadly amoebic disease, granulomatous amoebic encephalitis. On the other hand, *Acanthamoeba* Keratitis can also occur in immune competent individuals, and contact lens wearers in particular are more susceptible to infection (Lorenzo-Morales *et al.*, 2013). While, previously, keratitis was attributed to either bad hygiene or to corneal trauma caused by the lens, a recent study demonstrated that prolonged use of contact lenses may impair innate immunity at the ocular surface (Pan and Wu, 2012; Li & Sun, 2008; Thakur & Willcox, 2000). Overall therefore, it is the general consensus that the immune system is critical in determining the outcome of *Acanthamoeba* diseases in humans.

Macrophages play an essential role during microbial infections. Upon activation, macrophages release pro-inflammatory mediators, such as pro-inflammatory cytokines, in order to orchestrate the consequent innate and adaptive immune responses (Murray & Stow, 2014). During *Acanthamoeba* infections, macrophages have been observed within the infected tissues along with trophozoite forms (Harrison *et al.*, 2010; Knickelbein *et al.*, 2013). Furthermore macrophages have been reported as being essential in the resolution of the infections (Clarke *et al.*, 2006). Nevertheless, little is known about the interaction between *Acanthamoeba* and macrophages and in particular the pattern of macrophage pro-inflammatory cytokines that both whole trophozoites and amoeba-released products induce. Our studies have shown, for the first time, the profile and kinetics of *Acanthamoeba*-induced pro-inflammatory cytokines in murine BMD-macrophages post-infection. We

found that macrophages produced TNF- α , IL-12 and IL-6 in a time-dependent manner after incubation with trophozoites of *Acanthamoeba*. In particular, TNF- α was produced at significant levels compared with non-infected cultures after 6 h and these levels were maintained throughout the period of study. This would be consistent with the role of TNF- α as an “early cytokine”, rapidly released by macrophages to activate neutrophils and endothelial cells (Turner *et al.*, 2014). Interestingly, only the laboratory Neff strain induced this microbicidal cytokine from macrophages and not the clinical isolate and this may in part explain the virulence of the latter strain. By comparison, macrophage IL-12 and IL-6 levels increased progressively throughout the study period and was induced by both strains of *Acanthamoeba*. These cytokines, not only play important role in the activation of the innate immune cell functions, but they are also involved in the activation and proliferation of the adaptive immune cells (Ma, 2001; Jones, 2005). IL-12, in particular, plays a pivotal role in several microbial infections (Biron & Gazzinelli, 1995). For example, it induces phagocyte cytotoxic activity and the production of RNS and ROS; it stimulates IFN- γ production by natural killer (NK) cells and promotes T_H1 responses (Trinchieri, 2003). In addition IL-6 acts during early and late innate immune events; indeed, it damps the early innate immune responses by inducing neutrophils apoptosis and the production of IL-1 and TNF- α antagonists, initiating the late innate immune events, such as the recruitment of monocytes and their differentiation into macrophages. Subsequently IL-6 promotes T cells responses, enhancing their survival, inhibiting their apoptosis and modulating the differentiation of CD4+ cells into T_H1, T_H2, T_H17 and Treg cells (Jones, 2005). In our study, we also found that higher number of trophozoites induced higher cytokine production, suggesting that initiation of the immune response events can be dependent on trophozoite density at the site of infection.

Acanthamoeba can grow axenically in laboratory conditions. However, this can lead to loss of virulence factors, encystment capability and to less susceptibility to drugs (Koehsler *et al.*, 2009). Therefore, we compared the ability of *A.castellanii* Neff strain, a classical laboratory strain, and *A.castellanii* isolated from a case of bilateral keratitis to induce macrophage cytokine production. Interestingly, macrophages incubated with clinical isolate trophozoites produced significantly less cytokines than macrophages incubated with the Neff strain under similar conditions. It is known that *Acanthamoeba* induces cell damage with both contact dependent and contact independent mechanisms inducing cell lysis (Leher *et. al*, 1998) and apoptosis (Mattana *et al.*, 2001; Zheng *et al.* 2004). Therefore, lower cytokine production by macrophages incubated with the clinical strain could be due to this strain inducing comparatively more damage to macrophages than the Neff strain. Furthermore, pathogenic strains are more resistance to higher temperatures than non-pathogenic strains (Becker-Finco *et al.*, 2013). Indeed, when Neff trophozoites were incubated at 37°C, 5% CO₂, for 24h, their morphology changed significantly and the trophozoites became rounded and detached. By comparison, clinical isolate trophozoites morphologically appeared not to be affected by temperature. All these observations, indicate that clinical isolate trophozoites at high temperatures remain metabolically active and dividing, and therefore still able to influence macrophage activity and viability.

Macrophages were also stimulated with amoeba-derived cell free conditioned medium from either the Neff or clinical strains. The protocol for obtaining amoeba-derived cell free conditioned medium has been previously optimized and reported (Mattana *et al.*, 1997). Its characterization, through SDS-PAGE electrophoresis, showed 10 different bands presenting weights between 97 kDa and 16.4 kDa (Mattana *et al.*, 1997). Subsequently, the presence of ADP in these preparations,

was demonstrated by capillary electrophoresis (Mattana *et al.*, 2001). Although it has previously been demonstrated that amoeba-derived conditioned medium was capable of inducing pro-inflammatory cytokines IL-1 β , TNF- α , IL-6, by the monocytic cell line THP-1 (Mattana *et al.*, 2002), these metabolized supernatants did not induce murine macrophage cytokine production. This discrepancy in the results could be due to the different experimental conditions, such as period of stimulation, as well as with the different cellular model.

These results would also suggest that trophozoites activate macrophages to produce cytokines via molecules present on their surface rather than via excretory secretory products with a long half-life. However, whether the activation of macrophages in our trophozoite infection model is exclusively contact-dependent cannot be determined and soluble molecules with a short-half life or working in tandem with surface moieties may also be involved. Amoebic or even macrophage enzymes, such as ectonucleotidase (Deaglio & Robson, 2011), as well as binding between mammalian and amoebic surface moieties might be necessary for the activation and/or the release of the immunogenic molecules into the external milieu. In addition, stimulation of macrophages with amoeba-derived cell free conditioned medium did not reveal any significant differences between Neff and clinical strain derived media, reinforcing the conclusion that strain differences are dependent on the presence of active trophozoites.

The importance of amoebic proteases in pathogenicity (Alsam, 2005), immune evasion and differentiation mechanisms (Moon *et al.*, 2012; Leitsch *et al.*, 2010) has been widely discussed previously. However, more recently, studies have focused their attention on the role of these molecules in triggering the immune response (Tripathi *et al.*, 2012; Tripathi *et al.*, 2013; Tripathi *et al.*, 2014). Indeed, it has been demonstrated that the amoebic serine protease MIP-133, is not only involved in the

invasion of the trophozoites within the host tissue, but also it stimulates apoptosis and pro-inflammatory cytokine production in human corneal epithelial cell line, via the cytosolic phospholipase $A_{2\alpha}$ (Tripathi, *et al.* 2012). In the present study, it was demonstrated, for the first time, that both serine and cysteine amoebic proteases were capable of inducing IL-12 and IL-6 production by murine macrophages. Trophozoite-induced macrophage IL-12 production was inhibited equally when either leupeptin (serine and cysteine proteases inhibitor) or E64 (selective cysteine proteases inhibitor) were present, suggesting that IL-12 was equally stimulated by serine and cysteine proteases. Macrophage IL-6 production induced by either Neff or clinical strains decreased in the presence of either inhibitor. However, during Neff strain infection of macrophages, leupeptin was more effective than E64 in inhibiting IL-6 production, indicating that serine proteases might be the major protease responsible for inducing this cytokine. TNF- α detection was below the detectable levels and the ELISA assay did not provide robust results in comparison with IL-12 and IL-6, although optimization of the ELISA protocol was performed. On the other hand, TNF- α might be released during the early phase of co-incubation and due to its instability might be progressively degraded and therefore not found in the supernatant at 24 h. For all these reasons, exclusively IL-12 and IL-6 production was evaluated in the following experiments in order to investigate the mechanisms of interaction between macrophages and *Acanthamoeba*.

Real time imaging experiments indicate that the infection model we have used for our studies is efficient. Macrophage and trophozoites, cultured at 37°C 5%CO₂ interacted with each other in an active manner over the first hour of infection. The analysis of the images and data regarding the pro-inflammatory cytokine production suggested that macrophages could react differently in response to a pathogenic or a non-pathogenic *Acanthamoeba* strain. In particular the results indicated that

macrophages responded to trophozoites of a clinical isolate in a contact-dependent manner, attempting cytolysis and phagocytosis, as well producing cytokines. On the other hand macrophages appeared to respond to the non-pathogenic strain Neff, strain with less attempted phagocytosis and higher induction of cytokines. Live confocal microscopy and appropriate labelling of macrophages and trophozoites might be used to quantify their interactions and to fully understand their significance, as recently apply to understand the interaction between *Entamoeba* trophozoites and human cells (Ralston *et al.*, 2014).

The results presented so far have provided the supporting background information to identify the further questions to be addressed and the investigations required to determine the mechanisms by which *A. castellanii* trophozoites modulate macrophage function.

CHAPTER 4

Innate immune receptors expressed on murine macrophages recognise and respond to *Acanthamoeba castellanii* trophozoites

4.1 Abstract

Toll like receptors (TLRs) and protease activated receptors (PARs) are innate immune receptors expressed on immune cells, including macrophages. These receptors are involved in the recognition and response to pathogens. *Acanthamoeba* infections are characterized by the development of an intense innate immune response where a high influx of macrophages can be observed. Herein, using antibodies to inhibit receptors and bone-marrow macrophages derived from genetically modified mice, we investigated the activation of TLRs and PARs expressed on murine macrophages after co-incubation with *Acanthamoeba* trophozoites. Our results demonstrate that *Acanthamoeba*-induced IL-12 and IL-6 production by macrophages is predominantly MyD88-dependent. We demonstrate that TLR4 is the main TLR involved in the response to *Acanthamoeba*. In addition, *Acanthamoeba*-induced IL-12 production is partially PAR₁ dependent, but PAR₂ independent. This study shows for the first time the involvement of innate immune receptors, such as TLRs and PARs, expressed on macrophages, in the recognition and response to *Acanthamoeba* trophozoites.

4.2 Introduction

The innate immune system is the first line of defence against invading pathogens. Upon trauma or microbial infection, innate immune cells are recruited into the site of inflammation/infection where they elicit their antimicrobial functions (Chaplin, 2010). Toll-Like receptors are trans-membrane receptors strategically expressed by innate immune cells, such as macrophages and dendritic cells, as well as epithelial cells that promptly recognise pathogens and rapidly initiate an associated immune response (Kawasaki & Kawai, 2014). TLRs 1, 2, 4, 5, 6 are expressed on the plasma membrane, and they recognize pathogen associated structural moieties; whereas TLRs 3, 7, 8, 9 are expressed in the intracellular environment and are mainly involved in the recognition of viral, bacterial and protozoan nucleic acids (Kumar *et al.*, 2011). After ligand-binding, TLR intracellular signalling pathways are initiated with the activation of TIR containing adaptor molecules such as MyD88 and TRIF. The MyD88-dependent signalling pathway is associated with all TLRs, with the exception of TLR3, and it culminates with NF- κ B and MAPKinase activation and up-regulation of gene expression for production of pro-inflammatory cytokines and chemokines. The TRIF-dependent signalling pathway, associated with TLR3 and TLR4, leads to IRF3, Nf- κ B and MAPK activation, leading to type I IFN and pro-inflammatory cytokine production (Kawai & Akira, 2010). PARs are expressed throughout the body and they elicit important functions in preserving tissue homeostasis and in the defence mechanisms (Macfarlane *et al.*, 2001). Four different PARs have been identified and PAR₁ and PAR₂ are expressed on innate immune cells, such as monocytes and macrophages. PARs are activated by proteases and play a role in the recruitment of immune cells, oedema and release of pro-inflammatory cytokines and chemokines at the site of infection (Vergnolle, 2003; Shpacovitch *et al.*, 2007; Gieseler *et al.*, 2013).

Studies of *Acanthamoeba* recognition by TLRs have been reported only very recently. These studies have focused on TLRs expressed on epithelial corneal cells (Ren *et al.*, 2010; Ren & Wu, 2011; Alizadeh *et al.*, 2014). Similarly, the role of PARs in *Acanthamoeba* infections has only very recently acquired attention (Tripathi *et al.*, 2014). Although macrophages are heavily recruited during the development of both GAE and AK, the potential role of TLRs and PARs expressed on this immune cell population so far, has not been investigated.

Our previous results detailed in chapter 3 of this thesis indicate that *Acanthamoeba*-induced cytokine production in murine macrophages, is dependent on incubation time and co-incubation ratio. Furthermore both serine and cysteine amoebic proteases stimulate macrophage IL-12 and IL-6 production. Therefore we investigated the involvement of TLR2 and TLR4 as well as PAR1 and PAR2, expressed on macrophages, in the *in vitro* *Acanthamoeba* trophozoites/macrophages co-culture model validated in the chapter 3.

4.3 Materials and Methods

4.3.1 Inhibition of TLR2 and TLR4 expression on BMD murine macrophages with specific IgG antibody

In order to inhibit TLR2 and TLR4 expression on murine macrophages, specific functional grade purified antibodies were used: Anti-Human/Mouse CD282 (TLR2) murine monoclonal antibody (IgG1) and Anti-Mouse TLR4/MD-2 Complex rat monoclonal antibody (IgG2a, kappa) (eBioscience, Ltd., Hatfield, UK). Both antibodies supplied sterile in an aqueous buffer, without sodium azide. In order to identify the optimal concentration and the optimal experimental conditions, different antibody concentrations were tested: 10 µg/ml, and 20 µg/ml, for both TLR2 and TLR4 inhibition; 40 µg/ml was also tested for TLR4 inhibition.

At day 10, macrophages were harvested and plated 1×10^6 /well as described in the general Materials and Methods. The day after, cRPMI in the wells was discarded and replaced with 200 µl of either anti-TLR2 or anti-TLR4 antibody solution in cRPMI. 200 µl of cRPMI without anti-TLRs antibody were added in the wells for the control condition. Plates were then incubated at 37°C, 5% CO₂ for one hour. Subsequently, 800 µl of the specific agonist solution or cRPMI were added to the well. Plates were incubated at 37°C, 5% CO₂ and after 24 h, samples were collected and analysed.

4.3.2 Stimulation of PAR₂ deficient BMD macrophages with specific PAR₂ agonist

The synthetic peptide 2-Furoyl-LIGRL-Orn-NH₂ (Peptide Synthetics, Fareham, UK) was used as specific PAR₂ agonist. 2-Furoyl-LIGRL-Orn-NH₂ work solution was freshly reconstituted in cRPMI, prior to use.

At day 10, macrophages were harvested and plated 1×10^6 /well as described in the general Materials and Methods. The day after, cRPMI in the wells was discarded and replaced with 500 μ l of cRPMI. Subsequently 500 μ l of 2-Furoyl-LIGRL-Orn-NH₂ was added, obtaining a final concentration in the well of 12.5 μ M. Due to the small amount of the product, optimization of the concentration to use for the stimulation could not be performed. The concentration of PAR₂ agonist used in the experiment was determined based on the literature and on the availability of the product. Plates were incubated at 37°C, 5% CO₂. After 24 h, samples were collected and analysed.

4.3.3 Inhibition of PAR₁ using RWJ 56110 synthetic antagonist and stimulation with PAR₁ agonist

In order to inhibit PAR₁, expressed on murine macrophages, the selective PAR₁ antagonist RWJ56110 (Tocris Bioscience, Bristol, UK) has been used. Initially, stock solution was prepared in sterile distilled H₂O, aliquoted and stored at -20°C. RWJ 56110 work solution was freshly reconstituted in cRPMI and filter sterilised prior to use. Thr-Phe-Leu-Leu-Arg-NH₂ trifluoroacetate salt (TFLLR-NH₂) (Sigma-Aldrich, Paisley, UK) has been used as a PAR₁ selective agonist. Initially, stock solution was prepared dissolving the powder in sterile RPMI and subsequently aliquoted and stored at -20°C. TFLLR-NH₂ work solution was freshly reconstituted in cRPMI, prior to use. Due to the small amount of the product, optimization of the concentration to use for the stimulation could not be performed. The concentration of PAR₁ agonist and of RWJ 56110 PAR₁ antagonist used in the experiment was determined based on the literature and on the availability of the product.

At day 10, macrophages were harvested and plated 1×10^6 /well as described in the general Materials and Methods. The day after, cRPMI in the wells was discarded

and replaced with either 500 μ l of RWJ56110 solution 20 μ M, or 500 μ l of cRPMI for the control condition. Plates were then incubated at 37°C 5% CO₂ for 10 min. Subsequently 500 μ l of TFLLR-NH₂ solution was added at a final concentration in the well of 100 μ M. Plates were incubated at 37°C, 5% CO₂. After 24 h, samples were collected and analysed.

4.3.4 Statistical analyses

Experiments were performed in triplicate and repeated at least twice. Data are shown as the mean \pm s.e.m. of 3 replicates. Statistical analyses was performed using GraphPad Prism 5 Software. Student's *t*-test was applied to evaluate the significant differences between the conditions.

4.4 Results

4.4.1 *Acanthamoeba*-induced IL-12 and IL-6 production is MyD88-dependent and partially TRIF-dependent

Previously we have demonstrated that *Acanthamoeba* trophozoites can stimulate cytokine production by murine macrophages. Consequently, the following step was to understand what signalling pathway was involved in these events. Towards this purpose, C57BL/6 mice deficient for either MyD88 or TRIF genes and C57BL/6 wild type mice were used. BMD macrophages were obtained from these different mouse strains and co-incubated with trophozoites of *Acanthamoeba castellanii* Neff strain or *Acanthamoeba castellanii* clinical strain at ratio 1:1 and 1:2 as described in Chapter 3. As positive control macrophages were stimulated with LPS, natural TLR4 ligand, or with the synthetic double stranded RNA POLY I:C, selective TLR3 agonist. Production of IL-12 and IL-6 was then measured at 24 h after infection.

LPS induced IL-12 production in WT macrophages (2.515 ng/ml) but this effect was significantly diminished in MyD88^{-/-} macrophages ($p < 0.0001$). POLY I:C stimulated IL-12 production from WT macrophages (2.063 ng/ml) and this production was partially diminished using MyD88^{-/-} macrophages (Fig 4.1-A). IL-6 production by WT macrophages was strongly induced by LPS (2.998 ng/ml) and in much lower concentrations by POLY I:C (0.027 ng/ml). IL-6 production induced by LPS was completely ablated in MyD88^{-/-} macrophages ($p < 0.0001$), as well as after challenge with POLY I:C ($p = 0.0009$) in comparison with WT macrophages (Fig 4.2-B). Both IL-12 and IL-6 production, by WT macrophages were significantly induced by trophozoites of either Neff strain or clinical isolates at both the infection ratios studied. MyD88^{-/-} macrophages co-incubated with trophozoites of either Neff strain or clinical isolate did not produce IL-12 and IL-6 (Fig 4.1-A, B).

Stimulation of WT and TRIF^{-/-} macrophages with specific agonists presented the following features. IL-12 production, by WT macrophages, was detected following stimulation with LPS (2.387 ng/ml) and POLY I:C (4.007 ng/ml). This production was significantly diminished in TRIF^{-/-} macrophages stimulated with either LPS (p=0.0001) or POLY I:C (p<0.0001). Similarly, IL-6 production, by WT macrophages, was induced by LPS (0.601 ng/ml) and by POLY I:C (0.499 ng/ml). IL-6 production by TRIF^{-/-} macrophages was significantly diminished after challenge with either LPS (p<0.0001) or POLY I:C (p<0.0001) in comparison to WT macrophages (Fig 4.2-B). IL-12 production by WT macrophages was induced by trophozoites of both Neff strain and clinical isolate at both of the ratios investigated. IL-12 production was significantly inhibited in TRIF^{-/-} macrophages co-incubated with trophozoites of either the Neff strain or clinical isolate in comparison with WT macrophages (Fig. 4.2-A). IL-6 production by WT macrophages, was induced only by trophozoites of the Neff strain at the highest ratio, and this production was significantly diminished using TRIF^{-/-} macrophages (p=0.0014) (Fig. 4.2-B).

Fig 4.1 Release of IL-12 (A) and IL-6 (B): comparison between C57BL/6 WT and C57BL/6 MyD88^{-/-} macrophages at 24 h after co-incubation with *Acanthamoeba* trophozoites. 1x10⁶ murine macrophages, obtained from either C57BL/6 WT or C57BL/6 MyD88^{-/-} mice, were challenged with either 1x10⁶ or 5x10⁵ trophozoites of either *A. castellanii* Neff strain (respectively Neff 1:1 and Neff 1:2) or clinical isolate (respectively clinical 1:1 and 1:2). LPS and POLY I:C at respectively 200 ng/ml (LPS) and 10 µg/ml (POLY I:C) were used to stimulate macrophages as positive controls. Uninfected macrophages (Control) were considered the negative control. The experiment was performed twice. Results represent the mean ± standard error of n=3. Student's *t*-test was applied to evaluate differences between C57BL/6 WT and the C57BL/6 MyD88^{-/-} macrophage cytokine production. In the graphs, significances between C57BL/6 WT and the C57BL/6 MyD88^{-/-} macrophages are indicated as follow: for values of p<0.005 °°; p<0.0005 °°°. IL-12 and IL-6 production in trophozoites/MyD88^{-/-} macrophages co-incubation is completely ablated in comparison to trophozoites/WT macrophages co-incubation, suggesting that the production of these pro-inflammatory cytokines by macrophages, in response to *Acanthamoeba*, is MyD88-dependent.

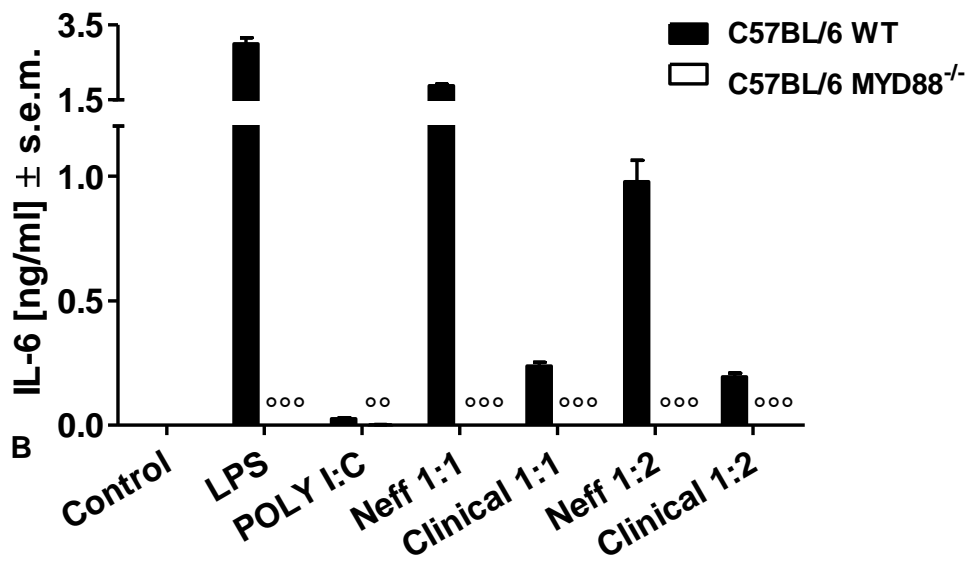
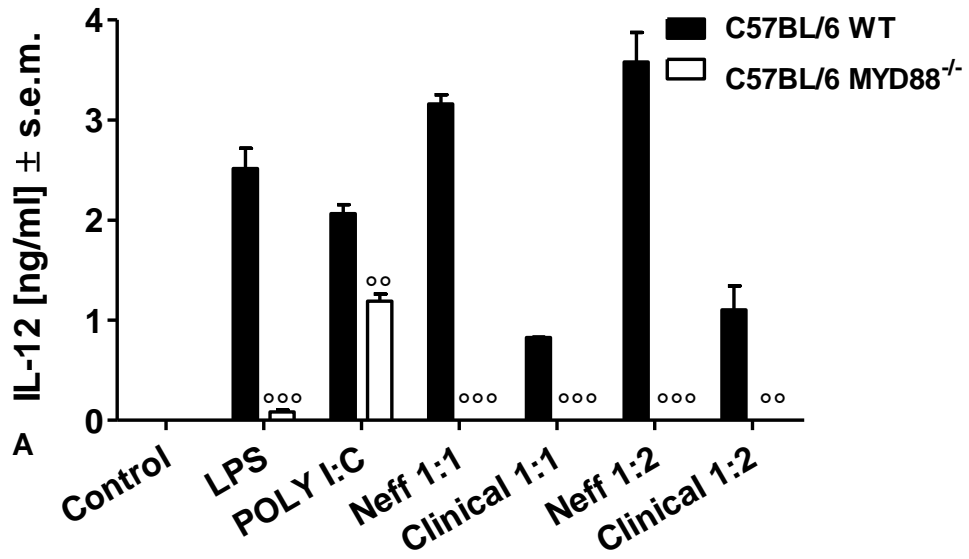
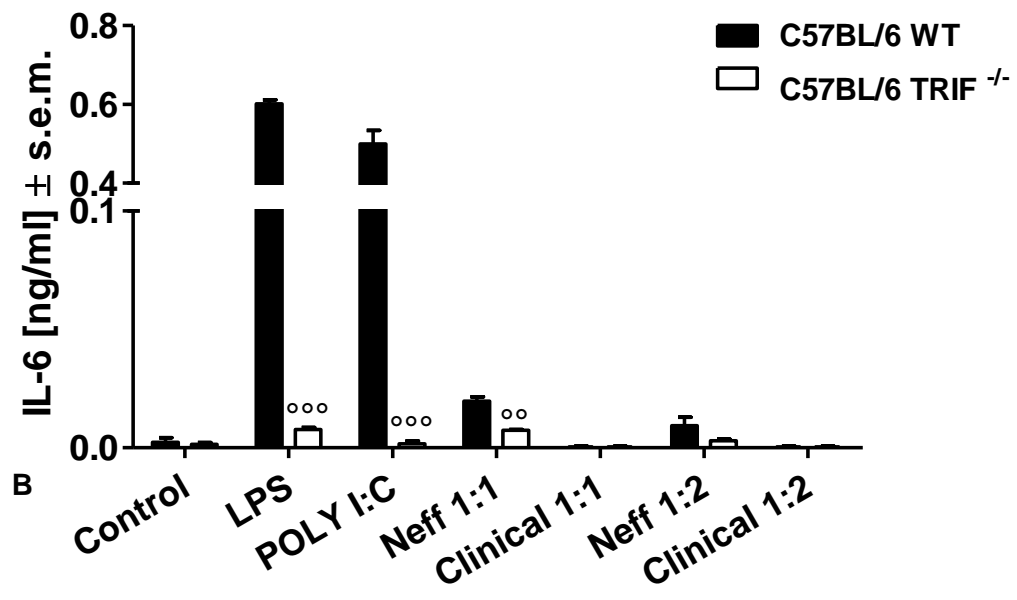
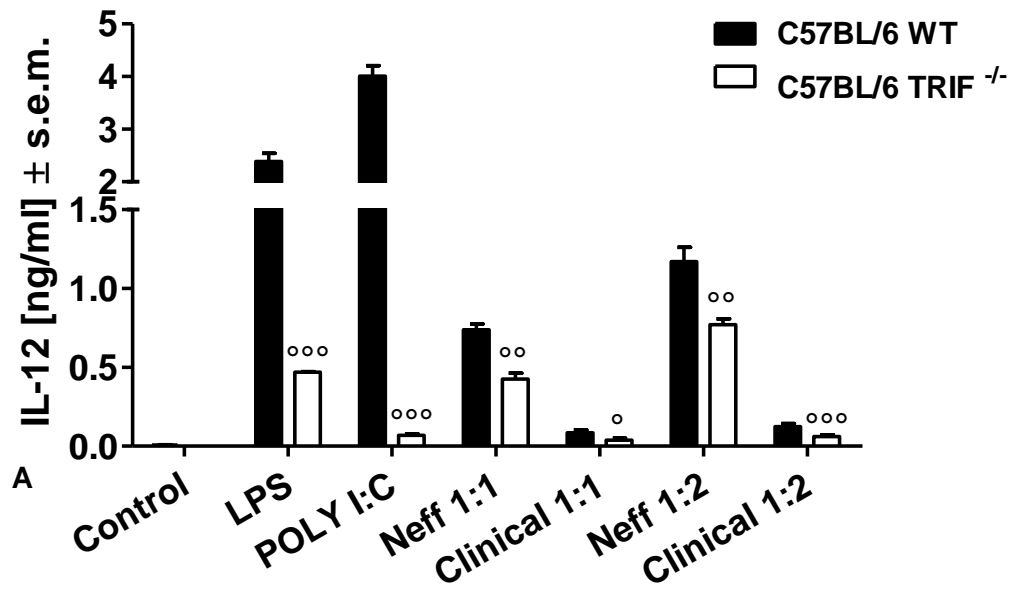


Fig 4.2 Release of IL-12 (A) and IL-6 (B): comparison between C57BL/6 WT and C57BL/6 TRIF^{-/-} macrophages at 24 h after co-incubation with *Acanthamoeba* trophozoites. 1x10⁶ murine macrophages, obtained from either C57BL/6 WT or C57BL/6 TRIF^{-/-} mice, were challenged with either 1x10⁶ or 5x10⁵ trophozoites of either *A. castellanii* Neff strain (respectively Neff 1:1 and Neff 1:2) or clinical isolate (respectively clinical 1:1 and 1:2). LPS and POLY I:C at respectively 200 ng/ml (LPS) and 10 µg/ml (POLY I:C) were used to stimulate macrophages as positive controls. Uninfected macrophages (Control) were considered the negative control. The experiment was performed twice. Results represent the mean ± standard error of n=3. Student's *t*-test was applied to evaluate differences between C57BL/6 WT and the C57BL/6 TRIF^{-/-} macrophages. Values of p<0.05 were considered significant. In the graphs, significances between C57BL/6 WT and the C57BL/6 TRIF^{-/-} conditions are indicated as follow: for values of p<0.05 °; p<0.005 °°; p<0.0005 °°°. IL-12 and IL-6 production in trophozoites/TRIF^{-/-} macrophages co-incubation is significantly diminished in comparison with trophozoites/WT macrophages co-incubation condition suggesting that the production of these pro-inflammatory cytokines by macrophages in response to *Acanthamoeba*, might be in part TRIF-dependent, although this does not appear to be the main signalling pathway involved during *Acanthamoeba* stimulation.



4.4.2 Anti-CD282 (TLR2) monoclonal antibody inhibits IL-12 and IL-6 cytokine production by murine macrophages in response to PAM3CSK4

The efficacy of specific antibodies for TLR2 and TLR4 in blocking the receptors was tested in order to determine whether they were appropriate for co-incubation experiments. Therefore murine macrophages were pre-treated or not treated with different concentrations of either anti IgG-TLR2 or anti IgG-TLR4 and subsequently stimulated with either the synthetic Triacetylated lipopeptide PAM3CK4, a TLR2/TLR1 agonist, or LPS a TLR4 agonist. In addition, in order to evaluate the intrinsic activity of the antibody, unstimulated macrophages pre-treated with either anti IgG-TLR2 or anti IgG-TLR4 were also included in the experimental design. IL-12 and IL-6 production was evaluated at 24 hr after stimulation.

Pre-treatment with only anti IgG-TLR2 (Fig. 4.3) or anti IgG-TLR4 (Fig. 4.4), at any of the concentrations used did not induce either IL-12 or IL-6 production by murine macrophages showing values similar to unstimulated non pre-treated macrophages.

IL-12 production by macrophages was induced by PAM3CK4 (Fig 4.3-A₁, A₂). This production was significantly inhibited in the presence of anti IgG-TLR2 antibody used at either 10 µg/ml ($p < 0.0001$) (Fig 4.3-A₁) or 20 µg/ml ($p < 0.0001$) (Fig 4.3-A₂). Similarly, IL-6 production was induced by PAM3CK4 (Fig 4.3-B₁, B₂) and significantly inhibited by the presence of anti IgG-TLR2 antibody used at either 10 µg/ml ($p = 0.0001$) (Fig 4.3-B₁) or 20 µg/ml ($p < 0.0001$) (Fig 4.3-B₂).

LPS stimulated IL-12 production by macrophages (Fig.4.4). However, pre-incubation with anti IgG-TLR4 did not inhibit LPS-induced IL-12 production by murine macrophages at either 10 µg/ml ($p = 0.09$ ns) (Fig 4.4-A₁) or 40 µg/ml ($p = 0.08$ ns)

(Fig 4.4-A₃). On the other hand, pre-treatment with 20 µg/ml anti IgG-TLR4 induced a small, but significant decrease of the LPS-induced IL-12 production ($p=0.0054$) (Fig 4.4-A₂). By comparison with IL-12 production, however, the pre-treatment with anti IgG-TLR4 did not inhibit LPS-induced IL-6 production at any concentration applied (Fig 4.4-B₁, B₂, B₃).

Fig 4.3 IL-12 (A), and IL-6 (B) production by murine macrophages after 24h pre-treatment with anti IgG TLR2 antibody. 1×10^6 murine macrophages, obtained from BALB/c mice, were pre-treated with anti IgG TLR2 antibody (+ Anti IgG-TLR2) or not pre-treated (- Anti IgG-TLR2). Antibody was used at two different concentration: 10 $\mu\text{g/ml}$ (A_1 , B_1) or 20 $\mu\text{g/ml}$ (A_2 , B_2) for 1 h at 37°, 5% CO_2 . Subsequently, pre-treated or non pre-treated macrophages were stimulated with PAM3CSK4 at a concentration of 320 ng/ml (PAM3CSK4). Unstimulated macrophages, pre-treated or not pre-treated with antibody were included in the experimental design (Control). The experiment was performed twice. Results represent the mean \pm standard error of $n=3$. Student's *t*-test was applied to evaluate differences between - Anti IgG-TLR2 and + Anti IgG-TLR2 conditions. In the graphs, significances between - Anti IgG-TLR2 and + Anti IgG-TLR2 conditions are indicated as follow: for values of $p < 0.0005$ °°. Data shown in the graphs suggest that the functional inhibition of TLR2, using specific antibody, was effective. Indeed, PAM3CSK4-induced IL-12, and IL-6 production was significantly reduced by pre-treatment Anti IgG-TLR2 antibody. Furthermore, TLR2 antibody itself did not stimulate either IL-12 or IL-6 production.

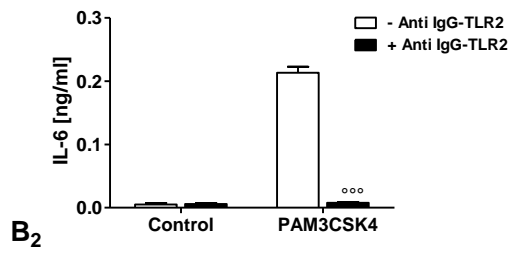
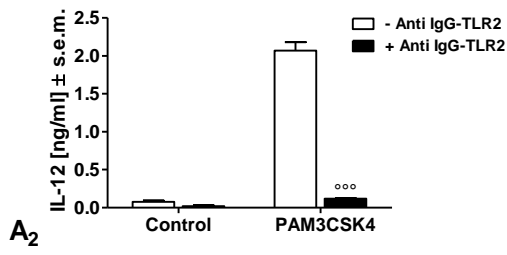
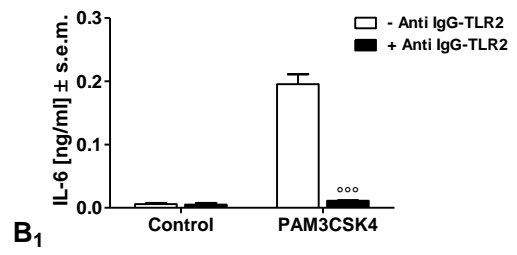
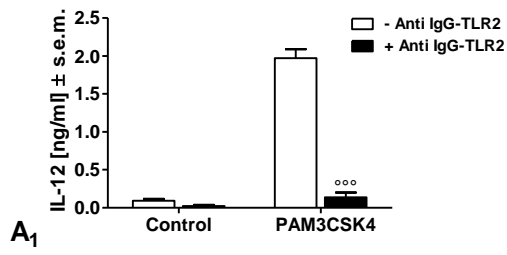
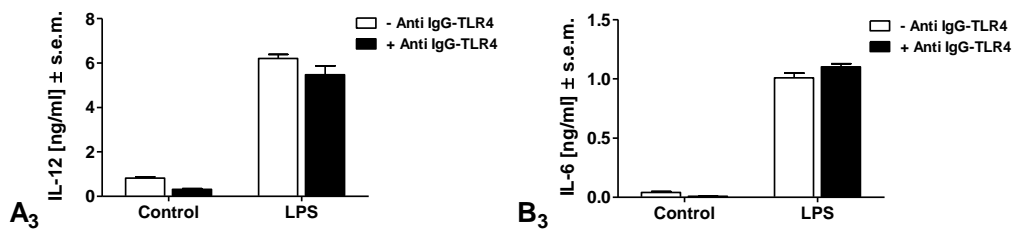
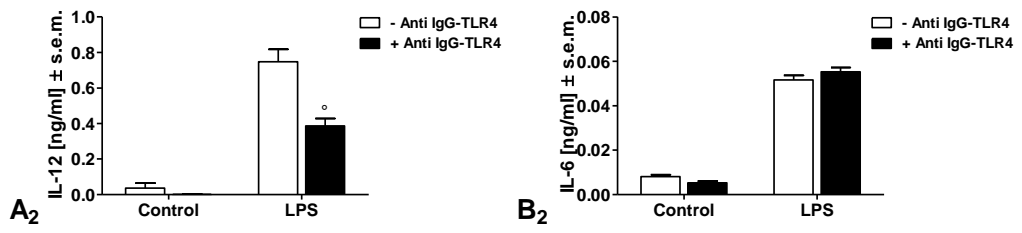
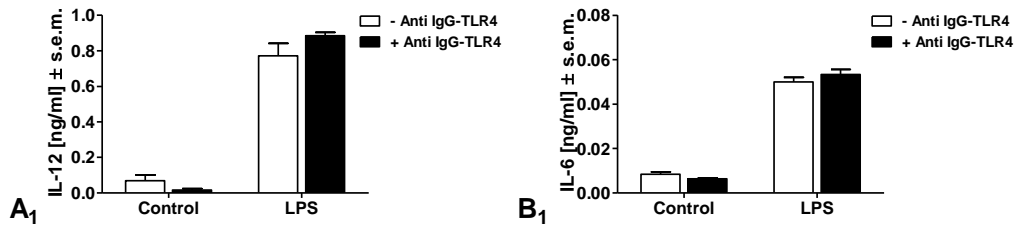


Fig 4.4 IL-12 (A), and IL-6 (B) production by murine macrophages after 24h pre-treatment with anti IgG TLR4 antibody. 1×10^6 murine macrophages, obtained from BALB/c mice, were pre-treated with anti IgG TLR4 antibody (+ Anti IgG-TLR4) or not pre-treated (- Anti IgG-TLR4). Antibody was used at three different concentration: 10 $\mu\text{g/ml}$ (A_1 , B_1) or 20 $\mu\text{g/ml}$ (A_2 , B_2) or 40 $\mu\text{g/ml}$ (A_3 , B_3) for 1 h at 37° 5% CO_2 . Subsequently, pre-treated or non pre-treated macrophages were stimulated with LPS at a concentration of 200 ng/ml (LPS). Unstimulated macrophages, pre-treated or not with antibody, were included in the experimental design (Control). The experiment was performed twice. Results represent the mean \pm standard error of $n=3$. Student's *t*-test was applied to evaluate differences between - Anti IgG-TLR4 and + Anti IgG-TLR4 conditions. In the graphs, significances between - Anti IgG-TLR4 and + Anti IgG-TLR4 conditions are indicated as follow: for values of $p < 0.05$ °. Data shown in the graphs suggest that the inhibition of TLR4 using specific antibody was not effective. Indeed, although TLR4 antibody did not possess an intrinsic effect in stimulating cytokine production LPS-induced IL-12 and IL-6 production was not significantly reduced overall in the presence of Anti IgG-TLR4 antibody.



4.4.3 *Acanthamoeba*-induced macrophage IL-12 and IL-6 production is TLR4-dependent but TLR2-independent

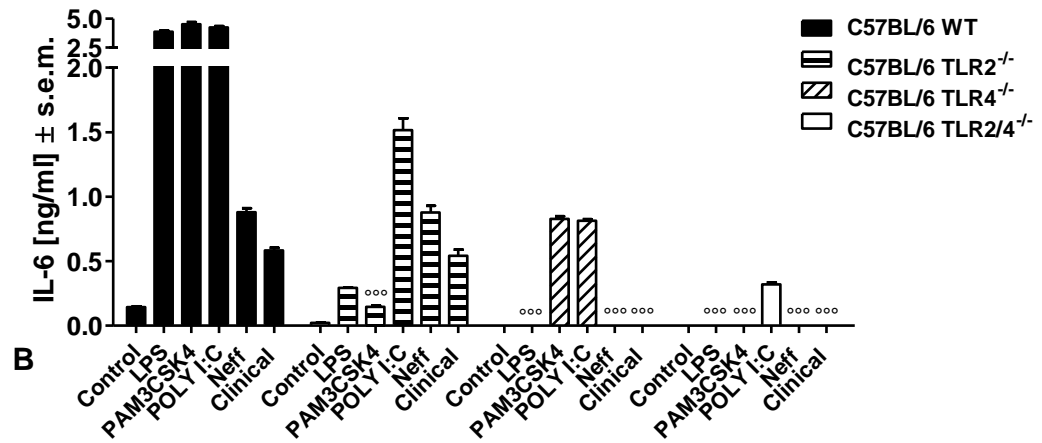
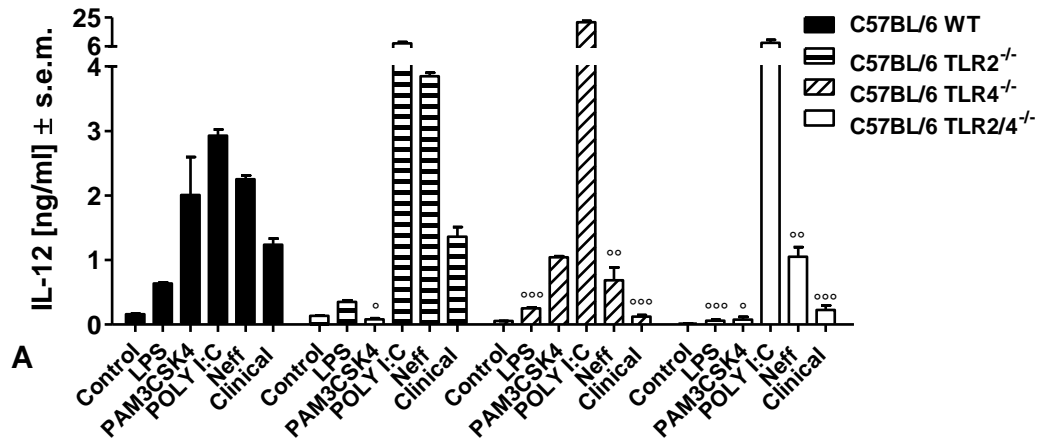
Previously we have demonstrated that *Acanthamoeba* trophozoites can stimulate IL-12 and IL-6 production by murine macrophages in a MyD88 dependent manner. The following step was to understand what specific TLR was involved in this event. TLR2 and TLR4 were considered the potential targets for our investigation since they are localized on cell surface and associated with the MyD88-dependent signalling pathway. Therefore preliminary inhibition experiments using specific TLR antibodies were performed. However, they were not only prohibitively expensive, but not effective for both receptors. Therefore the study to determine roles for these TLRs was performed using macrophages derived from gene deficient C57BL/6 mice for either TLR2 or TLR4 or TLR2/TLR4. BMD macrophages, trophozoites of *Acanthamoeba castellanii* Neff strain or *Acanthamoeba castellanii* clinical strain were used in co-incubation experiments at a ratio of 1:1. As positive control, macrophages were stimulated with either LPS or PAM3CKS4 or RNA POLY I:C. Production of IL-12 and IL-6 was then measured at 24 h after infection.

IL-12 production by WT macrophages was detected following stimulation with LPS (0.636 ng/ml) and, as expected, LPS-induced IL-12 production was significantly diminished in TLR4^{-/-} macrophages (p<0.0001) and TLR2/4^{-/-} macrophages (p<0.0001). PAM3CSK4-induced IL-12 production by WT macrophages (2.007 ng/ml) was significantly decreased in TLR2^{-/-} macrophages (p=0.015) and TLR2/4^{-/-} macrophages (p=0.015). POLY I:C-induced IL-12 production was higher in TLR2 and TLR4 and both TLR2/TLR4 deficient macrophages than WT macrophages (Fig 4.5-A). IL-6 production by WT macrophages was induced by all three agonists to similar values. LPS-induced IL-6 production was completely ablated in TLR4^{-/-} and TLR2/4^{-/-} macrophages in comparison with WT macrophages. PAM3CSK4-induced

IL-6 production was significantly diminished in TLR2^{-/-} macrophages (p<0.0001) and completely ablated in TLR2/4^{-/-} macrophages in comparison with WT macrophages. POLY I:C-induced IL-6 production was reduced in comparison with WT macrophages when either TLR2 or TLR4 or both receptors were not expressed on macrophages (Fig 4.5-B).

Macrophages/trophozoites co-incubation presented the following features. Both IL-12 and IL-6 production by WT macrophages was induced by trophozoites of either Neff strain or clinical isolate. Production of these cytokines was not diminished in TLR2^{-/-} macrophages (Fig 4.5-A, B). Conversely, IL-12 production by TLR4^{-/-} macrophages was significantly lower in comparison with WT macrophages, after challenge with either Neff strain (p=0.0009) or clinical isolate (p=0.0002) (Fig 4.5-A). In comparison with the WT macrophages, the absence of TLR4 on macrophages completely ablated IL-6 production induced by both Neff strain and clinical isolate (Fig 4.5-B). The absence of both TLR2 and TLR4 on macrophages was characterized by significantly lower IL-12 production when co-incubated with either Neff strain (p=0.0009) or clinical isolate trophozoites (p=0.0002), in comparison with WT macrophages (Fig 4.5-A). TLR2/4^{-/-} macrophages co-incubated with either Neff strain or clinical isolate trophozoites did not produce IL-6 (Fig 4.5-B).

Fig 4.5 Release of IL-12 (A) and IL-6 (B): comparison between C57BL/6 WT and C57BL/6 TLR2^{-/-}, TLR4^{-/-}, TLR2/4^{-/-} macrophages 24 h after co-incubation with *Acanthamoeba* trophozoites. 1x10⁶ murine macrophages, obtained from C57BL/6 WT and KO mice, were challenged with 1x10⁶ trophozoites of either *A. castellanii* Neff strain (Neff) or clinical isolate (Clinical). LPS, PAM3CSK4 and POLY I:C at respectively 200 ng/ml, 320 ng/ml and 10 µg/ml were used to stimulate macrophages as positive controls. Uninfected macrophages (Control) were considered the negative control. The experiment was performed twice. Results represent the mean ± standard error of n=3. Student's *t*-test was applied to evaluate differences between C57BL76 WT and the C57BL/6 TLR2^{-/-}, TLR4^{-/-}, TLR2/4^{-/-} conditions. In the graphs, significances between C57BL76 WT and the C57BL/6 TLR2^{-/-}, TLR4^{-/-}, TLR2/4^{-/-} conditions are indicated as follow: for values of p<0.05 °; p<0.005 °°; p<0.0005 °°°. IL-12 and IL-6 production in trophozoites/TLR2^{-/-} macrophages co-incubation was not significantly diminished in comparison with trophozoites/WT macrophages co-incubation condition, suggesting that the production of these pro-inflammatory cytokines by macrophages in response to *Acanthamoeba* is not TLR2-dependent. On the other hand, in the absence of TLR4, trophozoites-induced IL-12 production by macrophages was significantly decreased, whereas IL-6 production was completely ablated. The same pattern was observed when both TLR2 and TLR4 were not expressed. Therefore, TLR4 appeared to be the main TLR involved in the recognition and response to *Acanthamoeba castellanii*.



4.4.4 *Acanthamoeba*-induced IL-12 and IL-6 production by murine macrophages is PAR₂-independent

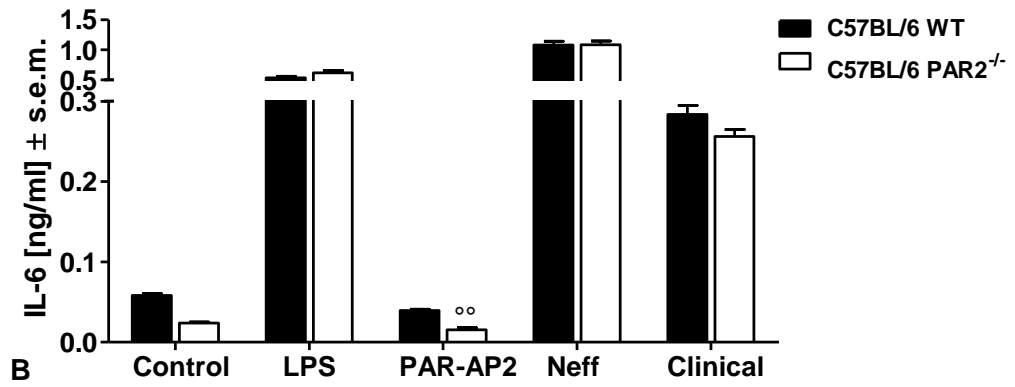
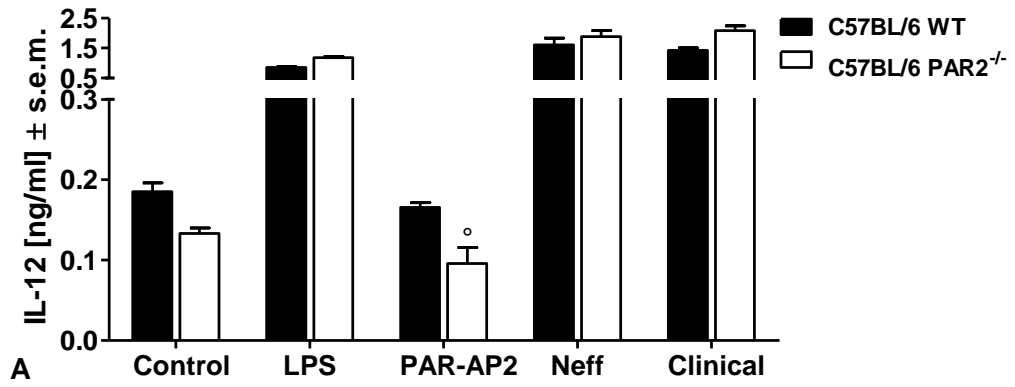
From our previous experiments, it was demonstrated that amoebic serine and cysteine proteases could stimulate IL-12 and IL-6 production by murine macrophages. Therefore, we investigated if PARs were involved in this event. PAR₂ was considered a potential target for our investigation, since it is an extracellular receptor widely expressed on immune cells and involved in inflammatory and immunological processes. The study was performed using C57BL/6 wild type mice and C57BL/6 mice deficient for the PAR₂ gene. BMD macrophages were obtained from these different mouse strains and co-incubated with trophozoites of *Acanthamoeba castellanii* Neff strain or *Acanthamoeba castellanii* clinical strain at a ratio of 1:1. As positive control macrophages were stimulated with the synthetic peptide 2-Furoyl-LIGRL-Orn-NH₂, a selective and potent PAR₂ agonist (PAR-AP2) that, by mimicking the tethered peptidic sequence, directly activates PAR₂ expressed on target cells (Ramachandran *et al.*, 2012). In addition, macrophages were stimulated with LPS. Production of IL-12 and IL-6 was then measured at 24 h after infection.

IL-12 production, by WT macrophages, was induced after stimulation with LPS (0.857 ng/ml); this production was not significantly reduced in PAR₂^{-/-} macrophages. PAR-AP2 did not induced an increased of IL-12 production by WT macrophages (0.165 ng/ml) in comparison with control WT macrophages (0.185 ng/ml). Nevertheless, PAR₂^{-/-} macrophages were less responsive to PAR-AP2, presenting a significant decrease in IL-12 production in comparison with WT macrophages stimulated with PAR-AP2 (p=0.014). IL-12 production by WT macrophages, was induced by trophozoites of either Neff strain (1.605 ng/ml) or clinical isolate (1.426 ng/ml). IL-12 production by PAR₂^{-/-} macrophages co-incubated with trophozoites of

either Neff strain (1.880 ng/ml) or clinical isolate (2.085 ng/ml) was not significantly reduced in comparison with the WT macrophage co-incubation condition (Fig 4.6-A).

LPS-induced IL-6 production by PAR₂^{-/-} macrophages did not present significant differences in comparison with similarly stimulated WT macrophages (0.532 ng/ml). PAR-AP2 failed to induce IL-6 production by WT macrophages. However, IL-6 production was significantly decreased in PAR₂^{-/-} macrophages in comparison with WT macrophages when incubated in the presence of PAR-AP2. Similar to IL-12, IL-6 production by WT macrophages was detected after incubation with trophozoites of either Neff strain (1.079 ng/ml) or clinical isolate (0.283 ng/ml). *Acanthamoeba*-induced IL-6 production by PAR₂^{-/-} macrophages presented similar concentration values as the WT macrophages under co-incubation conditions (Fig 4.6-B).

Fig 4.6 Release of IL-12 (A) and IL-6 (B): comparison between C57BL/6 WT and C57BL/6 PAR₂^{-/-} macrophages at 24 h after co-incubation with *Acanthamoeba* trophozoites. 1x10⁶ murine macrophages, obtained from C57BL/6 WT and KO mice, were challenged with 1x10⁶ trophozoites of either *A. castellanii* Neff strain (Neff) or clinical isolate (Clinical). 2-Furoyl-LIGRL-Orn-NH₂ (PAR-AP2) at a concentration of 12.5 μM was used to stimulate macrophages as positive controls. LPS at 200 ng/ml (LPS) was also included in the experimental design. Uninfected macrophages (Control) were considered the negative control. The experiment was performed twice. Results represent the mean ± standard error of n=3. Student's *t*-test was applied to evaluate differences between C57BL/6 WT and the C57BL/6 PAR₂^{-/-} conditions. In the graphs significances between C57BL/6 WT and the C57BL/6 PAR₂^{-/-} conditions are indicated as follow: for values of p<0.05 °; p<0.005 °°. IL-12 and IL-6 production in trophozoites/PAR₂^{-/-} macrophages co-incubation presented the same concentration values as in trophozoites/WT macrophages co-incubation condition, suggesting that the production of these pro-inflammatory cytokines by macrophages, in response to *Acanthamoeba*, is not PAR₂-dependent.



4.4.5 *Acanthamoeba castellanii* clinical strain induces IL-12 production by murine macrophages in a PAR₁-dependent manner

From previous experiments it was demonstrated that amoebic serine and cysteine proteases can stimulate IL-12 and IL-6 production by murine macrophages, and that this event was not PAR₂-dependent. Further investigations were then undertaken to determine whether PAR₁ was involved. Similar to PAR₂, PAR₁ is an extracellular receptor widely expressed on immune cells and involved in inflammatory and immunological processes. PAR₁^{-/-} mice were not available to perform this study, and therefore the synthetic antagonist, selective for PAR₁, RWJ 56110, was used to block the receptor activity. RWJ 56110 presents a chemical structure that mimics a peptide chain in which is included an heterocycle. This synthetic compound can directly bind to PAR₁ blocking its activation and internalization without interfering with the cleavage of the N-terminus of the receptor (Maryanoff *et al.*, 2003).

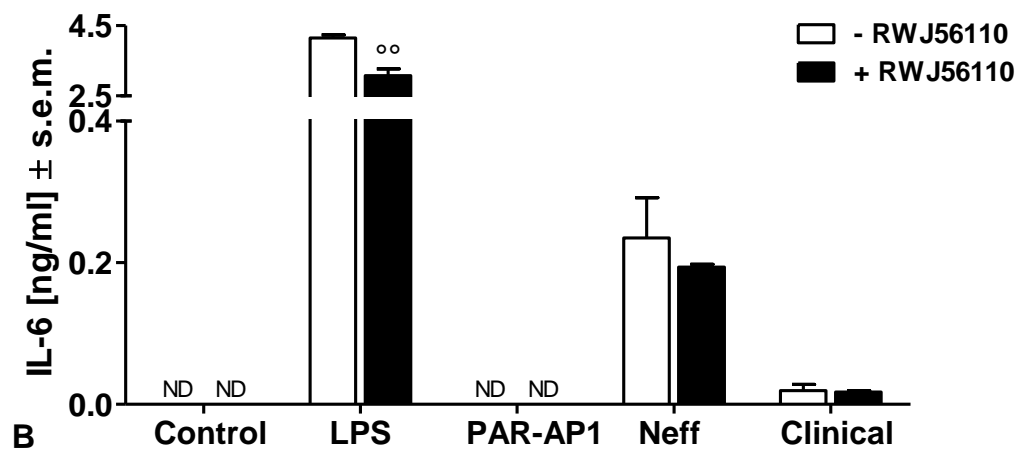
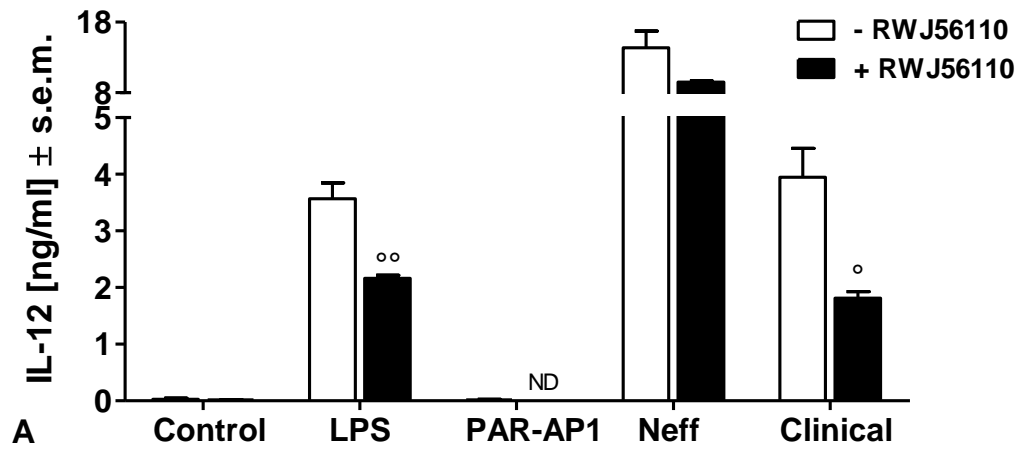
BMD macrophages were either pre-treated or not treated with RWJ 56110. Subsequently, macrophages were stimulated with TFLLR-NH₂ a PAR₁ agonist (PAR-AP1) (Ramachandran *et al.*, 2012), or LPS. In order to evaluate the role of PAR₁ in *Acanthamoeba* infection macrophages were co-incubated with *Acanthamoeba castellanii* trophozoites of either Neff strain or clinical isolate at a ratio of 1:1. In addition, in order to evaluate the intrinsic activity of the antagonist, unstimulated macrophages pre-treated with RWJ56110 were included in the experimental design. IL-12 and IL-6 production was evaluated at 24 h.

Pre-treatment with RWJ 56110 did not induce either IL-12 or IL-6 production by murine macrophages, showing values similar to non pre-treated unstimulated macrophages (Fig 4.7-A, B). Stimulation of macrophages with PAR-AP1 and LPS, in the presence or absence of RWJ 56110 presented the following unexpected

features. Neither IL-12 nor IL-6 production by macrophages, whether pre-treated or not pre-treated with RWJ56110, was observed after stimulation with PAR-AP1 (Fig 4.7-A, B). LPS-induced IL-12 and IL-6 production by non pre-treated macrophages, decreased when macrophages were pre-treated with RWJ 56110 (respectively $p=0.0039$; $p=0.0032$) (Fig 4.7-A, B).

IL-12 production by RWJ56110 non-treated macrophages was induced by Neff strain trophozoites. However, the PAR₁ inhibition through pre-treatment with RWJ 56110 did not significantly modify Neff strain-induced IL-12 production. IL-12 production by RWJ56110 non-treated macrophages was also induced by clinical isolate trophozoites and this production was significantly decreased by pre-treatment with RWJ 56110 ($p=0.0075$) (Fig 4.7-A). IL-6 production by RWJ56110 non-treated macrophages was induced after co-incubation with either Neff strain or clinical isolate trophozoites. Macrophage pre-treatment with RWJ 56110 did not modify the *Acanthamoeba*-induced IL-6 production (Fig 4.7-B).

Fig 4.7 IL-12 (A), and IL-6 (B) production by murine macrophages after 24 h pre-treatment with the PAR₁ antagonist RWJ 56110. 1×10^6 murine macrophages, obtained from BALB/c mice, were pre-treated with 20 μ M RWJ 56110 solution (+ RWJ56110) or not pre-treated (- RWJ56110). Macrophages were incubated for 10 min at 37° 5% CO₂. Subsequently, macrophages were stimulated with either TFLLR-NH₂ (PAR-AP1) at a concentration of 100 μ M, or LPS at a concentration of 200 ng/ml (LPS). Unstimulated macrophages, treated or not treated with antibody, were included in the experimental design (Control). The experiment was performed twice. Results represent the mean \pm standard error of n=3. Student's *t*-test was applied to evaluate differences between - RWJ56110 and + RWJ56110 conditions. In the graphs, significances between - RWJ56110 and + RWJ56110 conditions are indicated as follow: for values of $p < 0.05$ °; $p < 0.005$ °°. Data shown in the graphs suggest that IL-12 and IL-6 production by murine macrophages induced by Neff strain trophozoites is not PAR₁-dependent. On the other hand, clinical isolate-induced IL-12 production appears at least in part to be PAR₁-dependent, although it does not appear to be the main receptor involved in this event.



4.5 Discussion

The role of innate immune receptors such as toll like receptors has been widely described during protozoan infections (Kumar *et al.*, 2011). Both intracellular and extracellular eukaryotic parasites are recognized by TLRs and their activation leads to important immunological events, such as production of pro-inflammatory cytokines, activation of iNOS synthase and activation of cell-mediated immunity: essential mechanisms to control parasite growth and dissemination within host tissues (Maldonado-Bernal *et al.*, 2005). TLR2 and TLR4 are the main TLRs involved in the recognition of parasitic protozoans such as *Leishmania spp.*, *Trypanosoma cruzii*, *Toxoplasma gondii*, *Plasmodium falciparum* and *Entamoeba histolytica* (Uematsu & Akira, 2008). Only recently the involvement of TLRs during *Acanthamoeba* infections were reported (Ren *et al.*, 2010; Ren & Wu, 2011; Alizadeh *et al.*, 2014). Epithelial and endothelial barriers are crucial components of the innate immune system that help avoid the invasion of *Acanthamoeba* trophozoites and its progression into the deeper layers of tissue. Recent studies have demonstrated that *Acanthamoeba* trophozoites can activate TLR4 expressed on corneal epithelial cells, inducing pro-inflammatory cytokines and chemokines at the ocular surface (Ren *et al.*, 2010). The activation of TLRs at the ocular surface by *Acanthamoeba* and the release of cytokines and chemokines, can be the triggering event for the recruitment of innate immune cells such as macrophages and neutrophils.

So far, the activation of TLRs expressed on macrophages, during *Acanthamoeba* infections has not been studied. Previously we reported that IL-12 and IL-6 production by murine macrophages was induced by trophozoites of *A. castellanii*. Therefore our aim was to evaluate whether TLRs, expressed on macrophages, were involved in these events. Initially, by using either MyD88 or TRIF deficient

macrophages, we observed that *Acanthamoeba*-induced IL-12 and IL-6 production by murine macrophages was completely ablated in MyD88^{-/-} macrophages and slightly decreased in TRIF^{-/-} macrophages, suggesting that *Acanthamoeba*-induced macrophage pro-inflammatory cytokine production not only occurs mainly through a MyD88-dependent pathway, but also through in part through a MyD88-independent pathway. These observations implicated TLR4, which is known to initiate both MyD88 and TRIF dependent signalling events, as a logical candidate innate immune receptor responsible for *Acanthamoeba* induced activation of macrophages (Kawai & Akira, 2010). To investigate this, the role of TLR4 and TLR2 was investigated in our co-infection model. IL-12 production was not decreased in TLR2^{-/-} macrophages compared with wild type control macrophages after challenge with *Acanthamoeba* trophozoites (and potentially even upregulated). However, IL-12 production was unambiguously reduced in TLR4^{-/-} macrophages compared with wild type control macrophages. Furthermore, *Acanthamoeba*-induced macrophage IL-12 production was also reduced in TLR2/4^{-/-} macrophages, in comparison with WT macrophages. These data suggest that *Acanthamoeba*-induced IL-12 production by macrophages is largely TLR4-dependent although it might not be the only receptor involved in this event. *Acanthamoeba*-induced macrophage IL-6 production was not shown to be increased, or decreased in TLR2^{-/-} macrophages in comparison with the WT macrophages. Interestingly IL-6 production, unlike IL-12 was completely ablated in TLR4 and in TLR2/4 deficient macrophages, suggesting that *Acanthamoeba*-induced IL-6 production by macrophages is totally TLR4-dependent. Summarising, TLR4 expressed on macrophages is therefore involved in the recognition of *Acanthamoeba* and its activation leads to production of pro-inflammatory cytokines mainly through the MyD88 signalling pathway but also, to a lesser extent through the TRIF-dependent signalling pathway. These suggestions are reinforced by the

unique characteristic of TLR4 as the only TLR associated utilising both MyD88-dependent and TRIF signalling pathways (Kawai & Akira, 2010).

The results obtained suggest that *Acanthamoeba* might present on its surface molecules that are recognized by TLR4 inducing an innate immunological response. Glycosylphosphatidylinositol (GPI)-anchors are structures consisting of a glycan conserved core anchored to the plasma membrane by fatty acids chains GPI-anchors can be linked to glycoproteins forming GPI-anchored protein; or they can be linked to repeated phosphorylated carbohydrate units (from 5 to 40 units), forming lipophosphoglycans (LPG). Free GPI-anchors, therefore not linked to glycoproteins or phosphoglycans, also exist and they are called glycoinositolphospholipids (GIPLs) (Ropert & Gazzinelli, 2000). GPI-anchors are highly expressed in several parasitic protozoa (Ropert & Gazzinelli, 2000) and are highly immunogenic, inducing a response by cells of both the myeloid and lymphoid lineages (Uematsu & Akira, 2008). These structures are recognized by TLRs, mainly TLR2, TLR4 and TLR3 and they are therefore considered as protozoan PAMPs (Kumar *et al.*, 2011). According to a study in the early seventies (Korn *et al.*, 1974) the plasma membrane of *A. castellanii* is composed for 31% of its mass of lipophosphoglycans. This data has been confirmed and further characterised by a more recent study using Gas Chromatography-Mass Spectrometry techniques, where the chemical nature of *Acanthamoebic* LPG was identified and recognized as glycoinositolphosphosphingolipids (GIPSL) (Karaś & Russa, 2013). Although it cannot be confirmed with the present study, these structural moieties might be the target of the *Acanthamoeba*-associated molecular pattern able to stimulate TLRs expressed on macrophages.

During parasitic infections proteases are known to be important virulence factors and to be involved in cell differentiation, food acquisition and immune evasion

mechanisms (Rascón Jr & McKerrow, 2013; McKerrow *et al.*, 2006). In addition to their role in the invasion and immune evasion mechanisms recently it has been demonstrated that the *Acanthamoeba*-serine protease, MIP-133, and *Acanthamoeba* plasminogen activator factor stimulate the production of pro-inflammatory cytokines and chemokines by corneal epithelial cells (Tripathi *et al.*, 2012; Tripathi *et al.*, 2013). In addition, we have previously demonstrated (Chapter 3) that *Acanthamoeba* serine and cysteine proteases stimulate IL-12 and IL-6 production by murine macrophages. Protease activated receptors are trans-membrane receptors that are activated by the proteolytic activity of endogenous and exogenous proteases. In particular PAR₁ and PAR₂ are the receptors mainly associated with immune responses and mainly expressed on epithelial, endothelial and innate immune cells (Shpacovitch *et al.*, 2007; Vergnolle, 2003). Therefore, we investigated if PAR₁ and PAR₂, expressed on macrophages were activated by *Acanthamoeba* proteases leading to IL-12 and IL-6 production. By using PAR₂ deficient macrophages, we found that *Acanthamoeba*-induced IL-12 and IL-6 production was PAR₂-independent. On the other hand, *Acanthamoeba*-induced IL-12 production by macrophages was shown to be at least partially PAR₁-dependent, as the pre-treatment of macrophages with specific PAR₁ antagonist significantly inhibited IL-12 production induced by *Acanthamoeba*. Interestingly, a very recent study has reported that *Acanthamoeba* plasminogen activator factor stimulates IL-8 production by human corneal epithelial cells in a PAR₂-dependent, but PAR₁-independent manner (Tripathi *et al.*, 2014). Furthermore, it has been demonstrated, by using an *in vivo* murine model, that *Acanthamoeba* trophozoites and their excreted/secreted molecules stimulate allergic responses and induce T_H2 responses through the activation of DC in a PAR₂-dependent manner (Park *et al.*, 2014).

In this study we report, for the first time, a role for TLR4 and PAR₁ expressed on macrophages in the stimulation of pro-inflammatory cytokine production by *A. castellanii*. In particular, *Acanthamoeba*-induced IL-12 production by macrophages was demonstrated to be both TLR4-dependent and PAR₁-dependent. Cross-talk between the two receptors might also occur, either directly (receptor association) or indirectly at the signalling level. Examples of TLRs-PARs cross-talk, especially involving PAR₂, have been reported and known to be associated with bacterial, viral and fungal infections, but none as yet during protozoan infections (Gieseler *et al.*, 2013). For this reason, it would be interesting to further investigate the interactions between PARs and TLRs during *Acanthamoeba* infections and how these might influence the *Acanthamoeba*-induced pro-inflammatory cytokine production by macrophages.

Appropriate agonists were used for our studies in order to evaluate the efficiency of the system, viability of the cells and the real receptor deficiency. Unexpectedly both PAR-AP2 and PAR-AP1 did not stimulate a significant IL-12 and IL-6 production by WT macrophages. PAR-AP2 and PAR-AP1 concentrations used in our systems were obtained based on the pre-existing literature, since dose-response experiments could not be performed due to the low amount of product and for economic reasons. A possible reason for the lack of agonistic effect might be due to an inappropriate dose or time of exposure to these products. Future studies need to be undertaken to understanding these events. Interestingly, LPS-induced IL-12 and IL-6 production by murine macrophage was inhibited by the pre-incubation with PAR₁ antagonist RWJ 56110. This event might be associated with the direct effect of LPS (Saban *et al.*, 2007) or to extracellular secondary molecules induced by LPS such thrombin-like serine proteases (Mansell *et al.*, 2001).

So far we have found that stimulation of macrophages with *A. castellanii* trophozoites leads to production of pro-inflammatory products in a TLR-dependent manner, therefore promoting the development of an inflammatory/antimicrobial phenotype in macrophages. The ability of *Acanthamoeba* to modulate arginine metabolism in macrophages by shifting it either towards a killing phenotype, by inducing NO production, or toward a wound healing/tissue repairing phenotype by inducing polyamines synthesis in murine macrophages is investigated in the following chapter.

CHAPTER 5

***Acanthamoeba* trophozoites induce arginase activity in murine macrophages**

5.1 Abstract

Macrophages are considered the sentinels of the innate immune system and within all tissues they perform important functions during health and disease. Macrophages have the ability to metabolise L-arginine via iNOS or arginase leading to nitric oxide (NO) production or to polyamine and proline synthesis respectively. The expression of these two enzymes, and the effect of their induction during protozoan infections have been already broadly studied. Induction of iNOS is generally anti-microbial through the production of NO, whereas arginase is normally associated with wound healing. However, arginase induction can also deprive pathogens of arginine. Macrophages respond to *Acanthamoeba* by the production of pro-inflammatory cytokines but their amoebicidal effects against *Acanthamoeba* are NO-independent. In the present study, we investigate the ability of *Acanthamoeba* to interfere with arginine metabolism and its products. Arginase activation and NO production were investigated by incubating murine BMD macrophages, obtained from BALB/c mice, with either trophozoites of *Acanthamoeba* or amoeba-derived conditioned medium. Results demonstrate that *Acanthamoeba* trophozoites stimulate murine macrophages arginase activity, whereas NO-production was not detected. *Acanthamoeba*-induced arginase activity by macrophages was TLR2-independent, as blocking macrophage TLR2 activity with antibody had no effect. In addition, LPS-induced NO production by macrophages was significantly reduced by the co-incubation with live trophozoites. Taken together, these results demonstrate an “alternative” macrophage activation by *A. castellanii*, that could also be considered an immune evasion mechanism.

5.2 Introduction

In the site of infection, macrophages are activated by host proteins, inflammatory mediators and/or by microbial components (Murray & Wynn 2011). Initially, macrophage activation was associated with a killing, pro-inflammatory phenotype attributed to the production of reactive oxygen metabolites and nitric oxide, now termed 'classical activation'. However, the finding that macrophages could be activated by IL-4 or IL-13 in the presence, or absence of LPS modified the concept of macrophage activation. This activation state, termed 'alternative activation' was associated with an anti-inflammatory phenotype (Stein *et al.*, 1992). Macrophages are now known to exhibit many often time-dependent activation states, with confusing and inconsistent nomenclature (Murray *et al.*, 2014) (Fig 5.1). Classically activated macrophages also termed M1 are characterized by a pro-inflammatory and killing phenotype, whereas alternatively activated macrophages termed M2 are considered anti-inflammatory and are associated with tissue remodelling, wound-healing and an immune-regulatory phenotype (Stein *et al.*, 1992; Goerdts & Orfanos, 1999; Mills *et al.*, 2000). M1 macrophages are induced by interferon- γ in combination with microbial components (TLR ligands), such as LPS and they are characterized by high expression of IL-12, IL-23 and iNOS and a low expression of IL-10 (Mantovani *et al.*, 2007). M2 macrophages are induced by IL-4 and IL-13, immune complexes, IL-10, glucocorticoids, transforming growth factor- β (TGF- β), IL-21 and IL-33 (Biswas & Mantovani, 2010). These macrophages express low IL-12, low IL-23, high IL-10, Arg 1, fizz-1 and ym-1 (Mantovani *et al.*, 2007). Macrophages that have only been exposed to LPS or potentially other TLR ligands, are sometimes termed 'innate macrophages' have characteristics similar to M1 macrophages such as high expression of IL-12, IL-23 and iNOS, but also express Arg 1 in a time-dependent manner. This indicates a shifting of phenotype, where arginine activity is

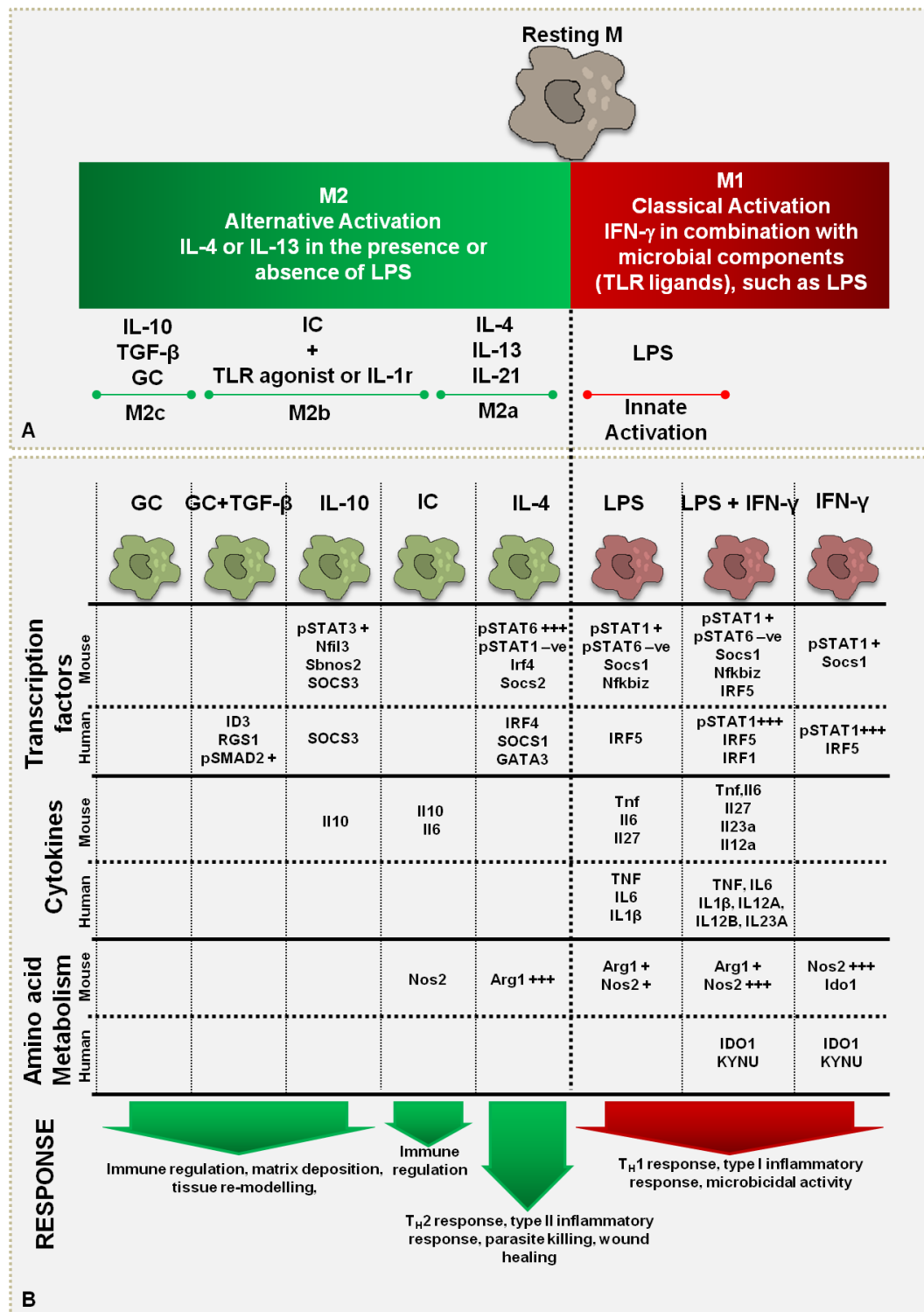
shifted from the production of NO (killing phenotype) to the production of polyamines and proline (wound healing and tissue repair) (Wang *et al.*, 1995; Sonoki *et al.*, 1997; Menzies *et al.*, 2010). Perhaps due this complexity it is better to consider macrophage phenotypes as a spectrum similar to that proposed by Mosser and Edwards (2008) which is subject to temporal movement as previously reported (Wang *et al.*, 1995; Sonoki *et al.*, 1997; Menzies *et al.*, 2010).

Notwithstanding the difficulties in defining macrophage activations states, arginine metabolism would appear to be important in terms of their activation states and function. The relative expression of inducible nitric oxide synthase (iNOS) and arginase 1 (Arg 1) is clearly functionally important. iNOS catabolises L-arginine to L-citrulline and NO, therefore inducing anti-proliferative, anti-microbial functions; on the other hand, arginase metabolizes arginine into ornithine and urea, leading to proliferative and tissue repair functions (Rath, *et al.*, 2014).

We have previously demonstrated that *Acanthamoeba* trophozoites induce pro-inflammatory cytokines through TLR4 and PAR₁ expressed on murine macrophages. Therefore, in this chapter, we investigated *Acanthamoeba*-induced L-arginine metabolism pathways in murine macrophages. Specifically, we evaluated the induction of arginase activity and the production of NO, after challenge with either trophozoites or amoeba-derived conditioned medium. In addition we dissected the involvement of TLRs in these events.

Fig 5.1 Macrophage Activation. Similarly to the TH1/TH2 nomenclature, macrophages were initially distinguished into classically activate (M1) or alternative activated (M2) (Stein *et al.*, 1992; Mills, 2012). Sub-classification of M2 macrophages into M2a, M2b and M2c was then reported, accordingly to the wide range of stimuli discovered. Furthermore, innate activation of macrophages, induced by LPS only, was also demonstrated. The paradigm M1/M2, macrophages might be visualized as two independent and opposite phenotypes, either fighting the infection or fixing the injured tissue (Mills, 2012). However, it has been demonstrated that, this simplistic classification does not reflect the actual complexity of macrophages activation and of their spectrum of functions. Indeed, macrophages are actually plastic cells that adapt, accordingly to the stimuli, microenvironment and stage of infection/inflammation, acquiring either the M1 or the M2 phenotype in a continuous and incremental sequence of functional and temporal events (Mantovani *et al.*, 2002; Menzies *et al.*, 2010; Sica & Mantovani, 2012; Barros *et al.*, 2013). Recently, there have been difficulties and confusion regarding the nomenclature used for the description of macrophage activation, the over simplistic use of single markers to discriminate between M1 and M2 macrophages and the experimental techniques used. Consequently a diverse group of researchers has formulated guidelines in order to standardise the methods for obtaining macrophages, their activation method as well as the nomenclature to use and the identification of collectively accepted activation markers (Murray *et al.*, 2014). The M1/M2 classification of macrophages, observed *in vitro*, might be difficult to find in an *in vivo* context (Barros *et al.*, 2013); indeed, the source of the stimuli and the microenvironment in which it is released cannot be fully recreated *in vitro* since in an infectious/inflammatory site, different stimuli coexist and can potentially be recognized by macrophages and induce their activation (Sica & Mantovani, 2012; Martinez & Gordon,

2014). Previously used nomenclature and the recently proposed nomenclature are illustrated in A (reviewed by Liu & Yang, 2013) and B (Murray *et al.*, 2014), respectively.



5.3 Materials and methods

All methods not described here were carried out as described in Chapter 2.

5.3.1 Effect of *Acanthamoeba* on LPS-induced NO production by murine macrophages

In order to evaluate the effect that either *Acanthamoeba* trophozoites or the amoeba-derived cell free conditioned medium had on LPS-induced NO production, macrophages were incubated with either trophozoites or amoeba-derived conditioned medium of either Neff strain or clinical isolate prior to stimulation with LPS.

Bone marrow-derived macrophages, obtained from BALB/c mice as described in materials and methods, were harvested and plated at 1×10^6 /well. Following incubation overnight, cRPMI in the wells was discarded and replaced with either 200 μ l of trophozoite suspension (1×10^6 trophozoites/well) or 200 μ l of amoeba-derived conditioned medium. Plates were incubated for 1 h at 37°C 5% CO₂. Subsequently, macrophages, pre-incubated or not pre-incubated with *Acanthamoeba*, were stimulated with either 800 μ l of cRPMI or 800 μ l of LPS, at a final concentration in the well of 200 ng/ml. Plates were then incubated at 37°C, 5% CO₂ for 24 h after which the supernatants were collected and analyzed.

5.3.2 Bioinformatical analysis

Flavo-hemoglobins (FlaHb) protein sequences were obtained from NCBI protein data base (<http://www.ncbi.nlm.nih.gov/guide/proteins/>). From the organisms possessing FlaHb enzymes, 4 protozoa and 1 fungi were selected: *Dictyostelium discoideum* Flavo-hemoglobin A, *Dictyostelium discoideum* Flavo-hemoglobin B, *Dictyostelium fasciculatum*, *Giardia intestinalis*, *Giardia lamblia*, *Saccharomyces cerevisiae*. A.

castellanii FlaHb predicted protein sequence was obtained by blasting *G. intestinalis* FlaHb CDS in AmoebaDB (<http://amoebadb.org/amoeba/>). Sequence alignment was performed using the platform <http://multalin.toulouse.inra.fr/multalin/> (Corpet, 1988).

5.4 Results

5.4.1 *Acanthamoeba* trophozoites induce murine macrophage arginase activity; whereas *Acanthamoeba*-induced macrophage NO production was not significantly induced

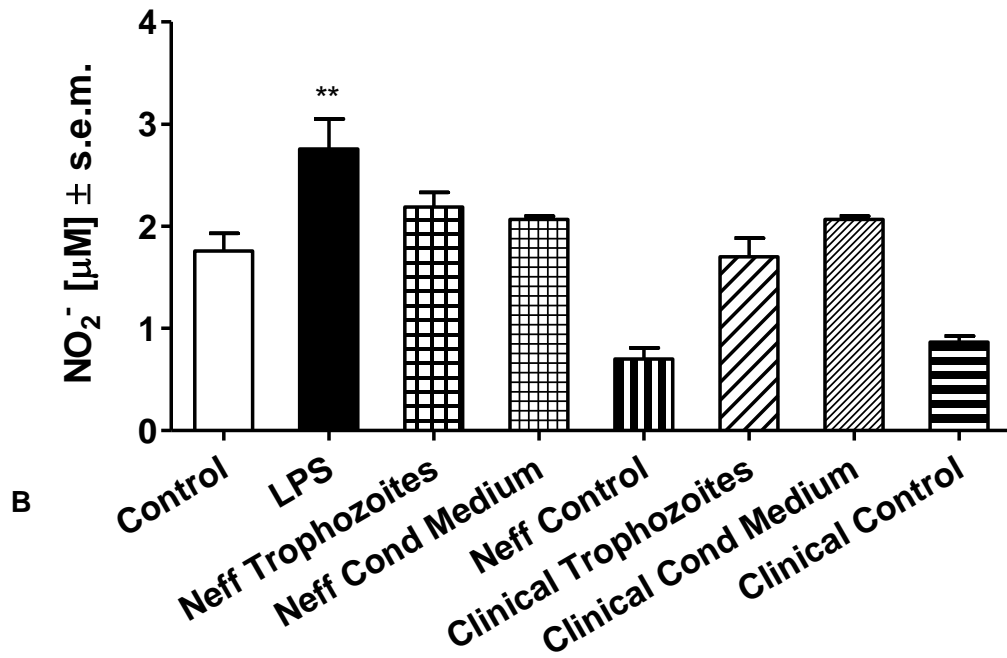
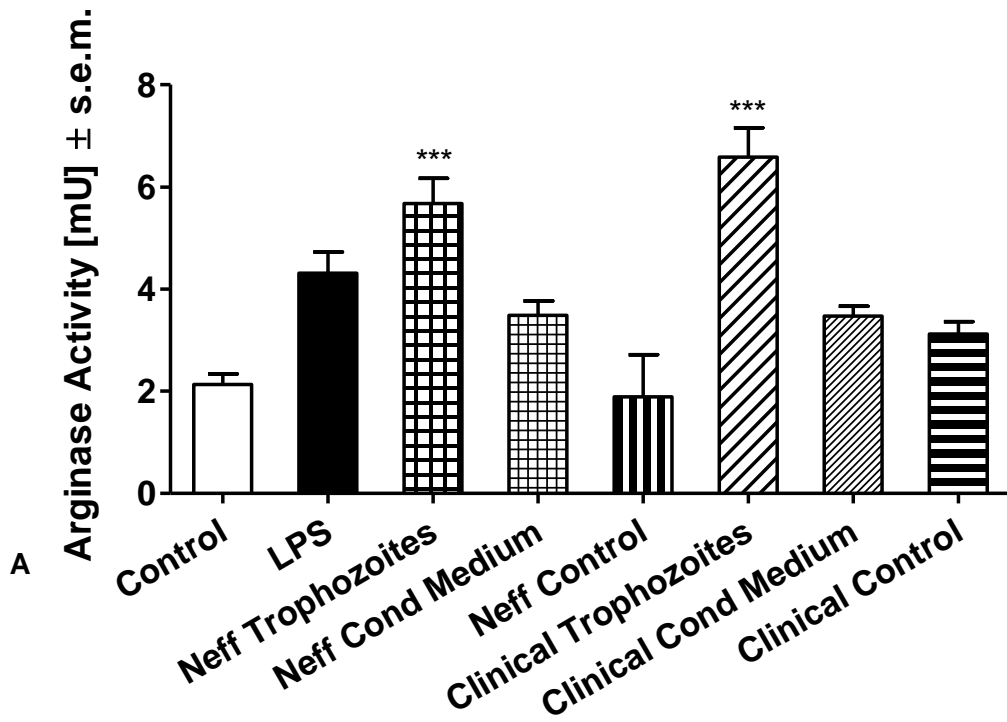
In order to evaluate if *A. castellanii* was able to induce arginase activity or iNOS by murine macrophages, BMD macrophages were obtained and co-incubated with either trophozoites, of either *A. castellanii* Neff strain or *A. castellanii* clinical strain at a ratio 1:1, or amoeba-derived conditioned medium, obtained from either Neff or clinical cultured trophozoites. Although IL-4 is highly and unequivocally used to induce arginase activity by murine macrophages, LPS has been used as positive control in these experiments. Indeed LPS has been demonstrated capable of inducing macrophage innate activation, characterized by late expression of arginase and arginase activity by murine macrophages (Menzies *et al.*, 2010). Since, *Acanthamoeba* expresses an arginase gene in its genome (Clarke *et al.*, 2013), arginase activity by both Neff and clinical trophozoites, maintained at the same incubation conditions, was also evaluated. After 24 h incubation at 37°C, 5% CO₂, arginase activity was determined and nitric oxide (NO) production was assessed by quantifying the nitrite (NO₂⁻), the end product of the NO oxidation pathway expressed in stimulated macrophages, present in the supernatants.

Arginase activity by macrophages was significantly induced by both Neff (5.674 mU, p<0.05) and clinical trophozoites (6.586 mU, p<0.05) in comparison with un-stimulated macrophages. In contrast, both amoeba-derived conditioned media derived from either the Neff strain or clinical isolate failed to significantly up-regulate arginase activity relative to control un-stimulated macrophages. Only low levels of arginase, similar to levels detected in un-stimulated macrophages were detected in

Neff and clinical trophozoites, (1.892 and 3.118 mU, respectively). Stimulation with LPS also induced arginase activity by macrophages (4.31 mU) (Fig 5.2-A).

NO production by macrophages was significantly induced by LPS in comparison with un-stimulated macrophages (2.755 μ M versus 1.755 μ M, respectively; $p < 0.05$). Neither trophozoites nor amoeba-derived conditioned medium from either strain induced significant NO production by macrophages, in comparison with the control macrophage cultures. In trophozoite mono-culture supernatant the level of NO detected was below the control values (Fig 5.2-B).

Fig 5.2 Arginase activity (A) and NO₂⁻ concentration (B) at 24 h after infection. 1x10⁶ murine macrophages, obtained from BALB/c mice, were challenged with 1x10⁶ trophozoites of either *A. castellanii* Neff strain (Neff trophozoites) or clinical isolate (clinical trophozoites). Furthermore, they were stimulated with undiluted and non-fractionated amoeba-derived conditioned medium obtained from either the Neff (Neff cond medium) or clinical (clinical cond medium) strains. LPS at 200 ng/ml (LPS) was used to stimulate macrophages as positive controls. Uninfected macrophages (Control) were considered the negative control. Monoculture of either Neff strain (Neff control) or clinical isolate (Clinical control) trophozoites were included in the experimental design. The experiment was performed twice. Results represent the mean ± standard error of n=3. One way ANOVA was applied and Dunnett's multiple comparison test was performed to evaluate differences between each condition and the control. In the graphs, significant differences between each stimuli and control were represented as follows: p<0.005 **, p<0.0005 ***. Arginase activity was detected in trophozoite/macrophage co-incubation cultures. Conversely, amoeba-derived conditioned medium, obtained from either Neff strain or clinical, failed to induce significant arginase activity in murine macrophages. Arginase activity associated with trophozoites of either Neff or clinical strains was lower (Neff trophozoites) or similar (clinical trophozoites) to control values. NO could be detected in the supernatant of macrophages stimulated with LPS, whereas it could not be significantly detected in *Acanthamoeba*/macrophages co-incubation.



5.4.2 PAM3CSK4-induced arginase activity by macrophages is TLR2-dependent

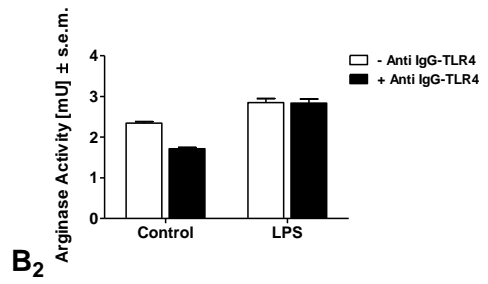
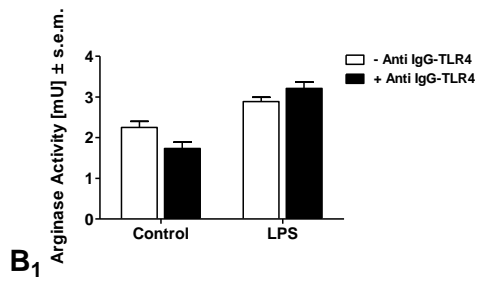
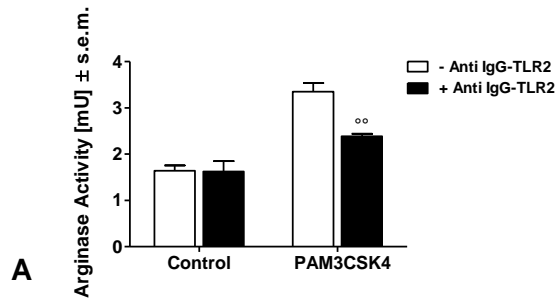
It is known that LPS-induced arginase activity is TLR4-dependent, whereas little is known about the involvement of TLR2 agonist in this event. As a preliminary investigation, in order to evaluating the role of TLR2 and TLR4 expressed on macrophages in *Acanthamoeba*-induced arginase activity, the efficiency of TLR blocking antibody in inhibiting agonist-induced arginase activity was evaluated. Therefore, murine macrophages were pre-treated or not with different concentrations of either anti IgG-TLR2 or anti IgG-TLR4 and subsequently stimulated with either the synthetic triacetylated lipopeptide PAM3CKS4, TLR2/TLR1 agonist, or LPS, a TLR4 agonist. In addition, in order to evaluate the intrinsic activity of the antibody, un-stimulated macrophages pre-treated with either anti IgG-TLR2 or anti IgG-TLR4 were also included in the experimental design. Arginase activity was evaluated at 24 h after stimulation.

Pre-treatment of macrophages with either anti IgG-TLR2 (Fig 5.3-A) or anti IgG-TLR4 alone (Fig 5.3-B₁, B₂), irrespective of the concentration used, did not induce arginase activity, showing values similar to un-stimulated non pre-treated macrophages.

Arginase activity by macrophages was induced by PAM3CSK4 (3.352 mU) (Fig 5.3-A). This production was significantly inhibited in the presence of anti IgG-TLR2 antibody used at 10 µg/ml (2.383 mU, $p=0.0038$) (Fig 5.3-A). While macrophage arginase activity was also induced by LPS, this activity was not inhibited by the pre-incubation with anti IgG-TLR4 at either 10 µg/ml ($p=0.1543$) (Fig 5.3-B₁) or 40 µg/ml ($p=0.4648$) (Fig 5.3-B₂). Consequently, this antibody was not used in further studies.

Fig 5.3 Arginase activity by murine macrophages at 24 h, either pre-treated or not pre-treated with either anti IgG TLR2 antibody (A), or anti IgG TLR4 antibody (B).

1×10^6 murine macrophages, obtained from BALB/c mice, were pre-treated with anti IgG TLRs antibody (+ Anti IgG-TLRs) or not pre-treated (- Anti IgG-TLRs). Anti IgG TLR2 antibody was used at a concentration of 10 $\mu\text{g/ml}$ (A), whereas anti IgG TLR4 antibody was used at a concentration of either 10 $\mu\text{g/ml}$ (B₁) or 40 $\mu\text{g/ml}$ (B₂) and incubated for 1 h at 37° 5% CO₂. Subsequently, pre-treated or non pre-treated macrophages were stimulated with either PAM3CSK4, at a concentration of 320 ng/ml (PAM3CSK4) or LPS, at a concentration of 200 ng/ml (LPS). Un-stimulated macrophages, pre-treated or not pre-treated with antibody were included in the experimental design (Control). The experiment was performed twice. Results represent the mean \pm standard error of n=3. Student's *t*-test was applied to evaluate differences between - Anti IgG-TLRs and + Anti IgG-TLRs conditions. In the graphs, significances between - Anti IgG-TLRs and + Anti IgG-TLRs conditions are indicated as follow: for values of $p < 0.005$ °°. Data shown in the graphs suggest that the functional inhibition of TLR2 using specific antibody, was effective. Indeed, PAM3CSK4-induced arginase activity was significantly reduced by the pre-treatment with anti IgG-TLR2 antibody. On the other hand, pre-treatment with anti-IgG TLR4 antibody did not inhibit LPS-induced arginase activity.

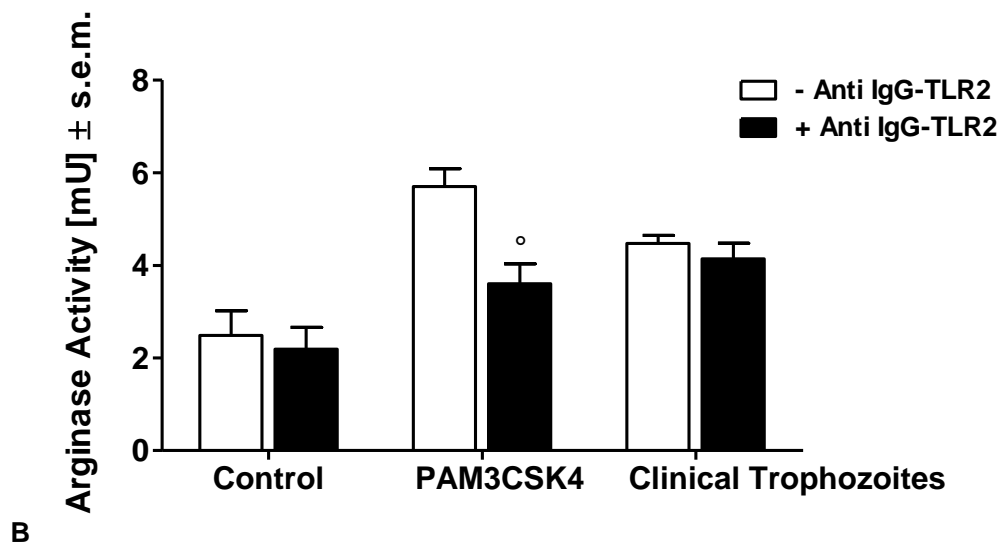
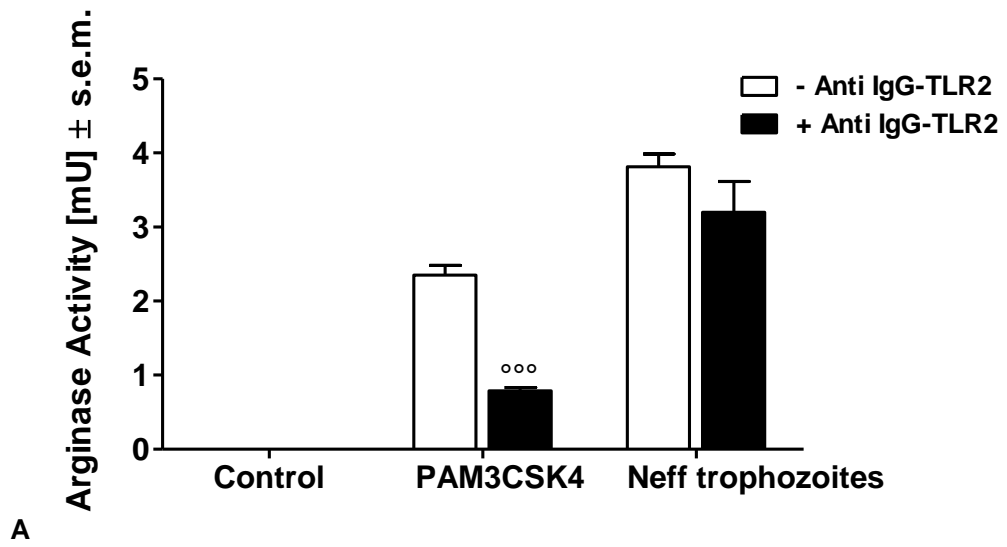


5.4.3 Trophozoite-induced arginase activity by macrophages is TLR2-independent

Since PAM3CSK4-induced arginase activity could be inhibited with specific anti-IgG TLR2 antibody, this experimental design could be applied in the trophozoites/macrophages co-incubation experiment, in order to evaluate the role of TLR2 in *Acanthamoeba*-induced arginase activity. Anti-IgG TLR4 antibody did not inhibited LPS-induced arginase macrophage activity. We could not therefore investigate the role of TLR4 by using this experimental design. Consequently, murine macrophages were pre-treated or not pre-treated with 10 µg/ml anti IgG-TLR2 solution and subsequently stimulated with trophozoites of either Neff strain or clinical isolate at a ratio of 1:1. The synthetic triacetylated lipopeptide PAM3CKS4 was used as a positive control. Un-stimulated macrophages pre-treated with anti IgG-TLR2 were also included in the experimental design. Arginase activity was evaluated following 24 h stimulation.

Macrophage arginase activity was induced by both Neff (3.815 mU) (Fig 5.4-A) and clinical (4.476 mU) (Fig 5.4-B) trophozoites, however the pre-treatment of macrophages with anti-IgG TLR2 antibody did not inhibit trophozoite-induced arginase activity.

Fig 5.4 *Acanthamoeba*-induced murine macrophage arginase activity at 24 h pre-treated or not pre-treated with anti IgG TLR2 antibody. 1×10^6 murine macrophages, obtained from BALB/c mice, were pre-treated with anti IgG TLR2 antibody (+ Anti IgG-TLR2) or not pre-treated (- Anti IgG-TLR2) for 1 h at 37° 5% CO_2 . Subsequently, pre-treated or non pre-treated macrophages were stimulated with PAM3CSK4, at a concentration of 320 ng/ml (PAM3CSK4) or with 1×10^6 of either Neff (Neff trophozoites) (A) or clinical trophozoites (Clinical trophozoites) (B). Un-stimulated macrophages, pre-treated or not pre-treated with antibody were included in the experimental design (Control). The experiment was performed twice. Results represent the mean \pm standard error of $n=3$. Student's *t*-test was applied to evaluate differences between - Anti IgG-TLR2 and + Anti IgG-TLR2 conditions. In the graphs, significances between - Anti IgG-TLR2 and + Anti IgG-TLR2 conditions are indicated as follow: for values of $p < 0.05$ °; $p < 0.0005$ °°. Data shown in the graphs suggest that trophozoites-induced arginase activity by macrophages is not TLR2-dependent.

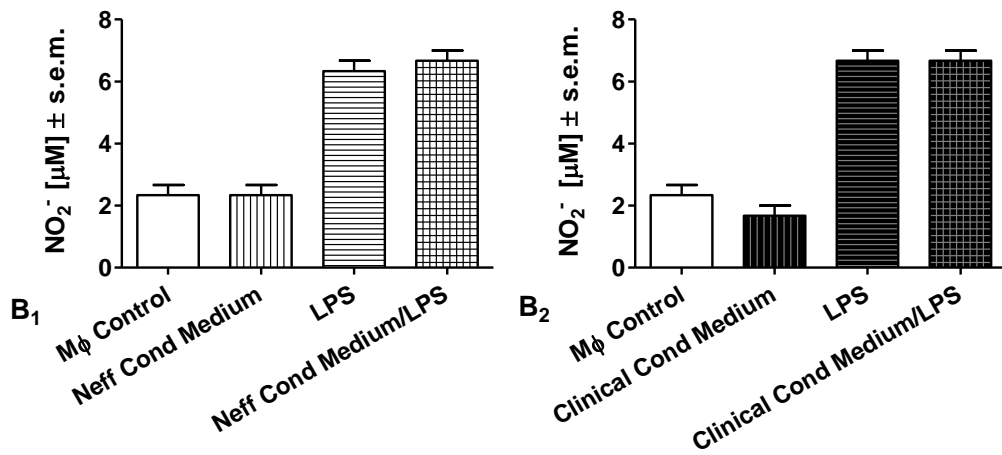
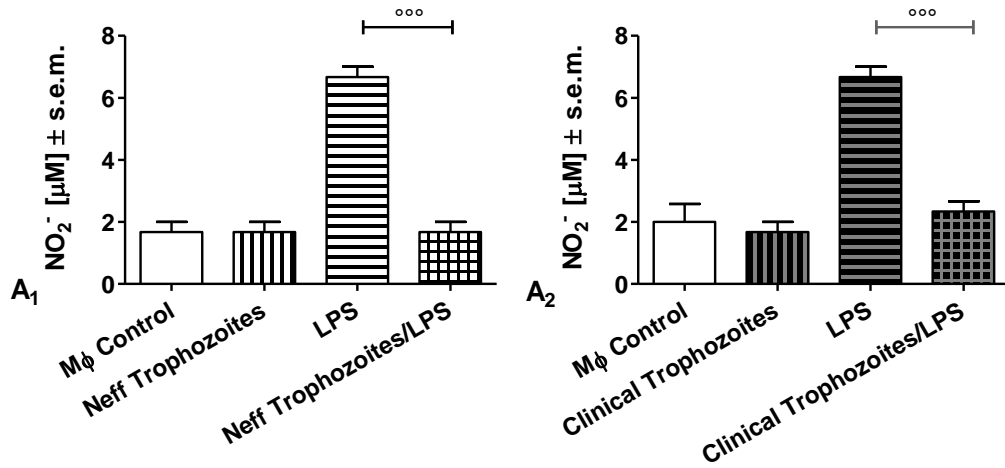


5.4.4 LPS-induced NO production by macrophages is reduced by *Acanthamoeba* trophozoites

In order to evaluate if *Acanthamoeba* might possess a NO-detoxifying system, macrophages were pre-incubated for one hour at 37°C 5% CO₂, with either Neff or Clinical trophozoites at a ratio of 1:1 or with amoeba-derived conditioned medium obtained by either Neff or clinical trophozoite culture. Macrophages were then stimulated with LPS or left untreated. Macrophages not pre-incubated with *Acanthamoeba*, and not stimulated with LPS were considered the negative control. NO production by BMD macrophages was assessed by quantifying the nitrite (NO₂⁻), end product of NO oxidation pathway expressed in stimulated macrophages, present in the supernatants after 24 h incubation at 37°C, 5% CO₂.

Both trophozoites and supernatants of either Neff strain or clinical isolate did not induce significant NO-production by macrophages, presenting concentration values similar to un-stimulated macrophages (Fig 5.5). LPS induced NO production by macrophages (6.666 μM) and this production was significantly decreased by the presence of trophozoites of either the Neff strain (1.666 μM p=0.0002) (Fig 5.5-A₁) or clinical isolate (2.333 μM p=0.0004) (Fig 5.5-A₂). Amoeba-derived conditioned medium, obtained from either Neff or clinical isolate trophozoites did not reduce LPS-induced NO production by macrophages (Fig 5.5-B₁, B₂ respectively).

Fig 5.5 LPS-induced NO₂⁻ production by macrophages following pre-incubation with, or without, *Acanthamoeba* trophozoites (A), or amoeba-derived conditioned medium (B). 1x10⁶ murine macrophages, obtained from BALB/c mice, were pre-incubated or not pre-incubated with 1x10⁶ trophozoites, of either *A. castellanii* Neff strain (Neff trophozoites) or clinical isolate (clinical trophozoites), or with 200 µl of amoeba conditioned medium derived from either Neff (Neff Cond Medium) or clinical (Clinical Cond Medium) trophozoites for 1 h at 37°C, 5% CO₂. Macrophages pre-incubated or not pre-incubated with either trophozoites or conditioned medium were then stimulated with LPS at 200 ng/ml (respectively trophozoite or Cond Medium/LPS and LPS). Macrophages non pre-treated with either trophozoites, or conditioned medium and not stimulated with LPS (Mφ control) were considered the negative control. The experiment was repeated twice. Results represent the mean ± standard error of n=3. Student's *t*-test was applied to evaluate differences between pre-incubation and non pre-incubation with *Acanthamoeba* conditions. In the graphs, significances between pre-incubation and non pre-incubation with *Acanthamoeba* conditions are indicated as follow: for values of p<0.0005 °°. In the graphs, LPS-induced NO production by macrophages was decreased by the pre-incubation with both Neff strain and clinical isolate trophozoites. On the other hand, pre-incubation of amoeba-derived conditioned medium did not induced a decreased of LPS-induced NO production by macrophages.



5.4.5 *Acanthamoeba* FlaHb putative protein presents a similar amino acid sequence to other FlaHb protein sequences.

In order to evaluate the presence of flavohemoglobins in *Acanthamoeba* genome, protein multi-alignment studies were performed.

A FlaHb putative protein was identified, in *Acanthamoeba* genome, presenting similarities to the FlaHb amino acid sequences in *Dictyostelium*, *Giardia* and *Saccharomyces* (Fig 5.6). The alignment demonstrates a degree of similarity between this putative protein from *A. castellanii* Neff with other FlaHb protein sequences, although many residues conserved in the other taxa are not identifiable in the *Acanthamoeba* sequence.

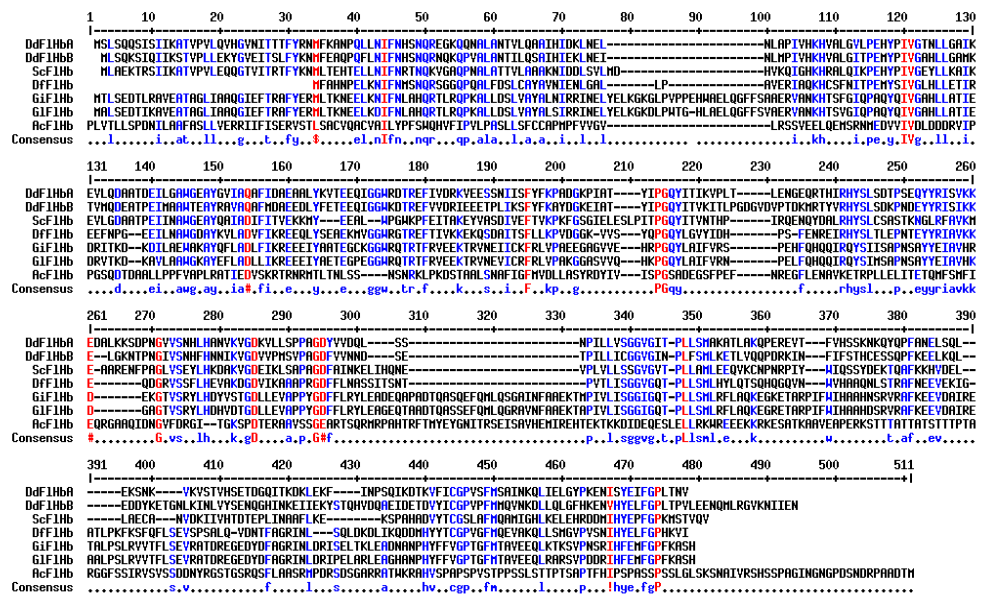


Fig 5.6 Flavohemoglobin protein sequence multi-alignment across several organisms and comparison with *A. castellanii* FlaHb predicted protein sequence. Protein sequence was obtained from NCBI protein data base. From the organisms missing FlaHb enzymes, 4 protozoa and 1 fungi were selected: *Dictyostelium discoideum* Flavohemoglobin A (DdFlHbA), *Dictyostelium discoideum* Flavohemoglobin B (DdFlHbB), *Dictyostelium fasciculatum* (DfFlHb), *Giardia intestinalis* (GiFlHb), *Giardia lamblia* (GfFlHb), *Saccharomyces cerevisiae* (ScFlHb). *A. castellanii* FlaHb (AcFlHb) predicted protein sequence was obtained by blasting *G. intestinalis* FlaHb CDS in AmoebaDB. E score was 0.045. Identical amino acids among the protein sequence are showed in red, whereas homologous are showed in blue.

5.5 Discussion

The catabolism of L-arginine, by either arginase or iNOS, plays an essential role in the immune responses controlling many intracellular and extracellular microbial pathogens (Das *et al.*, 2010). The balance between these two enzyme activities within macrophages is crucial for the development of appropriate immune responses contributing to control of parasites and recovery of tissue functions (Rath *et al.*, 2014). Both arginase and iNOS compete for the same substrate, L-arginine, and consequently excessive arginase activity can cause a depletion of L-arginine, limiting NO production through iNOS activity. This in turn can result in uncontrolled parasite replication e.g. with *Leishmania* infection (Raes *et al.*, 2007). On the other hand excessive iNOS activity can cause tissue damage (Raes *et al.*, 2007).

Given the importance of NO in parasite killing it is not surprising that some intracellular parasites have evolved the ability to modulate host cell L-arginine metabolism in order to survive and to disseminate within the host tissues. *T. cruzi* produces a cysteine protease, cruzipain, that induces arginase activity in heart tissue leading to polyamine synthesis which is necessary for parasite growth, whereas it does not induce iNOS activity (Aoki *et al.*, 2004). Similarly, *Leishmania* spp. infects macrophages, and in order to survive within these cells, it modulates their L-arginine metabolism increasing arginase activity, and therefore polyamine synthesis, necessary for parasite survival and proliferation (Kropf *et al.*, 2005). Increased host arginase activity and polyamine synthesis, rather than NO production, is the crucial event for *L. major* survival (Gaur *et al.*, 2007). In *L. mexicana* infections, endogenous arginase activity within the parasite plays an essential role in its survival and virulence, through depletion of L-arginine which limits NO production, (Gaur *et al.*, 2007). In one study, *T. gondii* has been demonstrated to induce Arg 1 expression in host cells, thus evading NO-induced

parasite killing (Das *et al.*, 2010). However in another study inhibition of arginase in mice was demonstrated to promote the growth of *T. gondii* (Woods *et al.*, 2013). The apparent contradictory results is likely due to *T. gondii* being auxotrophic for this amino acid meaning that L-arginine depletion as well as NO production can both have detrimental effects on this parasite (Woods *et al.*, 2013).

It was previously demonstrated that macrophage-induced amoebicidal activity against *Acanthamoeba* is iNOS-independent (Alizadeh *et al.*, 2007). We have demonstrated for the first time that *Acanthamoeba* can induce arginase activity but not iNOS in murine macrophages. Indeed, we demonstrate that *A. castellanii* trophozoite induces an increase in arginase activity in murine macrophages after 24 h co-incubation. This increased arginase activity by macrophages was not observed after stimulation with amoeba-derived conditioned medium. In addition, neither trophozoites nor amoeba-derived conditioned medium induce significant macrophage NO production. Interestingly, transcripts for an arginase enzyme were previously noted in the *A. castellanii* Neff strain genome (Kim *et al.*, 1987; Clarke *et al.*, 2013). However, arginase activity was not detected at significant levels in trophozoites maintained in the same experimental conditions as co-incubation of trophozoites with macrophages studies, suggesting that all arginase activity measured and any related down-regulation of NO production was associated with a direct effect of trophozoites on macrophage function.

It is known that Arg1 is expressed in many systems and organs and that L-arginine depletion by arginase induces a down-regulation of T-cell proliferation and functions, promoting immune suppression in cancer and in human placenta (Fu *et al.*, 2011). Corneal endothelial and epithelium cells cultured *in vitro*, express arginase and its activation leads to a down regulation of T-cell proliferation supporting the corneal immune privileged condition (Fu *et al.*, 2011). Therefore, *Acanthamoeba*-induced

arginase activity in macrophages, and also potentially its endogenous arginase activity, could represent a dual immune evasion mechanism limiting iNOS activity and down-regulating T-cell proliferation and functions. Extracellular parasitic protozoans, such as *Entamoeba* and *Giardia*, also possess endogenous arginase activity. It has been demonstrated that these protozoans can consume L-arginine, present in the external environment, inhibiting NO-production by host cells and enabling evasion of the anti-microbial actions of NO (Elnekave *et al.*, 2003; Stadelmann *et al.*, 2012; Echmann *et al.*, 2000). From our results, a slightly higher arginase activity was evident in macrophages incubated with the clinical strain trophozoites rather than the Neff strain. Clinical isolate trophozoites also had a higher endogenous arginase activity than Neff trophozoites. This raises the intriguing possibility that these factors could contribute to the ability of *Acanthamoeba* to cause clinical disease. More studies will be required to test this possibility.

It is known that LPS, through TLR4, can induce early expression of iNOS and late expression of Arg 1 in murine macrophages (Menzies *et al.*, 2010) It has also been shown that TLR2 is involved in the development of alternative activated macrophages in a murine model of neurocysticercosis (Gundra *et al.*, 2011). In the present report it was found that *Acanthamoeba*-induced arginase activity was TLR2-independent. Other TLRs, such as TLR4, could be involved in these events, however this cannot be confirmed in the present study due to limitations in the reagents available to us. Furthermore, future experiments will also include non specific agonist in the experimental design to verify the real selective and specific inhibition of the antibody used.

NO was not detected at significant levels in trophozoite/macrophage co-incubation supernatants, or after stimulation of macrophages with amoeba-derived conditioned

medium. This is consistent with the fact that arginase, rather than iNOS, is induced in macrophages by *Acanthamoeba* trophozoites. However, we hypothesise a possible detoxification mechanism expressed by *Acanthamoeba*, in order to protect itself from NO-dependent cytotoxic effects, that might account for the ability of *Acanthamoeba* to interfere with LPS-induced NO production. We found that LPS-induced NO production by macrophages was significantly diminished by the pre-incubation and presence of *Acanthamoeba* trophozoites. In contrast, pre-incubation with amoeba-derived conditioned medium did not reduce LPS-induced NO production by macrophages.

Some microbial pathogens have developed enzymes that catalysed the conversion of NO into inactive and less harmful molecules as a defence mechanism. For example, flavohemoglobins (FlaHb) are microbial enzymes that in aerobic conditions detoxify NO into nitrate NO_3^- . They are highly expressed in microbes that live in NO and related species-rich environments (Mastronicola *et al.*, 2010). Furthermore, microbial pathogens increase FlaHb expression during infections, suggesting their role in pathogenic events (Mastronicola *et al.*, 2010). FlaHb have been identified in bacteria (Stevanin *et al.*, 2007; Crawford & Goldberg, 1998), fungi (Collette *et al.*, 2014) and thus far 2 protozoans, *Dictyostelium discoideum* (Iijima *et al.*, 2000) and *Giardia intestinalis* (Mastronicola *et al.*, 2010). Although it has not fully been confirmed in this study, FlaHb, or other detoxifying systems, may be expressed by *Acanthamoeba*, allowing this organism to live in natural environments, as well as to survive in the NO-rich inflammatory environment. Of significance, through interrogation of the *Acanthamoeba* genome and protein multi-alignment studies, we identified a putative protein with similarities to the FlaHb amino acid sequence in *Dictyostelium*, *Giardia* and *Saccharomyces*. The alignment demonstrates a degree of similarity between this putative protein from *A. castellanii* Neff with other FlaHb

protein sequences, although many residues conserved in the other taxa are not identifiable in the *Acanthamoeba* sequence. Thus further investigations are required to establish if FlaHb or another enzyme with similar function is responsible for the detoxification of NO by *Acanthamoeba*.

This report indicates for the first time that *Acanthamoeba* can induce arginase activity, but does not induce NO-production by murine macrophages. Furthermore, live trophozoites decrease LPS-induced NO production by macrophages. The increased *Acanthamoeba*-induced arginase activity by macrophages, and the absence of NO-production, or its detoxification, could be considered as a potential immune evasion mechanism. On the other hand it can also be an attempt by the host cells to recover from excessive cell damage caused by both trophozoites and inflammatory mediators. The results suggest that *Acanthamoeba* and host cells have a bi-directional interaction involving, receptors and enzymes, expressed by immune cells, and enzymes expressed by *Acanthamoeba*. Subtle differences in this interaction might determine the chances of *Acanthamoeba* establishing an infection in its occasional host. For this reason, it could be interesting to investigate metabolic pathways in *Acanthamoeba* trophozoites, and if *Acanthamoeba* can modulate and interfere with host metabolic pathways and ultimately affect the immune response generated.

CHAPTER 6

Qualitative characterization of macrophage metabolism after stimulation with amoeba-derived cell free conditioned medium: preliminary data.

6.1 Abstract

The development of “-omics” techniques, such as genomics, transcriptomics and metabolomics have allowed researchers to obtain a global and rapid overview about the biology of protozoan parasites, their hosts and host/parasite interactions. The term metabolome refers to a steady picture of all metabolites, including upstream intermediates and downstream products, present in a biological system at a determined time or/and under a specific condition. Metabolomic techniques combine separation and detection systems with computational analytical techniques to allow the analysis of the metabolome. This can be achieved in a target cell, tissue, organ, body fluid or whole organism at a predefined time and in the context of drug treatment, neoplastic, infectious or metabolic diseases. Herein, the composition of conditioned media from *Acanthamoeba* Neff strain and clinical isolate used in previous chapters, is characterised by LC/MS. The results demonstrate that conditioned media from the clinical strain of *Acanthamoeba* contains L-kynurenine, L-glutamine and ATP. The ability of these preparations and LPS to modify murine macrophage metabolism was investigated by analysis of macrophage intracellular and excreted metabolites. This preliminary metabolomics study suggests that *Acanthamoeba*-derived conditioned medium unlike LPS does not induce important up regulation of glycolysis, nor catabolism of L-arginine in macrophages. Interestingly, ATP was released by macrophages after incubation with either LPS or amoeba-derived conditioned medium. The results indicate that *Acanthamoeba* secrete products that are potentially involved in the modulation of immune response at the site of infection.

6.2 Introduction

In the site of infection/inflammation macrophages can be differently activated and initiate a perfectly tailored immune response against endogenous or exogenous threats (Murray & Wynn 2011). Macrophage activation phenotypes and their functions have been widely studied and discussed in the literature (Murray *et al.*, 2014). Immunological, biochemical and molecular studies, performed both *in vivo* and *in vitro*, have allowed researchers to identify the nature of the stimuli, the receptors and enzymes involved, and the genes expressed in differently activated macrophages (Biswas & Mantovani, 2012). These biochemical and transcriptional modifications are then used to characterize M1 pro-inflammatory and M2 anti-inflammatory, wound-healing immune-regulatory macrophage phenotypes (Biswas & Mantovani, 2012).

Cellular metabolism essential for the production of energy, and the maintenance of cellular and tissue functions in physiological conditions, can change in response to pathological and infectious conditions (Biswas & Mantovani, 2012). The concept that cellular metabolism could significantly change within activated macrophages has been studied and demonstrated since the early 1970s (Galván-Peña & O'Neill, 2014). More recently different macrophage activation states have been studied in terms of their metabolic profiles (Galván-Peña & O'Neill, 2014). L-arginine metabolism characterizes the paradigm M1/M2. Indeed, activation of macrophages by LPS (innate activation) is known to rapidly induce iNOS expression which converts arginine substrate to nitric oxide and L-citrulline (Rath *et al.*, 2014). These macrophages subsequently express Arg 1 which converts arginine to ornithine (Menzies *et al.*, 2010). IFN- γ accentuates iNOS expression and thus nitric oxide and citrulline production, but inhibits Arg 1 and ornithine production (Menzies *et al.*, 2010). M2 activation as a consequence of ligation of IL-4R α alone or in combination

with TLR4 also results in arginase expression with the production of L-ornithine. L-ornithine produced by macrophages is subsequently metabolized into polyamines and proline (Rath *et al.*, 2014). L-tryptophan metabolism by indoleamine 2,3-dioxygenase (IDO1) can occur in macrophages stimulated both in an IFN- γ -dependent and independent manner (TLR ligand) (Jung *et al.*, 2007). Induction of IDO in macrophages leads to depletion of extracellular L-tryptophan and release of its catabolites into the external milieu resulting in immune regulatory events (Murakami *et al.*, 2013).

Carbohydrate metabolism has been shown to be differently driven in M1 and M2 macrophages (Galván-Peña & O'Neill, 2014). Glycolysis is principally induced in classically activated macrophages characterized by the uptake of glucose from the external milieu and the conversion of pyruvate into lactate allowing resistance to an inflammatory hypoxic microenvironment (Galván-Peña & O'Neill, 2014). Attenuated respiratory chain reactions and the activation of pentose phosphate pathway allow and enhance ROS and NOS production, promoting the macrophage killing phenotype (Galván-Peña & O'Neill, 2014). Furthermore, glycolysis facilitates phagocytosis, which requires a sustained energy supply (Biswas & Mantovani, 2012). In contrast, M2 macrophages promote fatty acid oxidation and oxidative phosphorylation, which support a prolonged energy supply for the tissue remodeling processes. In addition, pentose phosphate metabolism is attenuated in M2 macrophages (Biswas & Mantovani, 2012).

Upon infection, intracellular and extracellular pathogens can interfere and modulate cellular metabolism by inducing production of the metabolites necessary for their survival or/and by depleting metabolites essential for host cells metabolic functions. These mechanisms have evolved to facilitate their survival within the host cells/tissue and to avoid the immune response (Muraille *et al.*, 2014). The host has

evolved counter measures that through changes to metabolism deprive pathogens of essential nutrients such as tryptophan or arginine or produce toxic moieties such as NO that kills pathogens. In addition, endogenous and pathogen-released metabolites can interfere with cellular homeostasis and induce or modulate immune and inflammatory events (Grohmann and Bronte, 2010). For these reasons, studies based on “-omics” techniques are gaining momentum as a way to elucidate pathogen metabolism and innate immune cell metabolism modification during infectious disease (Kafsack & Llinás, 2010; Lamour *et al.*, 2012; Sana *et al.*, 2013).

Results reported in the previous chapters suggest that *Acanthamoeba* is capable of inducing pro-inflammatory cytokines that are normally associated with innate or M1 activated macrophages. Furthermore our previous results would suggest that *Acanthamoeba* stimulates arginase activity in murine macrophages. The following studies were therefore undertaken to characterize products that *Acanthamoeba* secrete and to determine if these products can modulate macrophage metabolism. *Acanthamoeba* are clearly metabolically active protozoa and it is impossible to separate macrophages and trophozoites metabolites post co-infection, thus it was not practicable to determine the effects of live *Acanthamoeba* trophozoites on macrophage metabolism.

6.3 Materials and Methods

6.3.1 Extraction of metabolites from whole macrophages, from macrophage spent medium and amoeba-derived conditioned medium.

BMD macrophages, obtained from BALB/c mice, were stimulated with amoeba-derived conditioned medium obtained from either *A. castellanii* Neff strain or *A. castellanii* clinical isolate as described in the general Materials and Methods. In this experimental design, amoeba-derived conditioned media obtained from either *A. castellanii* Neff strain or *A. castellanii* clinical isolate were seeded into empty wells or into the wells containing 1×10^6 macrophages. Plates were incubated at 37°C, 5% CO₂, for 24 hrs after which metabolite extraction was performed.

Chloroform/methanol/water (20:60:20 v/v/v) extraction mixture was used for extraction of metabolites from macrophages and chloroform/methanol (20:60 v/v) extraction mixture for extraction of metabolites from the spent medium or amoeba-derived conditioned media controls. Extraction mixtures were prepared using HPLC grade solvents, and chilled at 4°C along with required plastics (microcentrifuge tubes and 24 well plates), PBS and tube holders. All centrifugation steps were carried out at 4°C.

After incubation, the plate was observed under the inverted microscope to evaluate the state of cells and identify any contamination. The plate was placed on ice in order to arrest the metabolism. 75 µl of macrophage spent medium, 75 µl of amoeba-derived conditioned medium, and 75 µl of cRPMI were transferred into a fresh pre-chilled 24 well plate. The remaining macrophages were washed with 1 ml of chilled PBS that was discarded throughout. 200 µl of chloroform/methanol/water (20:60:20 v/v/v) was added to macrophage monolayers and 300 µl of

chloroform/methanol (20:60 v/v) extraction mixture was added to the spent medium, amoeba-derived conditioned medium and cRPMI samples. Plates were then sealed and incubated for 1 hr at 140 rpm on a plate shaker at 4°C. Extraction samples were transferred into pre-chilled microcentrifuge tubes and centrifuged for 10 min at 13000 rpm at 4°C. Supernatants were removed from the microcentrifuge tubes without perturbing the underlying white layer, and transferred into 0.2 ml clear flat bottom glass micro tubes inserted into transparent screw cap vials (LC/MS auto sampler vial kit) (Thermo scientific, Hemel Hempstead, UK). Extraction samples were stored at -80°C until LC/MS analysis.

6.3.2 Liquid chromatography and mass spectrometry

Extraction samples were analysed through high-performance liquid chromatography (HPLC) and mass spectrometry (MS) systems. The liquid chromatography system (UltiMate® 3000 LC System, Dionex, Thermo scientific, Hemel Hempstead, UK) was connected to an Extractive Mass Spectrometer (Orbitrap, Thermo scientific, Hemel Hempstead, UK). The auto sampler tray was loaded as follows: initially 2 vials containing solvent blank (chloroform/methanol/water mixture), then 4 vials containing mixed metabolite standard; lastly the extraction samples were randomly loaded into the auto sampler tray (Storm *et al.*, 2014). 10 µl from each vial were introduced into SeQuant® ZIC®-pHILIC, 5 µm polymeric particles, 150 mm x 4.6 mm, metal-free HPLC column (Millipore, Merck, Darmstadt, Germany) (Storm *et al.*, 2014). The mobile phase consisted of two solvent solutions: 20 mM ammonium carbonate in HPLC grade water (solvent A) and acetonitrile (solvent B). Metabolites were separated, through the column, applying the following gradient elution protocol: the starting point was 80% of B and 20% of A which was maintained for 30 min; followed by 20% of B and 80% of A for a 1 min; followed by 5% solvent B and 95% solvent A for 6 min; and finally 80% solvent B and 20% solvent A for 10 min (Storm

et al., 2014). For each sample the total elution time was 46 min. Eluted metabolites through LC were positively and negatively ionized by electrospray ionization (ESI) and identified by mass spectrometry in relation to mass/charge ratio.

6.3.3 Data processing

LC/MS data processing is a three-phase process. The first phase is the conversion of raw LC data to accessible mzXML files. Chromatograms were extracted from these files and stored into PeakML files (Berg *et al.*, 2013). Subsequently PeakML files corresponding to replicates were matched and peaks that were not equally detected were discarded. The second phase is operated by mzMatch software, which applies intensity filter, noise filter, and a final filter that re-integrates peaks deleted by preceding filters. mzMatch, allows the identification of putative metabolites through mass databases (Berg *et al.*, 2013). The last phase is the import of mzMatch peak list into an IDIOM Microsoft excel file which allows the identification of the putative metabolites present in the extraction samples on the basis of mass and retention time (Berg *et al.*, 2013). IDIOM provides relative intensity values which provides the relative levels of metabolites detected (Creek *et al.*, 2012).

6.3.4 Data analysis

Data obtained from IDIOM excel files were analysed as follow. Metabolites with a high confidence value (in relation to the match with known metabolite standards, RT and mass match) were included in our analysis. By using IDIOM tools, comparative analysis was performed between control and stimulated samples. Increased or decreased relative intensity expressed as fold change values between control and stimulations were calculated and differences of Log_2 fold change $> \pm 1$ were considered to indicate differences within the conditions (Silva *et al.*, 2011).

6.4 Results

6.4.1 *Acanthamoeba* modifies the complete RPMI composition by the release and the uptake of metabolites

Approximately 230 metabolites were detected by LC-MS in the amoeba-derived conditioned medium extracts. Metabolically active trophozoites, of both Neff strain and clinical isolate were able to modify the composition of RPMI media by withdrawing and/or secreting metabolites (Fig 6.1). Both strains of *Acanthamoeba* secreted 15 metabolites in common at high levels into their media (urocanate, N2-(D-1-Carboxyethyl)-L-arginine, 2-oxoglutarate, phosphoenolpyruvate, cis-aconitate, D-ribose 5-phosphate, nicotinate, cytidine, inosine, CMP, (-)-ureidoglycolate, orotate, N-carbamoyl-L-aspartate, 1-(5'-Phosphoribosyl)-5-amino-4-(N-succinocarboxamide)-imidazole, AMP) (Fig 6.1). In addition, the clinical isolate secreted an additional 13 unique metabolites (L-kynurenine, 2-oxoglutaramate, L-glutamate, (2S)-2-isopropylmalate, 2-hydroxy-6-ketonoatrienedioate, D-glucose 6-phosphate, 3-phospho-D-glycerate, D-sedoheptulose 7-phosphate, sucrose, ATP, 2',3'-cyclic CMP, xanthosine 5'-phosphate, icosadienoic acid) and the Neff strain secreted an additional 2 unique metabolites (3-(3-hydroxy-phenyl)-propanoic acid, 8-Amino-7-oxononanoate) into the media (Fig 6.1). Both strains of *Acanthamoeba* withdrew folate, cysteate and urate from the media. In addition, the clinical isolate withdrew (3-(4-hydroxyphenyl)pyruvate, N-acetylisatin, LPA (0:0/18:1(9Z)), LPA (0:0/18:2(9Z,12Z))) (Fig 6.1).

A number of differences in the quantities of metabolites released into the media were noted between the *Acanthamoeba* strains (Fig 6.2). L-kynurenine, 2-oxoglutaramate and L-glutamate were increased >1 fold in conditioned medium from the clinical isolate, but not from the Neff strain. Although, urocanate was detected in

conditioned medium from both strains, Neff conditioned medium extracts had a higher fold change value of >2. N²-(D-1-Carboxyethyl)-L-arginine (D-octopine) was increased to a similar extent in both Neff and clinical conditioned media (Fig 6.2).

2-oxoglutarate, phosphoenolpyruvate and cis-aconitate were detected at >2 fold increases in both conditioned media. D-ribose 5-phosphate was detected in both conditioned media, however it was present at higher levels in the medium derived from the clinical isolate. D-glucose 6-phosphate, 3-phospho-D-glycerate, and D-sedoheptulose 7-phosphate and sucrose were only detected at high levels in conditioned medium from the clinical isolate (Fig 6.2). ATP was detected in conditioned medium from the clinical strain at >2 fold increase, but not in the conditioned medium from the Neff strain (Fig 6.2).

Depletion of folate (fold change > -2) from the cRPMI could be observed in conditioned medium from both the Neff strain and clinical strain of *Acanthamoeba*. Nicotinate was highly increased in conditioned media derived from both strains of *Acanthamoeba* (Fig 6.2).

Metabolites derived from nucleotide metabolism were raised in both Neff strain and clinical isolate conditioned medium extracts. However, conditioned medium, from the clinical strain, but not the Neff strain had increased levels of 2',3'-cyclic CMP and xanthosine 5' phosphate (Fig 6.2).

Fig. 6.1 Characterization of amoeba-derived conditioned medium. Venn diagram schematically indicates the number and the specific metabolites withdrawn or released by 4×10^6 *Acanthamoeba* trophozoites/ml incubated at room temperature in RPMI 20 mM Hepes for 2 h. Prior to use, amoeba-derived conditioned medium was supplemented with 10% FCS. The experiment was performed once, and conditions were in triplicate. Metabolites decreased >1 fold (blue), in relation with cRPMI, were considered withdrawn and used by *Acanthamoeba* trophozoites, whereas metabolites increased by >1 fold (red) in relation with cRPMI, were considered secreted by *Acanthamoeba* trophozoites. The number of metabolites, either withdrawn, or released by either Neff strain (pink) or clinical isolate (green) trophozoites are represented. The overview provided by the Venn diagram suggests that conditioned medium derived from clinical isolate presents a richer and a peculiar metabolic composition compared with conditioned medium derived from Neff strain trophozoites. Analysis of the metabolic composition of these preparations gives insight into the biology of the *Acanthamoeba* and is essential to know what metabolites are added or are missing when amoeba-derived conditioned medium is used to stimulate macrophages *in vitro*.

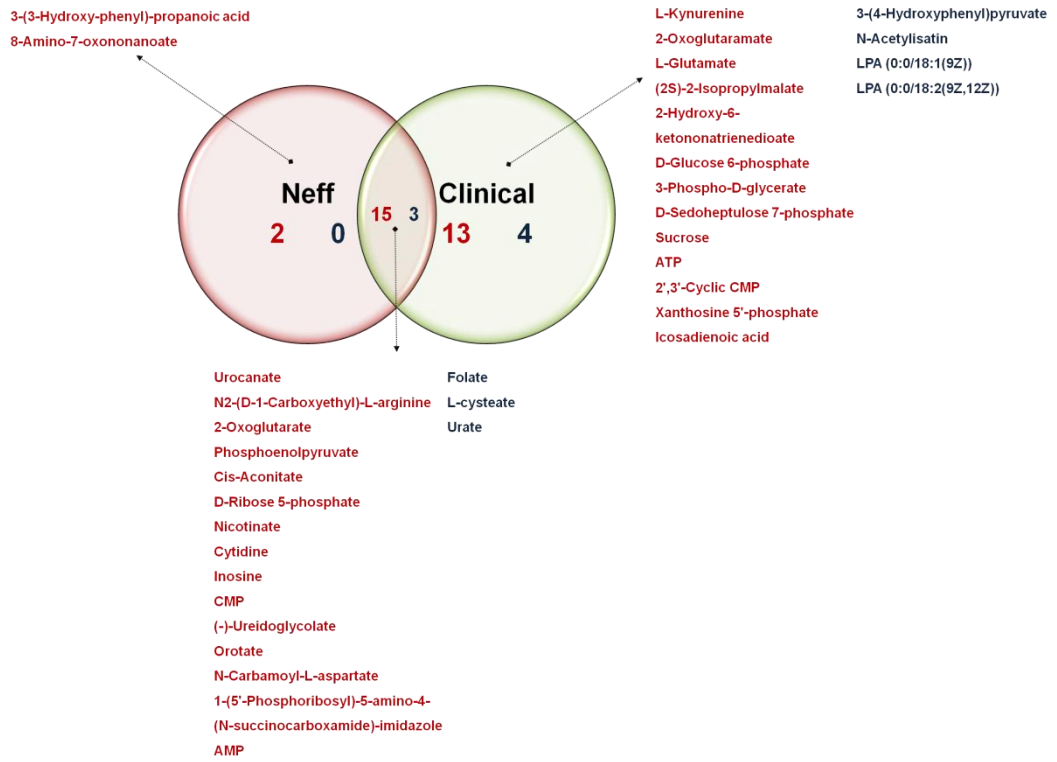


Fig 6.2 Fold change differences of metabolites in amoebic-derived conditioned medium. Metabolites with fold change values of either ≥ 1 (shades of red) or ≥ -1 (shades of blue) in comparison with the extract of cRPMI are considered potentially important. Metabolites not detected are indicated with an empty box.

$$\text{Metabolite fold change} = \frac{\text{Amoeba-derived cond medium relative intensity value mean}}{\text{cRPMI relative intensity value mean}} \text{ Log2}$$



Amino Acid Metabolism	Neff Cond Medium	Clinical Cond Medium
L-Kynurenine		
L-Alanine		
Creatine		
2-Oxoglutarate		
L-Glutamate		
enol-Phenylpyruvate		
L-Methionine S-oxide		
3-(3-Hydroxy-phenyl)-propanoic acid		
2,3,4,5-Tetrahydrodipicolinate		
N-Acetyl-L-glutamate 5-semialdehyde		
(2S)-2-Isopropylmalate		
3-(4-Hydroxyphenyl)pyruvate		
2-Hydroxy-6-ketono-natrienedioate		
Urocanate		
L-Cysteate		
N-Acetylisatin		
Indolelactate		
N2-(D-1-Carboxyethyl)-L-arginine		
Carbohydrate Metabolism	Neff Cond Medium	Clinical Cond Medium
2-Oxoglutarate		
D-Glucose 6-phosphate		
Dihydroxyfumarate		
2-Dehydro-3-deoxy-L-rhamnonate		
Phosphoenolpyruvate		
cis-Aconitate		
D-Fructose		
3-Phospho-D-glycerate		
D-Ribose 5-phosphate		
UDP-D-xylose		
D-Sedoheptulose 7-phosphate		
Sucrose		
Energy Metabolism	Neff Cond Medium	Clinical Cond Medium
ATP		
Metabolism of Cofactors and Vitamins	Neff Cond Medium	Clinical Cond Medium
Nicotinate		
Folate		
Isopyridoxal		
8-Amino-7-oxononanoate		
2-Amino-4-hydroxy-6-(D-erythro-1,2,3-trihydroxypropyl)-7,8-dihydropteridine		
Nucleotide Metabolism	Neff Cond Medium	Clinical Cond Medium
Hypoxanthine		
Cytidine		
Inosine		
CMP		
(-)-Ureidoglycolate		
Orotate		
N-Carbamoyl-L-aspartate		
2',3'-Cyclic CMP		
Xanthosine 5'-phosphate		
1-(5'-Phosphoribosyl)-5-amino-4-(N-succinocarboxamide)-imidazole		
Oxalureate		
Urate		
Allantoate		
AMP		
Lipid Metabolism	Neff Cond Medium	Clinical Cond Medium
sn-glycero-3-Phosphoethanolamine		
LPA(0:0/18:1(9Z))		
sn-Glycerol 3-phosphate		
(9Z)-Hexadecenoic acid		
Icosadienoic acid		
LPA(0:0/18:2(9Z,12Z))		

6.4.2 Amoeba-derived conditioned medium and LPS differently modulate macrophage metabolism.

Approximately 250 metabolites were identified in the whole macrophage extraction samples. Although no major differences in the total number of metabolites detected in the three different conditions could be observed there were clear quantitative differences. 27 metabolites were upregulated in LPS-stimulated macrophage extract compared with unstimulated control macrophages. These included urea cycle intermediates, glycolysis and TCA cycle metabolites, pentose phosphate pathway (PPP) metabolites, vitamin and co-factors metabolites and nucleotide metabolites. Macrophages stimulated with conditioned media derived from either strain of *Acanthamoeba* had less pronounced changes to their metabolism. Conditioned media from both strains substantially increased N-(L-arginino)succinate, xanthine and Deamino-NAD⁺ levels over control un-stimulated macrophages. In addition, macrophages stimulated with conditioned media from the Neff strain trophozoites produced L-kynurenine while those stimulated with conditioned media from the clinical isolate produced nicotinate. Pyridoxine phosphate was detected at high levels in both LPS and macrophages stimulated with conditioned media derived from the clinical isolate of *Acanthamoeba*. Among the urea cycle intermediates, L-arginino-succinate was detected at similarly high levels within macrophages stimulated with LPS or Neff or clinical-derived conditioned medium. L-citrulline levels were low within macrophages stimulated with conditioned media from the clinical isolate of *Acanthamoeba*, but raised in macrophages stimulated with LPS. Deoxyinosine and deoxyguanosine detection was equally low in both macrophages stimulated with Neff and clinical conditioned medium; deoxycytine relative intensity was found low in macrophages stimulated with either amoeba-derived conditioned media or LPS, whereas several metabolites associated with either purine or

pyrimidine metabolism were found at high levels within LPS-stimulated macrophages, but not those stimulated with amoebic conditioned media (Fig 6.3).

230 metabolites were identified in the spent media from macrophages stimulated with LPS or the amoebic conditioned medias. The spent medium of LPS-stimulated macrophages was altered more than the media of macrophages stimulated with either amoeba-derived conditioned media. 5 metabolites (ATP, inosine, AMP, xanthine, CMP) were found at similarly high levels in the spent medium of macrophages stimulated with either LPS or conditioned media. 8 metabolites (D-glucose 6-phosphate, D-glyceraldehyde 3-phosphate, 3-phospho-D-glycerate, hypoxanthine, xanthosine 5'-phosphate, (-)-ureidoglycolate, 2',3'-cyclic CMP, deoxyuridine) were found in similar quantities in macrophages stimulated with LPS or conditioned medium from the clinical isolate of *Acanthamoeba*. Fewer common metabolites were found in the spent media from macrophages stimulated with LPS and conditioned medium from the Neff strain of *Acanthamoeba*.(Fig 6.4).

6.4.2.1 Amino acid metabolism

LPS induced changes in the urea cycle intermediates produced by macrophages. N-L-arginino succinate, L-arginine, L-ornithine and L-citrulline were detected in LPS-stimulated macrophages extracts at higher levels in comparison with un-stimulated whole macrophages extracts. L-citrulline and N-L-arginino succinate relative intensities were also higher in the spent medium of LPS-stimulated macrophages, in comparison with un-stimulated macrophages. L-proline, a metabolite derived from arginine catabolism was also higher within LPS-stimulated macrophages in comparison with un-stimulated macrophages. Conditioned media from either strain of *Acanthamoeba* did not induce such modifications of arginine metabolism. However N-L-argininosuccinate was raised within macrophages following stimulation with either Neff or clinical derived conditioned media. L-

citrulline was found at reduced levels in macrophages stimulated with clinical-derived conditioned medium compared with control, un-stimulated macrophages (Fig 6.5).

Tryptophan metabolism was not notably modified in macrophages stimulated with LPS or amoeba-derived conditioned media. L-kynurenine was found in the extracts of macrophages stimulated with conditioned media derived from the Neff or clinical strain of *Acanthamoeba*, but not LPS. Levels of this metabolite were notably higher in macrophages stimulated with conditioned media from the Neff strain than those stimulated with media from the clinical isolate (Fig 6.5).

Glutathione was reduced within macrophages stimulated with LPS in comparison with un-stimulated macrophages. A similar pattern was observed for macrophages stimulated with amoeba-derived conditioned media although changes were modest (less than 1 fold change). Glutathione disulfide relative intensity was increased in spent medium from LPS-stimulated macrophages, but not spent media from macrophages stimulated with conditioned media from either strain of *Acanthamoeba* (Fig 6.5).

6.4.2.2 Carbohydrate metabolism

Carbohydrate metabolism was increased in LPS-stimulated macrophages, but not macrophages stimulated with conditioned media derived from Neff or the clinical isolate of *Acanthamoeba* (Fig 6.6). Thus, LPS-stimulated macrophages had increased intracellular D-glucose levels and culture media showed a concomitant decrease in D-glucose levels. Intracellular glucose levels in macrophages stimulated with Neff or clinical conditioned media were generally reduced although not by greater than 1 fold.

Glycolysis intermediates, such as D-glyceraldehyde 3-phosphate, 3-phospho-D-glycerate and phosphoenolpyruvate were increased within macrophages and in their spent medium after stimulation with LPS. Conditioned media derived from Neff and the clinical strain of *Acanthamoeba* did not induce glycolysis in macrophages. However increased levels of D-glucose 6-phosphate, D-glyceraldehyde 3-phosphate and 3-phospho-D-glycerate were evident in the spent medium of macrophages stimulated with clinical conditioned medium at similar levels to the conditioned medium used as stimulant (Fig 6.6).

Pyruvate levels were only modestly altered in LPS-stimulated macrophages but intracellular and extracellular levels of (R)-lactate were substantially increased over control, un-stimulated macrophages. The TCA cycle intermediates 2-oxoglutarate and succinate were also increased in LPS stimulated macrophages. Macrophages stimulated with either Neff or clinical conditioned media had not notable differences in (R)-lactate levels or difference in the TCA cycle relative to control un-stimulated macrophages (Fig 6.6).

Oxidative phosphorylation and energy metabolites associated with energy metabolism such as ADP, ATP, NAD⁺ and NADH were detectable within LPS-stimulated macrophages, although not notably increased in comparison with un-stimulated macrophages. Macrophages stimulated with either Neff or clinical conditioned media had little change in any of these parameters. Interestingly ATP was markedly increased (>2 fold) in the spent media of macrophages stimulated with either LPS or amoeba-derived conditioned media (Fig 6.6).

Pentose phosphate pathway metabolites, such as D-erithrose-4-phosphate and sedoheptulose 7-phosphate were highly detected within LPS-stimulated macrophages, but not within macrophages stimulated with amoeba-derived

conditioned media. Pentose phosphate pathway metabolites such as ribose 5-phosphate and sedoheptulose 7-phosphate were found in high levels (similar to levels introduced by the conditioned medium) in the spent medium of macrophages stimulated with clinical conditioned medium (Fig 6.6).

Fig 6.3 Characterization of whole stimulated-macrophages metabolome. Venn diagram schematically indicates the number and the specific metabolites highly detected or low detected in the extract of 1×10^6 whole macrophages, obtained from BALB/c mice, stimulated with LPS (blue), or Neff-derived free cell conditioned medium (orange) or clinical-derived conditioned medium (green), for 24 h at 37°C, 5% CO₂. The experiment was performed once, and conditions were in triplicate. Metabolites decreased >1 fold (blue) or increased by >1 fold (red), in relation with un-stimulated macrophages, were considered respectively less or highly detected. The overview provided by the Venn diagram suggests that LPS induces more intense metabolic modification/activation within macrophages, in comparison with both amoeba-derived conditioned media. Furthermore, not many similarities or differences can be observed between the stimulations.

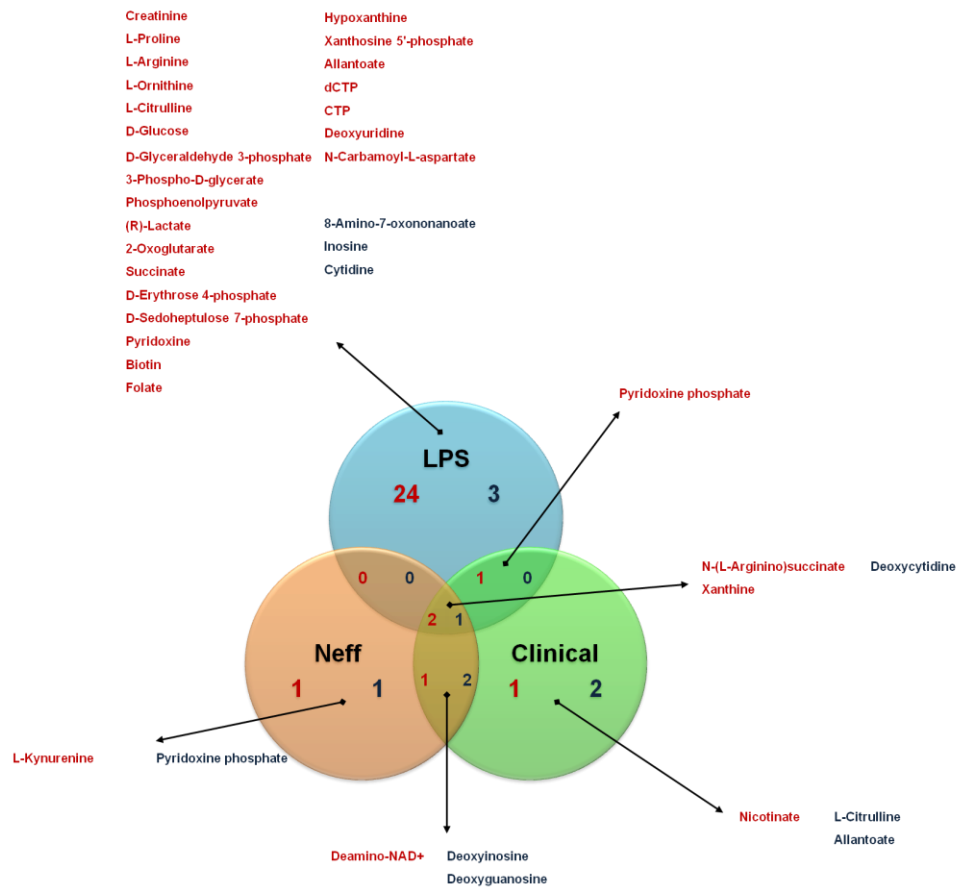
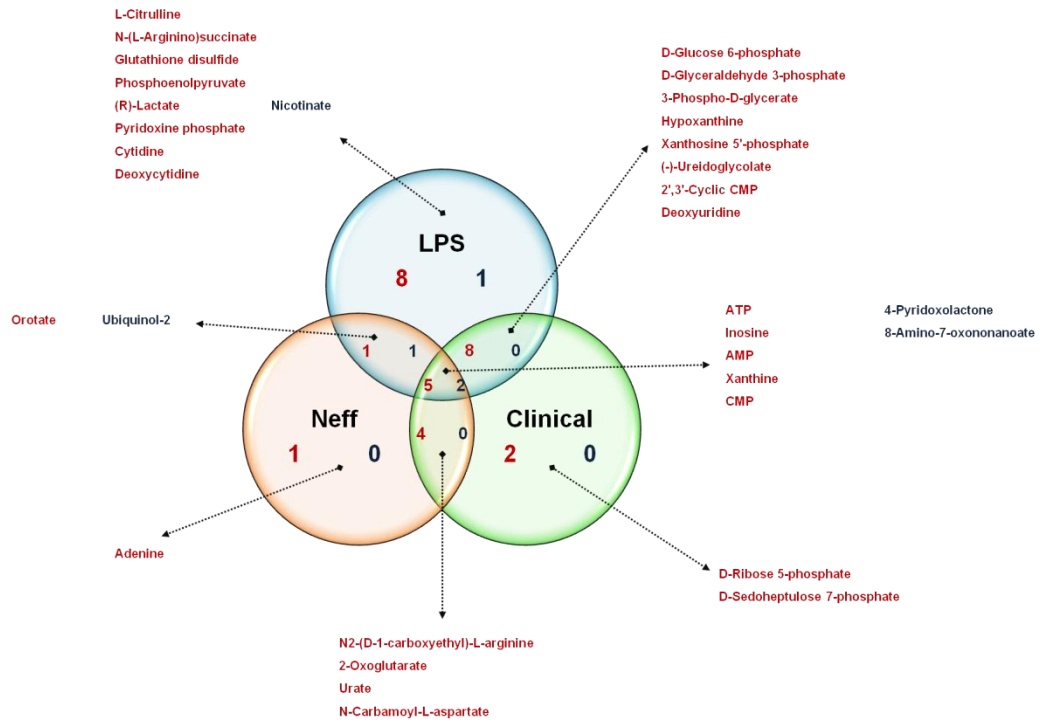
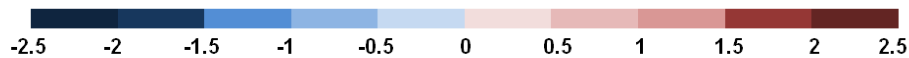


Fig 6.4 Characterization of the metabolome of the spent medium from stimulated macrophage cultures. Venn diagram schematically indicates the number and the specific metabolites highly detected or low detected in the medium metabolized by 1×10^6 macrophages, obtained from BALB/c mice, after stimulation with LPS (blue), or Neff-derived free cell conditioned medium (orange) or clinical-derived conditioned medium (green) for 24 h at 37°C, 5% CO₂. The experiment was performed once, and conditions were in triplicate. Metabolites decreased >1 fold (blue) or increased by >1 fold (red) were considered respectively less or highly detected in relation to un-stimulated macrophages. The overview provided by the Venn diagram suggests that LPS induces more intense metabolic modification of the spent medium in comparison with both amoeba-derived conditioned media, however a higher degree of similarity can be observed within the three different stimulations. When analysing these data the initial metabolic composition of amoeba-derived conditioned medium has to be taken in consideration.



$$\text{Metabolite fold change} = \frac{\text{stimulated macrophages' relative intensity value mean}}{\text{un-stimulated macrophages' relative intensity value mean}} \text{Log2}$$



Arginine Metabolism	LPS		Neff Cond Medium		Clinical Cond Medium	
	in	out	in	out	in	out
Creatinine						
L-Proline						
L-Arginine						
L-Ornithine						
L-Glutamate						
L-Citrulline						
N-(L-Arginino)succinate						
N2-(D-1-Carboxyethyl)-L-arginine						

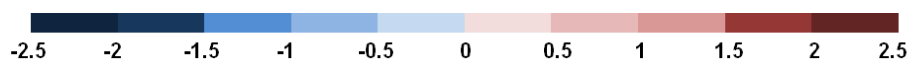
Tryptophan Metabolism	LPS		Neff Cond Medium		Clinical Cond Medium	
	In	Out	In	out	in	out
L-Tryptophan						
L-Kynurenine						
Kynurenate						
L-Formylkynurenine						

Glutathione Metabolism	LPS		Neff Cond Medium		Clinical Cond Medium	
	in	out	in	out	in	out
Glutathione						
Glutathione disulfide						

Fig 6.5 Schematic representation of the amino acid metabolism detected by LC/MS.

Fold changes of metabolites' relative intensity value means detected in both the whole macrophage extract (in) and in the macrophage spent medium (out) were calculated and schematically reported in the table. Metabolites with fold change values of either ≥ 1 (shades of red) or ≥ -1 (shades of blue), in comparison with the extract of un-stimulated macrophage conditions, are considered potentially important. Metabolites not detected are indicated with an empty box.

$$\text{Metabolite fold change} = \frac{\text{stimulated macrophages' relative intensity value mean}}{\text{un-stimulated macrophages' relative intensity value mean}} \text{Log2}$$



Carbohydrate Metabolism Glycolysis, TCA cycle, Oxidative phosphorylation, Pentose phosphate pathway	LPS		Neff Cond Medium		Clinical Cond Medium	
	in	out	in	out	in	out
D-Glucose	Red	Blue	Blue	Red	Blue	Red
D-Glucose 6-phosphate	Red	Red	Red	Red	Red	Red
D-Glyceraldehyde 3-phosphate	Red	Red	Blue	Red	Blue	Red
3-Phospho-D-glycerate	Red	Red	Blue	Red	Blue	Red
Phosphoenolpyruvate	Red	Red	Blue	Red	Blue	Red
Pyruvate	Red	Blue	Red	Red	Red	Blue
(R)-Lactate	Red	Red	Red	Red	Blue	Red
Citrate	Red	Blue	Blue	Red	Blue	Red
Oxalosuccinate	Red	Blue	Red	Red	Blue	Red
2-Oxoglutarate	Red	Red	Blue	Red	Blue	Red
Succinate	Red	Blue	Red	Red	Red	Blue
Fumarate	Red	Blue	Red	Red	Red	Blue
(S)-Malate	Red	Red	Blue	Blue	Blue	Blue
Oxaloacetate	Blue	Blue	Blue	Blue	Blue	Blue
ADP	Red	Red	Red	Red	Red	Red
ATP	Red	Red	Blue	Red	Blue	Red
NAD+	Red	Red	Blue	Red	Blue	Red
NADH	Red	Red	Blue	Red	Blue	Red
D-Ribose 5-phosphate	Red	Red	Blue	Red	Blue	Red
D-Erythrose 4-phosphate	Red	Red	Blue	Red	Blue	Red
D-Sedoheptulose 7-phosphate	Red	Red	Red	Red	Red	Red

Fig 6.6 Schematic representation of the carbohydrate metabolism detected by LC/MS. Fold changes of metabolites' relative intensity value means detected in both the whole macrophages extract (in) and in the macrophage spent medium (out), were calculated and schematically reported in the table. Metabolites with fold change values of either ≥ 1 (shades of red) or ≥ -1 (shades of blue), in comparison with the extract of un-stimulated macrophage conditions, are considered potentially important. Metabolites not detected are indicated with an empty box.

6.5 Discussion

In the site of infection, innate immune cells respond to pathogens or pathogen-associated molecules with a wide range of transcriptional, functional and phenotypic modifications (Muraille *et al.*, 2014). These modifications culminate in alteration of receptors or surface molecules, cytokine production and cellular metabolism (Saric *et al.*, 2010; Muraille *et al.*, 2014; Galván-Peña & O'Neill, 2014).

The ability of *Acanthamoeba* to alter its growth medium through depletion and secretion of metabolites, or to influence the metabolism of mammalian cells has not been studied at a global level. Therefore LC/MS studies were undertaken to define the metabolic composition of the conditioned medium derived from each strain of *Acanthamoeba* and to determine its effect on macrophage metabolism. The analysis of conditioned medium revealed subtle differences between the Neff strain and clinical isolate of *Acanthamoeba*, but many similarities between the conditioned media. The conditioned medium derived from the clinical isolate of *Acanthamoeba* had a higher number of metabolites expressed at >1 fold difference over the RPMI medium compared with conditioned medium derived from the Neff strain.

By analysing the extracts of whole stimulated macrophages and of their spent medium it is possible to draw conclusions about what is used or accumulated in our *in vitro* system. Several metabolites found in the amoeba-derived conditioned medium could be found in the spent medium of macrophages stimulated with these preparations suggesting that they are not used by macrophages. Others such as ATP which was present in the conditioned medium derived from the clinical isolate of *Acanthamoeba* was also produced by macrophages stimulated with either LPS or amoeba-derived conditioned media, indicating that this important metabolite might be secreted by macrophages into their external microenvironment irrespective of

stimulant. However, ATP released by the clinical isolate of *Acanthamoeba* might also be important in immune regulation. L-kynurenine and L-glutamate were exclusively found in conditioned medium derived from the clinical isolate of *Acanthamoeba*. The absence of these two metabolites in the spent medium of macrophages stimulated with this conditioned medium suggests that they might be internalized and quickly metabolized within macrophages.

Acanthamoeba is able to synthesise folate but can also scavenge folate from external pools (Henriquez *et al.*, 2014). Depletion of folate from culture medium was indeed observed as both amoeba-derived conditioned media had considerably less folate than the RPMI. LPS-stimulated macrophages had increased intracellular and decreased extracellular levels of folate. Macrophages stimulated with either amoeba-derived conditioned media, further depleted folate from the culture medium. The reduction of folate in amoeba-derived conditioned media and its further depletion by macrophages might affect macrophage functions and homeostasis (Kolb & Petrie, 2013).

After characterizing the metabolic composition of amoebic conditioned medium, the effect of these preparations on the amino acid and carbohydrate metabolism within macrophages in comparison with LPS-stimulated macrophages was investigated. LPS appears to induce intense modifications of the amino acid and carbohydrate macrophage metabolism, whereas amoeba conditioned medium did not induce such dramatic changes. The ability of LPS to induce changes to the metabolism of murine macrophages, including increased intracellular detection of the urea cycle intermediates L-citrulline and L-ornithine, depletion of D-glucose from the external milieu, and increased detection of intracellular lactate have previously been described and suggested as characteristics of innate and classically activated macrophages (Galván-Peña & O'Neill, 2014; Biswas & Mantovani, 2012). These

same characteristics are not observed within macrophages stimulated with amoeba-derived conditioned media. For instance, L-citrulline is depleted within macrophages stimulated with conditioned medium derived from the clinical isolate of *Acanthamoeba*. High intracellular levels of L-citrulline have been observed in other infectious systems such as malaria (Sana *et al.*, 2013). The depletion of this urea cycle intermediate, to the best of our knowledge, has never been reported. Carbohydrate metabolism within macrophages stimulated with amoeba-derived conditioned medium, in contrast to LPS stimulated macrophages where it was substantially augmented, was only modestly modified with certain intermediates increased and others reduced in comparison with control macrophages. This was somewhat surprising as glycolysis is generally greatly up-regulated during other infectious diseases (Saric *et al.*, 2010; Sana *et al.*, 2013; Biswas & Mantovani, 2012). Increased extracellular ATP was observed in the spent medium of macrophages stimulated with both LPS and amoeba-derived conditioned media. It is logical that increased glycolysis and TCA cycle activity could provide the ATP released from LPS stimulated macrophages. The source of ATP in macrophages stimulated with amoeba-derived conditioned media might be through the modest increase in glycolysis evident through small increases in intracellular pyruvate. Alternatively ATP production could be through β -oxidation of fatty acids and oxidative phosphorylation that have been described for M2 macrophage activation (Galván-Peña & O'Neill, 2014).

Although amoebic-derived conditioned medium did not induce intense metabolic organization within macrophages or similar metabolic effects as observed in those stimulated with LPS, high levels of L-kynurenine, L-glutamate and ATP were detected in conditioned medium derived from the clinical isolate of *Acanthamoeba*.

These metabolites have the potential to modulate the inflammatory/immune response of the host.

Previous studies in other systems have demonstrated that L-kynurenine, derived from the catabolism of L-tryptophan by IDO is capable of modulating immune responses (Murakami *et al.*, 2013). For example, it has been demonstrated that synthesis of L-kynurenine by dermal fibroblasts induces the production of metallo-proteases 1 and 3 and collagen type I (Salimi Elizei *et al.*, 2014). Topical administration of L-kynurenine in an experimental wound healing model decreased expression of pro-inflammatory cytokines and chemokines, as well as inhibition of T-cell responses, while not affecting macrophage infiltration (Salimi Elizei *et al.*, 2014). In addition, L-kynurenine can have an inhibitory effect on pro-inflammatory cytokine expression by DCs, inducing SOCS2 expression (McBerry *et al.*, 2012). Thus L-kynurenine produced by *Acanthamoeba* has the potential to inhibit or reduce pro-inflammatory cytokine production by macrophages, and to reduce T-cell responses.

The detection of L-glutamate within conditioned medium from the clinical isolate might have implications for the pathogenesis of GAE. L-glutamate has been demonstrated to also be produced during inflammatory events in the brain and to induce cell damage within cerebral tissues, both *in vivo* and *in vitro* (Thomas *et al.*, 2014) and it has been associated with several neurodegenerative disorders (Ye *et al.*, 2014).

ATP is released by damaged cells or by activated immune cells in the site of infection/inflammation (Idzko *et al.*, 2014; Ren *et al.*, 2014). By activating purinergic receptors expressed on immune cells and non immune cells such as endothelial and epithelial, ATP induces a wide range of immune functions, including pro-inflammatory cytokine and chemokine release (Gabel, 2007), neutrophil chemotaxis

(Junger, 2008), and epithelial wound repair (Gendaszewska-Darmach, 2011). It is known that macrophages can release ATP in the extracellular milieu in response to PAMPs (Sakaki *et al.*, 2012). A recent study has demonstrated that LPS-induced ATP release by murine macrophages was TLR4-dependent (Ren *et al.*, 2014) and our metabolomic data confirm the release of ATP in the external milieu by macrophages stimulated with LPS. Interestingly, both Neff strain and clinical isolate conditioned medium induced ATP extracellular release by macrophages. Our previous studies indicate that IL-12 and IL-6 production by *Acanthamoeba* trophozoites is TLR4-dependent, and therefore *Acanthamoeba*-induced ATP release by macrophages could be associated with the activation of TLR4, although this requires further investigation. Of interest is the ability of the clinical strain of *Acanthamoeba* to produce and secrete ATP. ATP released at the site of infection, from both macrophages and from trophozoites, could alter the outcome of the inflammatory/immune response. Extracellular nucleotides are known to stimulate cell motility, and to induce wound healing by activating P2Y2 receptors (Klepeis *et al.*, 2004). However, it has also been reported that high concentrations of ATP inhibit epithelial cell migration associated with wound healing (Klepeis *et al.*, 2004), and inhibit the development of Th1 cells (la Sala *et al.*, 2001). These suggestions are important in the context of *Acanthamoeba* keratitis where the balance of immune activation, immune privilege and wound healing is likely to determine the disease outcome.

A growing number of studies have applied metabolomics as a means to understand protozoan parasites (Creek *et al.*, 2012; Lakshmanan *et al.*, 2011; Jeelani & Nozaki, 2014), to evaluate their drug susceptibilities (Creek & Barrett, 2014), and to understand their interactions with their hosts (Sana *et al.*, 2013; Lamour *et al.*, 2012; Olszewski *et al.*, 2009). Recently a metabolomics protocol for the analysis of the

metabolome of *Acanthamoeba* Neff strain trophozoites, cultured in a chemically defined media, has been optimized and performed in our laboratories. *Acanthamoeba* Neff strain showed a high metabolic activity characterized by the intrinsic biosynthesis of amino acids as well as the removal and the release of metabolites from the media (on going analysis). *Acanthamoeba* trophozoites are impossible to separate from macrophages post co-infection; for this reason, amoeba-derived free cell conditioned media was used instead of live *Acanthamoeba* trophozoites in this series of experiments. However, future studies can be performed with living trophozoites by introducing the appropriate controls in the experimental design, such as monoculture of trophozoites in cRPMI along with the macrophage and trophozoite co-incubation conditions. Cell sorting by flow cytometry can furthermore be applied to separate macrophages from trophozoites from co-incubation conditions, after optimization of the staining protocols.

Although the results reported in this study are preliminary and of a qualitative nature, they provide valuable insights and will stimulate further studies. Furthermore, identifying peculiar aspects of *Acanthamoeba* metabolism that may facilitate disease progression might indicate chemotherapeutic targets. Such interventions might ameliorate damaging aspects of the immune response and/or deprive *Acanthamoeba* of essential host metabolites.

CHAPTER 7

Conclusion

The immunology of *Acanthamoeba* infections has only recently garnered interest. The apparent lack of interest might have been due to the low incidence of human disease in spite of evidence of common exposure through serological studies (Cursons *et al.*, 1980).

The main aim of our study was to investigate the effect of *A. castellanii* on the activation of resting macrophages. For this purpose, bone marrow derived murine macrophages were co-incubated with either a classical laboratory strain of *A. castellanii*, named Neff or *A. castellanii* isolated from a case of bilateral keratitis in Italy. Both the laboratory strain and the clinical isolate belong to genotype T4, which is most commonly associated with *Acanthamoeba* infections.

Initial studies demonstrated that *Acanthamoeba* Neff strain trophozoites were capable of inducing pro-inflammatory cytokine production, TNF- α , IL-12 and IL-6, by murine macrophages in a time-dependent manner. Although both *Acanthamoeba* (Neff) and clinical strain trophozoites could induce pro-inflammatory cytokines there were certain differences. Indeed, the clinical strain did not induce TNF- α production and IL-12 and IL-6 production induced by clinical isolate was significantly lower in comparison with Neff strain. The reduced cytokine production by macrophages co-incubated with the clinical strain relative to those co-incubated with the Neff strain might be associated with increased cytotoxicity. Proteases which have been suggested as virulence factors (de Souza Carvalho *et al.*, 2011) and capable of potentially degrading cytokines (Harrison *et al.*, 2010) could be responsible for the apparent lower levels of cytokines in macrophages co-incubated with the clinical strain of *Acanthamoeba*. All these suggestions are consistent with the higher pathogenic nature of the clinical strain of *Acanthamoeba* being capable of inducing infectious disease in comparison with the laboratory strain, which is considered non-

pathogenic and might have lost its virulence as a consequence of long-term culture *in vitro* (Koehsler *et al.*, 2009).

We tested the hypothesis that amoebic-secreted serine and cysteine proteases were capable of influencing pro-inflammatory cytokine production by macrophages by using a selection of protease inhibitors. Results implicate a role for amoebic-proteases in the induction of IL-12 and IL-6 production by macrophages co-incubated with trophozoites of either strain, rather than their degradation. In particular, both serine proteases and, to a lesser extent cysteine proteases were involved in these events. We have observed that amoebic-cell free conditioned medium was not capable of inducing pro-inflammatory cytokine production by macrophages, suggesting that macrophage/trophozoite interaction might be an important factor for the release of proteases by *Acanthamoeba* trophozoites as previously reported (Hurt *et al.*, 2003).

The subsequent aim was to determine which macrophage signalling pathways were activated by *A. castellanii* isolates and which macrophage PPRs may be involved. Towards this purpose, macrophages were obtained from C57BL/6 mice deficient for either MyD88 or TRIF genes and their wild type counterparts. MyD88^{-/-} macrophages co-incubated with trophozoites were unable to make IL-12 and IL-6. In contrast, TRIF^{-/-} macrophages were still able to produce IL-12 and IL-6 when co-incubated with trophozoites although at diminished levels in comparison with WT macrophages. TLR2 and TLR4 are innate immune receptors expressed on the cell membrane of macrophages and are both associated with the MyD88-dependent signalling pathway. Therefore to determine the role of these receptors macrophages were obtained from TLR2, TLR4 or TLR2/4 gene deficient mice and were co-incubated with *Acanthamoeba* trophozoites. It was found that *Acanthamoeba*-induced IL-12 and IL-6 production was not diminished in TLR2^{-/-} macrophages co-

incubated with trophozoites. On the other hand, IL-12 production was diminished and IL-6 production ablated in TLR4^{-/-} macrophages co-incubated with trophozoites, These results demonstrate that recognition of *Acanthamoeba* trophozoites is predominately through TLR4 that induces MyD88, and to a lesser extent TRIF-dependent signalling and cytokine production. This is in accordance with the unique ability of TLR4 to induce both MyD88-dependent and TRIF signalling pathways (Kawasaki & Kawai, 2014).

PAR₁ and PAR₂ G-protein coupled receptors expressed on innate immune cells, as well as endothelial and epithelial cells, can be activated by endogenous or/and exogenous proteases resulting in immune/inflammatory responses (Vergnolle, 2003). We have previously observed that *Acanthamoeba*-induced IL-12 and IL-6 production by macrophages was associated with amoebic serine and cysteine proteases. Therefore our subsequent aim was to investigate whether PAR₁ and PAR₂ were involved in these events. To this end PAR₂ deficient macrophages were co-incubated with *Acanthamoeba* trophozoites and it was found that *Acanthamoeba*-induced IL-12 and IL-6 production was not PAR₂-dependent. On the other hand, by using specific PAR₁ antagonist, RWJ 56110, it was found that *Acanthamoeba*-induced macrophage IL-12 was partially PAR₁-dependent. Thus TLR4 and PAR₁ both play a role in IL-12 production induced by *Acanthamoeba*, suggesting a potential cross-talk between the two receptors in response to *Acanthamoeba*. In literature, it has been reported TLRs/PARs cross-talk, during bacterial, viral and fungal infections, in particular involving PAR₂ (Gieseler *et al.*, 2013), however this event has never been reported in protozoan infections yet.

Our study indicates that TLR4 and PAR₁, expressed on macrophages, are involved in the recognition of *Acanthamoeba* trophozoites, and that their activation leads to pro-inflammatory cytokines production. The roles of TLRs and PARs expressed on

corneal cells, have already been observed in *Acanthamoeba* infections (Ren *et al.*, 2010; Alizadeh *et al.*, 2014; Tripathi *et al.*, 2014). On one hand, our study confirms TLR4 as the main receptor involved in the recognition and response to *Acanthamoeba* trophozoites, accordingly to what has been observed in corneal epithelial cells (Ren *et al.*, 2010). On the other hand, we showed a different activation pattern of PARs expressed on macrophages, by *Acanthamoeba*, in comparison with what has been observed in corneal epithelial cells (Tripathi *et al.*, 2014). Indeed we have demonstrated that *Acanthamoeba* is capable of activating PAR₁, but not PAR₂ expressed on macrophages.

So far it has been demonstrated that *Acanthamoeba* is capable of inducing a pro-inflammatory, antimicrobial phenotype in macrophages, characterized by the activation of innate immune receptors and pro-inflammatory cytokine release. At this point our aim was also to evaluate whether *Acanthamoeba* could modulate arginine metabolism within macrophages, driving this pathway towards either the production of NO by macrophages and therefore a killing phenotype or alternatively the synthesis of polyamines and the development of a wound healing/tissue repair phenotype (Murray *et al.*, 2014). Interestingly *Acanthamoeba* trophozoites, but not amoeba-derived free cell conditioned medium, induce arginase activity and not iNOS in murine macrophages. Trophozoites of the clinical isolate induced slightly higher arginase activity in comparison with trophozoites of the Neff strain. Furthermore, a higher intrinsic arginase activity was observed in clinical trophozoite compared with Neff strain trophozoite monoculture maintained at the same experimental conditions. Interestingly LPS-induced NO production was diminished by the pre-incubation and presence of *Acanthamoeba* trophozoites. These results demonstrate that *Acanthamoeba* is capable of driving the catabolism of arginine by macrophages towards the synthesis of polyamines by inducing arginase activity.

Macrophage NO production was not induced by *Acanthamoeba* and potentially trophozoites might possess NO-detoxifying systems, as it has been observed in other microorganisms (Mastronicola *et al.*, 2010). The ability to induce arginase and not iNOS, as well as perhaps to neutralize NO, can be considered as an immune evasion mechanism by *Acanthamoeba*. Alternatively it might be a response by the host cells to recover tissue homeostasis and mitigate excessive damage caused by both trophozoites and inflammatory mediators.

Different macrophage phenotypes can be characterized by the specific pattern of the released immune mediators, as well as through the analysis of their cellular metabolism (Galván-Peña & O'Neill, 2014). Therefore, macrophage metabolic modification following stimulation with *Acanthamoeba* was investigated. Although we have previously demonstrated that amoeba cell-free conditioned medium was not capable of inducing pro-inflammatory cytokines or to induce arginase activity by murine macrophages, our hypothesis was that amoeba-secreted products could modulate the host's cell metabolism or directly interfere with immune/inflammatory responses. Furthermore, the use of amoebic-derived conditioned medium, for this experiment, was preferred to live trophozoites for technical reasons, due to the difficulty in separating trophozoites from macrophages, after the period of co-incubation. For these reasons, by using a metabolomics approach, the metabolic composition of both Neff and clinical-derived conditioned medium was identified and subsequently the metabolic pattern of macrophages stimulated with either Neff or clinical-derived conditioned medium was qualitatively analysed. Results showed that amoebic-derived conditioned medium did not induce important metabolic changes in macrophages and very few similarities with LPS-stimulated macrophages could be found. Interestingly, increased detection of extracellular ATP could be observed in response to both LPS and amoeba conditioned medium. Three metabolites,

characterized by their immunological significance, were detected at high levels exclusively within clinical strain trophozoite-derived conditioned medium: ATP, L-kynurenine and L-glutamate.

All this considered, the main aim of our study was fulfilled: we found that *Acanthamoeba* trophozoites not only promoted the development of a pro-inflammatory macrophage phenotype, through the activation of PPRs and the induction of pro-inflammatory signalling pathways, but also somewhat paradoxically the development of a wound healing macrophage phenotype, characterized by the increase of arginase activity and the inhibition of NO production. The *Acanthamoeba*/macrophage *in vitro* co-incubation model presents a characteristic metabolic signature, where both host cell and amoeba derived metabolites might operate to modulate the development of the immune response. (Fig 7.1).

The main aim of this study was therefore achieved and from the results obtained the project can be taken forward to confirm and further dissect the nature of *Acanthamoeba*-induced macrophage phenotypes. For instance, the production of the anti-inflammatory cytokine IL-10 can be evaluated in macrophage/*Acanthamoeba* co-incubation *in vitro* systems, to evaluate if *Acanthamoeba* can also induce an anti-inflammatory response in order to persist in the site of infection. Analysis of the macrophage transcriptome, after stimulation with *Acanthamoeba*, as well as fluorescence activated cell sorting (FACS) analysis can provide a deeper and more detailed picture about the macrophage activation states induced by *Acanthamoeba*.

Further interesting questions and hypotheses have arisen for future studies. It will be interesting to identify the nature of *Acanthamoeba*-associated PAMPs expressed by the trophozoite life-cycle stage. Karaś & Russa (2013) reported the method to

extract and purify LPG from *Acanthamoeba* trophozoites. By applying this extraction and purification method, purified LPG from *Acanthamoeba* can be used to stimulate macrophages and evaluate the mechanisms of recognition and the consequent immune responses towards these amoebic structures (Maldonado-Bernal *et al.*, 2005). The role of amoeba-derived proteases in the production of pro-inflammatory cytokines requires further investigation and whether they are essential for the exposure and subsequent recognition of the as yet to be identified PAMPs has to be elucidated. Using gel electrophoresis techniques, the pattern of proteins present in the medium of macrophages stimulated with *Acanthamoeba* trophozoites, in comparison with unstimulated macrophages and trophozoites mono-culture, can be characterized. Identification of amoebic secreted proteases in the co-incubation model and the production of recombinant protein would help in understanding the role of the amoebic proteases in the induction of immune events. We previously suggested that there could be TLRs/PARs cross-talk, during *Acanthamoeba* infections. After identifying the amoebic PAMPs involved and secreted amoebic proteases, it could be interesting to investigate receptor cross-talk using both macrophages and corneal epithelial *in vitro* systems. These experiments can be performed by combining macrophages from genetically modified mice and specific antagonists or antibodies. The ability of *Acanthamoeba* to inhibit LPS-induced NO production has never been reported and it could be interesting to investigate the mechanisms by which *Acanthamoeba* may elicit this effect, as well as how the activity of the amoeba-derived arginase, might influence the metabolism of arginine, which is essential for immune defence as well as for the recovery of homeostatic conditions. Finally, the analysis of the amoeba-derived cell free conditioned medium metabolome has provided an interesting starting overview from which immunological, diagnostic and chemotherapy studies can be developed.

The study of the immunological mechanisms involved in these rather rare, but insidious infectious diseases, might be useful for future practical applications. For instance, TLR activation by *Acanthamoeba* trophozoites suggests the expression of amoebic PAMPs that, once identified, can be used as new adjuvants for vaccine production. *Acanthamoeba*, which mainly causes diseases within the eye and the brain, could be used as an experimental model for studies destined to understand the immune mechanisms operating within these immune privilege sites. *Acanthamoeba*-associated PAMPs, characterized by their immunogenic properties, and peculiar metabolites released into the site of infection, can be used for more economic and quicker diagnosis from corneal scraps, biopsies and cerebrospinal liquid. Finally, the major challenge for *Acanthamoeba* treatment is to associate the eradication of the micro-organism with the amelioration of the associated inflammatory symptoms. For this reason, the knowledge of the mechanisms through which *Acanthamoeba* triggers immune responses can be useful for the development of new drugs. The modulation of receptor activity and of signalling pathways, as well as interventions to the metabolism at the site of infection might mitigate exacerbated immune/inflammatory responses while controlling infection.

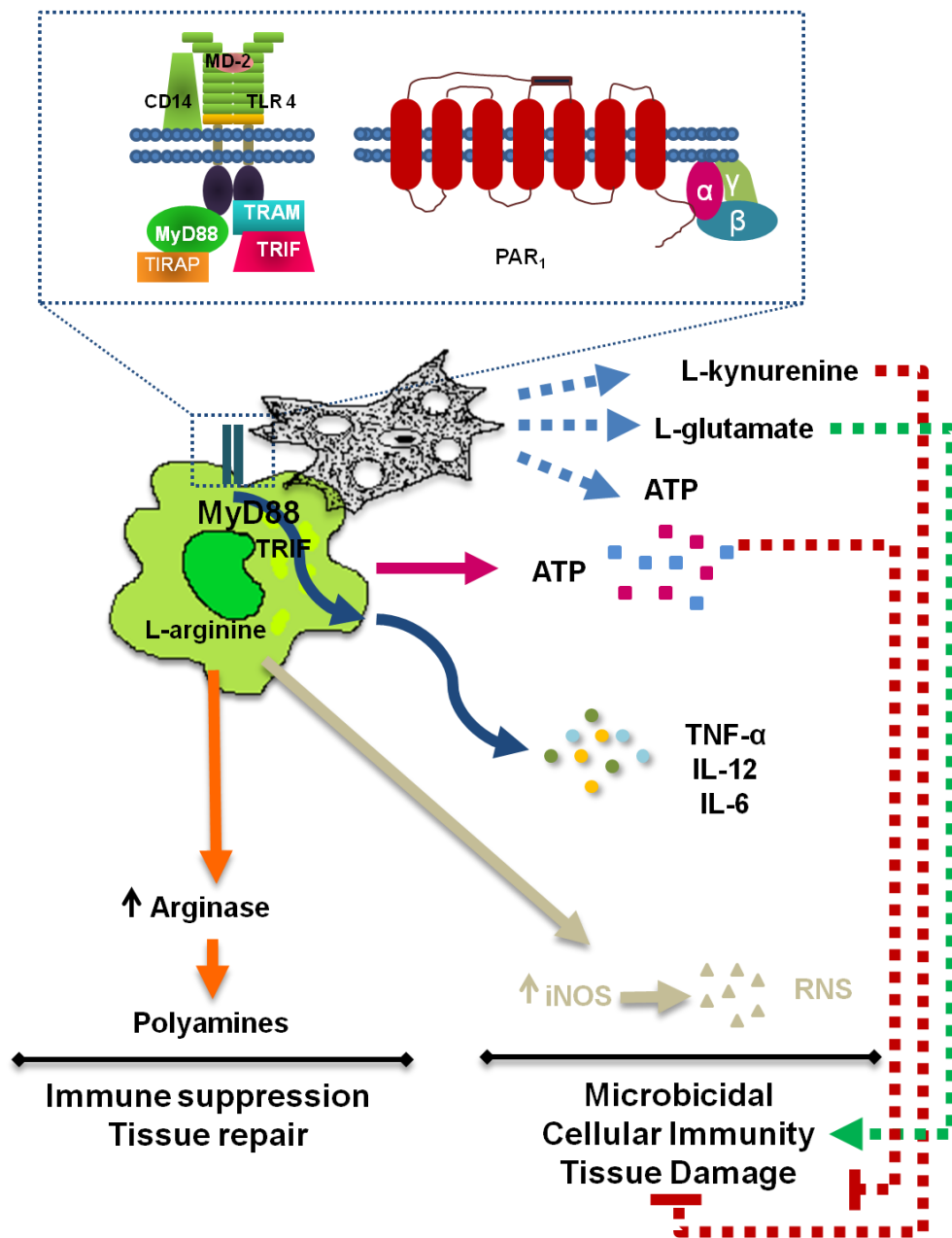


Fig 7.1 Schematic summary of the results. *Acanthamoeba* trophozoites promote the development of a pro-inflammatory macrophage phenotype inducing pro-inflammatory cytokine production, although the production of RNS was not detected. On the other hand, by driving L-arginine catabolism toward L-ornithine synthesis *Acanthamoeba* also induces anti-inflammatory and healing phenotype in murine macrophages. *Acanthamoeba*-released metabolites can modulate immune responses either enhancing or inhibiting pro-inflammatory responses.

CHAPTER 8

References

Adams MN, Ramachandran R, Yau MK, Suen JY, Fairlie DP, Hollenberg MD & Hooper JD, 2011. Structure, function and pathophysiology of protease activated receptors. *Pharmacol Ther.*, Vol. 130, No 3, p. 248-82.

Afshar K, Boydking A, Ganesh S, Herrington C & McFadden PM, 2013. Rapidly fatal disseminated acanthamoebiasis in a single lung transplant recipient. *Ann Transplant.*, Vol. 18, p. 108-11.

Aichelburg AC, Walochnik J, Assadian O, Prosch H, Steuer A, Perneczky G, Visvesvara GS, Aspöck H & Vetter N, 2008. Successful treatment of disseminated *Acanthamoeba* sp. infection with miltefosine. *Emerg Infect Dis.*, Vol. 14, No 11, p. 1743-1746.

Akpek G, Uslu A, Huebner T, Taner A, Rapoport AP, Gojo I, Akpolat YT, Ioffe O, Kleinberg M & Baer MR, 2011. Granulomatous amebic encephalitis: an under-recognized cause of infectious mortality after hematopoietic stem cell transplantation. *Transpl Infect Dis.*, Vol. 13, No 4. P. 366-73.

Alfieri SC, Correia CE, Motegi SA & Pral EM, 2000. Proteinase activities in total extracts and in medium conditioned by *Acanthamoeba polyphaga* trophozoites. *J Parasitol.*, Vol. 86, No 2, p. 220-7.

Alizadeh H, Apte S, El-Agha MS, Li L, Hurt M, Howard K, Cavanagh HD, McCulley JP & Niederkorn JY, 2001. Tear IgA and serum IgG antibodies against *Acanthamoeba* in patients with *Acanthamoeba* keratitis. *Cornea.*, Vol. 20, No 6, p. 622-7.

Alizadeh H, He Y, McCulley JP, Ma D, Stewart GL, Via M, Haehling E & Niederkorn JY, 1995. Successful immunization against *Acanthamoeba* keratitis in a pig model. *Cornea.*, Vol. 14, No 2, p. 180-6.

Alizadeh H, Li H, Neelam S & Niederkorn JY, 2008. Modulation of corneal and stromal matrix metalloproteinase by the mannose-induced *Acanthamoeba* cytolytic protein. *Exp Eye Res.*, Vol. 87, No 3, p. 286-91.

Alizadeh H, Neelam S & Niederkorn JY, 2007. Role of activated macrophages in *Acanthamoeba* keratitis. *J Parasitol.*, Vol. 93, No 5, p. 1114-20.

Alizadeh H, Pidherney MS, McCulley JP & Niederkorn JY, 1994. Apoptosis as a mechanism of cytolysis of tumor cells by a pathogenic free-living amoeba. *Infect Immun.*, Vol. 62, No 4, p. 1298-303.

Alizadeh H, Tripathi T, Abdi M & Smith AD, 2014. Pathogenic strains of *Acanthamoeba* are recognized by TLR4 and initiated inflammatory responses in the cornea. *PLoS One*, Vol. 9, No 3, e92375.

Alsam S, Kim KS, Stins M, Rivas AO, Sissons J & Khan NA, 2003. *Acanthamoeba* interactions with human brain microvascular endothelial cells. *Microb Pathog.*, Vol. 35, No 6, p. 235-41.

Alsam S, Sissons J, Jayasekera S & Khan NA, 2005. Extracellular proteases of *Acanthamoeba castellanii* (encephalitis isolate belonging to T1 genotype) contribute to increased permeability in an in vitro model of the human blood–brain barrier. *Journal of Infection*, Vol 51, No 2, p. 150-156

Aoki MP, Guiñazú NL, Pellegrini AV, Gotoh T, Masih DT & Gea S, 2004. Cruzipain, a major *Trypanosoma cruzi* antigen, promotes arginase-2 expression and survival of neonatal mouse cardiomyocytes. *Am J Physiol Cell Physiol.*, Vol. 286, No 2, p. 206-12.

Arnalich-Montiel F, Lorenzo-Morales J, Irigoyen C, Morcillo-Laiz R, López-Vélez R, Muñoz-Negrete F, Piñero JE & Valladares B, 2013. Co-isolation of

Vahlkampfia and *Acanthamoeba* in acanthamoeba-like keratitis in a Spanish population. *Cornea*, Vol. 32, No. 5, p. 608-14.

Astorga B, Lorenzo-Morales J, Martín-Navarro CM, Alarcón V, Moreno J, González AC, Navarrete E, Piñero JE & Valladares B, 2011. *Acanthamoeba* belonging to T3, T4, and T11: genotypes isolated from air-conditioning units in Santiago, Chile. *J. Eukaryot. Microbiol.* Vol 58, No 6, p. 542–544.

Barete S, Combes A, de Jonckheere JF, Datry A, Varnous S, Martinez V, Ptacek SG, Caumes E, Capron F, Francès C, Gibert C & Chosidow O, 2007. Fatal disseminated *Acanthamoeba lenticulata* infection in a heart transplant patient. *Emerg Infect Dis.*, Vol. 13, No 5, p. 736-8.

Barros MH, Hauck F, Dreyer JH, Kempkes B & Niedobitek G, 2013. Macrophage polarisation: an immunohistochemical approach for identifying M1 and M2 macrophages. *PLoS One*, Vol. 8, No. 11:e80908. doi: 10.1371/journal.pone.0080908. eCollection 2013.

Becker-Finco A, Costa AO, Silva SK, Ramada JS, Furst C, Stinghen AE, De Figueiredo BC, De Moura J & Alvarenga LM, 2013. Physiological, morphological, and immunochemical parameters used for the characterization of clinical and environmental isolates of *Acanthamoeba*. *Parasitology*, Vol 140, No 03, p. 396-405.

Berg M, Vanaerschot M, Jankevics A, Cuypers B, Breitling R & Dujardin JC, 2013. LC-MS metabolomics from study design to data-analysis using a versatile pathogen as a test case. *Comput Struct Biotechnol J.*, Vol. 4, e201301002.

Binesh F, Karimi M & Navabii H, 2011. Unexpected postmortem diagnosis of *Acanthamoeba* meningoencephalitis in an immunocompetent child. *BMJ Case Rep.*, pii: bcr0320113954. doi: 10.1136/bcr.03.2011.3954.

Biron CA & Gazzinelli RT, 1995. Effects of IL-12 on immune responses to microbial infections: a key mediator in regulating disease outcome. *Curr Opin Immunol.*, Vol. 7, No 4, p. 485-96.

Biswas SK & Mantovani A, 2010. Macrophage plasticity and interaction with lymphocyte subsets: cancer as a paradigm. *Nat Immunol.*, Vol. 11, No 10, p. 889-96.

Bogler SA, Zaley CD, Burianek LL, Fuerst PA & Byers TJ, 1983. Interstrain mitochondrial DNA polymorphism detected in *Acanthamoeba* by restriction endonuclease analysis. *Mol Biochem Parasitol.* Vol. 8, No 2 p. 145-63.

Booton GC, Joslin CE, Shoff M, Tu EY, Kelly DJ & Fuerst PA. 2009. Genotypic identification of *Acanthamoeba* sp. isolates associated with an outbreak of *Acanthamoeba* keratitis. *Cornea*, Vol. 28, No 6, p. 673-6.

Booton GC, Visvesvara GS, Byers TJ, Kelly DJ & Fuerst PA, 2005. Identification and distribution of *Acanthamoeba* species genotypes associated with nonkeratitis infections. *J Clin Microbiol.*, Vol. 43, No 4; p. 1689–93.

Brisette-Storkus CS, Reynolds SM, Lepisto AJ & Hendricks RL, 2002. Identification of a novel macrophage population in the normal mouse corneal stroma. *Invest Ophthalmol Vis Sci.*, Vol. 43, No 7, p. 2264-71.

Cabral GA & Marciano-Cabral F., 2004. Cannabinoid-mediated exacerbation of brain infection by opportunistic amoebae. *J Neuroimmunol.*, Vol 147, No 1-2, p. 127-30.

Cabral GA, Raborn ES, Griffin L, Dennis J & Marciano-Cabral F, 2008. CB2 receptors in the brain: role in central immune function. *Br J Pharmacol.*, Vol. 153, No 2, p. 240-51.

Cariello AJ, Passos RM, Yu MC & Hofling-Lima AL, 2011. Microbial keratitis at a referral center in Brazil. *Int Ophthalmol.*, Vol. 31, No 3, p. 197-204.

Castellani A, 1930. An amoeba found in culture of yeast: Preliminary note. *J Fop Med Hyg.*, p.160.

Castillo RD, Garza JX, Shamszadeh M, Reiff AO & Marzan KA, 2012. *Acanthamoeba* meningoencephalitis presenting as neuropsychiatric lupus in a pediatric patient. *Clin Exp Rheumatol.*, Vol. 30, No 2, p. 272-6.

Chaplin DD, 2010. Overview of the immune response. *J Allergy Clin Immunol.*, 125(2 Suppl 2), p. S3-23.

Chawla A, Armstrong M & Carley F, 2014. *Acanthamoeba* keratitis - an increasing incidence. *Cont Lens Anterior Eye.*, Vol 37, No 2, p:120.

Cho JH, Na BK, Kim TS & Song CY, 2000. Purification and characterization of an extracellular serine proteinase from *Acanthamoeba castellanii*. *IUBMB Life.*, Vol. 50, No 3, p. 209-14.

Clarke B, Sinha A, Parmar DN & Sykakis E, 2012. Advances in the diagnosis and treatment of *Acanthamoeba* keratitis. *Journal of Ophthalmology* Volume 2012, Article ID 484892, 6 pages doi:10.1155/2012/484892

Clarke DW & Niederkorn JY, 2006. The pathophysiology of *Acanthamoeba* keratitis. *Trends Parasitol.*, Vol. 22, No 4, p. 175-80.

Clarke DW, Alizadeh H & Niederkorn JY, 2005. Failure of *Acanthamoeba castellanii* to produce intraocular infections. *Invest. Ophthalmol. Vis.Sci.*, Vol. 46, p. 2472-2478.

Clarke DW, Alizadeh H & Niederkorn JY, 2006. Intracorneal instillation of latex beads induces macrophage-dependent protection against *Acanthamoeba* keratitis. *Invest Ophthalmol Vis Sci.*, Vol. 47, No 11, p. 4917

Clarke M, Lohan AJ, Liu B, Lagkourdos I, Roy S, Zafar N, Bertelli C, Shilde C, Kianianmomeni A, Bürglin TR, Frech C, Turcotte B, Kopec KO, Synnott JM, Choo C, Paponov I, Finkler A, Heng Tan CS, Hutchins AP, Weinmeier T, Rattei T, Chu JS, Gimenez G, Irimia M, Rigden DJ, Fitzpatrick DA, Lorenzo-Morales J, Bateman A, Chiu CH, Tang P, Hegemann P, Fromm H, Raoult D, Greub G, Miranda-Saavedra D, Chen N, Nash P, Ginger ML, Horn M, Schaap P, Caler L & Loftus BJ, 2013. Genome of *Acanthamoeba castellanii* highlights extensive lateral gene transfer and early evolution of tyrosine kinase signaling. *Genome Biol.*, Vol. 14, No. 2, R 11.

Collette JR, Zhou H & Lorenz MC, 2014. *Candida albicans* suppresses nitric oxide generation from macrophages via a secreted molecule. *PLoS One.*, Vol. 9, No 4:e96203.

Corraliza IM, Campo ML, Soler G & Modolell M, 1994. Determination of arginase activity in macrophages: a micromethod. *J Immunol Methods.*, Vol. 174, No 1-2, p. 231-5.

Costas M & Griffiths AJ, 1985. Enzyme composition and the taxonomy of *Acanthamoeba*. *J Protozool.*, Vol 32, No 4, p. 604-7M.

Crawford MJ & Goldberg DE, 1998. Role for the *Salmonella* flavohemoglobin in protection from nitric oxide. *J Biol Chem.*, Vol. 273, No 20, p. 12543-7.

Creek DJ & Barrett MP, 2014. Determination of antiprotozoal drug mechanisms by metabolomics approaches. *Parasitology*, Vol. 141, No 1, p. 83-92.

Creek DJ, Anderson J, McConville MJ & Barrett MP, 2012. Metabolomic analysis of trypanosomatid protozoa. *Mol Biochem Parasitol.*, Vol. 181, No 2, p. 73-84.

Creek DJ, Jankevics A, Burgess KE, Breitling R & Barrett MP, 2012. IDEOM: an Excel interface for analysis of LC-MS-based metabolomics data. *Bioinformatics.*, Vol. 28, No 7, p. 1048-9.

Culbertson CG, Smith JW & Minner JR, 1958. *Acanthamoeba*: observations on animal pathogenicity. *Science*, Vol. 1, No 27, p. 1 506.

Culbertson CG, Smith JW, Cohen HK & Minner JR, 1959. Experimental infection of mice and monkeys by *Acanthamoeba*. *Am J Pathol*, Vol. 35, p. 1851 97.

Cursons RT & Brown TJ, 1978. Use of cell cultures as an indicator of pathogenicity of free-living amoebae. *J Clin Pathol.*, Vol. 31, No 1, p. 1-11.

Cursons RT, Brown TJ, Keys EA, Moriarty KM & Till D, 1980. Immunity to pathogenic free-living amoebae: role of humoral antibody. *Infect Immun.*, Vol. 29, No 2, p. 401-7.

Dart JK, Saw VP & Kilvington S, 2009. *Acanthamoeba* keratitis: diagnosis and treatment update 2009. *Am J Ophthalmol.*, Vol. 148, No 4, p. 487-499.

Das P, Lahiri A, Lahiri A & Chakravortty D, 2010. Modulation of the arginase pathway in the context of microbial pathogenesis: a metabolic enzyme moonlighting as an immune modulator. *PLoS Pathog.*, Vol. 6, No 6.

Davies LC, Jenkins SJ, Allen JE & Taylor PR, 2013. Tissue-resident macrophages. *Nat Immunol.*, Vol. 14, No 10, p. 986-95.

De Jonckheere JF, 1980. Growth characteristics, cytopathic effect in cell culture, and virulence in mice of 36 type strains belonging to 19 different *Acanthamoeba* spp. *Appl Environ Microbiol.*, Vol. 39, No. 4, p. 681-5.

de Souza Carvalho FR, Carrijo-Carvalho LC, Chudzinski-Tavassi AM, Foronda AS & de Freitas D, 2011. Serine-like proteolytic enzymes correlated with differential pathogenicity in patients with acute *Acanthamoeba* keratitis. *Clin Microbiol Infect.*, Vol. 17, No 4, p. 603-9.

Deaglio S & Robson SC, 2011. Ectonucleotidases as regulators of purinergic signaling in thrombosis, inflammation, and immunity. *Adv Pharmacol.*, Vol 61, p. 301-32

Di Cave D, D' Alfonso R, Dussey Comlavi KA, D' Orazi C, Monno R & Berrilli F, 2014. Genotypic heterogeneity based on 18S-rRNA gene sequences among *Acanthamoeba* isolates from clinical samples in Italy. *ExpParasitol.*, pii: S00144894(14)001234. doi: 10.1016/j.exppara.2014.05.009.

Di Cave D, Monno R, Bottalico P, Guerriero S, D'Amelio S, D'Orazi C & Berrilli F, 2009. *Acanthamoeba* T4 and T15 genotypes associated with keratitis infections in Italy. *Eur J Clin Microbiol Infect Dis.*, Vol. 28, No 6, p. 607-12.

Duarte AG, Sattar F, Granwehr B, Aronson JF, Wang Z & Lick S, 2006. Disseminated acanthamoebiasis after lung transplantation. *J Heart Lung Transplant.*, Vol. 25, No 2, p. 237-40.

Eckmann L, Laurent F, Langford TD, Hetsko ML, Smith JR, Kagnoff MF & Gillin FD, 2000. Nitric oxide production by human intestinal epithelial cells and competition for arginine as potential determinants of host defense against the lumen-dwelling pathogen *Giardia lamblia*. *J Immunol.*, Vol. 164, No 3, p. 1478-87.

Elnekave K, Siman-Tov R & Ankri S, 2003. Consumption of L-arginine mediated by *Entamoeba histolytica* L-arginase (EhArg) inhibits amoebicidal activity and nitric oxide production by activated macrophages. *Parasite Immunol.*, Vol. 25, No 11-12, p. 597-608.

Ferrante A & Abell TJ, 1986. Conditioned medium from stimulated mononuclear leukocytes augments human neutrophil-mediated killing of a virulent *Acanthamoeba* sp. *Infect Immun.*, Vol. 51, No 2, p. 607-17.

Ferrante A & Bates EJ, 1988. Elastase in the pathogenic free-living amoebae *Naegleria* and *Acanthamoeba* spp. *Infect Immun.*, Vol. 56, No 12, p. 3320-1.

Ferrante A & Rowan-Kelly B, 1983. Activation of the alternative pathway of complement by *Acanthamoeba culbertsoni*. *Clin Exp Immunol.*, Vol. 54, No 2, p. 477-85.

Forrester JV, Xu H, Lambe T & Cornall R, 2008. Immune privilege or privileged immunity? *Mucosal Immunol.*, Vol. 1, No 5, p. 372-81.

Fu H, Khan A, Coe D, Zaher S, Chai JG, Kropf P, Müller I, Larkin DF & George AJ, 2011. Arginine depletion as a mechanism for the immune privilege of corneal allografts. *Eur J Immunol.*, Vol.41, No 10, p. 2997-3005.

Fuerst PA, 2014. Insights from the DNA databases: approaches to the phylogenetic structure of *Acanthamoeba*. *Exp Parasitol.*, Vol. 145 Suppl:S39-45.

Fung KT, Dhillon AP, McLaughlin JE, Lucas SB, Davidson B, Rolles K, Patch D & Burroughs AK, 2008. Cure of *Acanthamoeba* cerebral abscess in a liver transplant patient. *Liver Transpl.*, Vol 14, No 3, p. 308-312.

- Gabel CA**, 2007. P2 purinergic receptor modulation of cytokine production. *Purinergic Signal.*, Vol. 3, No 1-2, p. 27-38.
- Galván-Peña S & O'Neill LA**, 2014. Metabolic reprogramming in macrophage polarization. *Front Immunol.*, Vol. 5, No. 420. doi: 10.3389/fimmu.2014.00420. eCollection 2014.
- Garate M, Cao Z, Bateman E & Panjwani N**, 2004. Cloning and characterization of a novel mannose-binding protein of *Acanthamoeba*. *J Biol Chem.*, Vol. 279, No 28, p. 29849-56.
- Garate M, Cubillos I, Marchant J & Panjwani N**, 2005. Biochemical characterization and functional studies of *Acanthamoeba* mannose-binding protein. *Infect Immun.*, Vol. 73, No 9, p. 5775-81.
- Garate M, Marchant J, Cubillos I, Cao Z, Khan NA & Panjwani N**, 2006. In vitro pathogenicity of *Acanthamoeba* is associated with the expression of the mannose-binding protein. *Invest Ophthalmol Vis Sci.* Vol.47, No 3, p. 1056-62.
- Garner A**, 1993. Pathogenesis of acanthamoebic keratitis: hypothesis based on a histological analysis of 30 cases. *British Journal of Ophthalmology*, Vol. 77, No 6, p. 366–370.
- Gast RJ, Ledee RD, Fuerst PA & Byers TJ**, 1996. Subgenus systematics of *Acanthamoeba*: four nuclear 18S rDNA sequence types. *J. Eukaryot. Microbiol.*, Vol 43, No 6, p. 498–504.
- Gatti S, Rama P, Matuska S, Berrilli F, Cavallero A, Carletti S, Bruno A, Maserati R & Di Cave D**, 2010. Isolation and genotyping of *Acanthamoeba* strains from corneal infections in Italy. *J Med Microbiol*, Vol. 59, No 11, p. 1324-1330

Gaur U, Roberts SC, Dalvi RP, Corraliza I, Ullman B & Wilson ME, 2007. An effect of parasite-encoded arginase on the outcome of murine cutaneous leishmaniasis. *J Immunol.*, Vol. 179, No 12, p. 8446-53.

Gautom RK, Lory S, Seyedirashti S, Bergeron DL & Fritsche TR, 1994. Mitochondrial DNA fingerprinting of *Acanthamoeba* spp. isolated from clinical and environmental sources. *J. Clin. Microbiol.*, Vol. 32, No 4, p.1070-73.

Gendaszewska-Darmach E & Kucharska M, 2011. Nucleotide receptors as targets in the pharmacological enhancement of dermal wound healing. *Purinergic Signal.*, Vol. 7, No 2, p. 193-206.

Gianinazzi C, Schild M, Wüthrich F, Müller N, Schürch N & Gottstein B, 2009. Potentially human pathogenic *Acanthamoeba* isolated from a heated indoor swimming pool in Switzerland. *Experimental Parasitology*, Vol. 121, No 2, p 180-186.

Gieseler F, Ungefroren H, Settmacher U, Hollenberg MD & Kaufmann R, 2013. Proteinase-activated receptors (PARs) – focus on receptor-receptor-interactions and their physiological and pathophysiological impact. *Cell Commun Signal.*, 11:86. doi: 10.1186/1478-811X-11-86.

Goerdts S & Orfanos CE, 1999. Other functions, other genes: alternative activation of antigen-presenting cells. *Immunity*, Vol. 10, No 2, p. 137-42.

Gonzalez MM, Gould E, Dickinson G, Martinez AJ, Visvesvara GS, Cleary TJ & Hensley GT, 1986. Acquired immunodeficiency syndrome associated with *Acanthamoeba* infection and other opportunistic organisms. *Arch Pathol Lab Med*, Vol. 110, No 8, p. 749-51.

Gordon S, Plüddemann A & Martinez Estrada F, 2014. Macrophage heterogeneity in tissues: phenotypic diversity and functions. *Immunol Rev.* Vol. 262, No 1, p. 36-55.

Gordon VR, Asem EK, Vodkin MH & McLaughlin GL, 1993. *Acanthamoeba* binds to extracellular matrix proteins *in vitro*. *Invest. Ophthalmol. Vis. Sci.*, Vol. 34, p. 658–662.

Griffin JL, 1972. Temperature tolerance of pathogenic and nonpathogenic free-living amoebas. *Science.*, Vol. 178, No 4063, p. 869-70.

Grohmann U & Bronte V, 2010. Control of immune response by amino acid metabolism. *Immunol Rev.*, Vol. 236, p. 243-64.

Grün AL, Stemplewitz B & Scheid P, 2014. First report of an *Acanthamoeba* genotype T13 isolate as etiological agent of a keratitis in humans. *Parasitol Res.*, Vol. 113, No 6, p. 2395-400.

Gullett J, Mills J, Hadley K, Podemski B, Pitts L & Gelber R, 1979. Disseminated granulomatous *Acanthamoeba* infection presenting as an unusual skin lesion. *Am. J. Med.*, Vol. 67, No 5, p. 891–896.

Gundra UM, Mishra BB, Wong K & Teale JM, 2011. Increased disease severity of parasite-infected TLR2^{-/-} mice is correlated with decreased central nervous system inflammation and reduced numbers of cells with alternatively activated macrophage phenotypes in a murine model of neurocysticercosis. *Infect Immun.*, Vol. 79, No 7, p. 2586-96.

Gupta D, Panda GS & Bakhshi S, 2008. Successful treatment of *Acanthamoeba* meningoencephalitis during induction therapy of childhood acute lymphoblastic leukemia. *Pediatr. Blood Cancer*, Vol 50, No 6, p. 1292–1293.

Hadaś E & Mazur T, 1993. Biochemical markers of pathogenicity and virulence of *Acanthamoeba* sp. strains. *Parasitol Res.*, Vol. 79, No 8, p. 696-8.

Harrison JL, Ferreira GA, Raborn ES, Lafrenaye AD, Marciano-Cabral F & Cabral GA, 2010. *Acanthamoeba culbertsoni* elicits soluble factors that exert anti-microglial cell activity. *Infect Immun.*, Vol. 78, No 9, p. 4001-11.

He YG, Niederkorn JY, McCulley JP, Stewart GL, Meyer DR, Silvany R & Dougherty J, 1990. *In vivo* and *in vitro* collagenolytic activity of *Acanthamoeba castellanii*. *Invest Ophthalmol Vis Sci.*, Vol. 31, No 11, p. 2235-40.

Henriquez FL, Campbell SJ, Sundararaj BK, Cano A, Muench SP & Roberts CW, 2014. The *Acanthamoeba* Shikimate Pathway has a Unique Molecular Arrangement and is Essential for Aromatic Amino Acid Biosynthesis. *Protist*, Vol 166, No 1, p. 93-105.

Holley MM, Zhang Y, Lehrmann E, Wood WH, Becker KG & Kielian T, 2012. Toll-like receptor 2 (TLR2)-TLR9 crosstalk dictates IL-12 family cytokine production in microglia. *Glia*. Vol. 60, No 1, p. 29-42.

Hurt M, Apte S, Leher H, Howard K, Niederkorn J & Alizadeh H, 2001. Exacerbation of *Acanthamoeba* keratitis in animals treated with anti-macrophage inflammatory protein 2 or antineutrophil antibodies. *Infect Immun.*, Vol. 69, No 5, p. 2988-95.

Hurt M, Niederkorn J & Alizadeh H, 2003. Effects of mannose on *Acanthamoeba castellanii* proliferation and cytolytic ability to corneal epithelial cells. *Invest Ophthalmol Vis Sci.*, Vol. 44, No 8, p. 3424-31.

Hurt M, Proy V, Niederkorn JY & Alizadeh H, 2003. The interaction of *Acanthamoeba castellanii* cysts with macrophages and neutrophils. *J Parasitol.*, Vol. 89, No 3, p. 565-72

Ibrahim YW, Boase DL & Cree IA, 2007. Factors affecting the epidemiology of *Acanthamoeba* keratitis. *Ophthalmic Epidemiol.*, Vol 14, No 2, p. 53-60.

Idzko M, Ferrari D & Eltzschig HK, 2014. Nucleotide signalling during inflammation. *Nature*, Vol. 509, No 7500, p. 310-7.

Iijima M, Shimizu H, Tanaka Y & Urushihara H, 2000. Identification and characterization of two flavohemoglobin genes in *Dictyostelium discoideum*. *Cell Struct Funct.*, Vol. 25, No 1, p. 47-55.

Iovieno A, Gore DM, Carnt N & Dart JK, 2014. *Acanthamoeba* Sclerokeratitis: Epidemiology, Clinical Features, and Treatment Outcomes. *Ophthalmology*. pii: S01616420(14)005673. doi:10.1016/j.ophtha.2014.06.033

Iovieno A, Oechsler RA, Ledee DR, Miller D & Alfonso EC, 2010. Drug-resistant severe *Acanthamoeba* keratitis caused by rare T5 *Acanthamoeba* genotype. *Eye Contact Lens.*, Vol. 36, No 3, p. 183-4.

Jager BV & Stamm WP, 1927. Brain abscesses caused by free-living amoeba probably of the genus *hartmannella* in a patient with Hodgkin's disease. *The Lancet*, Vol 2, No 7791, p. 1343-345.

Jaillon S, Galdiero MR, Del Prete D, Cassatella MA, Garlanda C & Mantovani A, 2013. Neutrophils in innate and adaptive immunity. *Semin Immunopathol.*, Vol. 35, No 4, p. 377-94.

- Jaison PL, Cao Z & Panjwani N**, 1998. Binding of *Acanthamoeba* to [corrected] mannose-glycoproteins of corneal epithelium: effect of injury. *Curr Eye Res.*, Vol. 17, No 8, p. 770-6.
- Jeelani G & Nozaki T**, 2014. Metabolomic analysis of *Entamoeba*: applications and implications. *Curr Opin Microbiol.*, Vol. 20, p. 118-24.
- John T, Desai D & Sahm D**, 1989. Adherence of *Acanthamoeba castellanii* cysts and trophozoites to unworn contact lenses. *Am J Ophthalmol.*; Vol. 108, No 6, p. 658–664.
- Jones BR, Visvesvara GS & Robinson NM**, 1975. *Acanthamoeba polyphaga* keratitis and *Acanthamoeba* uveitis associated with fatal meningoencephalitis. *Trans. Ophthalmol. Soc. U. K.*, Vol. 95, No 2, p. :221–232.
- Jones SA**, 2005. Directing transition from innate to acquired immunity: defining a role for IL-6. *J Immunol.*, Vol. 175, No 6, p. 3463-8.
- Jung ID, Lee CM, Jeong YI, Lee JS, Park WS, Han J & Park YM**, 2007. Differential regulation of indoleamine 2,3-dioxygenase by lipopolysaccharide and interferon gamma in murine bone marrow derived dendritic cells. *FEBS Lett.*, Vol. 581, No 7, p. 1449-56.
- Junger WG**, 2008. Purinergic regulation of neutrophil chemotaxis. *Cell Mol Life Sci.*, Vol. 65, No 16, p. 2528-40.
- Kafsack BF & Llinás M**, 2010. Eating at the table of another: metabolomics of host-parasite interactions. *Cell Host Microbe.*, Vol. 7, No 2, p. 90-9.

- Kao PM, Hsu BM, Che NH, Huang KH, Huang SW, King KL & Chiu YC**, 2012. Isolation and identification of *Acanthamoeba* species from thermal spring environments in southern Taiwan. *Exp Parasitol.*, Vol. 130, No 4, p. 354-8.
- Karáš MA & Russa R**, 2013. New long chain bases in lipophosphoglycan of *Acanthamoeba castellanii*. *Lipids*, Vol. 48, No 6, p. 639-50.
- Kaul DR, Lowe L, Visvesvara GS, Farmen S, Khaled YA & Yanik GA**, 2008. *Acanthamoeba* infection in a patient with chronic graft-versus-host disease occurring during treatment with voriconazole. *Transpl Infect Dis.*, Vol. 10, No 6, p. 437-41.
- Kawai T & Akira S**, 2009. The roles of TLRs, RLRs and NLRs in pathogen recognition. *Int Immunol.*, Vol. 21, No 4, p. 317-37.
- Kawai T & Akira S**, 2010. The role of pattern-recognition receptors in innate immunity: update on Toll-like receptors. *Nat Immunol.*, Vol. 11, No 5, p. 373-84.
- Kawasaki T & Kawai T**, 2014. Toll-like receptor signaling pathways. *Front Immunol.*, Vol. 5, No 461. doi: 10.3389/fimmu.2014.00461. eCollection 2014.
- Khan NA & Siddiqui R**, 2009. *Acanthamoeba* affects the integrity of human brain microvascular endothelial cells and degrades the tight junction proteins. *Int J Parasitol.*, Vol. 39, No 14, p. 1611-6.
- Khan NA**, 2006. *Acanthamoeba*: biology and increasing importance in human health. *FEMS Microbiol Rev.*, Vol 30, p 564–595.
- Khan NA**, 2008. *Acanthamoeba* and the blood–brain barrier: the breakthrough. *Journal of Medical Microbiology*, Vol. 57, No 9, p.1051–1057

Khan NA, Jarroll EL & Paget TA, 2002. Molecular and physiological differentiation between pathogenic and non-pathogenic *Acanthamoeba*. *Curr Microbiol.*, Vol. 45, No 3, p. 197-202.

Khan NA, Jarroll EL, Panjwani N, Cao Z & Paget TA, 2000. Proteases as markers for differentiation of pathogenic and non pathogenic species of *Acanthamoeba*. *J Clin Microbiol.*, Vol. 38, No 8, p. 2858-61.

Kilvington S, 1993. *Acanthamoeba* trophozoite and cyst adherence to four types of soft contact lens and removal by cleaning agents. *Eye*, Vol. 7, No (Pt 4), p. 535–538.

Kim BG, Sobota A, Bitonti AJ, McCann PP & Byers TJ, 1987. Polyamine metabolism in *Acanthamoeba*: polyamine content and synthesis of ornithine, putrescine, and diaminopropane. *J Protozool.*, Vol. 34, No 3, p. 278-84.

Kim EC & Kim MS, 2010. Bilateral *Acanthamoeba* keratitis after orthokeratology. *Cornea.*, Vol. 29, No 6, p. 680-2.

Kim JY, Na BK, Song KJ, Park MH, Park YK & Kim TS, 2012. Functional expression and characterization of an iron containing superoxide dismutase of *Acanthamoeba castellanii*. *Parasitol Res.*, Vol. 111, No 4, p. 1673-82.

Kim SY, Syms MJ, Holtel MR & Nauschuetz KK, 2000. *Acanthamoeba* sinusitis with subsequent dissemination in an AIDS patient. *Ear Nose Throat J.*, Vol. 79, No 3, p.171-4.

Kim WT, Kong HH, Ha YR, Hong YC, Jeong HJ, Yu HS & Chung DI, 2006. Comparison of specific activity and cytopathic effects of purified 33 kDa serine proteinase from *Acanthamoeba* strains with different degree of virulence. *Korean J Parasitol.*, Vol. 44, No 4, p. 321-30.

Kinrear FB, 2003. Cytopathogenicity of *Acanthamoeba*, *Vahlkampfia* and *Hartmannella*: quantitative & qualitative in vitro studies on keratocytes. *J Infect.*, Vol. 46, No 4, p. 228-37.

Kinrear FB, 2004. *Acanthamoeba* pathogenicity for corneal cells. *J Infect.*, Vol. 49, No 4, p. 310-6.

Klepeis VE, Weinger I, Kaczmarek E & Trinkaus-Randall V, 2004. P2Y receptors play a critical role in epithelial cell communication and migration. *J Cell Biochem.*, Vol. 93, No 6, p. 1115-33.

Klotz SA, Misra RP & Butrus SI, 1987. Carbohydrate deposits on the surfaces of worn extended-wear soft contact lenses. *Arch Ophthalmol.*, Vol. 105, No 7, p. 974-7

Knickelbein JE, Kovarik J, Dhaliwal DK & Chu CT, 2013. *Acanthamoeba* keratitis: a clinicopathologic case report and review of the literature. *Hum Pathol.*, Vol. 44, No 5, p. 918-22.

Koehsler M, Leitsch D, Duchêne M, Nagl M & Walochnik J, 2009. *Acanthamoeba castellanii*: growth on human cell layers reactivates attenuated properties after prolonged axenic culture. *FEMS Microbiol Lett.*, p 1-7

Kolb AF & Petrie L, 2013. Folate deficiency enhances the inflammatory response of macrophages. *Mol Immunol.*, Vol. 54, No 2, p. 164-72.

Kong HH, Kim TH & Chung DI, 2000. Purification and characterization of a secretory serine proteinase of *Acanthamoeba healyi* isolated from GAE. *J Parasitol.*, Vol. 86, No 1, p. 12-7.

Kong HH, Shin JY, Yu HS, Kim J, Hahn TW, Hahn YH, & Chung DI, 2002. Mitochondrial DNA Restriction Fragment Length Polymorphism (RFLP) and 18S

Small-Subunit Ribosomal DNA PCR-RFLP Analyses of *Acanthamoeba* Isolated from Contact Lens Storage Cases of Residents in Southwestern Korea. *Journal Of Clinical Microbiology*, Vol 40, No 4, p. 1199–1206.

Korn ED, Dearborn DG & Wright PL, 1974. Lipophosphoglycan of the plasma membrane of *Acanthamoeba castellanii*. Isolation from whole amoebae and identification of the water-soluble products of acid hydrolysis. *J Biol Chem.*, Vol. 249, No 11, p. 3335-41.

Kropf P, Fuentes JM, Fähnrich E, Arpa L, Herath S, Weber V, Soler G, Celada A, Modolell M & Müller I, 2005. Arginase and polyamine synthesis are key factors in the regulation of experimental leishmaniasis in vivo. *FASEB J.*, Vol. 19, No 8, p.1000-2.

Ku JY, Chan FM & Beckingsale P, 2009. *Acanthamoeba* keratitis cluster: an increase in *Acanthamoeba* keratitis in Australia. *Clin Experiment Ophthalmol.*, Vol. 37, No 2, p. 181-90.

Kumar H, Kawai T & Akira S, 2011. Pathogen recognition by the innate immune system. *Int Rev Immunol.*, Vol. 30, No 1, p. 16-34.

la Sala A, Ferrari D, Corinti S, Cavani A, Di Virgilio F & Girolomoni G, 2001. Extracellular ATP induces a distorted maturation of dendritic cells and inhibits their capacity to initiate Th1 responses. *J Immunol.*, Vol. 166, No 3, p. 1611-7.

Lackner P, Beer R, Broessner G, Helbok R, Pfausler B, Brenneis C, Auer H, Walochnik J & Schmutzhard E, 2010. Acute granulomatous *Acanthamoeba* encephalitis in an immunocompetent patient. *Neurocrit Care.*, Vol 12, No 1, p. 91-4.

Lakshmanan V, Rhee KY & Daily JP, 2011. Metabolomics and malaria biology. *Mol Biochem Parasitol.*, Vol. 175, No 2, p. 104-11.

Lalitha P, Lin CC, Srinivasan M, Mascarenhas J, Prajna NV, Keenan JD, McLeod SD, Acharya NR, Lietman TM & Porco TC, 2012. *Acanthamoeba* keratitis in South India: a longitudinal analysis of epidemics. *Ophthalmic Epidemiol.*, Vol. 19, No 2, p. 111-5.

Lambiase A, Micera A, Sacchetti M, Mantelli F & Bonini S, 2011. Toll-like receptors in ocular surface diseases: overview and new findings. *Clin Sci (Lond)*, Vol. 120, No 10, p. 441-50.

Lamour SD, Choi BS, Keun HC, Müller I & Saric J, 2012. Metabolic characterization of *Leishmania major* infection in activated and nonactivated macrophages. *J Proteome Res.*, Vol. 11, No 8, p. 4211-22.

Lang R, Song PI, Legat FJ, Lavker RM, Harten B, Kalden H, Grady EF, Bunnett NW, Armstrong CA & Ansel JC, 2003. Human corneal epithelial cells express functional PAR-1 and PAR-2. *Invest Ophthalmol Vis Sci.*, Vol. 44, No 1, p. 99-105.

Larkin DF & Easty DL, 1991. Experimental *Acanthamoeba* keratitis: II. Immunohistochemical evaluation. *Br J Ophthalmol.*, Vol. 75, No 7, p. 421-4.

Lasjerdi Z, Niyati M, Haghghi A, Shahabi S, Biderouni FT, Taghipour N, Eftekhar M & Nazemalhosseini Mojarad E, 2011. Potentially pathogenic free-living amoebae isolated from hospital wards with immunodeficient patients in Tehran, Iran. *Parasitology Research*, Vol. 109, No 3, p 575-580.

Ledee DR, Iovieno A, Miller D, Mandal N, Diaz M, Fell J, Fini ME & Alfonso EC, 2009. Molecular identification of t4 and t5 genotypes in isolates from *Acanthamoeba* keratitis patients. *J Clin Microbiol.*, Vol. 47, No 5, p. 1458-62.

Leher H, Alizadeh H, Taylor WM, Shea AS, Silvany RS, Van Klink F, Jager MJ & Niederkorn JY, 1998a. Role of mucosal IgA in the resistance to *Acanthamoeba* keratitis. *Invest Ophthalmol Vis Sci.*, Vol. 39, No 13, p. 2666-73.

Leher H, Kinoshita K, Alizadeh H, Zaragoza FL, He Y & Niederkorn J, 1998. Impact of oral immunization with *Acanthamoeba* antigens on parasite adhesion and corneal infection. *Invest Ophthalmol Vis Sci.*, Vol. 39, No 12, p. 2337-43.

Leher H, Silvany R, Alizadeh H, Huang J & Niederkorn JY, 1998. Mannose induces the release of cytopathic factors from *Acanthamoeba castellanii*. *Infect Immun.*, Vol. 66, No 1, p. 5-10.

Leher H, Zaragoza F, Taherzadeh S, Alizadeh H & Niederkorn JY, 1999. Monoclonal IgA antibodies protect against *Acanthamoeba* keratitis. *Exp Eye Res.*, Vol. 69, No 1, p. 75-84.

Leitsch D, Köhsler M, Marchetti-Deschmann M, Deutsch A, Allmaier G, Duchêne M & Walochnik J, 2010. Major role for cysteine proteases during the early phase of *Acanthamoeba castellanii* encystment. *Eukaryot Cell.*, Vol. 9, No 4, p. 611-8.

Li L & Sun X, 2008. Impaired innate immunity of ocular surface is the key bridge between extended contact lens wearing and occurrence of *Acanthamoeba* keratitis. *Med Hypotheses.*, Vol. 70, No 2, p. 260-4.

Li S, Li B, Jiang H, Wang Y, Qu M, Duan H, Zhou Q & Shi W, 2013. Macrophage depletion impairs corneal wound healing after autologous transplantation in mice. *PLoS One*, Vol. 8, No 4:e61799. doi: 10.1371/journal.pone.0061799.

Liu G & Yang H, 2013. Modulation of macrophage activation and programming in immunity. *J Cell Physiol.*, Vol. 228, No 3, p. 502-12.

Lorenzo-Morales J, Martínez-Carretero E, Batista N, Alvarez-Marín J, Bahaya Y, Walochnik J & Valladares B, 2007. Early diagnosis of amoebic keratitis due to a mixed infection with *Acanthamoeba* and *Hartmannella*. *Parasitol Res.*, Vol. 102, No 1, p. 167-9.

Lorenzo-Morales J, Martín-Navarro CM, López-Arencibia A, Arnalich-Montiel F, Piñero JE & Valladares B, 2013. *Acanthamoeba* keratitis: an emerging disease gathering importance worldwide? *Trends Parasitol*, Vol. 29, No 4, p. 181-187.

Ma X, 2001. TNF-alpha and IL-12: a balancing act in macrophage functioning. *Microbes Infect*, Vol. 3, No 2, p. 121-9.

Macfarlane SR, Seatter MJ, Kanke T, Hunter GD & Plevin R, 2001. Proteinase-activated receptors. *Pharmacol Rev.*, Vol. 53, No 2, p. 245-82.

Maciver SK, Asif M, Simmen MW & Lorenzo-Morales J, 2013. A systematic analysis of *Acanthamoeba* genotype frequency correlated with source and pathogenicity: T4 is confirmed as a pathogen-rich genotype. *European Journal of Protistology*, Vol 49, p. 217–221.

Magnet A, Henriques-Gil N, Galván-Díaz AL, Izquierdo F, Fenoy S & del Aguila C, 2014. Novel *Acanthamoeba* 18S rRNA gene sequence type from an environmental isolate. *Parasitology Research*, Vol. 113, No 8, p. 2845-2850.

Maldonado-Bernal C, Kirschning CJ, Rosenstein Y, Rocha LM, Rios-Sarabia N, Espinosa-Cantellano M, Becker I, Estrada I, Salazar-González RM, López-Macías C, Wagner H, Sánchez J & Isibasi A, 2005. The innate immune response to *Entamoeba histolytica* lipopeptidophosphoglycan is mediated by toll-like receptors 2 and 4. *Parasite Immunol.*, Vol. 27, No 4, p. 127-37.

Mann A & Tighe B, 2013. Contact lens interactions with the tear film. *Exp Eye Res.*, Vol. 117, p. 88-98.

Mansell A, Reinicke A, Worrall DM & O'Neill LA, 2001. The serine protease inhibitor antithrombin III inhibits LPS-mediated NF-kappaB activation by TLR-4. *FEBS Lett.*, Vol. 508, No. 3, p. 313-7

Mantovani A, Sica A & Locati M, 2007. New vistas on macrophage differentiation and activation. *Eur J Immunol.*, Vol. 37, No 1, p. 14-6.

Mantovani A, Sozzani S, Locati M, Allavena P & Sica A, 2002. Macrophage polarization: tumor-associated macrophages as a paradigm for polarized M2 mononuclear phagocytes. *Trends Immunol.*, Vol. 23, No 11, p. 549-55.

Marciano-Cabral F & Cabral G, 2003. *Acanthamoeba* spp. as Agents of Disease in Humans. *Clinical Microbiology Reviews*, Vol 16, No 2, p. 273–307

Marciano-Cabral F & Toney DM, 1998. The interaction of *Acanthamoeba* spp. with activated macrophages and with macrophage cell lines. *J Eukaryot Microbiol.*, Vol. 45, No 4, p. 452-8.

Marciano-Cabral F, Ludwick C, Puffenbarger RA & Cabral GA, 2004. Differential stimulation of microglial pro-inflammatory cytokines by *Acanthamoeba culbertsoni* versus *Acanthamoeba castellanii*. *J Eukaryot Microbiol.*, Vol. 51, No 4, p. 472-9.

Marciano-Cabral F, Puffenbarger R & Cabral GA, 2000. The increasing importance of *Acanthamoeba* infections. *J Eukaryot Microbiol.*, Vol. 47, No 1, p. 29-36.

Maritschnegg P, Sovinz P, Lackner H, Benesch M, Nebel A, Schwinger W, Walochnik J & Urban C, 2011. Granulomatous amebic encephalitis in a child with

acute lymphoblastic leukemia successfully treated with multimodal antimicrobial therapy and hyperbaric oxygen. *J Clin Microbiol.*, Vol 49, No 1, p: 446-8.

Martinez AJ & Visvesvara GS, 1997. Free-living, Amphizoic and Opportunistic Amebas. *Brain Pathology*, Vol 7, p. 583-598.

Martinez AJ, 1980. Is *Acanthamoeba* encephalitis an opportunistic infection? *Neurology*, Vol. 30, No 6, p. 567-574.

Martinez FO & Gordon S, 2014. The M1 and M2 paradigm of macrophage activation: time for reassessment. *F1000Prime Rep.*, Vol. 6. 10.12703/P6-13. eCollection 2014.

Maryanoff BE, Zhang HC, Andrade-Gordon P & Derian CK, 2003. Discovery of potent peptide-mimetic antagonists for the human thrombin receptor, protease-activated receptor-1 (PAR-1). *Curr Med Chem Cardiovasc Hematol Agents.*, Vol. 1, No 1, p. 13-36.

Mastronicola D, Testa F, Forte E, Bordi E, Pucillo LP, Sarti P & Giuffrè A, 2010. Flavohemoglobin and nitric oxide detoxification in the human protozoan parasite *Giardia intestinalis*. *Biochem Biophys Res Commun.*, Vol. 399, No 4, p. 654-8.

Mattana A, Bennardini F, Usai S, Fiori PL, Franconi F & Cappuccinelli P, 1997. *Acanthamoeba castellanii* metabolites increase the intracellular calcium level and cause cytotoxicity in wish cells. *Microb Pathog.*, Vol. 23, No 2, p. 85-93.

Mattana A, Cappai V, Alberti L, Serra C, Fiori PL & Cappuccinelli P, 2002. ADP and other metabolites released from *Acanthamoeba castellanii* lead to human monocytic cell death through apoptosis and stimulate the secretion of proinflammatory cytokines. *Infect Immun.*, Vol. 70, No 8, p. 4424-32.

- Mattana A, Tozzi MG, Costa M, Delogu G, Fiori PL & Cappuccinelli P**, 2001. By releasing ADP, *Acanthamoeba castellanii* causes an increase in the cytosolic free calcium concentration and apoptosis in wish cells. *Infect Immun.*, Vol. 69, No 6, p. 4134-40.
- McBerry C, Gonzalez RM, Shryock N, Dias A & Aliberti J**, 2012. SOCS2-induced proteasome-dependent TRAF6 degradation: a common anti-inflammatory pathway for control of innate immune responses. *PLoS One*. Vol. 7, No 6, e38384.
- McClellan K, Howard K, Mayhew E, Niederkorn J & Alizadeh H**, 2002. Adaptive immune responses to *Acanthamoeba* cysts. *Exp Eye Res.*, Vol. 75, No 3, p. 285-93.
- McClellan SA, Huang X, Barrett RP, van Rooijen N & Hazlett LD**, 2003. Macrophages restrict *Pseudomonas aeruginosa* growth, regulate polymorphonuclear neutrophil influx, and balance pro- and anti-inflammatory cytokines in BALB/c mice. *J Immunol.*, Vol. 170, No 10, p. 5219-27.
- McClure R & Massari P**, 2014. TLR-dependent human mucosal epithelial cell responses to microbial pathogens. *Front Immunol.*, Vol. 5, No 386. doi: 10.3389/fimmu.2014.00386. eCollection 2014.
- McKerrow JH, Caffrey C, Kelly B, Loke P & Sajid M**, 2006. Proteases in parasitic diseases. *Annu Rev Pathol.*, Vol. 1, p. 497-536.
- Menzies FM, Henriquez FL, Alexander J & Roberts CW**, 2010. Sequential expression of macrophage anti-microbial/inflammatory and wound healing markers following innate, alternative and classical activation. *Clin Exp Immunol.*, Vol. 160, No 3, p. 369-79.
- Mills CD**, 2012. M1 and M2 macrophages: oracles of health and disease. *Crit Rev Immunol.*, Vol. 32, No 6, p. 463-88.

- Mills CD, Kincaid K, Alt JM, Heilman MJ & Hill AM**, 2000. M-1/M-2 macrophages and the Th1/Th2 paradigm. *J Immunol.*, Vol. 164, No 12, p. 6166-73.
- Mitra MM, Alizadeh H, Gerard RD & Niederkorn JY**, 1995. Characterization of a plasminogen activator produced by *Acanthamoeba castellanii*. *Mol Biochem Parasitol.*, Vol. 73, No 1-2, p. 157-64.
- Mitro K, Bhagavathiammai A, Zhou OM, Bobbett G, McKerrow JH, Chokshi R, Chokshi B & James ER**, 1994. Partial characterization of the proteolytic secretions of *Acanthamoeba polyphaga*. *Exp Parasitol.*, Vol. 78, No 4, p. 377-85.
- Moon EK, Hong Y, Chung DI & Kong HH**, 2012. Cysteine protease involving in autophagosomal degradation of mitochondria during encystation of *Acanthamoeba*. *Molecular & Biochemical Parasitology*, Vol. 185, No 2, p: 121-126
- Morton LD, McLaughlin GL & Whiteley HE**, 1991. Effects of temperature, amebic strain, and carbohydrates on *Acanthamoeba* adherence to corneal epithelium in vitro. *Infect Immun.*, Vol. 59, No 10, p. 3819-22.
- Mosser DM & Edwards JP**, 2008. Exploring the full spectrum of macrophage activation. *Nat Rev Immunol.*, Vol. 8, No 12, p. 958-69
- Moura H, Wallace S & Visvesvara GS**, 1992. *Acanthamoeba healyi* n. sp. and the isoenzyme and immunoblot profiles of *Acanthamoeba* spp., groups 1 and 3. *J Protozool.*, Vol 39, No 5, p. 573-83.
- Muraille E, Leo O & Moser M**, 2014. TH1/TH2 paradigm extended: macrophage polarization as an unappreciated pathogen-driven escape mechanism? *Front Immunol.*, Vol. 5, No 603. doi: 10.3389/fimmu.2014.00603. eCollection 2014.

Murakami Y, Hoshi M, Imamura Y, Arioka Y, Yamamoto Y & Saito K, 2013. Remarkable role of indoleamine 2,3-dioxygenase and tryptophan metabolites in infectious diseases: potential role in macrophage-mediated inflammatory diseases. *Mediators Inflamm.*, Vol. 2013, No 391984. doi: 10.1155/2013/391984. Epub 2013 Feb 18.

Murphy K, 2011. Janeway's immunobiology. 8th edition. London and New York: Garland Science Taylor & Francis Group.

Murray PJ & Wynn TA, 2011. Protective and pathogenic functions of macrophage subsets. *Nat Rev Immunol.*, Vol. 11, No 11, p. 723-37.

Murray PJ, Allen JE, Biswas SK, Fisher EA, Gilroy DW, Goerdts S, Gordon S, Hamilton JA, Ivashkiv LB, Lawrence T, Locati M, Mantovani A, Martinez FO, Mege JL, Mosser DM, Natoli G, Saeij JP, Schultze JL, Shirey KA, Sica A, Suttles J, Udalova I, van Ginderachter JA, Vogel SN & Wynn TA, 2014. Macrophage activation and polarization: nomenclature and experimental guidelines. *Immunity.* Vol. 41, No 1, p. 14-20.

Murray RZ & Stow JL, 2014. Cytokine secretion in macrophages: SNAREs, Rabs, and membrane trafficking. *Front Immunol.*, Vol. 5, No 538.

Mutreja D, Jalpota Y, Madan R & Tewari V, 2007. Disseminated *Acanthamoeba* infection in a renal transplant recipient: a case report. *Indian J Pathol Microbiol.*, Vol. 50, No 2, p. 346-8.

Na BK, Cho JH, Song CY & Kim TS, 2002. Degradation of immunoglobulins, protease inhibitors and interleukin-1 by a secretory proteinase of *Acanthamoeba castellanii*. *Korean J Parasitol.*, Vol. 40, No 2, p. 93-9.

Na BK, Kim JC & Song CY, 2001. Characterization and pathogenetic role of proteinase from *Acanthamoeba castellanii*. *Microb Pathog.*, Vol. 30, No 1, p. 39-48.

Nachega JB, Rombaux P, Weynand B, Thomas G & Zech F, 2005. Successful treatment of *Acanthamoeba* rhinosinusitis in a patient with AIDS. *AIDS Patient Care STDS.*, Vol. 19. No 10, p. 621-5.

Nagington J, Watson PG, Playfair TJ, McGill J, Jones BR & Steele AD, 1974. Amoebic infection of the eye. *The Lancet*, Vol 2, No 7896, p. 1537–1540.

Nagyová V, Nagy A & Timko J, 2010. Morphological, physiological and molecular biological characterisation of isolates from first cases of *Acanthamoeba* keratitis in Slovakia. *Parasitol Res.*, Vol. 106, No 4, p. 861-72.

Niederhorn JY, 2006. See no evil, hear no evil, do no evil: the lessons of immune privilege. *Nat Immunol.*, Vol. 7, No 4, p. 354-9.

Nuprasert W, Putaporntip C, Pariyakanok L & Jongwutiwes S, 2010. Identification of a novel t17 genotype of *Acanthamoeba* from environmental isolates and t10 genotype causing keratitis in Thailand. *J Clin Microbiol.*, Vol. 48, No 12, p. 4636-40.

Oliva S, Jantz M, Tiernan R, Cook DL & Judson MA, 1999. Successful treatment of widely disseminated acanthamoebiasis. *South Med J*, Vol. 92, No 2, p. 55–7.

Olszewski KL, Morrissey JM, Wilinski D, Burns JM, Vaidya AB, Rabinowitz JD & Llinás M, 2009. Host-parasite interactions revealed by *Plasmodium falciparum* metabolomics. *Cell Host Microbe*, Vol. 5, No 2, p. 191-9.

Omaña-Molina M, González-Robles A, Iliana Salazar-Villatoro L, Lorenzo-Morales J, Cristóbal-Ramos AR, Hernández-Ramírez VI, Talamás-Rohana P,

Méndez Cruz AR & Martínez-Palomo A, 2013. Reevaluating the role of *Acanthamoeba* proteases in tissue invasion: observation of cytopathogenic mechanisms on MDCK cell monolayers and hamster corneal cells. *Biomed Res Int.*, 2013;2013:461329. doi: 10.1155/2013/461329

Omaña-Molina M, González-Robles A, Salazar-Villatoro LI, Cristóbal-Ramos AR, González-Lázaro M, Salinas-Moreno E, Méndez-Cruz R, Sánchez-Cornejo M, De la Torre-González E & Martínez-Palomo A, 2010. *Acanthamoeba castellanii*: morphological analysis of the interaction with human cornea. *Exp Parasitol.*, Vol. 126, No 1, p. 73-8.

Otri AM, Mohammed I, Abedin A, Cao Z, Hopkinson A, Panjwani N & Dua HS, 2010. Antimicrobial peptides expression by ocular surface cells in response to *Acanthamoeba castellanii*: an *in vitro* study. *Br J Ophthalmol.*, Vol. 94, No 11, p. 1523-7.

Owen J, Punt J & Stranford S, 2012. Kuby Immunology, 7th Edition. W. H. Freeman and Company, New York

Paget T, Haroune N, Bagchi S & Jarroll E, 2013. Metabolomics and protozoan parasites. *Acta Parasitol.*, Vol. 58, No 2, p. 127-31.

Pan H & Wu X, 2012. Hypoxia attenuates inflammatory mediators production induced by *Acanthamoeba* via Toll-like receptor 4 signaling in human corneal epithelial cells. *Biochemical and Biophysical Research Communications*, Vol 420, p. 685–691

Park MK, Cho MK, Kang SA, Park HK, Kim DH & Yu HS, 2014. *Acanthamoeba* protease activity promotes allergic airway inflammation via protease-activated receptor 2. *PLoS One*, Vol. 9, No 3, e92726. doi: 10.1371/journal.pone.0092726.

Pearlman E, Sun Y, Roy S, Karmakar M, Hise AG, Szczotka-Flynn L, Ghannoum M, Chinnery HR, McMenamin PG & Rietsch A, 2013. Host defense at the ocular surface. *Int Rev Immunol.*, Vol. 32, No 1, p. 4-18.

Petry F, Torzewski M, Bohl J, Wilhelm-Schwenkmezger T, Scheid P, Walochnik J, Michel R, Zöller L, Werhahn KJ, Bhakdi S & Lackner KJ, 2006. Early diagnosis of *Acanthamoeba* infection during routine cytological examination of cerebrospinal fluid. *J. Clin. Microbiol.*, Vol. 44, No 5, p. 1903-4.

Pettit DA, Williamson J, Cabral GA & Marciano-Cabral F, 1996. *In vitro* destruction of nerve cell cultures by *Acanthamoeba* spp.: a transmission and scanning electron microscopy study. *J Parasitol.*, Vol. 82, No 5, p. 769-77.

Pietrucha-Dilanchian P, Chan JC, Castellano-Sanchez A, Hirzel A, Laowansiri P, Tuda C, Visvesvara GS, Qvarnstrom Y & Ratzan KR, 2012. *Balamuthia mandrillaris* and *Acanthamoeba* amebic encephalitis with neurotoxoplasmosis coinfection in a patient with advanced HIV infection. *J Clin Microbiol.*, Vol. 50, No 3, p.1128-31.

Por YM, Mehta JS, Chua JL, Koh TH, Khor WB, Fong AC, Lim JW, Heng WJ, Loh RS, Lim L & Tan DT, 2009. *Acanthamoeba* keratitis associated with contact lens wear in Singapore. *Am J Ophthalmol.*, Vol. 148, No 1, p. 7-12.

Pumidonming W, Koehsler M, Leitsch D & Walochnik J, 2014. Protein profiles and immunoreactivities of *Acanthamoeba* morphological. *Exp Parasitol.*, 145 Suppl:S50-6.

Pumidonming W, Walochnik J, Dauber E & Petry F, 2011. Binding to complement factors and activation of the alternative pathway by *Acanthamoeba*. *Immunobiology*, Vol. 216, No 1-2, p. 225-33.

Pussard M & Pons R, 1977. Morphologie de la paroi kystique et taxonomie du genre *Acanthamoeba* (Protozoa, Amoebida). *Protistologica* 13, 557–598.

Qvarnstrom Y, Nerad TA & Visvesvara GS, 2013. Characterization of a new pathogenic *Acanthamoeba* Species, *A. byersi* n. sp., isolated from a human with fatal amoebic encephalitis. *J Eukaryot Microbiol.*, Vol. 60, No 6, p. 626-33.

Radford CF, Minassian DC & Dart JK, 2002. *Acanthamoeba* keratitis in England and Wales: incidence, outcome, and risk factors. *Br J Ophthalmol.* Vol. 86, No 5, p. 536-42.

Raes G, Beschin A, Ghassabeh GH & De Baetselier P, 2007. Alternatively activated macrophages in protozoan infections. *Curr Opin Immunol.*, Vol. 19, No 4, p.454-9.

Ralston KS, Solga MD, Mackey-Lawrence NM, Somlata, Bhattacharya A & Petri WA Jr, 2014. Trophocytosis by *Entamoeba histolytica* contributes to cell killing and tissue invasion. *Nature.* Vol. 508, No. 7497, p. 526-30.

Ramachandran R, Noorbakhsh F, Defea K & Hollenberg MD, 2013. Targeting proteinase-activated receptors: therapeutic potential and challenges. *Nat Rev Drug Discov.*, Vol. 11, No 1, p. 69-86.

Rascón AA Jr & McKerrow JH, 2013. Synthetic and natural protease inhibitors provide insights into parasite development, virulence and pathogenesis. *Curr Med Chem.*, Vol. 20, No 25, p. 3078-102.

Rath M, Müller I, Kropf P, Closs EI & Munder M, 2014. Metabolism via arginase or nitric oxide synthase: two competing arginine pathways in macrophages. *Front Immunol.*, Vol. 5, No 532. doi: 10.3389/fimmu.2014.00532.

- Reddy R, Vijayasradhi M, Uppin MS, Challa S, Jabeen A & Borghain R**, 2011. *Acanthamoeba* meningoencephalitis in an immunocompetent patient: an autopsy case report. *Neuropathology*, Vol. 31, No 2, p. 183-7.
- Ren H, Teng Y, Tan B, Zhang X, Jiang W, Liu M, Jiang W, Du B & Qian M**, 2014. Toll-like receptor-triggered calcium mobilization protects mice against bacterial infection through extracellular ATP release. *Infect Immun*. Vol. 82, No 12, p. 5076-85.
- Ren M, Gao L & Wu X**, 2010. TLR4: the receptor bridging *Acanthamoeba* challenge and intracellular inflammatory responses in human corneal cell lines. *Immunol Cell Biol.*, Vol. 88, No 5, p. 529-36.
- Ren MY & Wu XY**, 2011. Toll-like receptor 4 signalling pathway activation in a rat model of *Acanthamoeba* Keratitis. *Parasite Immunol.*, Vol. 33, No 1, p. 25-33.
- Reyes-Batlle M, Todd CD, Martín-Navarro CM, López-Arencibia A, Cabello-Vilchez AM, González AC, Córdoba-Lanús E, Lindo JF, Valladares B, Piñero JE & Lorenzo-Morales J**, 2014. Isolation and characterization of *Acanthamoeba* strains from soil samples in Gran Canaria, Canary Islands, Spain. *Parasitology Research*, Vol. 113, No 4 , p. 1383-1388.
- Ringsted J, Val Jager B, Suk D & Visvesvara GS**, 1976. Probable *Acanthamoeba* meningoencephalitis in a Korean child. *Am J Clin Pathol*, Vol. 66, No 4, p: 723–30.
- Risler A, Coupat-Goutaland B & Pélandakis M**, 2013. Genotyping and phylogenetic analysis of *Acanthamoeba* isolates associated with keratitis. *Parasitol Res.*, Vol. 112, No 11, p. 3807-16.
- Robert VB & Rorke LB**, 1973. Primary amebic encephalitis, probably from *Acanthamoeba*. *Ann Intern Med*, Vol 79, No 2, p. 174-179

Rocha-Azevedo BD, Jamerson M, Cabral GA & Marciano-Cabral F, 2010. *Acanthamoeba culbertsoni*: analysis of amoebic adhesion and invasion on extracellular matrix components collagen I and laminin-1. *Exp Parasitol.*, Vol. 126, No 1, p. 79-84.

Rocha-Azevedo BD, Jamerson M, Cabral GA, Silva-Filho FC & Marciano-Cabral F, 2009. *Acanthamoeba* interaction with extracellular matrix glycoproteins: biological and biochemical characterization and role in cytotoxicity and invasiveness. *J Eukaryot Microbiol.*, Vol. 56, No 3, p. 270-8.

Ropert C & Gazzinelli RT, 2000. Signalling of immune system cells by glycosylphosphatidylinositol (GPI) anchor and related structures derived from parasitic protozoa. *Curr Opin Microbiol.*, Vol. 3, No 4, p. 395-403.

Saban R, D'Andrea MR, Andrade-Gordon P, Derian CK, Dozmorov I, Ihnat MA, Hurst RE, Davis CA, Simpson C & Saban MR, 2007. Mandatory role of proteinase-activated receptor 1 in experimental bladder inflammation. *BMC Physiol.*, Vol. 7, No.4.

Said NA, Shoeir AT, Panjwani N, Garate M & Cao Z, 2004. Local and systemic humoral immune response during acute and chronic *Acanthamoeba* keratitis in rabbits. *Curr Eye Res.*, Vol. 29, No 6, p. 429-39.

Sakaki H, Tsukimoto M, Harada H, Moriyama Y & Kojima S, 2013. Autocrine regulation of macrophage activation via exocytosis of ATP and activation of P2Y11 receptor. *PLoS One*, Vol. 8, No 4, e59778.

Salimi Elizei S, Poormasjedi-Meibod MS, Li Y, Baradar Jalili R & Ghahary A, 2014. Effects of kynurenine on CD3+ and macrophages in wound healing. *Wound Repair Regen.*, doi: 10.1111/wrr.12252.

Sana TR, Gordon DB, Fischer SM, Tichy SE, Kitagawa N, Lai C, Gosnell WL & Chang SP, 2013. Global mass spectrometry based metabolomics profiling of erythrocytes infected with *Plasmodium falciparum*. *PLoS One.*, Vol. 8, No 4, e60840.

Sant'ana VP, Carrijo-Carvalho LC, Foronda AS, Chudzinski-Tavassi AM, de Freitas D & de Carvalho FR, 2014. Cytotoxic activity and degradation patterns of structural proteins by corneal isolates of *Acanthamoeba* spp. *Graefes Arch Clin Exp Ophthalmol.*, Aug 27. [Epub ahead of print]

Saric J, Li JV, Swann JR, Utzinger J, Calvert G, Nicholson JK, Dirnhofer S, Dallman MJ, Bictash M & Holmes E, 2010. Integrated cytokine and metabolic analysis of pathological responses to parasite exposure in rodents. *J Proteome Res.*, Vol. 9, No 5, p. 2255-64.

Satlin MJ, Graham JK, Visvesvara GS, Mena H, Marks KM, Saal SD & Soave R, 2013. Fulminant and fatal encephalitis caused by *Acanthamoeba* in a kidney transplant recipient: case report and literature review. *Transpl Infect Dis.*, Vol 15, No 6, p. 619-26.

Schroeder JM, Booton GC, Hay J, Niszl IA, Seal DV, Markus MB, Fuerst PA & Byers TJ, 2001. Use of subgenomic 18S ribosomal DNA PCR and sequencing for genus and genotype identification of acanthamoebae from humans with keratitis and from sewage sludge. *J Clin Microbiol.*, Vol. 39, No 5, p. 1903-11.

Schuster FL, Guglielmo BJ & Visvesvara GS, 2006. *In-vitro* activity of miltefosine and voriconazole on clinical isolates of free-living amebas: *Balamuthia mandrillaris*, *Acanthamoeba* spp., and *Naegleria fowleri*. *J Eukaryot Microbiol.*, Vol 53, No 2, p. 121-6.

Seal DV, 2003. *Acanthamoeba* keratitis update-incidence, molecular epidemiology and new drugs for treatment. *Eye (Lond)*., Vol. 17, No 8, p. 893-905.

Seijo Martinez M, Gonzalez-Mediero G, Santiago P, Rodriguez De Lope A, Diz J, Conde C & Visvesvara GS (2000) Granulomatous amebic encephalitis in a patient with AIDS: isolation of *Acanthamoeba* sp. Group II from brain tissue and successful treatment with sulfadiazine and fluconazole. *J Clin Microbiol*, Vol. 38, No 10, p. 3892-3895.

Selby DM, Chandra RS, Rakusan TA, Loechelt B, Markle BM & Visvesvara GS, 1998. Amebic osteomyelitis in a child with acquired immunodeficiency syndrome: a case report. *Pediatr Pathol Lab Med.*, Vol. 18, No 1, p. 89-95.

Shaharuddin B, Ahmad S, Meeson A & Ali S, 2013. Concise review: immunological properties of ocular surface and importance of limbal stem cells for transplantation. *Stem Cells Transl Med.*, Vol. 2, No 8, p. 614-24.

Sharma S, Ramachandran L & Rao GN, 1995. Adherence of cysts and trophozoites of *Acanthamoeba* to unworn rigid gas permeable and soft contact lenses. *CLAO J.*, Vol. 21, No 4, p. 247-51.

Shin HJ, Cho MS, Jung SY, Kim HI, Park S, Seo JH, Yoo JC & Im KI, 2001. Cytopathic changes in rat microglial cells induced by pathogenic *Acanthamoeba culbertsoni*: morphology and cytokine release. *Clin Diagn Lab Immunol.*, Vol. 8, No 4, p. 837-40.

Shin HJ, Cho MS, Kim HI, Lee M, Park S, Sohn S & Im KI, 2000. Apoptosis of primary-culture rat microglial cells induced by pathogenic *Acanthamoeba* spp. *Clin Diagn Lab Immunol.*, Vol. 7, No 3, p. 510-4.

Shpacovitch V, Feld M, Bunnett NW & Steinhoff M, 2007. Protease-activated receptors: novel PARtners in innate immunity. *Trends Immunol.*, Vol. 28, No 12, p. 541-50.

Sica A & Mantovani A, 2012. Macrophage plasticity and polarization: in vivo veritas. *J Clin Invest.* Vol. 122, No. 3, p. 787-95.

Siddiqui R & Khan NA, 2012. Biology and pathogenesis of *Acanthamoeba*. *Parasites & Vectors*, Vol. 5, No 6.

Silva AM, Cordeiro-da-Silva A & Coombs GH, 2011. Metabolic variation during development in culture of *Leishmania donovani* promastigotes. *PLoS Negl Trop Dis.*, Vol. 5, No. 12, e1451.

Sissons J, Alsam S, Jayasekera S & Khan NA, 2004. Ecto-ATPases of clinical and non-clinical isolates of *Acanthamoeba*. *Microb Pathog.*, Vol. 37, No 5, p. 231-9.

Sissons J, Alsam S, Jayasekera S, Kim KS, Stins M & Khan NA, 2004. *Acanthamoeba* induces cell-cycle arrest in host cells. *J Med Microbiol.*, Vol. 53, No 8, p. 711-7.

Sissons J, Kim KS, Stins M, Jayasekera S, Alsam S & Khan NA, 2005. *Acanthamoeba castellanii* induces host cell death via a phosphatidylinositol 3-kinase-dependent mechanism. *Infect Immun.*, Vol. 73, No 5, p. 2704-8.

Slater CA, Sickel JZ, Visvesvara GS, Pabico RC & Gaspari AA. Brief report: successful treatment of disseminated *Acanthamoeba* infection in an immunocompromised patient. *N Engl J Med*, Vol. 331, No 2, p. 85–7.

Sonoki T, Nagasaki A, Gotoh T, Takiguchi M, Takeya M, Matsuzaki H & Mori M, 1997. Coinduction of nitric-oxide synthase and arginase I in cultured rat peritoneal

macrophages and rat tissues in vivo by lipopolysaccharide. *J Biol Chem.*, Vol. 272, No 6, p. 3689-93.

Spanakos G, Tzanetou K, Miltsakakis D, Patsoula E, Malamou-Lada E & Vakalis NC, 2006. Genotyping of pathogenic *Acanthamoebae* isolated from clinical samples in Greece-report of a clinical isolate presenting T5 genotype. *Parasitol Int.*, Vol. 55, No 2, p. 147-9.

Stadelmann B, Merino MC, Persson L & Svärd SG, 2012. Arginine consumption by the intestinal parasite *Giardia intestinalis* reduces proliferation of intestinal epithelial cells. *PLoS One.*, Vol. 7, No 9:e45325.

Stein M, Keshav S, Harris N & Gordon S, 1992. Interleukin 4 potently enhances murine macrophage mannose receptor activity: a marker of alternative immunologic macrophage activation. *J Exp Med.*, Vol. 176, No 1, p. 287-92.

Steinberg JP, Galindo RL, Kraus ES & Ghanem KG, 2002. Disseminated acanthamebiasis in a renal transplant recipient with osteomyelitis and cutaneous lesions: case report and literature review. *Clin Infect Dis.*, Vol. 35, No 5, p. e43–9.

Stevanin TM, Read RC & Poole RK, 2007. The hmp gene encoding the NO-inducible flavohaemoglobin in *Escherichia coli* confers a protective advantage in resisting killing within macrophages, but not in vitro: links with swarming motility. *Gene*. Vol. 398, No 1-2, p. 62-8.

Stewart GL, Kim I, Shupe K, Alizadeh H, Silvany R, McCulley JP & Niederkorn JY, 1992. Chemotactic response of macrophages to *Acanthamoeba castellanii* antigen and antibody-dependent macrophage-mediated killing of the parasite. *J Parasitol.*, Vol. 78, No 5, p. 849-55.

Storm J, Sethia S, Blackburn GJ, Chokkathukalam A, Watson DG, Breitling R, Coombs GH & Müller S, 2014. Phosphoenolpyruvate carboxylase identified as a key enzyme in erythrocytic *Plasmodium falciparum* carbon metabolism. *PLoS Pathog.* Vol. 10, No 1, e1003876.

Stothard DR, Schroeder-Diedrich JM, Awwad MH, Gast RJ, Ledee DR, Rodriguez-Zaragoza S, Dean CL, Fuerst PA & Byers TJ, 1998. The evolutionary history of the genus *Acanthamoeba* and the identification of eight new 18S rRNA gene sequence types. *J. Eukaryot. Microbiol.*, Vol. 45, p. 45–54.

Stratford MP & Griffiths AJ, 1978. Variations in the properties and morphology of cysts of *Acanthamoeba castellanii*. *J. Gen. Microbiol.*, Vol. 108, p. 33–37.

Streilein JW, 1997. Regulation of ocular immune responses. *Eye (Lond)*., Vol. 11, (Pt 2), p. 171-5.

Sun Y, Karmakar M, Roy S, Ramadan RT, Williams SR, Howell S, Shive CL, Han Y, Stopford CM, Rietsch A & Pearlman E, 2010. TLR4 and TLR5 on corneal macrophages regulate *Pseudomonas aeruginosa* keratitis by signalling through MyD88-dependent and –independent pathways. *J Immunol.*, Vol 185, No 7, p. 4272-83.

Takaoka-Sugihara N, Yamagami S, Yokoo S, Matsubara M & Yagita K, 2012. Cytopathic effect of *Acanthamoeba* on human corneal fibroblasts. *Mol Vis.*, Vol. 18, p. 2221-8.

Takeda K & Akira S, 2004. TLR signalling pathways. *Semin Immunol.*, Vol. 16, No 1, p. 3-9.

Tanaka Y, Suguri S, Harada M, Hayabara T, Suzumori K & Ohta N, 1994. *Acanthamoeba*-specific human T-cell clones isolated from healthy individuals. *Parasitol Res.*, Vol. 80, No 7, p. 549-53.

Tanveer T, Hameed A, Muazzam AG, Jung S, Gul A & Mati A. 2013. Isolation and molecular characterization of potentially pathogenic *Acanthamoeba* genotypes from diverse water resources including household drinking water from Khyber Pakhtunkhwa, Pakistan. *Parasitology Research*, Vol. 112, No 8, p. 2925-2932.

Thakur A & Willcox MD, 2000. Contact lens wear alters the production of certain inflammatory mediators in tears. *Exp Eye Res*, Vol. 70, No 3, p. 255–9.

Thomas AG, O'Driscoll CM, Bressler J, Kaufmann W, Rojas CJ & Slusher BS, 2014. Small molecule glutaminase inhibitors block glutamate release from stimulated microglia. *Biochem Biophys Res Commun.*, Vol. 443, No 1, p. 32-6.

Torno MS Jr, Babapour R, Gurevitch A & Witt MD, 2000. Cutaneous acanthamoebiasis in AIDS. *J Am Acad Dermatol*, Vol. 42, No 22, p. 351–4.

Trabelsi H, Dendana F, Sellami A, Sellami H, Cheikhrouhou F, Neji S, Makni F & Ayadi A, 2012. Pathogenic free-living amoebae: Epidemiology and clinical review. *Pathol Biol (Paris)*. Vol. 60, No 6, p. 399-405.

Trinchieri G, 2003. Interleukin-12 and the regulation of innate resistance and adaptive immunity. *Nat Rev Immunol.*, Vol. 3, No 2, p. 133-46.

Tripathi T, Abdi M & Alizadeh H, 2013. Role of phospholipase A₂ (PLA₂) inhibitors in attenuating apoptosis of the corneal epithelial cells and mitigation of *Acanthamoeba* keratitis. *Exp Eye Res.*, Vol. 113, p. 182-91.

Tripathi T, Abdi M & Alizadeh H, 2014. Protease-activated receptor 2 (PAR2) is upregulated by *Acanthamoeba* plasminogen activator (aPA) and induces proinflammatory cytokine in human corneal epithelial cells. *Invest Ophthalmol Vis Sci.*, Vol. 55, No 6, p. 3912-21.

Tripathi T, Smith AD, Abdi M & Alizadeh H, 2012. *Acanthamoeba* cytopathic protein induces apoptosis and proinflammatory cytokines in human corneal epithelial cells by cPLA_{2α} activation. *Invest Ophthalmol Vis Sci.*, Vol. 53, No. 13, p. 7973-82.

Turner MD, Nedjai B, Hurst T & Pennington DJ, 2014. Cytokines and chemokines: At the crossroads of cell signalling and inflammatory disease. *Biochim Biophys Acta.*, Vol. 1843, No 11, p. 2563-2582.

Uematsu S & Akira S. Toll-Like Receptors (TLRs) and Their Ligands. Toll-Like Receptors (TLRs) and Innate Immunity. Handbook of Experimental Pharmacology 183. 2008. S. Bauer, G. Hartmann (eds.), Springer-Verlag Berlin Heidelberg

van Klink F, Alizadeh H, He Y, Mellon JA, Silvany RE, McCulley JP & Niederkorn JY, 1993. The role of contact lenses, trauma, and Langerhans cells in a Chinese hamster model of *Acanthamoeba* keratitis. *Invest Ophthalmol Vis Sci.*, Vol. 34, No 6, p. 1937-44.

van Klink F, Taylor WM, Alizadeh H, Jager MJ, van Rooijen N & Niederkorn JY, 1996. The role of macrophages in *Acanthamoeba* keratitis. *Invest Ophthalmol Vis Sci.*, Vol. 37, No 7, p. 1271-81.

Verani JR, Lorick SA, Yoder JS, Beach MJ, Braden CR, Roberts JM, Conover CS, Chen S, McConnell KA, Chang DC, Park BJ, Jones DB, Visvesvara GS &

- Roy SL**, 2009. National outbreak of *Acanthamoeba* keratitis associated with use of a contact lens solution, United States. *Emerg. Infect. Dis.*, Vol. 15, No 4, p. 1236–1242
- Vergnolle N**, 2003. The inflammatory response. Drug Development Research. Special Issue: Proteinases and Signalling: A Focus on Proteinase-Activated Receptors (PARs) — Part 1, Vol 59, No 4, p. 375-381.
- Visvesvara GS**, 1991. Classification of *Acanthamoeba*. *Reviews of Infectious Diseases*, Vol. 13, No 5, p. S369-72
- Visvesvara GS**, 2013. Infections with free-living amoebae. Handbook of Clinical Neurology, Vol. 114 (3rd series) Neuroparasitology and Tropical Neurology. Chapter 10.
- Visvesvara GS, Moura H & Schuster FL**, 2007. Pathogenic and opportunistic free-living amoebae: *Acanthamoeba* spp., *Balamuthia mandrillaris*, *Naegleria fowleri*, and *Sappinia diploidea*. *FEMS Immunol Med Microbiol*, Vol. 50, p 1–26
- Visvesvara GS, Sriram R, Qvarnstrom Y, Bandyopadhyay K, Da Silva AJ, Pieniazek NJ & Cabral GA**, 2009. *Paravahlkampfia francinae* n. sp. masquerading as an agent of primary amoebic meningoencephalitis. *J Eukaryot Microbiol.*, Vol. 56, No 4, p. 357-66.
- Walia R, Montoya JG, Visvesvera GS, Booton GC & Doyle RL**, 2007. A case of successful treatment of cutaneous *Acanthamoeba* infection in a lung transplant recipient. *Transpl Infect Dis.*, Vol. 9, No 1, p. 51-4.
- Walochnik J, Aichelburg A, Assadian O, Steuer A, Visvesvara G, Vetter N & Aspöck H**, 2008. Granulomatous amoebic encephalitis caused by *Acanthamoeba* amoebae of genotype T2 in a human immunodeficiency virus-negative patient. *J Clin Microbiol.*, Vol. 46, No 1, p. 338-40.

Walochnik J, Haller-Schober E, Kölli H, Picher O, Obwaller A & Aspöck H, 2000. Discrimination between clinically relevant and non relevant *Acanthamoeba* strains isolated from contact lens- wearing keratitis patients in Austria. *J Clin Microbiol.*, Vol. 38, No 11, p. 3932-6.

Walochnik J, Obwaller A & Aspöck H, 2000. Correlations between morphological, molecular biological, and physiological characteristics in clinical and nonclinical isolates of *Acanthamoeba* spp. *Appl Environ Microbiol.*, Vol. 66, No 10, p. 4408-13.

Walochnik J, Obwaller A, Haller-Schober EM & Aspöck H, 2001. Anti-*Acanthamoeba* IgG, IgM, and IgA immunoreactivities in correlation to strain pathogenicity. *Parasitol Res.*, Vol. 87, No 8, p. 651-6.

Walochnik J, Scheikl U & Haller-Schober EM, 2014. Twenty years of *Acanthamoeba* Diagnostics in Austria. *J Eukaryot Microbiol.*, doi: 10.1111/jeu.12149.

Wang WW, Jenkinson CP, Griscavage JM, Kern RM, Arabolos NS, Byrns RE, Cederbaum SD & Ignarro LJ, 1995. Co-induction of arginase and nitric oxide synthase in murine macrophages activated by lipopolysaccharide. *Biochem Biophys Res Commun.*, Vol. 210, No 3, p. 1009-16.

Webster D, Umar I, Kolyvas G, Bilbao J, Guiot MC, Duplisea K, Qvarnstrom Y & Visvesvara GS, 2012. Case Report: Treatment of Granulomatous Amoebic Encephalitis with Voriconazole and Miltefosine in an Immunocompetent Soldier. *Am. J. Trop. Med. Hyg.*, Vol 87, No 4, p. 715–718

Weekers PH & De Jonckheere JF, 1997. Differences in isoenzyme patterns of axenically and monoxenically grown *Acanthamoeba* and *Hartmannella*. *Antonie Van Leeuwenhoek.*, Vol 71, No 3, p. 231-7.

Woods S, Schroeder J, McGachy HA, Plevin R, Roberts CW & Alexander J, 2013. MAP kinase phosphatase-2 plays a key role in the control of infection with *Toxoplasma gondii* by modulating iNOS and arginase-1 activities in mice. *PLoS Pathog.*, Vol. 9, No 8:e1003535.

Yagi S, Schuster FL & Bloch K, 2007. Demonstration of presence of *Acanthamoeba* mitochondrial DNA in brain tissue and cerebrospinal fluid by PCR in samples from a patient who died of granulomatous amebic encephalitis. *J. Clin. Microbiol.*, Vol. 45 No 6, p. 2090-2091.

Yamagami S, Usui T, Amano S & Ebihara N, 2005. Bone marrow-derived cells in mouse and human cornea. *Cornea*. 24(8 Suppl):S71-S74.

Yang Z, Cao Z & Panjwani N, 1997. Pathogenesis of *Acanthamoeba* keratitis: carbohydrate-mediated host-parasite interactions. *Infect Immun.*, Vol. 65, No 2, p. 439-45.

Ye L, Huang Y, Zhao L, Li Y, Sun L, Zhou Y, Qian G & Zheng JC, 2013. IL-1 β and TNF- α induce neurotoxicity through glutamate production: a potential role for neuronal glutaminase. *J Neurochem.*, Vol. 125, No 6, p. 897-908.

Yoder JS, Verani J, Heidman N, Hoppe-Bauer J, Alfonso EC, Miller D, Jones DB, Bruckner D, Langston R, Jeng BH, Joslin CE, Tu E, Colby K, Vetter E, Ritterband D, Mathers W, Kowalski RP, Acharya NR, Limaye AP, Leiter C, Roy S, Lorick S, Roberts J & Beach MJ, 2012. *Acanthamoeba* keratitis: the persistence of cases following a multistate outbreak. *Ophthalmic Epidemiol.*, Vol. 19, No 4, p. 221-5.

Young AL, Leboeuf NR, Tsiouris SJ, Husain S & Grossman ME, 2010. Fatal disseminated *Acanthamoeba* infection in a liver transplant recipient

immunocompromised by combination therapies for graft-versus-host disease.
Transpl Infect Dis., Vol 12, No 6, p. 529-37.

Zheng X, Uno T, Goto T, Zhang W, Hill JM & Ohashi Y, 2004. Pathogenic *Acanthamoeba* induces apoptosis of human corneal epithelial cells. *Jpn J Ophthalmol.*, Vol. 48, No 1, p. 23-9.